# The Anti-inflammatory Effects of Vitamin D Receptor Agonists on Human White Preadipocytes

Thesis submitted in accordance with the requirements of the University of Liverpool
for the degree of Doctor of Philosophy
by
JingJing Zhu
April 2017

# Abstract


## Title: The anti-inflammatory effects of vitamin D receptor agonists on human white preadipocytes

Adipose tissue metaflammation in obesity is characterized by increased infiltration of immune cells and chronically increased gene expression and secretion of pro-inflammatory factors. It is proposed that VDR (vitamin D receptor) agonists could antagonize inflammatory response in adipose tissue. Hence, our study aimed to investigate whether VDR agonists [1α,25$(OH)_2D_3$ and its synthesized analogues ZK15922 and ZK191784] could inhibit inflammatory responses stimulated by THP-1-MacCM (macrophage conditioned medium)/IL-1β in human white preadipocytes.

Preadipocytes were either cultured alone (control), or with (25%) THP-1-MacCM alone, or with IL-1β (0.5 and 2 ng/ml) alone for 24 h. Further groups of cells were pretreated with VDR agonists [1α,25$(OH)_2D_3$ (0.01-10 nM), ZK15922 (10 nM and 1 μM) and ZK191784 (10 nM and 1 μM)] for 24 or 48 h, followed by treatment with (25%) THP-1-MacCM/IL-1β (0.5 and 2 ng/ml) and VDR agonists for a further 24 h before medium and lysate collection. The cell media were collected for measurement of cytokines using arrays and ELISA; the Trizol lysate for qPCR; buffer lysate for western blotting.

The results show that THP-1-MacCM/IL-1β enhanced the gene expression and secretion levels of IL-1β, IL-6, IL-8, MCP-1 and RANTES, whilst the pre- and treatment with VDR agonists significantly inhibited the gene expression and secretion of the major inflammatory factors in THP-1-MacCM/IL-1β-stimulated preadipocytes. Moreover, the combination of pretreatment with VDR agonists [1α,25$(OH)_2D_3$ (0.01-10 nM), ZK159222 (10 nM and 1μM) and ZK191784 (10 nM and 1μM)] and treatment with VDR agonist–MacCM significantly reduced the inflammatory gene expression and secretion from human preadipocytes, compared with THP-1-MacCM-stimulated preadipocytes. Taken together, VDR agonists could exert anti-inflammatory effects on the pro-inflammatory gene expression and secretion in THP-1-MacCM/IL-1β-stimulated preadipocytes.

In addition, VDR agonists significantly reduced the levels of phosphorylated relA of the NF-κB pathway, phosphorylated ERK of the MAPK pathways and phosphorylated eIF-2α of the UPR pathway, whilst increasing methylated relA of the NF-κB pathway and phosphorylated eIF-2α of the UPR pathway in THP-1-MacCM/IL-1β–stimulated preadipocytes. Therefore, it can be speculated that VDR agonists might inhibit metaflammation in adipose tissue by: 1, directly reducing pro-inflammatory gene expression; 2, modulating post-translational relAs and blocking phosphorylated ERK to attenuate pro-inflammatory gene expression; 3, reducing phosphorylated eIF-2α to inhibit the NF-κB pathway; 4, increasing phosphorylated eIF-2α to reduce pro-inflammatory translation.



**Zhu JingJing**

## Acknowledgements

*I hope to see my pilot face to face, when I have crossed the bar.*
*Alfred, Lord Tennyson*

I would like to express my gratitude to my supervisors Professor John Wilding and Dr Chen Bing for the research opportunities and guidance.

I sincerely thank my funder the China Scholarship Council for the tuition and living expenses.

I heartily thank Mr. Leif Hunter, Dr Sheila Ryan, Dr Feng LiangZhu (Soochow University), Mr. Liam Pope, Dr Cherlyn Ding, Miss Jessica Eyre, and Mr. Timothy Sale for the technical support; Mrs. Susan Jones for PGR support; Professor Luminita Paraoan and Professor Rob van't Hof for panel advising; my friends including Dr Yang MingMing, Dr Li DeJian and his family, Dr Li Yuxuan, Miss Wang DongMei, Mrs. Huang LiLi, Miss Huang ChenHong, Miss Zheng Yun, Dr Wang HaiRong, Dr Ma YanJuan, Mr. Pu Fei and Dr Xu JinMin for the emotional support.

I would like to give special thanks to Professor David Tappin (University of Glasgow), Professor Zhu JinXiang and Professor Zhou Yun (Soochow University) for encouraging me to undertake the PhD course in the first place.

Last but not least, I deeply thank my dearest mother for all that I have achieved.

# Table of contents

# Abbreviations

| | |
|---|---|
| AF-1 | activation function-1 |
| AF-NT | unclear factor of activated T cells |
| AMPK | 5’ adenosine monophosphate-activated protein kinase |
| AP | adipocyte-binding protein |
| AP-1 | activator protein-1 |
| APS | ammonium persulfate |
| AT ½ | angiotensin II type ½ |
| ATF-6 | transcription factor-6 |
| Atg | autophagy-related gene |
| Atg | Abelson-related gene |
| ATP | adenosine triphosphate |
| BAT | brown adipose tissue |
| bAT | beige adipose tissue |

| | |
|---|---|
| BCA | bicinchoninic acid |
| BMDMs | bone marrow-derived macrophages |
| BMI | body mass index |
| BMPs | bone morphogenetic proteins |
| BSA | bovine serum albumin |
| C/EBP | CCAAT enhancer binding proteins |
| cAMP | cyclic adenosine monophosphate |
| CBP | CREB binding protein |
| CCL | C-C ligand |
| CCR | C-C chemokine receptor |
| CD | cluster of differentiation |
| cDNA | complementary DNA |
| CHOP | CCAAT-enhancer-binding protein homologous protein |
| CISH | cytokine-inducible Src homology 2 containing protein |
| CNS | central nervous system |
| COX2 | cyclooxygenase 2 |
| CXCL | c-x-c motif ligand |
| CYP | cytochrome P450 |
| Cyt | cytochrome complex |
| DAG | diacylglycerol |
| DBD | DNA binding domain |
| DC | dendritic cells |
| DIO | diet-induced obesity |
| DKK1 | dickkopf1 |
| DRIP | VDR-interacting proteins |
| dSAT | deep subcutaneous adipose tissue |
| EC50 | half maximal effective concentration |
| EGF-R | epidermal growth factor receptor |
| eIF | eukaryotic translation initiation factor |
| ELISA | enzyme-linked immunosorbent assay |
| ER | endoplasmic reticulum |
| ERK | extracellular regulated kinase |
| FABP | fatty acid binding protein |
| FASN | Fatty acid synthase |
| FFA | free fatty acids |
| FGF | fibroblast growth factor |
| GLP-1 | glucagon-like peptide-1 |
| GLUT | glucose transporter |
| GM-CSF | granulocyte-macrophage colony-stimulating factor |
| HFD | high-fat-diet |
| HIF | hypoxia-inducible factor |
| HPLC | high-performance liquid chromatography |
| HRP | horseradish peroxidase |
| HSL-/- | hormone-sensitive lipase-deficient |

| | |
|---|---|
| HSP | heat shock proteins |
| ICAM | intracellular adhesion molecule |
| IFN | interferon |
| IKKβ | inhibitor of κ kinase β |
| IL | interleukin |
| IL-1RI | IL-1 type I receptor |
| IL2C | innate lymphoid type 2 cell |
| iNKT | invariant NNK |
| iNOS | inducible nitric oxide synthase |
| IP3R | inositol 1,4,5-trisphosphate receptor |
| IRE-1 | inositol-requiring enzyme-1 |
| IRF | interferon regulatory factor |
| IRS | insulin receptor substrate |
| IU | international unit |
| JAK/STAT | Janus kinase/signal transducers and activators of transcription |
| JNK | c-jun N-terminal kinase |
| KLF-4 | kruppel-like factor 4 |
| LBD | ligand binding domain |
| LC/MS | liquid chromatography mass spectrometry |
| LC3II | microtubule-associated protein 1A/1B-light chain 3 |
| LPL | lipoprotein lipase |
| LPS | lipopolysaccharide |
| MAC-1 | macrophage antigen 1 |
| MacCM | macrophage conditioned medium |
| MAO | metabolically abnormal obese |
| MAPK | mitogen-activated kinase |
| MCP-1 | monocyte chemoattractant protein-1 |
| M-CSF | macrophage colony-stimulating factor |
| Mfn | mitofusin |
| MGM | the whole THP-1-monocyte growth medium |
| MHC | major histocompatibility complex |
| MHO | metabolically healthy obese |
| MIP | macrophage inflammatory protein |
| miRNA | MicroRNA |
| MM | monocyte medium |
| MOMA | monocyte/macrophage marker antibody |
| MR | mannose receptor |
| MSCs | mesenchymal stem cells |
| mTOR | mammalian target of rapamycin |
| MyD88 | myeloid differentiation primary response gene 88 |
| NcoR | nuclear receptor co-repressor |
| NF | nuclear factor |
| NGF | nerve cell growth factor |
| NK | natural killer |

| | |
|---|---|
| NKT | natural killer T |
| NLRP3 | NLR pyrin domain containing 3 |
| NLRs | NOD-like receptors |
| NOD | nucleotide-binding oligomerization |
| OXPHOS | oxidative phosphorylation |
| P13K | phosphatidylinositol 3-kinase |
| PAI-1 | plasminogen activator inhibitor-1 |
| PAMPs | pathogen-associated molecular patterns |
| pCAF | p300/CBP-associated factor |
| PDGF | platelet-derived growth factor |
| PERK | PKR-like eukaryotic factor 2α kinase |
| PGM | the whole preadipocytes growth medium |
| PHD | prolyl hydroxylase domain |
| PK | Protein kinase |
| Pknox1 | PBX/knotted 1 homeobox 1 |
| PMA | Phorbol12-myristate13-acetate |
| PPARγ | nuclear-receptor peroxisome proliferator-activated receptor |
| PTH | parathyroid hormone |
| qPCR | real-time polymerase chain reaction |
| RANKL | receptor activator of NF-B ligand |
| RANTES | regulated on activation, normal T cell expressed and secreted |
| RICK | receptor-interacting serine/threonine-protein kinase 2, anaserine threonine kinase |
| ROX | reactive oxygen species |
| RSV | respiratory syncytial virus |
| RXR | retinoid X receptor |
| RyR | ryanodine receptor |
| SAT | subcutaneous adipose tissue |
| SCF | stem cell factor |
| SDS-PAGE | sodium dodecyl sulfate–polyacrylamide gel electrophoresis |
| SFRP2 | frizzled-related protein 2 |
| siRNA | small interfering RNA |
| SOCS | suppressor of cytokine signaling |
| SRC | steroid receptor coactivator |
| SREBP1c | sterol regulatory element-binding transcription factor 1c |
| sSAT | superficial subcutaneous adipose tissue |
| STAT | signal transducer and activator of transcription |
| T2D | type 2 diabetes |
| TEMED | tetramethylethylenediamine |
| TG | triglycerides |
| TGF | transforming growth factor |
| Th | T helper |
| TNF | tumor necrosis factor |
| TOF-SIMS | time-of-flight secondary ionmass spectrometry |
| Tregs | regulatory T cells |

| | |
|---|---|
| TRIF | toll-like receptor adaptor molecule 1 |
| TZDs | thiazolidinediones |
| UCP | uncoupling protein |
| UPR | unfolded protein response |
| VAT | visceral adipose tissue |
| VD | $1\alpha,25(OH)_2D_3$ |
| VDR | vitamin D receptor |
| VDREs | vitamin D response elements |
| VEGF | vascular endothelial growth factor |
| WAT | white adipose tissue |
| XBP | x-box binding protein |

# 1. Introduction

## 1.1. Metaflammation

More than 20 years ago, Hotamisligil et al. reported in an elegant series of studies that there is a state of inflammation characterized by increased expression levels of (tumor necrosis factor) TNF-α in adipose tissue of obese mice as well as humans (1). The discoveries were soon followed by a body of research dedicated to understanding the nature of this obesity-induced inflammation and the underlying mechanism of its pathogenesis (2-4).

Investigators now agree that this state of inflammation is distinctive and outside of the paradigm set up for the classical inflammation, which in addition to redness, swelling, heat and pain, is associated with the focused and rapid response to the origin of inflammation (5, 6). Based on the research evidence, Hotamisligil and Gregor summarized the hallmarks of the obesity-induced inflammation and termed it as “metaflammation”, in order to distinguish it from classical inflammation (7).

Studies suggest that it is a metabolically triggered-inflammatory response, characterized by dysfunction and infiltration of immune cells in adipose tissue (7). Though the early research revealed that metaflammation occurred in adipose tissue of humans and mice, the pancreas (8), liver (9), muscle (10) and brain (11) all endure this inflammatory insult (Figure 1.1).

**Figure 1.1** The occurrences of metaflammation onset and progression in some tissues (adipose tissue, muscle), organs (brain, liver), immune system and ecosystem (gut microbiota). Obtained from (12).

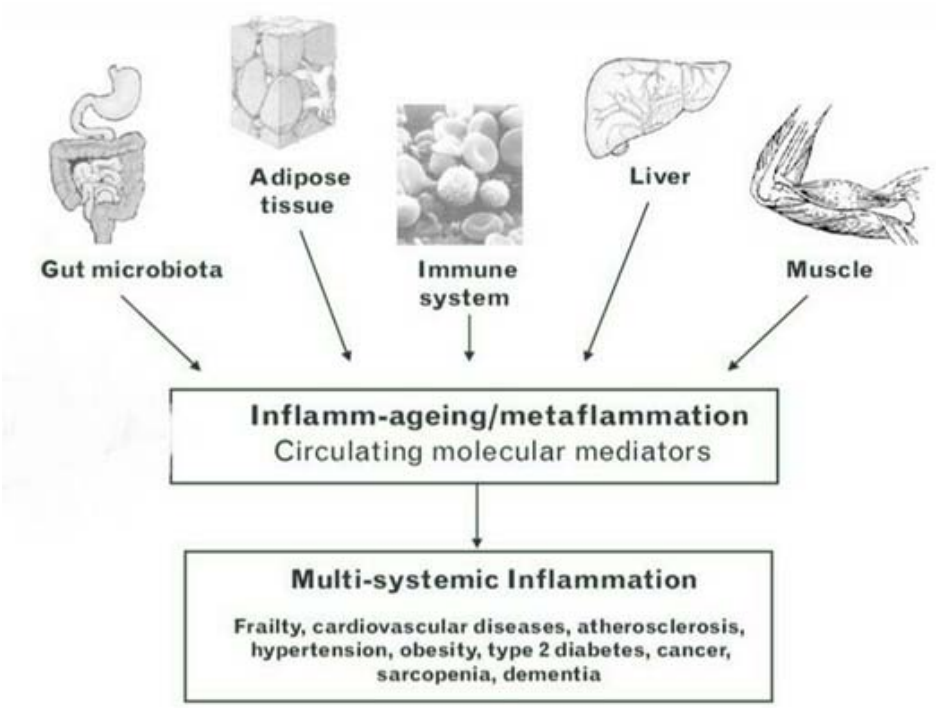


Adipose tissue expansion during the course of obesity is mediated by hypertrophy (enlarged adipocytes) and hyperplasia (increased number of adipocytes) (13). It has been proposed that metaflammation is highly associated with hypertrophic adipocytes, for its adoption of necrotic-like abnormalities, which may lead to disrupted homeostasis in adipose tissue and impaired function (14, 15). Moreover, due to a relative reduction in the vascularity as a result of rapid adipose expansion, adipose hypertrophy induces hypoxia in the local adipose tissue, up-regulating the gene expression levels of pro-inflammatory factors as well as angiogenic factors (16-18). For instance, as a transcription factor activated during the process of hypoxia, (hypoxia-inducible factor) HIF-1α can augment metaflammation in adipose tissue (19).

Another important feature of metaflammation is increased infiltration of immune cells into the afore-mentioned metabolic tissues (Figure 1.2). For example, the proportion of macrophage population is significantly higher in adipose tissue of mice fed a HFD (high-fat-diet) compared with the lean controls (20, 21). The mechanism is not yet fully understood, but it has been demonstrated that isolated bone marrow cells migrate towards the adipose explants from obese animals (22). The role of immune cells played in the pathogenesis of metaflammation will be discussed in details in *Introduction* Page 31-42. .

**Figure 1.2** Immune cell trafficking in obesity. (A) In lean adipose tissue, alternatively activated 'M2' macrophages are resident and their phenotype is maintained by the presence of T-regulatory (Treg) cells, Th2 cells, and eosinophils. (B) As white adipose tissue expands, recruited monocytes polarize to pro-inflammatory M1 macrophages. Moreover, the loss of eosinophils, Tregs and Th2 cells as obesity progresses is accompanied with the infiltration of CD4+ Th1 cells, CD8+ T cells, NK cells, and other granulocytes such as neutrophils and mast cells. Obtained from (23).

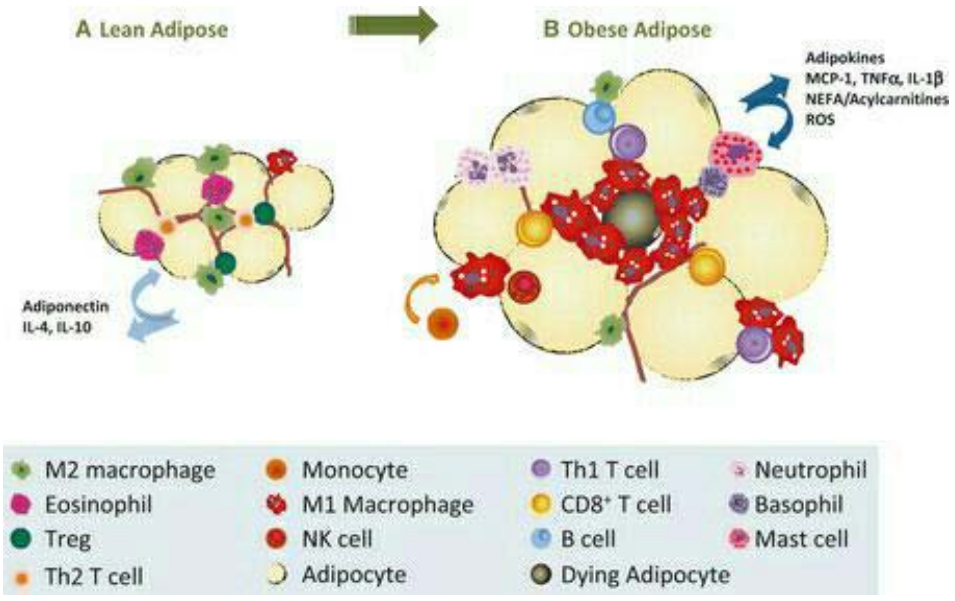


Metaflammation has also been suggested to be characterized by moderate local expression of pro-inflammatory factors in metabolic tissues (7). Since the discovery of TNF-α expression in the

obese adipose tissues of both humans and mice, an array of moderately expressed cytokines have been detected subsequently, such as IL-1β, IL-6 and other pro-inflammatory factors (critical in the induction and maintenance of metaflammation) as well as MCP-1(monocyte attractant protein 1) and other chemoattractants (responsible for the infiltration of immune cells into metabolic tissues) (24, 25). The underlying mechanisms have also been established based on the related investigations (Figure 1.3). For instance, during metaflammation, TNF-α as well as IL-1β activates JNK (c-jun N-terminal kinase), IKKβ (inhibitor of κ kinase β) and their down-stream cascades including the transcription factors AP-1 (activator protein-1) (by JNK) and (nuclear factor) NF-κB (by IKKβ) in the classical receptor-mediated way, thereby up-regulating the gene expression and secretion of pro-inflammatory factors (24). Likewise, JNK/AP-1 and IKKβ/NF-κB can be activated by pattern recognition receptors such as TLRs (toll like receptors) to mediate metaflammation (24). Conversely, the expression of nuclear-receptor (peroxisome proliferator-activated receptor) PPARγ was down-regulated when metaflammation occurred in adipose tissue (26). This may partly explain why the circulating level of adiponectin (a cytokine specifically secreted by adipocytes, essential for maintaining the homeostasis of adipose tissue) was negatively correlated with fat mass. TZDs (thiazolidinediones), which are potent PPARγ agonists, can significantly raise circulating levels of adiponectin when administered to both humans and mice (27, 28).

**Figure 1.3** The integration of metaflammatory signaling occurs at multiple levels, including at the receptor, organelle, kinase pathways, and gene expression. The three most heavily studied examples, PKC, JNK and IKK, can signal a multitude of immune (both innate and adaptive responses, resolution of inflammation) and metabolic responses (glucose, insulin and fatty acid metabolism). Obtained from (29).

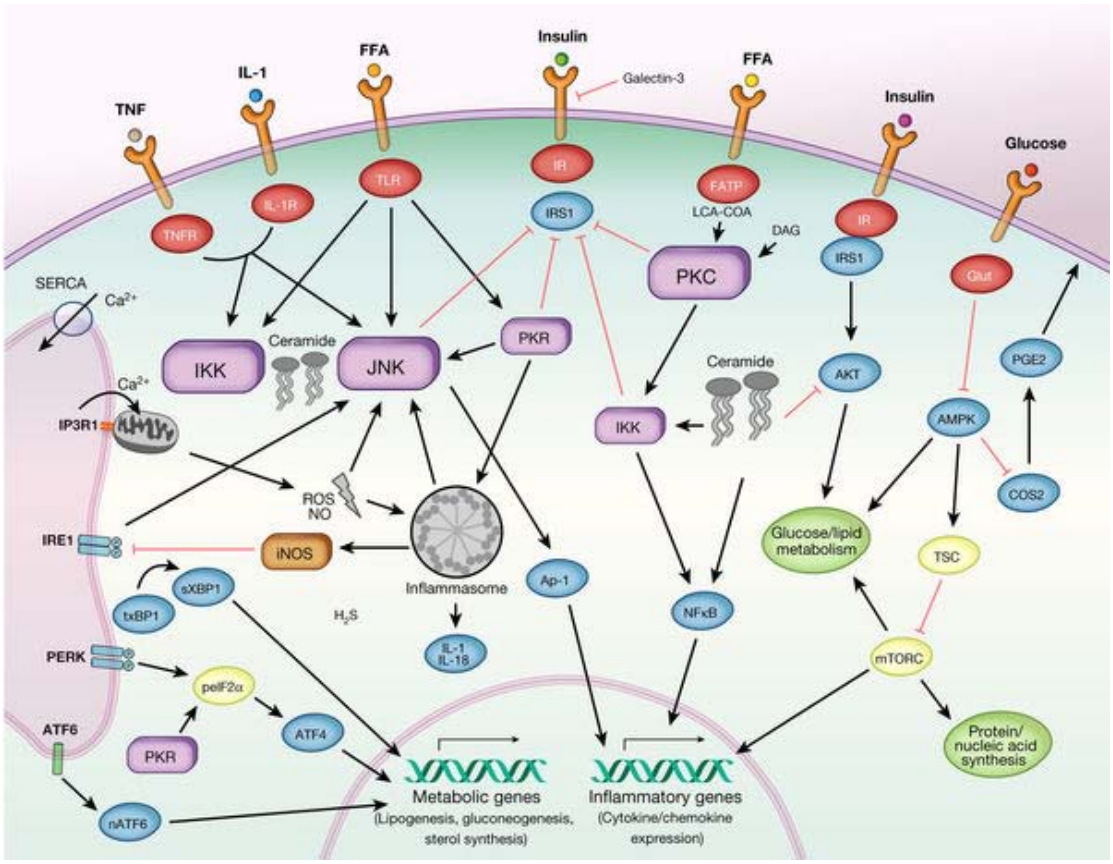


There is evidence that metaflammation is chronically maintained without apparent resolution (7). Metaflammation is characterized by maintenance in a chronic state, by contrast with the acute inflammatory response which is rapidly followed by resolution at the site of the insult. The plausible mechanism is that when induced merely by adipose expansion, metaflammation is not strong enough to stimulate a rapid and full program of resolution (7). Time-course analysis of the onset and progress of metaflammation by examining immune cell infiltration in adipose tissue has thoroughly been investigated in the mice on a HFD; wild-type C57BL/6J mice from the Jackson

Laboratory were on diet containing 10%, 45%, or 60% kcal from fat; from 4-5 weeks of age, and until 16 to 26 weeks. Global transcriptional profiling in these mice showed significantly enhanced gene expression of many macrophage-specific genes, such as MCP-1, MIP-1α (macrophage inflammatory protein) and MAC-1(macrophage antigen 1, CD11b). Moreover, this up-regulation appeared as early as 3 weeks after the initiation of HFD. Thus it was concluded that the expression of pro-inflammatory genes was positively correlated with the duration of fat mass expansion (20). In addition, adipose tissue can secrete IL-8 (a chemokine) which predominantly attracts neutrophils (30). Elgazar-Carmon et al. found that the number of infiltrating neutrophils in visceral fat of mice transiently increased at 3 and 7 days after starting HFD feeding (31). In parallel, the *in vitro* cellular system demonstrated that the interaction between adipose tissue and neutrophils was mediated by forming a protein complex (neutrophil CD 11b: adipocyte ICAM-1, intracellular adhesion molecule 1) (31). These results further reflect the chronicity of metaflammation, since it is in accordance with the characteristic of the progress of the chronic inflammation, which is that the transient infiltration of circulating neutrophils precedes the predominant infiltration of monocytes into the inflamed tissues. In the case of metaflammation, the infiltration largely consists of macrophages, as these tend to predominate in chronic inflammatory states (32).

## 1.2. Metaflammation in obesity

The accumulated evidence suggests that metaflammation is induced by excessive adiposity-obesity.

Obesity is attributed to excessive net energy gain, and characterized by accumulation of body fat. The World Health Organization reported that in 2014 more than 1.9 billion adults, 18 years and older, were overweight (body mass index-BMI is greater than or equal to 25 $kg/m^2$), of these over 600 million were obese (BMI is greater than or equal to 30 $kg/m^2$). More shocking is that 41 million children under the age of 5 were overweight or obese. Without intervention, these numbers are expected to rise in the future (33). An important contributor to the pandemic of obesity is the

so-called obesogenic environment, which is pictured as the modern, computer-dependent, sleep-deprived, physically inactive humans living chronically stressed in a society of food abundance (34). Although mild obesity is associated with some health benefits [i.e. now scarcely needed but apparent protection against starvation in times of food shortage (35), potential protection from osteoporosis and fractures in the elderly, etc (36)], nowadays obesity has become a leading global public health problem and is considered as a risk factor of a variety of diseases, such as T2D (type 2 diabetes), hepatic steatosis, biliary disease, neurodegeneration, cardiovascular diseases, musculoskeletal abnormalities and even some cancers (6). These obesity-associated maladies subsequently lead to reduced life expectancy and premature death. Hence, prevention of obesity-related diseases and treatment of obesity at the individual as well as population level is an important public health priority. Promotion of a life style combining balanced diet, healthy eating habits and moderate physical activity is critical to the treatment of obesity and prevention of its detrimental outcomes. Although weight loss is one approach to obesity management, it is not always effective, and if extreme may damage health. An alternative approach is to support weight loss with treatments that ameliorate the pathological processes that link obesity to disease, such as metaflammation (34). Moreover, weight loss does not significantly lower the risk of the obesity-associated metabolic diseases in a subgroup of obese individuals, who are classified as being MHO (metabolically healthy obese) (37).

MHO individuals are generally characterized as having a BMI greater or equal to 30 $kg/m^2$ but displaying favorable metabolic profiles. The concept of being MHO was initially described in the 1980s (38). Epidemiological evidence suggests that the proportion of MHO individuals may be up to 30% of the obese population (39). Although the existence of this subtype of obesity has been well recognized nowadays, the adequate standards to identify MHO individuals are yet to be established. The common clinical and biological criteria applied to identify MHO individuals include the absence of metabolic disorders (such as metaflammation, dyslipidemia and hypertension, etc) and presence of preserved insulin sensitivity (40). Most studies have used insulin sensitivity to divide obese individuals into being MHO and MAO (metabolically abnormal obese). Insulin sensitivity can be determined by the hyperinsulinemic–euglycemic clamp technique (invasive, expensive and time consuming) (41), the Matsuda index (oral glucose

tolerance test derived index) (42) or the homeostasis model assessment (fasting surrogate index) (43). Kloting et al. (44) reported that compared with MAO, MHO individuals have significantly lower mean omental adipocyte size (528 ± 76 vs. 715 ± 81 pl), a favorable metaflammation profile including lower number of macrophages in omental adipose tissue (4.9 ± 0.8 vs. 13.2 ± 1.4%), circulating CRP (C-reactive protein), progranulin, chemerin and retinol-binding protein-4 (all P values <0.05) and higher serum adiponectin (6.9 ± 3.4 vs. 3.4 ± 1.7 ng/ml, P<0.01). The strongest predictors of being MHO were macrophage infiltration together with circulating adiponectin ($r^2$ = 0.98, P<0.0001). Furthermore, Shin et al. (45) reported that plasma CRP (P<0.001), IL-6 (P<0.05) and oxidized LDL (low density lipoprotein) (P<0.001) were significantly lower in the MHO compared with the MAO individuals. Noteworthy, after a weight loss program for 12-week (the degree of weight loss between the two groups was similar and averaged 3.11% of initial body weight), the levels of CRP (P<0.05) and oxidized LDL (P<0.01) were significantly reduced in the MAO but not in the MHO group. Collectively, a favorable metaflammation profile may predispose, delay or protect obese individuals against obese-induced metabolic diseases. The mechanisms regarding the different metabolic outcomes of being obese still need to be clarified.

Adipose tissue expansion, characterized mainly by adipocyte hypertrophy and hyperplasia or both, is a potential contributor to metaflammation in obesity. Adipocyte hypertrophy as well as hyperplasia is regulated by environmental and genetic factors (13). However, it is still not clear how these two modes of expansion are regulated at the molecular level. The association of adipocyte hypertrophy with dysregulated adipocyte metabolism and increased adipocyte stress raised the hypothesis that adipocyte hypertrophy leads to obesity-associated adipocyte death. It has been subsequently demonstrated (46) that in the obese mice, humans and HSL-/- (hormone-sensitive lipase-deficient) mice (a model of adipocyte hypertrophy without increased adipose mass), the frequency of adipocyte death is positively correlated with hypertrophic adipocyte size, the WAT (white adipose tissue) of HSL-/- mice exhibited a 15-fold increase in necrotic-like adipocyte death and formation of macrophage syncytia, which coincides with the increased gene expression levels of metaflammation indicators including MAC-2 (a potent macrophage chemoattractant that promotes macrophage aggregation and survival at sites of inflammation due to its anti-apoptotic ability) and TNF-α by 7 and 5-fold (P<0.05) respectively in

perirenal WAT. Paradoxically, results generated from a large study of moderately obese, weight-stable individuals (47) showed that, an increased proportion of small adipose cells (hyperplasia) was positively correlated with metaflammation, as demonstrated by increased gene expression levels of IL-6 and MCP-1 ($P<0.05$) in subcutaneous adipose tissue, but the size of mature adipose cells (hypertrophy) was not. Therefore, based on the observed association between hypertrophic adipocyte size/hyperplasic small adipose cells and metaflammation, it is possible that other than adipocyte death, impaired adipogenesis and/or terminal differentiation in obesity is also closely associated with the pathogenesis of metaflammation.

ER stress, oxidative stress and hypoxia induced by adipose tissue expansion are potential triggers of metaflammation in obesity.

ER stress

Protein synthesis as well as folding takes place in the ER (endoplasmic reticulum). As a consequence of adipocyte hypertrophy (induced by excessive intake of energy and nutrients) in obesity, enhanced protein synthesis and insufficient chaperone proteins (helping correctly fold newly synthesized proteins) are thought to trigger ER stress (48). Since many chaperones belong to the family of HSP (heat shock proteins) that protect cells against conditions of chronic and acute stress, by either heat shock treatment or pharmacological means, the up-regulation of Hsp72 can inhibit JNK activation, thereby protecting against obesity-induced insulin resistance in mice (49). Similarly, exogenous chaperone proteins could alleviate ER stress in mouse fibroblasts and improve insulin sensitivity in the adipose tissue of obese and diabetic mice (50). Also, ER stress can be relieved by UPR (unfolded protein response) (Figure 1.4). The accumulation of incorrectly folded proteins in cytosol (the outcome of enhanced protein synthesis and insufficient chaperone proteins) triggers the UPR by activating PERK (PKR-like eukaryotic factor 2α kinase), IRE-1 (inositol-requiring enzyme-1) and ATF-6 (activating transcription factor-6) (48). The activation results in inhibition of protein synthesis, enhanced expression of chaperone proteins and clearance of incorrectly folded proteins, as well as stimulated ER biogenesis (51). However, by activating PERK or IRE-1, the UPR can induce crosstalk with the NF-κB pathway (52, 53). Activation of

IKK releases NF-κB, which in the nucleus acts as a key transcription factor mediating the inflammatory and immune response (54). When the UPR gets out of control, by activation of IRE-1, it leads to adipocyte apoptosis by inducing the crosstalk with JNK (51). JNK, on the other hand, can promote inflammatory gene expression by activation of AP-1 (55). Moreover, ER stress can increase the production of C/EBP (CCAAT enhancer binding proteins) homologous protein, which attenuates synthesis of adiponectin (18), thereby aggravating the inflammation (56).

Furthermore, in addition to protein synthesis, ER in adipocytes also controls lipid droplet formation, FFA (free fatty acids) uptake and synthesis; it has been shown that suppressed lipid-droplet formation in ER stress leads to massive FFA release from adipocytes into the circulation (57).

**Figure 1.4** The UPR is mediated by three proximal ER stress sensors, IRE-1α, PERK and ATF-6 and their respective signaling cascades. IRE-1α dimerization and autophosphorylation activates its kinase and endoribonuclease functions required to generate a potent transcription factor XBP-1s and protein cascade including TRAF-2, ASK-1 and (phosphorylated) JNK. Similarly, PERK dimerizes and autophosphorylates, activating the kinase domain that phosphorylates eIF-2α to abate general mRNA translation. Selective translation of the transcription factor ATF-4 under these conditions regulates the expression of genes involved in metabolism, redox control and nutrient uptake. ATF-6 on the other hand, moves to the Golgi complex to generate an active transcription factor [ATF-6(p50)] that mediates the expression of genes encoding ER chaperones, ER associated degradation components and enzymes involved in ER biogenesis. However, under conditions of irresolvable ER stress, expression levels of the transcription factor CHOP (CCAAT-enhancer-binding protein homologous protein) induced by ATF-4, and Cyt c (cytochrome complex) induced $Ca^{2+}$ and Mfn-2 (mitofusin) can reach a threshold that allows the execution of its pro-apoptotic activity via the regulation of various transcriptional targets. Obtained from (58).

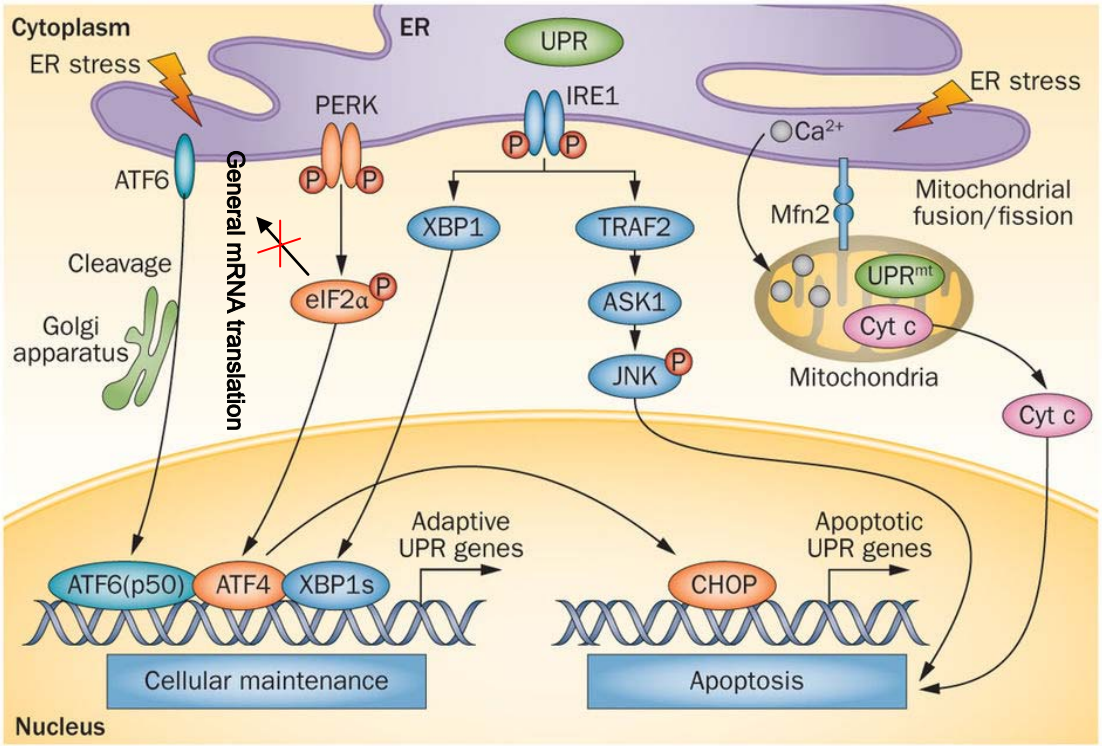

Oxidative stress

Oxidative stress can be taken as an integral part of ER stress and the UPR, because protein folding depends on redox potential (59). Importantly, oxidative stress arises when oxidative damage in cells, caused by ROS (reactive oxygen species, formed by reduction of molecular oxygen or by oxidation of water to yield superoxide radical, hydrogen peroxide and a hydroxyl radical) and exceeds antioxidant activity (54). Obesity induces oxidative stress by excessive formation of ROS, because important sources of oxidants are ER oxidoreductases and various membrane bound (nicotinamide adenine dinucleotide phosphate) NADPH-oxidases (59, 60); adipocytes synthesize and secrete all components of the RAS (renin-angiotensin system) including angiotensinogen, AT1 (angiotensin II type 1) and AT2 (angiotensin II type 2) receptors; the reinforced sympathetic nervous system induces RAS activation in obese adipose tissue (61), and then the local RAS production and activity subsequently leads to NADPH-oxidase activation via AT1 receptors and generation of ROS (62). Moreover, oxidative stress triggers metaflammation in 3T3-L1 adipocytes by activation of (protein kinase) PKB and JAK/STAT (Janus kinase/signal transducers and activators of transcription), thereby inhibiting the secretion of adiponectin and enhancing the expression of pro-inflammatory cytokines IL-6 and PAI-1 (plasminogen activator inhibitor-1) (63). Likewise, oxidative stress could induce metaflammation via activation of IKK (54). In turn, the expressed inflammatory cytokines, such as TNF-α, can further exacerbate oxidative stress by increasing ROS production (64).

Furthermore, by inhibiting FFA β-oxidation, the impaired mitochondrial biogenesis as well as function contributes to accumulated FFA in the cell and elevated FFA in blood, since ROS (mainly generated from mitochondria) severely damage the mitochondria themselves ( i.e. mtDNA, lipids, oxidative enzymes and other proteins). This phenomenon has been observed in adipose tissues as well as skeletal muscle, blood vessels, pancreas, liver and heart (54, 57).

FFA

Accumulated FFA in adipose tissue generated by ER stress (which could occur as a result of

increased FFA oxidation or decreased synthesis) and oxidative stress could stimulate TNF-α secretion from macrophages (65). Furthermore, TNF-α can promote the metabolism of FFA to fatty-acyl-CoA, DAG (diacylglycerol) and ceramides, these in turn activate serine/threonine kinases including MAPK (mitogen-activated kinase) family members [JNK , ERK (extracellular regulated kinase)], IKK, mTOR (mammalian target of rapamycin) and different types of conventional and atypical PKCs in adipose tissue, liver and skeletal muscle, to trigger inflammation and insulin resistance (6, 66). Leptin resistance (known to be associated with reduced appetite-suppressing action on hypothalamic centers to inhibit food intake, also leads to increased ER and oxidative stress and impairment of its peripheral action to promote FFA oxidation, which all contribute to lipotoxicity and metaflammation in obesity (67).

Hypoxia

Hypoxia can be seen as an adaptive response that prevents generation of toxic levels of ROS in oxidative stress (68), and concomitantly enhances proteins involved in the UPR to alleviate ER stress (69). The adipose tissue of obese mice is hypoxic, which was demonstrated by enhanced expression of hypoxia-inducible genes (18). This could partly be explained as the maximum adipocyte size was approximately 180 μm in diameter (70), while the diffusion distance of oxygen is 100 μm (71). Moreover, adipose tissue hypoxia is closely associated with inhibited adiponectin expression and enhanced expression of pro-inflammatory factors in diet-induced obesity in mice (17). An important contributor to metaflammation in obesity was shown to be HIF-1 (72). HIF-1 is a heterodimer consisting of HIF-1β and HIF-1α subunits, and the latter acts as an oxygen sensor. When $O_2$ level is sufficient, HIF-1α is continuously synthesized, but afterwards degrades. The degradation is accomplished through two-step hydroxylation by PHD (prolyl hydroxylase domain) enzymes and von Hippel-Lindau protein. Once combined with von Hippel-Lindau protein, HIF-1α is targeted to the degradation in the proteasome. When $O_2$ level is insufficient, PHD enzymes are inhibited to enable HIF-1α binding to (cyclic adenosine monophosphate) cAMP-binding protein/p300 subunit cofactor, thereby constitutively synthesizing HIF-1β. This renders HIF-1 to function as a transcription factor that up-regulates genes involved in inflammation, cellular stress, angiogenesis and extracellular matrix formation, etc. (69). For instance, the inhibited expression of

adiponectin and enhanced gene expression of angiopoietin-like factor 4, leptin, macrophage migration inhibitory factor, PAI-1, IL-6 and VEGF (vascular endothelial growth factor), were observed in human adipocytes cultured in media with 1% $O_2$, compared 21% $O_2$. In addition, except IL-6, the expression of these genes appeared to be HIF-1 dependent (73).

## 1.3. Adipose tissue in metaflammation

Although adipose tissue is the main site where metaflammation occurs, it is not homogeneous through the body. There are three types of adipose depots existing in the humans that are commonly classified by their color appearance: the white, the brown and the beige adipose tissue. Their specificities are tightly associated with cell composition, localization, pathways for homeostatic control, metabolic responsiveness and endocrine capacities. For instance, WAT stores energy as fat. Conversely, BAT (brown adipose tissue) burns fat to homeostatically maintain body temperature. Moreover, under certain circumstances, bAT (beige adipose tissue) characterized by thermogenic properties similar to BAT, emerges in WAT (74). Therefore, it's not hard to imply that these adipose depots may differentially contribute to or even counteract metabolic disorders (i.e. metaflammation, insulin resistance) induced by obesity.

### 1.3.1. White adipose tissue

The main white adipose depots can be divided into the SAT (subcutaneous adipose tissue) and VAT (visceral adipose tissue), which represent 80% and 20% of total body fat storage respectively (75). In humans, SAT can be anatomically divided by a stromal fascia (fascia superficialis) into superficial (sSAT) and deep subcutaneous adipose tissue (dSAT), whilst VAT can be further divided into perirenal, epididymal or perigonadal, epicardial, retroperitoneal, mesenteric and omental depots. Those adipose depots differ by their localization, venous drainage system as well as by their metabolic activity (75-77).

The distribution of SAT and VAT exhibits person-to-person variations and is dependent upon several factors including age, sex, nutrition and the energy homeostasis of the individual adipose tissue (78). For instance, visceral obesity is referred to as central abdominal obesity, while subcutaneous obesity mainly emphasizes excessive fat accumulation on hips and thighs. Hence the waist-to-hip ratio reflects the relative increase in visceral (waist) versus subcutaneous (hip) adiposity (74).

Though the total adipose tissue is important for the development of obesity associated metabolic disorders, it has been shown that some fat depots are more strongly associated with the risk factors than others, probably due to the existence of intrinsic differences in angiogenic capacity among different fat depots (79). For instance, recent tracing studies in mice revealed that the embryonic and stem cell precursor of preadipocytes differ in fat depots (80). During the course of obesity, progenitor cells (i.e. preadipocytes and adipocytes) from different depots have different potentials of proliferation and differentiation (81), which might determine the different metabolic outcomes of obesity.

Therefore, in the context of obesity or its related mal-metabolism, the differences in human adipose tissues entail caution when choosing which depots to study (82).

Subcutaneous adipose tissue

SAT is less metabolically active than VAT but important for storing TG (triglycerides) in periods of excess energy intake, and supplying the organism with FFAs in periods of fasting, starvation, or exercise. Another suggested role of SAT is playing as a buffer during intake of dietary lipids, thus to protect other tissues against lipotoxicity (83).

SAT has a higher expandability compared with VAT, because it has higher capillary density per adipocyte and angiogenic growth capacity (79, 81). Therefore, the enhanced expandability of storing lipids subcutaneously is realized by stimulation of adipogenesis rather than by hypertrophy in obesity, which might protect against early manifestation of obesity-associated metabolic

diseases. For example, MHO individuals appeared to have a preserved SAT expandability (44). However, the protection is relative and when adipogenesis is impaired, hypertrophic SAT subsequently participates in the pathogenesis of obesity associated metabolic disorders (i.e. insulin resistance and metaflammation), as obese animal models and humans (21, 84).

Though metaflammation is more important in VAT than in SAT (85), in the majority of the studies about obesity and metaflammation in the adipose tissue of humans, the authors analyzed the SCAT but not the VAT, because it is more readily accessible (86, 87). Moreover, Bigornia et al. concluded that by examining visceral and subcutaneous tissues during bariatric surgery, metaflammation in SAT could reflect that in VAT in the context of severe obesity (88). However, whether this is the general case in MAO individuals still remains to be clarified.

Visceral adipose tissue

VAT is a key risk factor to determine obesity associated metabolic complications, when compared with SAT, due to its intrinsic properties regarding, lipolytic activity, angiogenic potential, anatomy (89).

Firstly, it has been observed that the adipocytes of VAT have more mitochondria (the density of which was estimated by mitochondrial and genomic DNA) than those of SAT in rats, which confirms that VAT is metabolically more active, since in principle the metabolic activity of a cell is dependent on its mitochondrial content (90, 91). Moreover, VAT displayed increased lipolytic activity (75, 77) and protein secretion (91), compared with SAT. Similarly, by examining adipose tissues from the obese individuals undergoing bariatric surgery, the relative OXPHOS (oxidative phosphorylation) activity was found to be higher in omental VAT than SAT (92).

Secondly, the expandability of VAT is limited compared with SAT, since the adipogenesis of VAT is relatively restrained and depends largely on adipocyte hypertrophy, which is highly associated with obesity associated metabolic disorders, particularly metaflammation and insulin resistance (76).

Last but not least, the anatomical site of VAT could contribute to an increased cardio-metabolic risk, because VAT drains directly to the liver through the portal vein, the metabolites (i.e. FFA), adipokines as well as pro-inflammatory mediators have a hepatic first reach and pass at high concentration (75, 77, 93).

WAT is composed of mature white adipocytes (accounting for one third to two-thirds of total WAT cells) and a SVF (stromal vascular fraction) enclosing fibroblasts, endothelial cells, immune cells (i.e. macrophages) and preadipocytes (94). White adipocytes store energy as triglycerides. Triglycerides synthesis occurs in periods of positive energy balance. Whilst during energy deprivation, it is cleaved to release FFA and glycerol. Positive energy balance and its accumulated energy storage would eventually lead to excessive adiposity (obesity) (76), which not only induces metaflammation characterized by multi-immune cells infiltration (i.e. macrophages) and secretion of pro-inflammatory factors, but also contributes to a series of metabolic disorders, especially insulin resistance.

Adipocytes

Hypertrophy

Due to its ability to secrete a variety of pro-inflammatory and diabetogenic factors as well as a high capacity of lipolysis, hypertrophied adipocytes contribute to metaflammation and insulin resistance in obesity (95).

It has been shown that the size of human subcutaneous adipocytes was positively correlated with the secretion levels of pro-inflammatory cytokines including leptin, IL-6, IL-8, MCP-1 (96), basal and catecholamine-stimulated lipolysis (97), while negatively correlated with the levels of insulin-sensitivity related adipokines (e.g. adiponectin and IL-10) (44, 96, 98). Moreover, adipocyte hypertrophy is highly associated with loss of insulin sensitivity in both lean and obese conditions (44, 99, 100). Recently, a human adipocyte volume threshold of significantly increased risk for developing T2D has been described (99). Even though the threshold is most likely to be

cohort-specific, due to biological variations and technical differences in adipocyte size measurements, the concept of an adipocyte size threshold for increased T2D risk remains to be tested in different human populations (99), however there is probably a biological limit for adipocyte size of approximately 180 μm, above which there may be an increased risk of ectopic fat accumulation in liver, muscle and pancreas (101).

In addition, toxins may accumulate and induce intracellular stress in hypertrophic adipocytes (102, 103), which may trigger adipocyte apoptosis or autophagy, probably as a protective cellular event. These events may subsequently lead to impaired adipogenesis, adverse fat distribution, and chronically altered metabolic and immune signals from adipose tissue.

Apoptosis

Adipocyte apoptosis may represent an early event in immune cell infiltration and metaflammation by defining macrophage localization and function in adipose tissue (46, 104).

It has been reported that adipocyte apoptosis was increased in mice with DIO (diet-induced obesity) as well as humans (105-107). Increased Fas expression is associated with apoptosis (108) and its expression was found to be higher in isolated adipocytes from obese individuals compared with the lean controls, and in patients with T2D compared with the normal glucose tolerant control (105). Moreover, the activation of Fas in adipocytes, not only enhanced the expression of pro-inflammatory factors, but also interfered with insulin-stimulated glucose uptake and induced basal lipolysis (109, 110). Furthermore, apoptosis was significantly reduced in adipocytes from mice with genetic inactivation of Bid (a key pro-apoptotic molecule) and this also prevented immune cell infiltration of adipose tissue and protected against insulin resistance (107). Likewise, adipocyte specific deletion of the death receptor Fas (CD95), a member of the TNF receptor family, which plays a critical role in promoting apoptosis, significantly improved the insulin sensitivity and reduced hepatic steatosis as well as metaflammation in adipose tissue of mice fed a HFD (111).

Collectively, these data from mouse models suggest that adipocyte apoptosis may initiate macrophage infiltration into adipose tissue and induce insulin resistance in obesity, although this is yet to be confirmed in humans.

Autophagy

As mentioned before, autophagy (the naturally regulated destructive mechanism of the cell disassembling unnecessary or dysfunctional components) (112), has been considered as a cell protection mechanism against various stresses induced by obesity, and thus promotes cell survival. It has been demonstrated that autophagy is important for the regulation of lipid metabolism and pathophysiology of obesity (113, 114). However, the expression of autophagy genes was positively correlated with the degree of obesity, visceral fat distribution as well as adipocyte hypertrophy in both humans and rodent models (114, 115). For instance, it has been found that markers of autophagy, such as (autophagy-related) Atg5, Atg12-Atg5 complex as well as（microtubule-associated protein 1A/1B-light chain 3) LC3II were up-regulated in subcutaneous and (especially) visceral (omental) adipose tissue of obese persons (114). The mass of WAT were significantly reduced in mice with deletion of Atg7 gene, specifically in adipose tissue, compared with the wild type control (116). Moreover, insulin resistance was associated with up-regulation of different autophagy markers (Atg5, Atg7, LC3-II/LC3-1 ratio) in the subcutaneous and visceral (epididymal) adipose tissue of obese Wistar Ottawa Karlsburg W rats (115).

Taken together, it remains controversial whether autophagy may protect against obesity associated adipocyte dysfunction or be a symptom of impaired adipocyte function.

Preadipocytes

Differentiation/Hyperplasia

Adipocyte hyperplasia is realized by adipocyte precursor cells (i.e. preadipocytes) differentiating into adipocytes, which is a process regulated by various transcription factors and hormones.

Several *ex vivo* and *in vivo* studies have identified the types of adipocyte precursor cells (117, 118). In human subcutaneous WAT, adipocyte precursor cells are abundant among (cluster of differentiation) CD31 negative (-) and CD34 positive (+) stromal vascular fractions (117). In mice, the cell surface markers of highly pro-adipogenic precursor cells (subcutaneous and parametrial) include CD45–, CD31–, Ter119–, CD29+, CD34+, Sca-1+ and CD24+ (119). Subsequent studies have demonstrated that when transplanted into A/Zip lipodystrophic mice, these subpopulations of preadipocytes could differentiate into adipocytes and proliferate into fully functional WAT deposits *in vivo*. The transcription factors involved in regulating adipocyte hyperplasia include PPARγ and C/EBP (CCAAT enhancer binding protein) families, which play an important role in regulating the induction and maintenance of adipogenesis (120, 121); extracellular signals, such as BMPs (bone morphogenetic proteins), insulin-like growth factors and WNT, which modulate preadipocyte differentiation (122-124); and SREBP1c (sterol regulatory element-binding transcription factor 1c), which is responsible for enhancing the expression of lipogenic genes (e.g. acetyl-CoA carboxylase, fatty acid synthase and saturated fatty acid dehydrogenase). Moreover, it has been shown that the activation of ADD1 (adipocyte determination and differentiation-dependent factor 1)/SREBP1c could act as endogenous PPARγ ligands (lipid molecules) to initiate adipogenesis (demonstrated by enhanced mRNA expression of FASN and LPL) (125, 126) (Figure 1.5).

Interestingly, as mentioned in *Introduction* Page 7-8, a distinguishing feature of the MHO population is a lower number of infiltrated immune cells and a higher proportion of relatively small adipocytes in adipose tissues (40, 44). There also have been several mouse models showing similar MHO phenotype (127, 128). Moreover, *de novo* small adipocytes and enhanced insulin-dependent glucose uptake were detected in obese *db/db* mice treated with rosiglitazone [a TZD derived anti-diabetic reagent that promotes adipogenesis by binding to PPARγ to enhance the differentiation of preadipocytes (129, 130).

Collectively, although the molecular mechanisms of adipocyte hyperplasia and differentiation in normal and obese conditions remain elusive, these findings suggest that not only could *de novo* preadipocytes differentiating into adipocytes improve insulin sensitivity by providing additional

capacity to store excess energy, but also exert beneficial effects against metabolic complications induced by adipocyte hypertrophy in obesity (13).

**Figure 1.5** Preadipocyte differentiation is accompanied by an increased expression of C/EBPβ, which then induces the expression of PPAR-γ and C/EBPα forming a positive feed-back loop by activating each other's expression. This is followed by the coordinated expression of proteins responsible for establishing the mature adipocyte phenotype. CHOP is a major negative regulator of adipocyte differentiation. It blocks the transactivation of pro-adipogenic C/EBPs. The expression of CHOP is induced by the curcumin-like compound piceatannol. Obtained from (131).

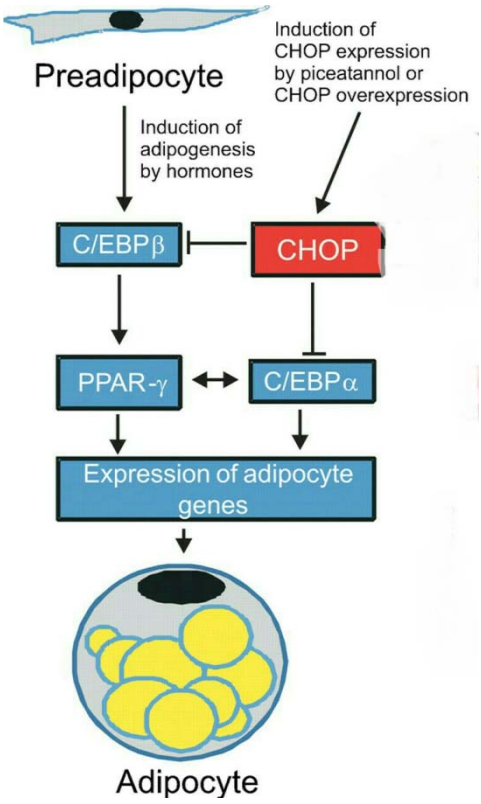


Interaction with macrophages

Several studies have shown that pre/adipocyte and monocyte/macrophage lineages have many

features in common. For instance, in inflammatory conditions, preadipocytes of the 3T3-L1 cell line as well as preadipocytes in primary culture exhibit phagocytic and microbicidal activities similar to that of macrophages (132, 133). Moreover, murine pre/adipocytes secrete numerous pro-inflammatory factors (i.e. IL-6) by LPS (lipopolysaccharide) activation (134). The link between pre/adipocyte and macrophage lineages was further strengthened by the detection of MOMA-2 (monocyte/macrophage marker antibody) antigen expressed on preadipocytes and adipocytes, which is also a marker of monocyte-macrophage lineage (133). Noteworthy, Charriere et al. demonstrated that having been injected into the peritoneal cavity of nude mice, the 3T3-L1 preadipocyte cell line rapidly and massively acquired high phagocytic activity, and 60-70% of preadipocytes expressed five macrophage-specific antigens: F4/80, Mac-1, CD80, CD86 and CD45 (135). In parallel, the *in vitro* experiments showed that cell-to-cell contact between preadipocytes and peritoneal macrophages partially induced this phenotype conversion (135). Therefore, not only preadipocytes and macrophages share some biological behaviors and characteristics, but also preadipocytes have the potential to be very efficiently and rapidly converted into macrophages, under certain situations.

More importantly, macrophages play a key role in influencing the proliferation, survival and differentiation of preadipocytes.

Firstly, even though Maumus et al. (136) reported that MacCM (macrophage conditioned medium) reduced adipose progenitor proliferation in culture, a body of evidence has shown that macrophages promote preadipocyte proliferation (137, 138). The proliferative effect is further supported by enhanced proliferation in situ, which is typically seen in obesity and characterized by increased infiltration of macrophages into human adipose tissue (139).

Secondly, it has been observed that 3T3-L1 preadipocytes undergo apoptosis when deprived of growth factors (serum withdrawal), but MacCM could exert cell protective and survival effects on serum deprived 3T3-L1 mouse preadipocytes. Further molecular studies identified that PDGF (platelet-derived growth factor) released by J774A.1 macrophages is a key component accounting for much of the survival of preadipocytes activity (140). Moreover, signaling as well as inhibitor

studies indicated that macrophage-secreted factors activate the PI3K-Akt and MEK-ERK1/2 pathway to promote the survival of preadipocytes (141). However, LPS-stimulated J774A.1 macrophages lost the suppressing effect on the apoptosis of 3T3-L1 preadipocyte, though PDGF activated signaling pathways are not attenuated, TNF-α expression in macrophages was significantly up-regulated. The pro-apoptotic effect of TNF-α was further shown by the observation that immuno-neutralization of TNF-α in the MacCM could restore its full pro-survival activity (142).

Last but not least, Constant et al. (143) reported that MacCM from mouse or human macrophage cell lines inhibited the differentiation of mouse 3T3-L1 and human preadipocytes. Furthermore, several macrophage-secreted factors also contribute to the anti-differentiating/adipogenic ability of MacCM, particularly IL-1β and Wnt-5a. For example, Lu et al. reported that the anti-adipogenic effect of macrophages (demonstrated by impaired preadipocyte differentiation) was significantly associated with the up-regulated expression of IL-1β, whereas immuno-neutralization of Wnt-5a in the J774-MacCM could antagonize the anti-adipogenic effect on 3T3-L1 preadipocytes (144).

In parallel, the signaling pathways involved in the anti-adipogenesis have also been clarified. For instance, THP-1-MacCM inhibited 3T3-L1 preadipocyte differentiation by acutely activating ERK1/2 phosphorylation. Pharmacological inhibition of the MEK-ERK1/2 pathway with PD98059 could partially block the anti-adipogenic effect (145). Moreover, the anti-adipogenic effect was associated with IKKβ phosphorylation and activation of NF-κB in the context of human THP-1-MacCM and human primary adipose progenitor cells, whereas the IKKβ inhibitor sc-514 could totally abrogate the anti-adipogenic ability of THP-1-MacCM and promote the differentiation of human preadipocytes (146).

Insulin resistance

Insulin is a pleiotropic hormone produced by beta cells of the pancreatic islets. It can stimulate nutrient (e.g. glucose) transport into cells, modify enzymatic activity, and regulate gene expression and energy homeostasis (147, 148). These functions are exerted across a variety of insulin target

tissues (e.g. liver, skeletal muscle and adipose tissue) through several intracellular signaling pathways. In skeletal muscle, insulin promotes glucose uptake by stimulating the translocation of (glucose transporter) GLUT-4 to the plasma membrane. In liver, insulin inhibits the expression of key gluconeogenic enzymes to suppress hepatic glucose production, and promotes glycogen and protein synthesis and accumulation of triglyceride in hepatocytes. In WAT, insulin prevents FFA efflux from adipocytes by down-regulating the activity of hormone sensitive lipase, and stimulating glucose uptake which is subsequently used for synthesis of glycerol for triglyceride formation (149).

Insulin signaling involves insulin receptor-IRS (insulin receptor substrate), which includes four distinct family members, IRS1-4; and its complex downstream signaling cascade. The signaling cascade branches into two main pathways. One is the (phosphatidylinositol 3-kinase) PI3K-Akt (also called PKB) pathway, which is largely responsible for insulin mediated glucose uptake and suppression of gluconeogenesis, the other is the Ras-MAPK pathway which regulates the gene expression, and exerts the crosstalk with the PI3K-Akt pathway to control protein synthesis, cell growth and differentiation (150).

The signaling pathways start from the activation of IRS1 by tyrosine phosphorylation, thereby initiating signal transduction. In obesity, elevated circulating FFA (released mainly by white adipocytes) lead to an increase in intracellular lipid products, including fatty acyl-CoA and ceramide (151-153), which consequently inhibit the insulin signaling cascade by activating a serine/threonine kinase – PKCθ. Moreover, if IRS1 is alternatively phosphorylated on serine 307, its downstream signaling ability is attenuated (154). The serine kinases that phosphorylate serine 307 include IKKβ of the NF-κB pathway and JNK1 of the JNK/AP-1 pathway, both of which can be activated during metaflammation (154). Other inflammation-related negative regulators of IRS proteins include the SOCS (suppressor of cytokine signaling). For instance, SOCS1 and SOCS3 (i.e. induced by macrophage polarization in metaflammation), can promote the ubiquitylation and subsequent degradation of IRS proteins (155). All of these cellular signals triggered by obesity contribute to exacerbated insulin sensitivity/insulin resistance.

As before mentioned, insulin sensitivity is the most important metabolic indicator to divide MAO and MHO, since insulin-resistant/compensatory hyperinsulinemic individuals are at greatly increased risk of being somewhat glucose-intolerant, dyslipidemic and hypertensive (156, 157). Furthermore, glucose intolerance/insulin resistance, dyslipidemia and essential hypertension represent important risk factors for cardiovascular disease. Last but not least, when insulin-resistant individuals cannot secrete the increased amounts of insulin to compensate for the insulin resistance, T2D occurs (157, 158).

Interleukin-1β

IL-1 is a potent endogenous pyrogen and plays an important role in many inflammatory diseases by initiating and potentiating immune and inflammatory responses. It consists of two major proteins, IL-1α and IL-1β. They have similar biological properties by binding to IL-1RI (IL-1 type I receptor), but minimal sequence homology. Moreover, they are fundamentally different in localization, maturation and secretion. IL-1α is secreted as a biologically active form, whereas IL-1β is translated as pro–IL-1β and has no biological activity until it is processed by the cysteine protease caspase-1 in the cytoplasm (159, 160).

Koenen et al. reported that the expression level of activated IL-1β was approximately 10-fold higher in the VAT (visceral adipose tissue), compared with the subcutaneous depot of overweight subjects (161). However, the main source of it is unclear. It has been proposed that infiltrated macrophages secrete high levels of IL-1β during the development of obesity, but adipocytes do express high levels of caspase-1 and are able to produce IL-1β, albeit at lower levels when compared with macrophages (161).

Besides participating in metaflammation, several studies suggest that IL-1β is involved in obesity-associated insulin resistance. Firstly, IL-1β could significantly inhibit the expression of insulin sensitivity genes PPARγ, adiponectin and GLUT-4, thereby attenuating adipocyte differentiation and inducing insulin resistance (162). Secondly, it has been shown that prolonged IL-1β treatment reduced the insulin-induced glucose uptake in murine 3T3-L1 adipocytes, which

was demonstrated by a marked inhibition of GLUT-4 translocation to the plasma membrane in response to insulin (163). Thirdly, IL-1β knockout mice were more insulin-sensitive, compared with the wild type control. The result was in parallel with that IL-1β-knockout protected the mice against HFD-induced metaflammation (164). Finally, it has been further shown that the treatment with IL-1 receptor antagonist anakinra has beneficial effects on patients with T2D (165).

Autophagy is a homeostatic mechanism that degrades large intracellular organelles or protein aggregates to change cellular structure during differentiation or to generate essential nutrients in times of nutrient deprivation (166, 167). It has been shown that adipose tissue of obese human individuals exhibited higher autophagic activity compared with the lean controls (114, 168). Hence, Tack et al. proposed that the pro-inflammatory factors, particularly IL-1β, released during metaflammation are highly associated with increased autophagy (169), and autophagy reciprocally functions to control the expression of IL-1β in adipose tissue, thereby alleviating metaflammation in obesity (170).

Interleukin-6

IL-6 is considered as an adipokine, since adipose tissue secretes one third of circulating IL-6 in healthy individuals. In the WAT only a fraction of IL-6 is produced by adipocytes, with the majority originating from macrophages (21). Importantly, IL-6 is a multifaceted, pleiotropic cytokine and plays a central role in the development of obesity-induced metabolic disorders (i.e. metaflammation, insulin resistance) (171). Hence, understanding and clarifying its role in the regulation of metabolism is of utmost importance.

Like leptin, it has been proved that the levels of circulating IL-6 are positively correlated with the percentage of body fat (172). Mice with a genetic deletion of IL-6 also developed adult-onset obesity, which suggests that IL-6 is involved in the chronic physiologic regulation of energy balance and decreased IL-6 signaling is highly associated with weight gain (173). Furthermore, Plata-Salaman reported that IL-6 is a powerful catabolic reagent that decreases food intake and increases energy expenditure in the CNS (central nervous system) (174). In conclusion, IL-6

secreted by adipose tissue contributes to energy homeostasis in the CNS in an endocrine manner, while inhibiting the secretion could potentially worsen obesity by negative feedback to hypothalamic areas that govern energy balance.

Moreover, IL-6 is a likely mediator of pro-inflammatory signaling in adipose tissue. Firstly, the plasma level of IL-6 is almost exclusively determined by whole-body adiposity, therefore it is not difficult to suggest that IL-6 is closely associated with obesity induced mal-metabolism, particularly metaflammation (175). Secondly, IL-6 action targeting endothelial cells and vascular smooth muscle cells leads to the increased expression of adhesion molecules and activation of local renin-angiotensin pathways, which may contribute to vascular wall inflammation and damage (175). Finally, IL-6 governs the production of CRP from human hepatocytes (176), and CRP is one of the strongest indicators of metabolic risk and may participate directly in inducing atherosclerotic lesions and cardiac events (177).

However, the role regarding IL-6 played in the pathogenesis of obesity and associated metabolic disorders are still controversial and unresolved. As mentioned previously, IL-6 is a potent catabolic agent that stimulates lipolysis, and increases FFA levels and whole body fat oxidation (178). It also inhibits the secretion of other adipokines, notably adiponectin as well as other markers of adipocyte differentiation in human adipocytes (179). Moreover, IL-6 could induce insulin secretion via enhancing the expression of GLP-1 (glucagon-like peptide-1) in pancreatic cells (180). All of these cellular events triggered by IL-6 may contribute to insulin resistance. Therefore, it is not surprising to have found that patients with obesity-related insulin resistance had significantly higher levels of IL-6, compared with the lean controls (181). In addition, IL-6 may enhance mesenchymal stem cell proliferation, thus to maintain the cells in an undifferentiated state and inhibit adipogenesis (182). Paradoxically, IL-6 has been demonstrated to increase glucose uptake in rat skeletal muscle, thereby promoting myogenesis and AMPK (5’ adenosine monophosphate-activated protein kinase)-mediated fatty acid oxidation during exercise (183). Taken together, IL-6 appears to function in a tissue and metabolic state-dependent manner (184).

Monocyte chemoattractant protein-1

MCP-1 secreted by hypertrophic adipocytes is thought to be responsible for macrophage infiltration in obese WAT. Kim et al. reported that MCP-1 secretion is significantly enhanced locally and in plasma of obese rodents and humans (185).

It has been long considered that the interaction of MCP-1 with its receptor [(C-C chemokine receptor) CCR-2] is pivotal for the recruitment of macrophages and pathogenesis of insulin resistance in obesity. Several groups have revealed that not only mice with CCR-2- or MCP-1-deficiency mice exhibit reduced number of infiltrated macrophages and attenuated metaflammation in the WAT, but also were protected against HFD-induced insulin resistance (185, 186). Moreover, adipose tissue-specific over-expression of MCP-1 was sufficient to increase the number of macrophages and induce insulin resistance in WAT of mice (187); *db/db* mice treated with a pharmacological antagonist of CCR-2 displayed decreased macrophage infiltration and improved insulin sensitivity in the WAT, as well as a decrease in body weight (188).

However, recently the role of MCP-1 in promoting macrophage recruitment and insulin resistance in adipose tissue has been challenged. For instance, MCP-1-deficient mice didn't exhibit reduced macrophage infiltration or improved metabolism (189, 190). Moreover, although Ccr-$2^{-/-}$ obese mice had fewer infiltrated macrophages in their WAT than that of the Ccr-$2^{+/+}$ obese mice, the number of macrophages in WAT or the level of insulin sensitivity of the CCR-2 deficient obese mice wasn't normalized to that of Ccr-$2^{-/-}$ lean control (186). These findings suggest that macrophage recruitment and insulin resistance in WAT are also regulated by MCP-1/CCR-2 independent signaling pathways.

C-C chemokine receptor type 5

CCR-5 is a G protein–coupled receptor functioning as a chemokine receptor in the C-C chemokine group. The cognate ligands of CCR-5 include (C-C ligand) CCL-3 (MIP-1α), CCL-4 (MIP-1β), CCL-3L1 and CCL-5 (RANTES, regulated on activation, normal T cell expressed and secreted) (191, 192). Kitade et al. identified and characterized a critical role for CCR-5 in the regulation of obesity-induced inflammatory response and insulin resistance in WAT (193). Firstly, the

expression of CCR-5 and its ligands including CCL-3, CCL-4, CCL-5, were significantly enhanced in the WAT of genetically (*ob/ob*) and HFD-induced obese mice, whereas CCR-5−/−mice were protected against HFD-induced insulin-resistance (characterized by hyperinsulinemia and glucose intolerance) by reducing macrophage accumulation in WAT. Secondly, the macrophage infiltration and crown-like structure formation were markedly reduced in obese WAT of CCR-5−/− mice, despite there being no significant difference in adipocyte size between the CCR-5−/− and the wild type control. Finally, CCR-5 deficiency led to the polarization of anti-inflammatory M2 macrophages in WAT, which suggests that interventions to reduce CCR-5 levels or an antagonist might have a beneficial therapeutic role to reduce adipose tissue inflammation in obesity. In addition, recent studies have also shown that the expression level of CCR-5 was positively correlated with the number of infiltrated macrophages in the WAT of morbidly obese individuals (194). Taken together, reducing CCR-5 activity may be a promising therapeutic target to attenuate metaflammation and improve insulin sensitivity in obesity.

### 1.3.2. Brown adipose tissue

BAT is composed of adipocytes containing numerous mitochondria, which contain iron, thus giving the darker color to BAT. In the presence of UCP-1 (uncoupling protein-1) which is specifically found in the mitochondria of BAT and bAT, energy from mitochondrial oxidation is dissipated as heat rather than coupled to ATP (adenosine triphosphate) synthesis. Contrary to the prevailing concept that BAT is only present in human neonates and young children, adults do have functional BAT and its activity is systematically reduced in obese individuals (195).

Due to its apparent thermogenic properties by depot enlargement via hypertrophic and hyperplasic processes (196), in the past BAT was mainly considered as a heat producing tissue to maintain the body temperature in human newborns upon cold exposure (197, 198). However, Rothwell et al. revealed that the activation of BAT upon overeating (‘diet-induced thermogenesis’) limited weight gain in rats (198). Furthermore, mice fed on HFD intermittently exposed to cold temperature, were not only protected against body weight gain, but also exhibited improved glucose homeostasis

(199), though the latter change was transient and subsequently counterbalanced by feeding a continuous HFD. Hence, a new concept has emerged based on these facts: it may be possible to treat obesity by activation of fat burning in BAT.

In addition, brown adipocytes express numerous factors, which have been demonstrated to act locally in an autocrine or paracrine manner, thereby modulating BAT metabolism. For instance, even though mainly produced by liver, activated BAT secretes FGF-21 (fibroblast growth factor) into the circulation (200), which is recognized as a protective factor against weight gain by increasing energy expenditure, and insulin resistance by promoting glucose utilization in many organs (201). Moreover, through a BAT transplantation study, Stanford et al. proposed that IL-6 production in brown adipose tissue could participate in preserving insulin sensitivity in endogenous BAT, WAT and heart muscle, which might protect against metabolic complications associated with obesity (202).

### 1.3.3. Beige adipose tissue

bAT is enclosed by WAT and composed of adipocytes with thermogenic properties. As with brown adipocytes, beige adipocytes have numerous mitochondria and high expression levels of UCP-1. However, unlike BAT expressing UCP-1 in the basal state, bAT only express it in response to specific activation (e.g. chronic cold exposure, agonists of the b-adrenergic receptor or PPARγ) (197). It has been described by Barbatelli et al. that bAT abundantly developed in the inguinal WAT of rodents in response to chronic cold exposure (203). Noteworthy, the switch from white to beige adipocytes is reversible. For example, in 5 weeks of warm adaptation, beige adipocytes will lose their UCP-1 activity and reverse to white adipocyte like cells without thermogenic properties (204). Similarly, it has been demonstrated that HFD over a long period of time could stimulate potent beige adipocyte precursors to differentiate into white adipocytes in mice (205). Whether this conversion from WAT to bAT to BAT (and the reverse) occurs within mature adipocytes or is a result of development of new adipocytes from preadipocytes, thus altering the ratio of cell types within adipose tissue is uncertain.

Even though global consequences of WAT transforming to bAT on adipose metabolism and insulin sensitivity are yet to be revealed, it can be anticipated that bAT may play a protective role by dissipating energy.

## 1.4. Immune cells in metaflammation

Adipose tissue can be isolated into an adipocyte fraction and a SVF by enzymatic digestion. The SVF is composed of innate and adaptive immune cells, preadipocytes, endothelial cells etc. In obese subjects, adipose tissue accounts for up to 50% of total body mass. Moreover, the studies of different adipose depots also have revealed that immune cells represent approximately two thirds of the SVF, which contains approximately 2 to 5 million cells/g of tissue (206). Among these immune cells, infiltrated macrophages (the hallmark of metaflammation) can make up to 75% of the whole immune population in the SVF (207). Therefore, the immune cells, especially macrophages in SVF, play a major role in the maintenance of metaflammation.

### 1.4.1. Neutrophils

Neutrophils present fundamental mechanisms of effector cells (e.g., complement activation, regulation of inflammation), participating in initiation of immune response as well as resolution of inflammation. It has been reported that low circulating adiponectin could induce the activity and increase the number of neutrophils in the peripheral blood of obese subjects (208). Moreover, a recent study revealed that a rapid increase in neutrophil number, lasting up to 90 days, and an increased expression of neutrophil elastase in parallel, occurs in the adipose tissue of DIO mice (31). Though the immediate trigger regarding the neutrophil infiltration into the adipose tissue following DIO is unknown, HFD is thought to induce acute stress after a brief surge in adipocyte precursor proliferation and this stress may be involved in recruiting neutrophils into the adipose tissue (209), whereas elastase deficiency or chemical inhibition of elastase alleviated the

metaflammation in mice upon 12 weeks of HFD feeding, compared with the wild type control. The plausible mechanism is that elastase seemed to promote macrophage infiltration and M1 polarization, since M2 macrophages were prevalent in obese mice that lacked this enzyme (210).

### 1.4.2. Eosinophils

Eosinophils play a critical role in local macrophage activity and polarization, they are the major IL-4-expressing cells in adipose tissue and activation of anti-inflammatory M2 macrophages is mainly driven by IL-4 (211). It has been shown that the M2 macrophage number was significantly decreased, when eosinophils were absent in adipose tissue (211).

### 1.4.3. Mast cells

Mast cells are important sensors of acute inflammation and play an important part in allergic reactions (212). They grow and proliferate in response to growth factors, such as SCF (stem cell factor), NGF (nerve cell growth factor) as well as cytokines (IL-3, IL-4, IL-9 and IL-10), and respond to microenvironment by releasing preformed contents of granules (histamine, heparin, tryptase and chymase) or *de novo* synthesis of pro-inflammatory cytokines such as IL-6, IL-8 and TNF-α. It has been demonstrated that mast cells accumulate in adipose tissue of DIO mice (213-215). Similarly, obese diabetic *db/db* mice were found to have a higher number of mast cells in adipose tissue (213). Furthermore, the development of obesity in diabetic *db/db* mice was associated with recruitment of largely immature mast cells from bone marrow into adipose tissue, whose maturation was in parallel with the metabolic abnormalities, whereas mast cell KitW-sh/W-sh deficient mice (lacking only mature mast cells) are resistant to diet-induced obesity (213), and the analysis of the VAT revealed the significantly reduced expression of pro-inflammatory factors and decreased number of macrophages (215), which suggests that the arrival of mast cell in adipose tissue precedes the infiltration of macrophages in the development of metaflammation.

In addition, in spite of the similar morphology of mast cells in both of the lean and obese subjects, the latter group has an increased rate of degranulation, whilst pharmacological inhibition of mast cell degranulation reproduced the metabolic phenotype seen in KitW-sh/W-sh-deficient mice (resistant to obesity and metaflammation) (216). Likewise, anti-fibrotic compounds such as angiotensin-converting enzyme inhibitors, silymarin, coupled with dietary intervention, could prevent mast cell maturation and degranulation, thus to reduce obesity associated metabolic disorders especially metaflammation (217).

### 1.4.4. Dendritic cells

DCs can be found in almost all tissues and are a heterogeneous group of mononuclear cells capable of acquiring, processing and presenting antigens to naïve T cells. Based on their phenotype and functional characteristics, they are divided into the following: conventional/myeloid DCs (CD11+), plasmacytoid DCs (CD11c−CD303+) and inflammatory DCs (inf-DCs), which are generated from in situ activation of monocytes recruited into the site of inflammation (218). Bertola et al. (219) revealed for the first time the accumulation of specific inf-DCs CD11chighF4/80low in adipose tissue of obese mice and CD11c+CD1c+ in adipose tissue of obese patients. The accumulation of these DCs was positively correlated with BMI and induced pro-inflammatory (T helper) Th17 cell responses as well as macrophage accumulation in obesity. It has been further demonstrated that adipose tissue DCs are among the early arrival of immune cells to maintain metaflammation induced by adipocyte expansion (220). In turn, by recruiting and activating other immune cells especially macrophages, the DCs could augment the inflammatory response in adipose tissue (220).

In parallel with these studies, it has been shown that in response to HFD, DCs (CD11+) expressed significantly higher levels of CCL-20 (a ligand of CCR-6) as well as IL-6, (transforming growth factor) TGF-β and IL-23 in adipose tissue, compared with the lean mice controls. Importantly, these cytokines are essential for Th17 cell proliferation and differentiation, thus to maintain and aggravate metaflammation (221). By contrast, the mice lacking DCs had a decreased number of

macrophages in the adipose tissue, whereas DC replacement in DC−/−mice can reverse this phenomenon (221). Similarly, the lean wild-type mice that received bone marrow-derived DCs exhibited macrophage infiltration in the adipose tissue, while the mice lacking DCs were resistant to the DOI induced weight gain and its subsequent metabolic disorders (220).

### 1.4.5. Natural killer cells and natural killer T cells

NK cells are a type of cytotoxic lymphocyte and function in the innate immune system analogous to cytotoxic T cells in the adaptive immune system. Compared with that of neutrophils, the increase in the numbers of NK cells appears to be delayed, occurring in weeks, rather than days after the initiation of HFD feeding in mouse adipose tissue (210). In contrast from neutrophils that are primarily of peripheral origin (210), NK cells increased partially or completely by proliferation of tissue-resident populations in adipose tissue. For instance, when the mice on HFD were intravenously injected with the labeled NK cells, only a small number of NK cells reach the adipose tissues from the periphery (migration), but BrdU labeling, as a marker of proliferation, was significantly increased in resident NK cells of adipose tissue, but not in splenic NK cells of peripheral origin (222).

It is now known that NKT cells can bridge innate and adaptive immune responses (223). There are three types of NKT cells: iNKT (invariant NNK), non-iNKT (non-invariant NKT) and NKT-like cells. iNKT and non-iNKT cells are both CD1d dependent (224). It has been shown that the NKT cell population and CD1d expression were significantly higher in adipose tissue of obese mice as well as that of humans, compared with the lean controls (225). For example, the iNKT and non-iNKT cell-deficient CD1d−/−mice gained little weight on HFD and displayed less metaflammation in the liver, compared with the wild type mice on the same diet (226). Paradoxically, the iNKT cell-deficient Jα18−/−mouse model on HFD became more obese and exhibited enhanced metaflammation in the adipose tissue since the early stage of DIO (225). Taken together, these data suggest NKTs especially iNTKs and non-iNTKs, play an ambiguous but important role in sustaining metaflammation in adipose tissue.

### 1.4.6. T cells

Adaptive immune cells including B and T lymphocytes can activate innate immunity induced-inflammatory response (227), whereas regulatory T cells (Tregs) can suppress metaflammation in the adipose tissue of obese mice (228).

For instance, Poutahidis et al. (229) found an association between western diet-associated obesity and CD4+ Th17 prevalent T cell phenotype in human subjects and mouse models. Similarly both CD4+ and CD8+ T cells have been found in the adipose tissue, and their number was positively correlated with BMI in obesity (230). Furthermore, adoptive transfer of CD8+ cells to CD8-deficient mice could induce M1 macrophage polarization and exacerbate metaflammation in adipose tissue (227). By contrast, the depletion of CD8+ cells or T cell receptor−/−in the obese mice was accompanied by a decreased number of macrophages in the adipose tissue and lowered expression of TNF-α and IL-6 (231). In addition, a novel subset of Tregs, Th22 has been shown to be associated with metaflammation induced by obesity. The proportion of circulating Th22 cells significantly increased in parallel with serum IL-22 level in the obese patients, when compared with lean subjects (232).

Paradoxically, Tregs could maintain tolerance/anti-inflammatory microenvironment by inducing IL-10 production. Yu et al. reported that the Tregs were abundant in VAT of the lean mice, whereas the number was significantly decreased in the DIO mice (228). Similarly, a reduced number of Foxp3+ Treg cells was found in VAT of obese humans (233). Moreover, Priceman et al. reported that the activity of STAT3 (signal transducer and activator of transcription) increased in parallel with the expression of IL-6 (a known inhibitor of Treg function) in adipose tissue of the obese mice, while the ablation of STAT3 could alleviate metaflammation and increase the ratio of Treg/Th1 cells as well as the number of anti-inflammatory M2 macrophages (234). Equally, by inducing Foxp3+Tregs and IL-10, the display of the profile of previously-mentioned proinflammatory immune cells could be prevented (229).

### 1.4.7. Macrophages

Diversity and plasticity are the hallmarks of macrophages. The phenotypes of activated-macrophages include classical M1 and alternative M2. The M1 phenotype is stimulated by microbial products (i.e. LPS, TLR ligand) or pro-inflammatory cytokines [(interferon) IFN-γ, TNF)] (235). M1 macrophages produce many pro-inflammatory cytokines including TNF-α, IL-1, IL-6, IL-12, Type I IFN, CXCL1-3, CXCL-5 and CXCL8-10, etc (236). In contrast, the M2 phenotype is observed "resting" in healing-type circumstances without infection and such resting and healing can be further amplified by IL-4, IL-10, or IL-13 (237). M2 macrophages produce anti-inflammatory cytokine such as IL-10 and very low level of pro-inflammatory cytokines such as IL-12 (238).

Under different pathophysiologic conditions, macrophages acquire distinguished functions by undergoing M1/M2 polarization. The polarization is a highly dynamic process and the phenotype of polarized macrophages can be switched (239, 240). Various inflammatory mediators, signaling molecules, and transcription factors are involved in regulating the process of polarization. Among them, canonical NF-κB and (interferon regulatory factor) IRF/STAT signaling pathways are central players. For example, the activation of IRF/STAT (via STAT1) by IFNs and TLR ligand will skew macrophage function towards the M1 phenotype, while the activation of IRF/STAT (via STAT6) signaling pathways by IL-4 and IL-13 will skew macrophage function toward M2 phenotype (236). The polarization can also be regulated by local microenvironmental conditions, such as hypoxia (241). Various diseases are highly associated with imbalances of the polarization. For instance, switching to M1 macrophages initiates and sustains the chronic inflammation, while skewing towards M2 means the anti-inflammatory resolution under such circumstance (237).

M1 macrophages

NF-κB signaling pathway (Figure 1.6)

In obese mice, macrophages make up to 40% of all cells of the adipose tissue, compared with 10%

of the lean control (21). Serum levels of FFAs, cholesterol and especially, LPS [a cell wall component from Gram-negative bacteria, associated with changes in the gut microbiota (metabolic endotoxemia)] are also elevated in obesity (242). TLR signaling, particularly TLR4 stimulated by LPS and other microbial ligands preferentially switches macrophages to M1 phenotype associated with chronic inflammation. MyD88 (myeloid differentiation primary response gene 88) and TRIF (toll-like receptor adaptor molecule 1) as adaptors mediate the signaling downstream of TLR4 (243). The signaling pathway through the MyD88 adaptor leads to the activation of NF-κB by activating a cascade of kinases, including IRAK4, TRAF6 and most importantly, IKKβ (243). When upstream signals converge at the IKK complex, firstly they activate IKKβ via phosphorylation, and then the activated IKKβ phosphorylates I-κB. Subsequently IκB degrades and releases NF-κB p65/p50 heterodimer from the NF-κB/I-κB complex. The NF-κB p65/p50 heterodimer translocates to the nucleus and binds to the promoters of inflammatory genes (244). As a key transcription factor associated with macrophage M1 activation, NF-κB regulates the expression of a large number of pro-inflammatory genes including TNF-α, IL-1β, COX2 (cyclooxygenase 2), IL-6, IL-12, MCP-1, as well as receptors including CCR-2 and CCR-5, which in turn augment metaflammation by recruiting more monocytes and other leukocytes into (murine) adipose tissue (244). In addition to binding to TLRs, some PAMPs (pathogen-associated molecular patterns, including LPS and other microbial ligands) are also recognized by a family of cytosolic nucleotide-binding receptors and NLRs (NOD-like receptors) (245). As the most well characterized members of the NLR family, (nucleotide-binding oligomerization) NOD1 is ubiquitously expressed and NOD2 is restricted to monocytes, macrophages, DCs (246). Both NOD1 and NOD2 induce the activation of NF-κB in a TLR-independent manner (247). Upon NOD1 or NOD2 stimulation, RICK/RIP2 (receptor-interacting serine/threonine-protein kinase 2, anaserine threonine kinase) undergoes polyubiquitination at K209 to activate IKK via TAK1 (transforming growth factor β-activated kinase 1), which is an essential step of the NOD1/NOD2-mediated activation of NF-κB (by phosphorylation and degradation of IκBs) and MAPKs. However, A20 deubiquitinase could severely decrease the ubiquitination to dampen the signaling activation (248, 249).

**Figure 1.6** IKKβ/NF-κB signals promote M1-type macrophage activation. The activation of the IKK complex (e.g. in response to TLR- or IL-1–mediated signals) leads to phosphorylation of IκB, triggering its proteasomal degradation. IκB degradation frees NF-κB to translocate to the nucleus and drive the expression of pro-inflammatory genes. In addition, the deletion of IKKβ in macrophages increases STAT-1 activation and promotes a shift toward the M1 phenotype. Obtained from (250).

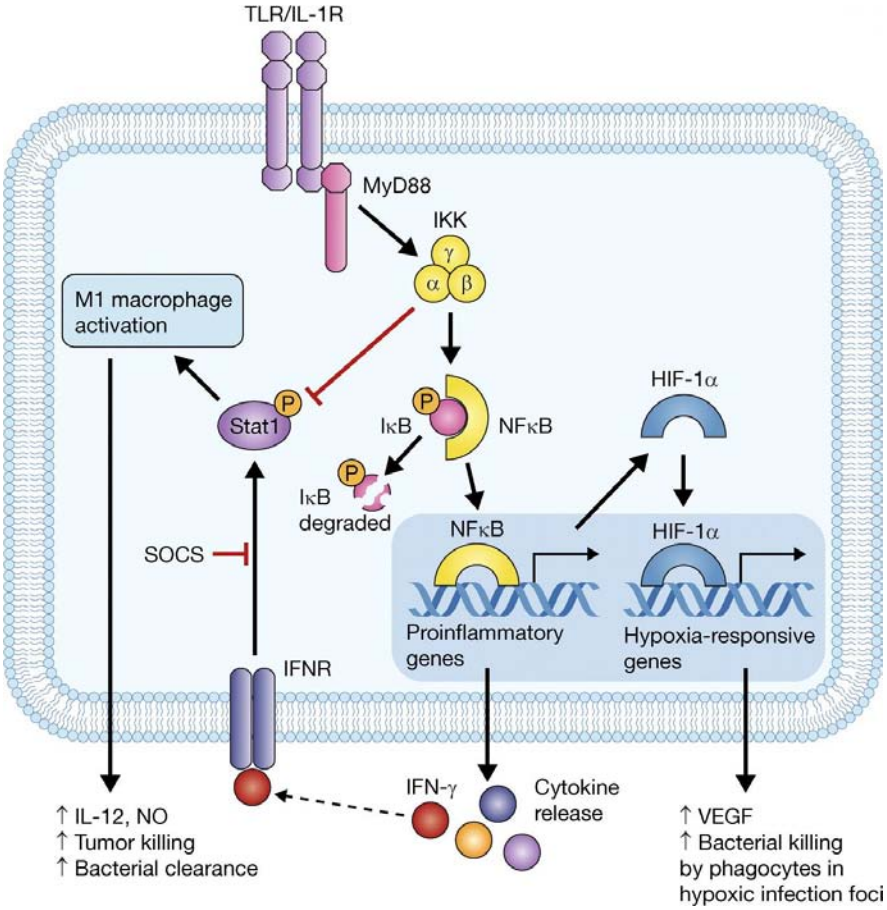


Inflammasome mediated pathways

The NLRs recognition leads to the activation of caspase-1 and subsequent proteolytic conversion of potent pro-inflammatory cytokines IL-1β and IL-18 from their precursors pro-IL-1β and pro-IL-18, respectively (251). This proteolytic conversion is mediated by a cytosolic caspase

1-activating protein complex, which is termed as inflammasome (251). The activation of switching to M1 macrophages is mediated by assembly of the NLR inflammasome and caspase-1 activation, which subsequently leads to the conversion of IL-1β and IL-18 into secreted active forms (252). With the cryptopyrin/NLRP3 (NLR pyrin domain containing 3) inflammasome serving as a sensor of obesity-associated metabolic signals, the progression of obesity can switch macrophages from “M2-like” to “M1-like” cells. For instance, Caspase-1 and IL-1β are both induced in the adipose tissue of DIO mice, whereas Nlrp3- and caspase-1-deficient mice both demonstrate a resistance to the DIO-induced inflammation (253). The mechanism underlying the protective effect may be driven by switch to M2 macrophages, since the nlrp3-knockout mice exhibit decreased M1, but increased M2 gene expression in macrophages of the adipose tissue.

IRF/STAT signaling pathways

As mentioned before, MyD88 and TRIF as downstream adaptors mediate the signaling pathways of M1 macrophages, which are activated by LPS. For instance, the TRIF-mediated signaling pathway activates transcription factor IRF3, which subsequently leads to the expression and secretion of type 1 IFN, such as IFN-α and IFN-β; by binding to the receptor of IFN, the secreted type 1 IFN consequently activate transcription factor STAT1 (243). It has been widely reported that IRF3 and IRF5 are involved in modulating M1 polarization and inducing the expression of M1-associated genes (254, 255), such as chemokine (c-x-c motif ligand) CXCL-9 and CXCL-10 (256), which are characteristic of classical M1 macrophage activation.

MicroRNAs

miRNAs, a class of 19–24 nucleotides non-coding RNAs that induce gene silencing at the post-transcriptional level, have emerged as an important factor in regulating gene expression in many immune cells including monocytes and macrophages (257). Functional miRNAs associated with macrophages have been identified. For instance, miR-155 could be induced in LPS-stimulated M1 macrophages; miR-146 might silence TNF receptor-associated factor 6 and IL-1 receptor-associated kinase 1 genes to attenuate TLR and cytokine signaling (258, 259). These

findings strongly suggest that miRNAs can modulate macrophage polarization in the course of various diseases (260).

Moreover, Zhuang et al. (261) reported that miR-223 modulates metaflammation in obesity via regulating macrophage activation. Though they demonstrated that miR-223 was up-regulated in LPS-stimulated macrophages (M1 like) but down-regulated in IL-4-stimulated mouse BMDMs (bone marrow-derived macrophages) (M2 like), the miR-223-deficient macrophages were hypersensitive to LPS-stimulation, and exhibited a delayed response to IL-4 compared with wild type mouse controls. Likewise, the miR-223-deficient mice exhibited an increased adipose tissue inflammatory response and decreased insulin sensitivity. In addition, Pknox1 (PBX/knotted 1 homeobox 1) as a miR-223 target in partially polarizing M2 to M1 macrophage was validated by gain and loss-of-function analyses in BMDMs.

M2 macrophages

Lymphocytes

The ratio of M1:M2 macrophages is 4:1 in lean adipose tissue (262). Even though M1 and M2 macrophage activities can exist without T or B cell influence (263), specialized or polarized T cells including Th1, Th2 and Tregs do play a role in macrophage polarization (264).

For example, Tregs can induce M2 macrophage differentiation in mice by secretion of IL-10 and TGF-β (265). Moreover, in the lean adipose tissue, Tregs are involved in the regulation of tissue homeostasis and maintenance of M2 macrophage population, whereas obesity is associated with decreased number of Tregs in adipose tissue (228). In addition, the presence of eosinophils and Tregs, which secrete cytokines IL-4/IL-13 and IL-10, respectively, together with adiponectin secreted by adipocytes, polarize macrophages toward an anti-inflammatory phenotype (M2 like) in the adipose tissue. In conclusion, these immune cells and their secretome maintain the positive balance of M2 macrophages in the lean AT (266).

A novel duo in modulating the polarization has also been identified: ILC2s (innate lymphoid type 2 cell) and IL-33. ILC2s are a regulatory subtype of ILCs, which are divided into three distinct populations, ILCs 1, 2 and 3 (267). With respect to the cytokine profile expression, these sub-populations are analogous to CD4+ T helper subsets: Th1, Th2 and Th17, respectively, though ILCs do not have T-cell receptors or specifically respond to antigenic signals (268). IL-33 is constitutively expressed in specialized populations of epithelial and endothelial cells of human as well as mice. Moreover, ST2 (interleukin 1 receptor-like 1, the receptor of IL-33) is highly expressed in ILC2s and Th2 lymphocytes and Tregs. Upon binding to ST2, IL-33 induces the secretion of anti-inflammatory cytokines including IL-5 and IL-13 by ILC2s in the adipose tissue, and the polarization of macrophages to an M2 phenotype (269). Furthermore, Han et al. proved that Tregs expressed higher levels of ST2 in adipose tissue of the lean mice, compared with the obese control, while IL-33 treatment restored the ST2-positive Treg population and alleviated metaflammation in the adipose tissue (270).

IRF/STAT signaling pathways

IL-10 induces the polarization to M2 phenotype by activating STAT3 via receptor (IL-10R). IL-10R is a heterodimer composed of IL-10R1 and IL-10R2 (271). Upon binding to IL-10, IL-10R undergoes autophosphorylation, thereby activating the transcription factor STAT3 to inhibit the expression of pro-inflammatory factors. It has been reported that IL-10 responds to TLR activation in the macrophages. The components in IL-10-induced macrophage transcriptome include TLR1, TLR8, MARCO (macrophage receptor with collagenous structure) and chemoattractants CXCL13 and CXCL4 (271).

In addition to IL-10, IL-4 as well as IL-13 induces the polarization to M2 phenotype by activating STAT6 of IRF/ STAT signaling pathways in the adipose tissue (272). Binding to IL-4 receptor alpha (IL-4Rα), IL-4 and IL-13 activate JAK1 and JAK3 respectively (273), thus to induce STAT6 activation and translocation. For example, during severe (respiratory syncytial virus) RSV-induced bronchiolitis, IL-4Rα/STAT6-dependent polarization to M2 macrophages significantly inhibited the inflammation and protected against the epithelial damage in lungs (274). Transcription factors

involved in the M2 polarization via IL-4 stimulation were demonstrated by transcriptome analysis, include various signaling mediators, such as CISH (cytokine-inducible Src homology 2 containing protein), SOCS1 and transcription factors, such as c-myc and IRF4, KLF-4 (Kruppel-like factor 4) (275). Moreover, besides being directly induced by TLR signaling, SOCS1 can also be up-regulated by IL-4 in concert with TLR, which in turn inhibits the action of STAT1 and STAT3 (276). In macrophages, SOCS proteins regulate the sensitivity of cells toward cytokines and modulate signaling via TLRs by Notch signaling (277).

It is noteworthy that PPARγ together with KLF-4 promote M2 polarization induced by IL-4 or IL-13. For example, mice with myeloid-specific deficiency of either PPARγ or KLF-4 resulted in the suppressed M2 polarization of macrophages (278). Similarly, IL-4 failed to promote the M2 polarization and suppress the secretion of IL-6 in macrophages deficient of PPARγ (279). In addition, other members of the PPAR family, PPARβ/δ, when stimulated by IL-4 and IL-13, also appear to promote the M2 polarization (280).

## 1.5. The vitamin D system

### 1.5.1. **Vitamin D metabolism** (Figure 1.7)

Vitamin D is a pleiotropic steroid hormone. Besides regulation of calcium homeostasis and bone turnover, it has anti-proliferative, pro-differentiation, immuno-modulatory, and anti-inflammatory properties in various cells and tissues in the body (281, 282).

Vitamin D (also known as cholecalciferol), is mainly generated in the skin where one of the rings of the precursor molecule (7-dehydrocholesterol) is broken by ultraviolet B light (sunlight), but can also be ingested from a number of foods, such as egg yolks, red meat and oily fish. Afterwards, to achieve the biologically active form $1\alpha,25(OH)_2D_3$ (calcitriol), vitamin D must first be hydroxylated at the carbon 25 position by 25-hydroxylase, to generate $25(OH)D_3$ (calcifediol) in

the liver. This hydroxylation is accomplished by several cytochrome P450 (CYP) isoforms including mitochondrial CYP27A1, the microsomal CYP2R1 (considered as the high-affinity 25-hydroxylase), CYP3A4 and CYP2J311 (283). $25(OH)D_3$ is the most plentiful and stable metabolite of vitamin D in human serum, the level of which is the best indicator of vitamin D status in body either from subcutaneous synthesis or from diet, as it binds serum vitamin D binding protein as well as other albumin super family members in the blood with high affinity (284). In general, $25(OH)D_3$ is not thought to exert much biologic activity in the body and is further circulated to the proximal tubule of kidneys, where it is hydroxylated at the 1 position to become $1\alpha,25(OH)_2D_3$ (calcitriol), which is the biologically active form of vitamin D (283). Interestingly, many other cells, especially macrophages in all tissues are capable of expressing 1-hydroxylase and synthesizing $1\alpha,25(OH)_2D_3$ locally (285). The hydroxylation is accomplished by the enzyme CYP27B1, the activity of which is essentially enhanced by PTH (parathyroid hormone) (286). Determination of circulating $1\alpha,25(OH)_2D_3$, at the present stage of the clinical knowledge, has very limited clinical utility. For though circulating $1\alpha,25(OH)_2D_3$ is diagnostic for several clinical conditions, including vitamin D-dependent rickets types I and II, hypercalcemia associated with sarcoidosis, tuberculosis, fungal infections, Hodgkin's disease, lymphoma, Wegener's granulomatosis and other clinical conditions involving the vitamin D endocrine system, including hypoparathyroidism, hyperparathyroidism and chronic renal failure [for which the assay of $1,25(OH)_2D_3$ is a confirmatory test], circulating $1\alpha,25(OH)_2D_3$ provides essentially no information with respect to the patient's nutritional vitamin D status (287).

Mediated by vitamin D receptor (VDR), $1\alpha,25(OH)_2D_3$ modulates the genomic or non-genomic response of numerous cells and tissues throughout the body, in an endocrine, autocrine or paracrine manner (285) (Figure 1.8).

**Figure 1.7** Vitamin D sources and metabolism. The recommended reference range for 25(OH)$D_3$ levels is 20-100 ng/ml (50-250 nM). Obtained from (284).

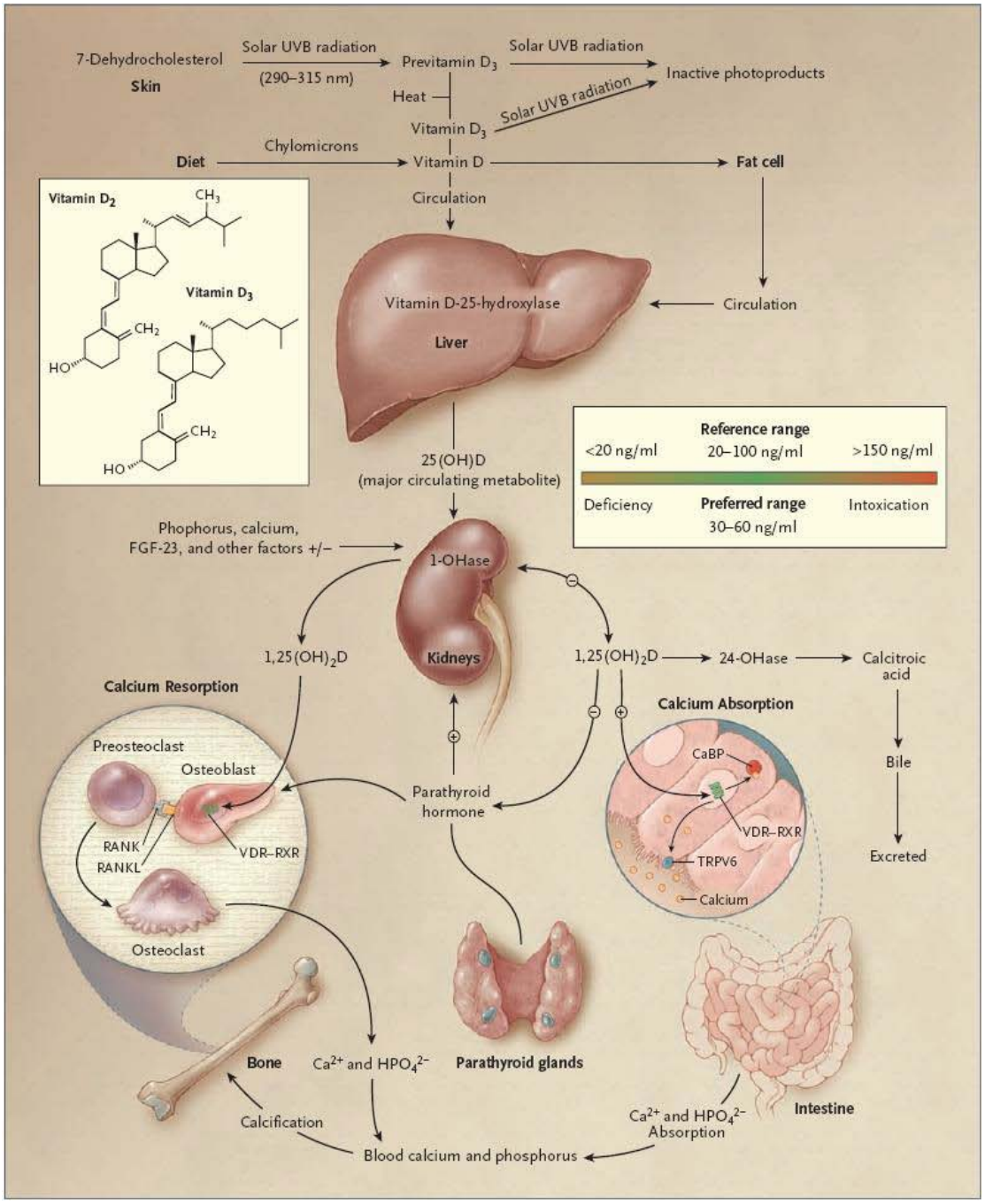

**Figure 1.8** Pathways for generating biological responses by $1,25(OH)_2D_3$. In the genomic pathway (left-hand side), occupancy of the VDR-RXR complex by $1,25(OH)_2D_3$ leads to an up- or down regulation of genes subject to hormone-receptor regulation. In the non-genomic pathway (right-hand side), occupancy of the VDR membrane receptor by $1,25(OH)_2D_3$ can lead to the initiation of rapid responses that are coupled through appropriate second-messenger systems (e.g. $Ca^{+2}$), either directly to the generation of the end biological responses or indirectly through modulation of genomic responses. Obtained from (288).

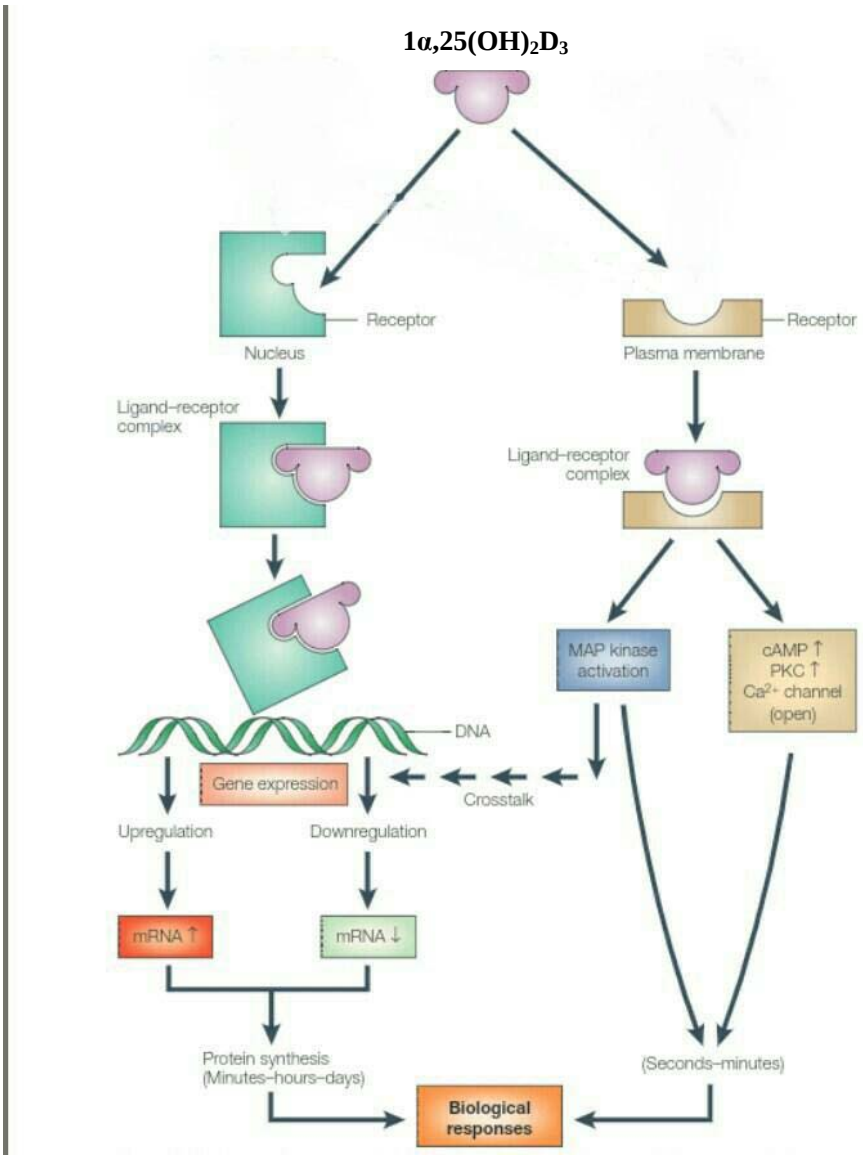

### 1.5.2. Vitamin D receptor

The gene for the VDR is located on chromosome 12 (12q13.11), and there is only one isoform encoded by this gene in humans and other organisms. Though 14 distinct transcripts of VDR (differing in their 5 termini) have been reported to be generated as a result of alternative splicing or differential promoter usage and some of them may be associated with the presence and/or severity of many rheumatic diseases (289), most of the variant transcripts produce the same classical VDR protein, consisting of 427 amino acids (290).

The VDR is a ligand-dependent transcription factor belonging to the super family normally referred to as the steroid/thyroid hormone receptors (291) and can be functionally divided into three regions with well-characterized functions: an $NH_2$-terminal region contains a ligand-independent transactivation function, AF-1 (activation function-1); a central region contains the DBD (DNA binding domain), which is composed of two C2-C2 type zinc fingers and responsible for targeting the VDR to VDREs (vitamin D response elements); and a C-terminal region contains a multi-functional domain consisting of the LBD (ligand binding domain), the RXR (retinoid X receptor) heterodimerization motif and a ligand-dependent transactivation function, AF-2, which is mainly present in cells of the bones, intestines, kidneys and parathyroid gland, and has traditionally been associated with calcemic activities (i.e. calcium and phosphorus homeostasis and maintenance of bone content). The presence of VDR in cells other than those organs has led to the recognition of non-calcemic actions of VDR ligands, such as pro-differentiation, immuno-modulation and anti-inflammation, etc (292). In the absence of ligand and serum in cellular systems, most of the VDR is present in the cytoplasm (293). When a VDR ligand binds to the LBD of VDR, the VDR forms a heterodimer with RXR, which is a nuclear receptor activated by 9-cis retinoic acid (vitamin A) and an obligate partner of VDR in mediating the action of VDR ligands (291). The ensuing conformational change enhances the formation of VDR-RXR heterodimer (294). Meanwhile the VDR ligand induces the translocation of the transcriptional complex (composed of the ligand and heterodimer) into the nucleus (295). Importantly, it has already been shown that only $1\alpha,25(OH)_2D_3$ and its synthesized analogues (VDR agonists) have high affinity of binding upon the VDR (296).

Besides directly inhibiting the expression of some genes by antagonizing the action of certain transcription factors [e.g. nuclear factor NF-AT (unclear factor of activated T cells) and NF-κB (297, 298)], the transcriptional complex can bind to VDREs [present in the promoter regions of vitamin D-responsive genes (299)] and cofactors, thereby positively or negatively regulating the gene transcription. Cofactors (which don't directly bind to DNA) possess the capability of modulating gene expression by acting as a bridge between the transcriptional complex and the basal Pol II transcription machinery. They consist of two functionally distinct families of proteins, namely coactivators and corepressors. Coactivators mediate the induction of transcription (positive regulation), whereas corepressors suppress the gene expression (negative regulation) (Figure 1.9) (292).

Positive regulation

Positive regulation is mediated by SRC (steroid receptor coactivator) and DRIP (VDR-interacting proteins) (300). The SRC family of cofactors includes SRC-1, SRC-2 and SRC-3. These SRC family members along with CBP (CREB binding protein)/p300 and pCAF (p300/CBP-associated factor), are histone acetyltransferases that destabilize the nucleosomal core by catalyzing the acetylation of lysine residues present in the N-terminal tails of histones (301). DRIP is a complex approximately 20 proteins and contains mediator factors that are required for the interaction with basal transcription factors and polymerase II. The transcriptional complex recruits the complete DRIP complex by ligand-mediated interaction with DRIP 205, which is a component of the DRIP complex (302).

The first step of the regulation involves the recruitment of the transcriptional complex-SRC or -histone acetyltransferase activity complex to a responsive promoter of VDREs, thereby facilitating the destabilization of the nucleosomal core to unwind vitamin D responsive genes. And then the transcriptional complex-DRIP complex targets the unwound DNA to promote the transcription (expression) of the genes (292).

Negative regulation

Negative regulation is mediated by three corepressors including (nuclear receptor co-repressor) NcoR-1, NcoR-2 and Hairless (301). The transcriptional complex-corepressor complex recruits histone deacetylase activities and subsequently deacetylates the lysine residues present in the N-terminally located in histone tails, thereby compacting the chromatin to silence of the genes (303).

The vitamin D-responsive genes modulated by the transcriptional complex include osteocalcin, osteopontin and RANKL (receptor activator of NF-κB ligand), which participate in extracellular bone matrix formation and bone remodeling (291); EGF-R (epidermal growth factor receptor), c-myc, K16 and PTH, which are involved in cell proliferation and differentiation (304-306); cytokines including IL-2, IL-12, TNF-α, IFN-γ and GM-CSF (granulocyte-macrophage colony-stimulating factor), which modulate inflammatory response in the tissues (307-310).

In addition, it has been recognized that by binding to VDR on the plasma membrane, $1,25(OH)_2D_3$ can exert non-genomic actions, such as the rapid intestinal absorption and reabsorption of $Ca^{2+}$ (transcaltachia), opening of voltage-gated $Ca^{2+}$ and $Cl^-$ channels in osteoblasts, migration of endothelial cells and secretion of insulin by beta pancreatic cells (288). The signaling molecules involved in these processes include sarcoplasmic reticulum $Ca^{2+}$-ATPase on plasma membranes, phospholipase C and phospholipase A2 (PLA2), PI3K, p21ras and a variety of second messengers ($Ca^{2+}$, cyclic AMP, fatty acids and 3-phosphoinositides such as phosphatidylinositol 3,4,5 triphosphate), accompanied by activation of protein kinases, such as PKA, PKC, MAPKs and $Ca^{2+}$-calmodulin kinase II, etc (311-314).

**Figure 1.9** The positive (by coactivator) and negative (by corepressor) genomic responses mediated by 1α,25(OH)$_2$D$_3$–VDR-RXR complex. Obtained from (315).

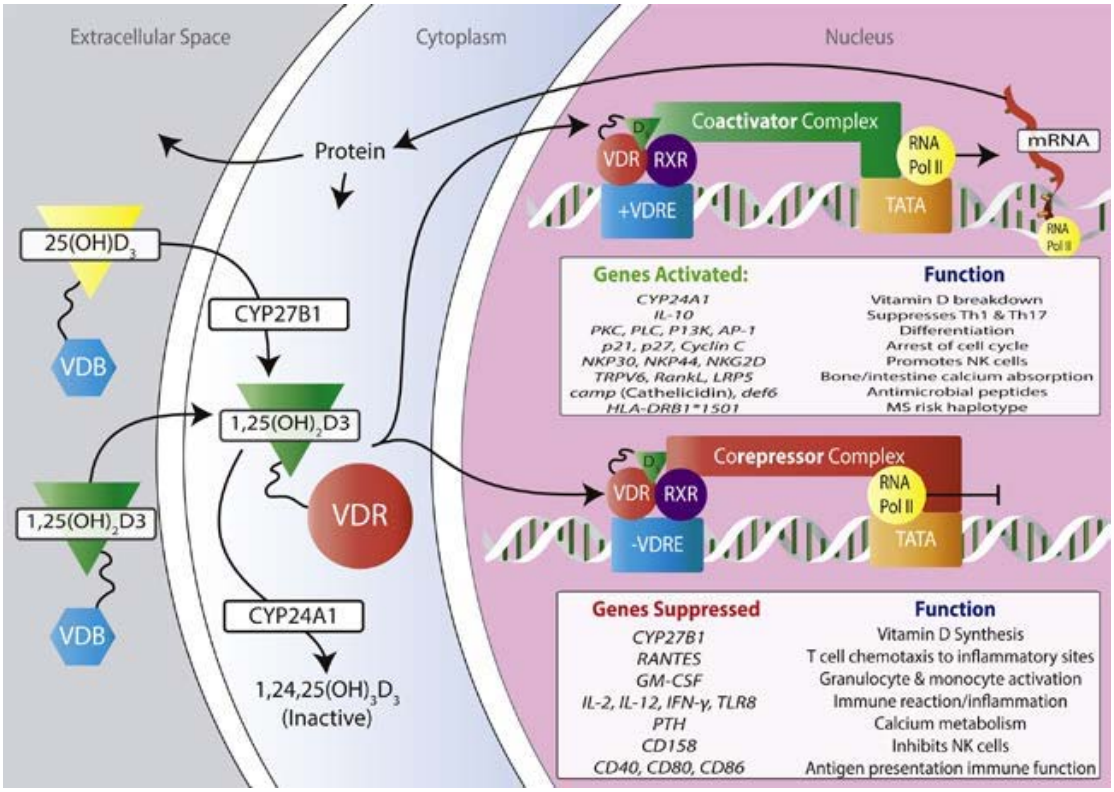


The expression of VDR in a variety of cell lines and primary cells, together with the increased evidence regarding its involvement in the processes of cell proliferation, differentiation, and immuno-regulation, has prompted testing of the therapeutic effect of 1α,25(OH)$_2$D$_3$ and other VDR agonists (e.g. ZK159222 and ZK191784) in several types of autoimmune diseases and cancers. Notably, it has been shown that 1α,25(OH)$_2$D$_3$ has anti-inflammatory properties on different human and mouse cells (292).

However, the immuno-modulatory (i.e. anti-inflammatory) properties of 1α,25(OH)$_2$D$_3$ are mostly achieved only if very high doses are applied, which can provoke hypercalcemia as a side effect. Hence, during recent decades there were many attempts to synthesize other VDR agonists [1α,25(OH)$_2$D$_3$ analogues] with the same or even stronger anti-inflammatory efficacy but lower

capacity in raising blood calcium levels (316). The development of agonists is mainly based on knowledge about the specific interactions of 1α,25$(OH)_2D_3$ or its analogues with the ligand binding pocket, which is in the LBD of VDR (Figure 1.10) (283).

To compare the efficacies of 1α,25$(OH)_2D_3$ with VDR antagonists, the mammalian one-hybrid assays (an expression vector for a fusion protein containing the DBD of the yeast transcription factor GAL4 and the LBD of the VDR together with a reporter gene construct containing a GAL4 binding site-driven luciferase gene) performed in HeLa cells demonstrated that 1α,25$(OH)_2D_3$ induced reporter gene activity in a typical dose response [EC50 (half maximal effective concentration)-value of $10^{-9}$ M], whereas ZK159222 showed very low ligand sensitivity (EC50-value of 1.2 x $10^{-7}$ M) (317). Similarly, the reporter gene assays [expression vectors for VDR and RXR and a reporter gene construct containing (directly repeated arrangements of two hexameric binding sites with three spacing nucleotides) DR3-type VDRE- driven luciferase gene] in Cos-7 cells exhibited that the EC-value of 1α,25$(OH)_2D_3$ is 1.7 x $10^{-9}$ M, while the ZK159222 is $10^{-8}$ M) (317). Moreover, the EC50-value was 2.3 x $10^{-10}$ M for 1α,25$(OH)_2D_3$ and 5.3 x $10^{-8}$ M for ZK191784, when inducing osteocalcin production (318).

**Figure 1.10** The molecular structure of VDR agonists.

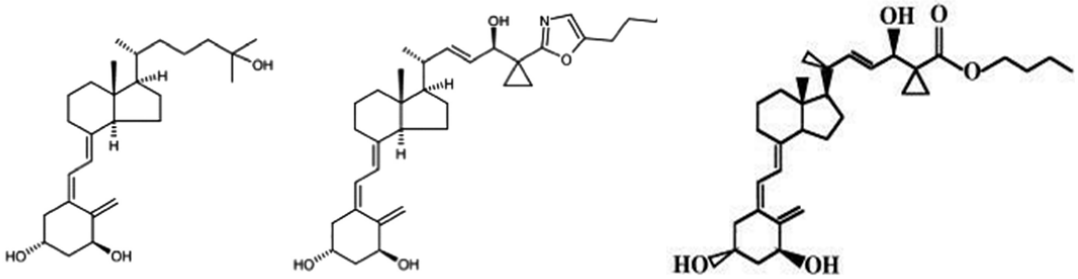


**1α,25$(OH)_2D_3$** **ZK191784** **ZK159222**

ZK159222

ZK 159222 is the first carboxylic ester analogues of $1\alpha,25(OH)_2D_3$ with a partial agonist profile. It has additional cyclopropyl rings and allylic alcohol substructures on its side chain, and an equal affinity to the nuclear VDR compared with $1\alpha,25(OH)_2D_3$. Metabolism studies *in vitro* indicate that its ester group is rapidly hydrolyzed in serum, thereby giving rise to the biologically less active carboxylic acid (319). Importantly, in rats ZK 159222 reduced the hypercalcemic and hypercalciuric activity by approximately 3000 times, when compared with $1\alpha,25(OH)_2D_3$ (320). Therefore, it is a promising new compound in vitamin D research.

Moreover**,** ZK 159222 inhibited lymphocyte proliferation, but induced osteocalcin synthesis in ROS 1712.8 cells (320). In HL60 cells (a promyelocytic leukemia cell line), ZK 159222 induced only a 10% differentiation (measured by nitroblue tetrazolium and demonstrated by reduction in CD14 expression) compared to that by $1\alpha,25(OH)_2D_3$ (320). Interestingly, ZK159222 also appears to be a competitive $1\alpha,25(OH)_2D_3$ antagonist. For instance, in MCF7 calls transiently transfected with a gene construct [DR3-vitamin D response element (a directly repeated arrangement of the hexameric binding sites with three spacing nucleotides, which represents an optimal binding site for VDR-RXR heterodimers) (321) and luciferase reporter], ZK 159222 displayed no agonistic but a $1\alpha,25(OH)_2D_3$ antagonistic effect with the similar potency as in HL60 cells (320).

Noteworthy, a recent study has shown that ZK159222 ($10^{-8,-6}$ M) [or ZK191784 ($10^{-8,-6}$ M), which will be discussed next in this section] significantly inhibited the release of pro-inflammatory factors including IL-6, IL-8, MCP-1 and RANTES from THP-1-MacCM-stimulated human white adipocytes. The anti-inflammatory effects are probably mediated by blocking phosphorylated NF-κB in the nucleus or phosphorylated MAPK p38 in the cytoplasm, thereby inhibiting the pro-inflammatory gene expression and secretion (24 h) (322).

ZK191784

ZK191784 contains a structurally modified side chain characterized by a 22,23-double bond, 24R-hydroxy group, 25-cyclopropyl ring and 5-butyloxazole unit, and competitively binds to the VDR with a similar affinity as $1\alpha,25(OH)_2D_3$ (323).

Nijenhuis et al. reported that ZK191784 normalized the $Ca^{2+}$ hyperabsorption and the expression of intestinal $Ca^{2+}$ transport proteins in TRPV5-/- mice (a phenotype displaying hypercalciuria, hypervitaminosis D, increased intestinal expression of the epithelial $Ca^{2+}$ channel TRPV6, the $Ca^{2+}$-binding protein calbindin-D9K and intestinal $Ca^{2+}$ hyperabsorption). Similarly, the compound decreased intestinal $Ca^{2+}$ absorption in WT mice as well as $1\alpha,25(OH)_2D_3$ –dependent $Ca^{2+}$ uptake by Caco-2 cells (318). Therefore, ZK197841 is associated with less hypercalcemic side effects compared with $1\alpha,25(OH)_2D_3$ or other analogues currently used in clinical practice.

Importantly, like $1\alpha,25(OH)_2D_3$, ZK191784 exhibited potent immune-suppressive and anti-inflammatory activity by inhibiting antigen-induced lymphocyte proliferation and cytokine secretion *in vitro*. Moreover, like ZK15922, it could also exert $1\alpha,25(OH)_2D_3$ -antagonistic effect on HL-60 cell differentiation (323, 324).

### 1.5.3. Vitamin D and adipose tissue

Storage

Vitamin D is a fat soluble secosteroid. It has been long shown that adipose tissue is the principal storage site for vitamin D and its metabolites, mainly in lipid droplets of adipocytes (325).

In humans, approximately 17% of orally-administered vitamin D dose is stored in adipose tissue whilst the rest is metabolized (326). Moreover, adipose tissue accumulates vitamin D proportionate to its concentration in plasma (327). Furthermore, the distribution of vitamin D and its metabolites in human adipose tissue have been studied by different analytical methods. For instance, with sensitivity less than 1 ng/g of tissue, HPLC (high-performance liquid chromatography) was used to measure the concentration of vitamin D in the human fat samples, which were obtained from autopsy (328). The concentrations were 45.3 ± 22.2 ng/g in the perirenal adipose tissue and 115.6 ± 52.4 ng/g in the axillary tissue. Similar results have been shown in the obese adults using LC/MS (liquid chromatography mass spectrometry) method (329).

Recently, a new technique called TOF-SIMS (time-of-flight secondary ion mass spectrometry) was used to the measurement purpose in human adipose tissue. This technique has several advantages: though it needs sophisticated sample preparation, the sample volume is relative low compared with the above-mentioned techniques; not only measuring vitamin D in different body compartments, but also it can specify the sub-cellular localization, by using ultracentrifugation to separate cellular components, and demonstrating it is found in adipocyte lipid droplets (325). In addition, adipose tissue also releases vitamin D at a much slower rate that is proportionate to its storage concentration (327).

Taken together, it has been suggested that adipose tissue functions as a vitamin D buffering system that prevents uncontrolled synthesis of $25(OH)D_3$ in the liver (330). Moreover, under fasting conditions, the slow release of vitamin D from adipose tissue may protect against the potential toxicity of vitamin D excess (331).

Production

25-hydroxylases including CYP2R1, CYP2J2, CYP27A1 andCYP3A4 [hydroxylating vitamin D at the carbon 25 position to generate $25(OH)D_3$ in the liver] have all been shown to be expressed in SAT as well as VAT (332, 333). Moreover, the expression of extra-renal $25(OH)D_3$-1α-hydroxylase (CYP27B1) also has been discovered in both rat and human adipose tissue. Noteworthy, 3T3-L1 preadipocytes express 1α-hydroxylase and were able to convert $^{3}H25(OH)D_3$ to $^{3}H1\alpha,25(OH)_2D_3$ (332, 334). But unlike the kidney, 1α-hydroxylase expressed by adipose tissue is not regulated by dietary calcium and vitamin D (335).

Degradation

The degradation of $1\alpha,25(OH)_2D_3$ by adipose tissue has been well established. CYP24A1, which catabolizes $25(OH)D_3$ and $1\alpha,25(OH)_2D_3$ to calcitroic acid and other inactive metabolites (336), is expressed in both human SAT and VAT (332). By induction of CYP24A1, $1\alpha,25(OH)_2D_3$ could stimulate its own degradation. In addition, it has been shown that over-expression of adipose

tissue CYP24A1 is associated with metabolic diseases, but the relevant pathophysiologic mechanisms still need further investigation.

Effects on adipogenesis

1α,25$(OH)_2D_3$ ($10^{-8}$ M) stimulated the differentiation of porcine MSCs (mesenchymal stem cells) toward adipocytic phenotype in a dose dependent manner. The differentiation was demonstrated by increased gene expression of PPARγ, LPL (lipoprotein lipase) and AP2 (adipocyte-binding protein2) (12 day) (337). Similarly, Narvaez et al. reported that in the presence of 1,25$(OH)_2D_3$ ($10^{-8}$ M), hASC (human adipose-derived stem cells) differentiated toward adipocytes with an increased expression of adipogenic marker genes [e.g. FABP4 (fatty acid binding protein) and PPARγ] and enhanced lipid accumulation (14 day) (338). Similarly, 1,25$(OH)_2D_3$ ($10^{-10, -8}$ M) promoted differentiation of already committed human subcutaneous preadipocytes by up-regulating the level of adipogenic FABP4 as well as enhancing the gene expression of LPL and PPARγ (334). In addition, the VDR is expressed in the earliest stages of adipocyte differentiation (4 h) (339). Knock down of the VDR by siRNA (small interfering RNA), the differentiation of 3T3-L1 cells was inhibited (340).

Paradoxically, besides inhibiting lipid droplet formation (7-8 day), 1α,25$(OH)_2D_3$ ($10^{-8}$ M) inhibited adipogenesis by suppressing the gene expression of C/EBPα and PPARγ, antagonizing the transacting activity of PPARγ, stabilizing the VDR protein (24 h) in 3T3-L1 preadipocytes (341). Moreover, 1α,25$(OH)_2D_3$ ($10^{-8}$ M) stimulated the expression of ETO (eight twenty-one, a C/EBP β corepressor) (24 h), thereby inhibiting the adipogenesis required transcriptional action of any remaining C/EBP β 3T3-L1 preadipocytes (340). In addition, the anti-adipogenic effect of 1α,25$(OH)_2D_3$ mediated by WNT signaling has emerged recently. For instance, 1α,25$(OH)_2D_3$ ($10^{-8}$ M) inhibits the differentiation of 3T3-L1 preadipocytes by maintaining the expression levels of WNT10B and nuclear β-catenin, thereby suppressing the level of PPARγ in 3T3-L1 adipocytes (342). Similarly, by suppressing DKK1 (dickkopf1) whilst enhancing the secretion of SFRP2 (frizzled-related protein 2) via VDR mediated WNT signaling (48 h), 1,25$(OH)_2D_3$ ($10^{-8}$ M) inhibited mouse BMSCs differentiation into adipocytes (343).

It is obvious that the conflicting results concerning the effects of $1\alpha,25(OH)_2D_3$ and its interactions with PPARγ in modulating adipogenesis/lipogenesis, likely reflect not only different models but also the end points reported. With respect to different models, some cells produce PPARγ ligands upon treatment with adipogenic media endogenously, while others require exogenous supplementation with synthetic PPARγ ligands for differentiation, and these uncertainties make it difficult to unravel the interactions between PPARγ and VDR activity (338). In addition, single cell profiling techniques have shown that changes in adipogenic marker genes do not strictly correlate with lipid droplet accumulation (344), not to mention that most of the above-mentioned studies, especially those of $1\alpha,25(OH)_2D_3$ exerting potent anti-proliferative effects, did not normalize lipid droplets formation by cell density.

Effects on adipocyte apoptosis

By microarray analysis of gene expression, it has been demonstrated that $1\alpha,25(OH)_2D_3$ ($10^{-8}$ M) significantly inhibited adipocyte apoptosis in human SAT *in vitro* (345). The anti-apoptotic effect also has been observed in differentiated 3T3-L1 cells (346). The underlying mechanism of anti-apoptosis is probably that physiological (low) doses ($<10^{-7}$ M) of vitamin $D_3$ could inhibit apoptotic gene expression, such as caspase-1 and caspase-2, but stimulate anti-apoptotic gene expression, such as BCL-2 (B-cell lymphoma 2) (347).

Paradoxically, an increased intake of vitamin $D_3$ [25 IU per os for 10 weeks] was associated with weight loss displayed by induction of apoptosis in WAT of the obese mice on HFD (348). Similarly, high dose ($10^{-7}$ M) of $1\alpha,25(OH)_2D_3$ stimulated the apoptosis of differentiated 3T3-L1 cells (346).

The apoptosis induced by $1\alpha,25(OH)_2D_3$ ($10^{-7}$ M) is mediated by $Ca^{2+}$ signaling (347). In mature 3T3-L1 adipocytes, $1\alpha,25(OH)_2D_3$ ($10^{-7}$ M) rapidly stimulates the voltage-dependent as well as voltage-insensitive $Ca^{2+}$ influx and triggers $Ca^{2+}$ release from ER stores through the (inositol 1,4,5-trisphosphate receptor) IP3R/$Ca^{2+}$ release channels and (ryanodine receptor) RyR/$Ca^{2+}$ release channels (day 1). Consequently the sustained increase of intracellular calcium initiates

apoptosis by activation of $Ca^{2+}$-dependent protease calpain and $Ca^{2+}$/calpain-dependent caspase-12 (day 3) (349). Noteworthy, the susceptibility of mature adipocytes to $1\alpha,25(OH)_2D_3$ induced-effect of increasing intracellular $Ca^{2+}$, depends upon $Ca^{2+}$-buffering capacity of these cells (350).

Effects on metaflammation

Though in a randomized controlled trial including fifty-five obese subjects, oral supplementation of vitamin D 7000 IU (international unit) per day over 26 weeks neither affected inflammatory markers in the circulation nor in the adipose tissue (351), there is a body of evidence suggesting that $1\alpha,25(OH)_2D_3$ is anti-inflammatory. In LPS-stimulated 3T3-L1 cells, $1\alpha,25(OH)_2D_3$ ($10^{-7}$ M) significantly reduced the release of IL-6 (24 h) (352). Similar results have also obtained in adipocytes from human subcutaneous WAT. For instance, $1,25(OH)_2D_3$ ($10^{-7,\ -8}$ M) attenuated TNF-α induced MCP-1 secretion (24 h) (353); inhibited THP-1-MacCM-induced gene expression of pro-inflammatory factors, such as MCP-1, IL-6 and IL-8 (24 h) (354). In addition, dietary supplementation of vitamin D (0.05 mg/kg of diet for 4 weeks) significantly reduced the secretion of IL-6 from epididymal adipose tissue of the mice on HFD (352).

It has been demonstrated that the anti-inflammatory effects of $1,25(OH)_2D_3$ ($10^{-8}$ M) were mediated by inhibition of the NF-κB and MAPK signaling pathways (354). The activation of these two pathways is essential in the signal transduction of pro-inflammatory factors in adipocytes, whereas $1\alpha,25(OH)_2D_3$ ($10^{-8}$ M) attenuated the activation by inhibiting the phosphorylation of relA as well as of p38 (24 h) (355, 356).

Interestingly, $1\alpha,25(OH)_2D_3$ ($10^{-8}$ M) also inhibited inflammation by enhancing the suppressive activity of human Tregs (357, 358). However, the underlying mechanism needs to be understood.

## 1.6. Aims and Hypotheses

### 1.6.1. Hypotheses

1. That VDR agonists [including $1\alpha,25(OH)_2D_3$ and its synthesized (pharmacological) analogues (ZK159222 and ZK191784)] reduce inflammatory responses in human adipose tissue;
2. These anti-inflammatory effects of VDR agonists on preadipocytes are mediated by modulation of multiple intracellular signaling, including the NF-κB, MAPK or unfolded protein response (UPR) pathways.

### 1.6.2. Aims

1. To study the anti-inflammatory effects of VDR agonists on MacCM (macrophage conditioned medium) or IL-1β-stimulated human white preadipocytes (an *in vitro* model of metaflammation in adipose tissue). This was achieved by measurement of the reduction of gene expression using qPCR (including IL-1β, IL-6, IL-8, MCP-1 and RANTES) or secretion using proteome array and ELISA (including IL-1β, IL-6, IL-8, MCP-1 and RANTES) for important mediators of inflammation in the model.
2. To investigate by which signaling molecules VDR agonists exert the anti-inflammatory effects. This was achieved by measurement of the reduction of phosphorylated relA of the NF-κB pathway, phosphorylated ERK (p42/44) or phosphorylated p38 of the MAPK pathways; or increase of methylated relA of the NF-κB pathway; or modulation of XBP-1 or phosphorylated eIF-2α of the UPR pathways (using western blotting).

# 2. Materials and Methods

## 2.1. THP-1-monocytes/macrophages

The THP-1 cell line was originally isolated from the peripheral blood of a 1-year old male patient suffering from acute monocytic leukemia (359). This cell line (in the monocyte as well as macrophage-like state) has been widely applied to studies regarding immune responses. THP-1 monocytes can be differentiated into a macrophage-like phenotype using either PMA (Phorbol12-myristate13-acetate), $1\alpha,25(OH)_2D_3$ or M-CSF (macrophage colony-stimulating factor) (360, 361). (Non-activated) M0 macrophages can develop from THP-1 monocytes by PMA stimulation in 48 h, such as adhering to culture plates, altering their morphology into flat and amoeboid in shape, with rough ER, large numbers of ribosomes, and well-developed Golgi apparatuses in the cytoplasm (362).

The advantages of THP-1 cell line include:

a) Under growing conditions with RPMI 1640 supplemented with 10% FBS, THP-1 cells can quadruple within three and a half days (363);
b) The cell line is relatively easy and safe to use since there hasn't been any reported evidence for the presence of infectious viruses or toxic products in THP-1 cells (363);
c) THP-1 cell line can be cultured *in vitro* up to passage 25 or recovered after being stored for a number of years and by following an appropriate protocol, without changes of cell sensitivity and activity (363);
d) The homogeneous genetic background of THP-1 minimizes the degree of variability in the cell phenotype, which renders reproducibility of findings (364),

THP-1 cells have been long used as an *in vitro* model of human monocytes and macrophages in mechanistic studies of inflammatory diseases (365, 366). It has been demonstrated that macrophage infiltration occurs in MAO (6). In *in vitro* experiments, the macrophages are often described as being in an M1-activated state, which can be obtained by stimulating

THP-1-macrophages with LPS (367, 368). The studies have shown that LPS significantly up-regulates the expression of the NF-κB transcription factor, which subsequently orchestrates a network of gene expression leading to cell proliferation, differentiation, migration, survival, and importantly the activation of inflammation, which is mediated through the release of pro-inflammatory factors including IL-1β, IL-6, IL-8 and TNF-α (367, 368).

## 2.2. Culture of THP-1-monocytes

Strict aseptic techniques are applied to the following protocols. All the procedures (except the centrifuging step) are performed under a laminar flow cabinet.

1. Prepare supplies as shown in Table 2.2.1.

**Table 2.2.1 Supplies needed for culture of THP-1-monocytes**

| Supply | Catalogue Number | Supply | Catalogue Number |
|---|---|---|---|
| THP-1-monocytes | - | RPMI 1640 medium | Sigma R8758-500 ML |
| Penicillin-Streptomycin | Gibco 15140122 | T75 flask | Sigma CLS430641U-100EA |
| FBS (Fetal bovine serum) | Gibco 16000044 | Filter (0.22 μm) | TPP 99250 |
| Pipette and Pipette Tip | - | Glovers | - |
| 10% Virkon (in water) | - | 70% Ethanol (in water) | Sigma51976-500 ML-F |
| Incubator | - | PBS | Gibco 10010023 |
| Hemocytometer | Digital Bio 2-7723-23 | Microscope | - |
| 1.5 ml Eppendorf tube (sterile) | - | 250 ml beaker | - |
| Distilled water | - | 50 ml centrifuge tube | - |

2. Prepare MGM (the whole THP-1-monocyte growth medium) and MM (monocyte medium) as shown in Table 2.2.2. Filter the medium and apply them to the following experiments.

**Table 2.2.2 Preparation of MGM and MM**

| Type | Recipe |
|---|---|
| MGM | 10% FBS in RPMI 1640 Medium,<br>1 x penicillin-Streptomycin (10,000 U/ml) |
| MM | RPMI 1640 Medium,<br>1 x penicillin-Streptomycin (10,000 U/ml) |

### 2.2.1. Culture of THP-1-monocytes

Protocol for cryo-preserved cells

1. Fill T75 flasks with MGM (25 ml/T75 flask). Place the flasks in an incubator (37°C, 5% $CO_2$) for 30 min.
2. Remove a cryovial of THP-1-monocytes [$10^7$ cells/vial, kindly provided by Professor Helen R Griffiths (Aston University, UK)] from the liquid nitrogen container and immediately place it on dry ice. Briefly twist the cap a quarter turn to relieve pressure, and then re-tighten it. Immerse the vial into a water bath (37°C) just to the screw cap for 2 min. Ensure that no water enters the thread of the screw cap.
3. Thoroughly rinse the cryovial with 70% ethanol. Aspirate the excess ethanol from the thread area of the screw cap. Open the vial and transfer the whole 1 ml of the cells into the T75 flask containing the pre-warmed MGM.
4. Place the flasks in an incubator (37°C, 5% $CO_2$) for cell growing. Replace the medium in every 48 h.

Cell counting

Take the flasks out of the incubator and spray the screw caps thoroughly with 70% ethanol and let them air dry. Transfer the cell suspension into 50 ml centrifugation tubes [1 flask (25 ml)/tube]. Draw out 100 µl as a sample then dilute it 9 times in PBS. Load 10 µl of the diluted sample onto a

hemocytometer to measure the cell density (= $\frac{100,000}{\#\text{of squares}}$ cell/ml).

### 2.2.2. Protocol for subculture of THP-1 monocytes

1. Subculture is to be initiated when the density of THP-1 monocytes has reached 1 x $10^6$/ml·T75 flask (confirmed by cell counting) (Figure 2.1).
2. Warm MGM for 30 minutes in 37°C water bath.
3. Transfer the cell suspension into a 50 ml centrifuge tube and centrifuge it at 150 x g for 10 min.
4. Resuspend the monocytes in the pre-warmed MGM.

**Figure 2.1 The suspension of THP-1 monocytes (cell density: 1 x $10^6$/ml)**

## 2.3. THP-1-monocytes treatments

Strict aseptic techniques are applied to the following protocols. All the procedures (except the centrifuging step) are performed under a laminar flow cabinet.

### 2.3.1. Generation of THP-1-MacCM (THP-1-macrophage conditioned medium)

1. Prepare reagents and supplies as shown in Table 2.3.1, 2.

**Table 2.3.1 Reagents needed for preparation of THP-1-MacCM**

| | Catalog Number | Stock Concentration |
|---|---|---|
| PMA(Phorbol12-myristate13-acetate) | Sigma P1585-1mg | 2 μg/μl [in DMSO(dimethyl sulfoxide)] |
| LPS | Sigma L3024-5mg | 5 mg/ml (in water) |
| ATP (Adenosine 5′-triphosphate) | Sigma FLAAS-1VL | - |

**Table 2.3.2 Supplies needed for preparation of THP-1-MacCM**

| Supply | Catalogue Number | Supply | Catalogue Number |
|---|---|---|---|
| RPMI 1640 medium | Sigma R8758-500 ML | FBS (Fetal Bovine Serum) | Gibco 16000044 |
| Penicillin-Streptomycin | Gibco 15140122 | Dnase-free water | ThermoFisher 10977015 |
| Filter (0.22 μm) | TPP 99722 | Pipette and Pipette Tip | - |
| Incubator | - | Glovers | - |
| 10% Virkon (in water) | - | 70% Ethanol (in water) | Sigma 51976-500 ML-F |
| Microscope | - | Paper towel | - |
| 1.5 ml Eppendorf tube | - | 15 ml and 50 ml centrifuge tube | - |
| Centrifuge | - | 250 ml beaker | - |
| Distilled water | - | Marker (pen) | - |
| Syringe (20 ml) | - | | |

2. When the density of THP-1 monocytes has reached 1 x $10^6$/ml·T75 flask, transfer the cell suspension into a 50 ml centrifuge tube and centrifuge it at 150 x g for 10 min.
3. Resuspend the cells in 100 nM PMA (diluted in MGM, 25 ml/T75 flask) to induce the differentiation for 48 h (Figure 2.2.).
4. Replace the differentiation medium with 1 μg/ml LPS, 1 mM ATP (diluted in MM, 25 ml/T75 flask) to activate the THP-1-macrophages for 24 h.

5. Collect the THP-1-MacCM, filter and store it at -80°C for further use.

### 2.3.2. THP-1-macrophage treatments

1. Prepare reagents and supplies as shown in Table 2.3.3, 4.

**Table 2.3.3 Reagents needed for treatments of THP-1-macrophages**

| | Catalog Number | Stock Concentration |
|---|---|---|
| PMA | Sigma P1585-1mg | 2 μg/μl (in DMSO) |
| LPS | Sigma L3024-5mg | 5 mg/ml (in water) |
| ATP | Sigma FLAAS-1VL | - |
| $1\alpha,25(OH)_2D_3$ | EnzoB ML-DM2000-0050 | 10 μg/ml (in DMSO) |
| ZK159222 | Bayer | 1 μg/μl |
| ZK191784 | Bayer | 1 μg/μl |

**Table 2.3.4 Supplies needed for treatments of THP-1-macrophages**

| Supply | Catalogue Number | Supply | Catalogue Number |
|---|---|---|---|
| RPMI 1640 medium | Sigma R8758-500 ML | FBS (Fetal Bovine Serum) | Gibco 16000044 |
| Penicillin-Streptomycin | Gibco 15140122 | Dnase-free water | ThermoFisher 10977015 |
| Syringe filter | TPP 99722 | Pipette and Pipette Tip | - |
| Incubator | - | Glovers | - |
| 10% Virkon (in water) | - | 70% Ethanol (in water) | Sigma 51976-500 ML-F |
| Microscope | - | Paper towel | - |
| 1.5 ml Eppendorf tube | - | 15 ml and 50 ml centrifuge tube | - |
| Centrifuge | - | 250 ml beaker | - |
| Distilled water | - | Marker | - |

2. When the density of THP-1 monocytes has reached 1 x $10^6$/ml·T75 flask (confirmed by cell counting), transfer the cell suspension into a 50 ml centrifuge tube and centrifuge it at 150 x g for 10 min.
3. Resuspend the cells in 100 nM PMA (diluted in MGM, 25 ml/T75 flask) to induce the differentiation for 48 h.
4. Replace the differentiation medium with 1 μg/ml LPS, 1 mM ATP to stimulate the THP-1-macrophages (diluted in GM, 25 ml/T75 flask), or at the same time treating the stimulated THP-1-macrophages with VDR agonists for 24 h, as shown in Table 2.3.5.
5. Collect the untreated and treated THP-1-MacCMs, filter and store them at -80°C for further

use.

**Table 2.3.5 Treatment plan for THP-1-macrophages**

| | Treatment (in GM, 25 ml/T75 flask) |
|---|---|
| THP-1-MacCM | 1 μg/ml LPS, 1 mM ATP |
| ZK159222(10nM)-MacCM | 1 μg/ml LPS, 1 mM ATP, 10 nM ZK159222 |
| ZK159222(1μM)-MacCM | 1 μg/ml LPS, 1 mM ATP, 1 μM ZK159222 |
| ZK191784(10nM)-MacCM | 1 μg/ml LPS, 1 mM ATP, 10 nM ZK191784 |
| ZK191784(1μM)-MacCM | 1 μg/ml LPS, 1 mM ATP, 1 μM ZK191784 |
| $1\alpha,25(OH)_2D_3$(10nM)-MacCM | 1 μg/ml LPS, 1 mM ATP, 10 nM $1\alpha,25(OH)_2D_3$ |

**Figure 2.2 THP-1-macrophages** (adhering to culture plates, adopting flat and amoeboid shape, at 48 h after induction of differentiation)

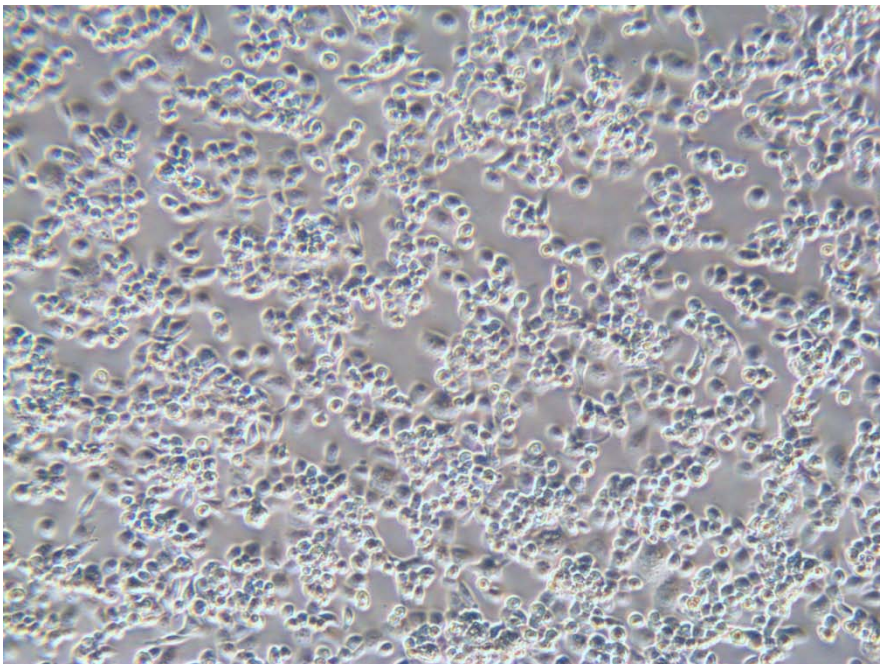

## 2.4. Human white preadipocytes

WAT consists of approximately one third of mature adipocytes. This not only serves as a storage depot of lipids, it is also a remarkable endocrine organ secreting a large number of adipokines, whose primary role is the integration of multiple functions, such as energy balance, food intake and appetite, immunity, insulin sensitivity, blood pressure, and reproduction (369). Dysfunctional secretion of adipokines accompanied by a dysregulated disposal of glucose and lipids, are crucial pathogenetic factors contributing to the development of several metabolic disorders, particularly metaflammation and insulin-resistance state of obesity (370).

The remaining two thirds are a combination of small blood vessels, nerve tissue, fibroblasts and preadipocytes in various stages of development (371). Noteworthy, preadipocytes have the capability of proliferating and differentiating into mature adipocytes, which confers adipose tissue a constant functional plasticity to expand throughout the entire lifespan (372). Human primary preadipocytes can be isolated and cultured from fat tissue explants. In particular culture conditions (i.e. IL-1β and THP-1-MacCM), adipokine secretion (i.e. pro-inflammatory factors) from preadipocytes can be induced and investigated *in vitro* (355). However, the major drawbacks of primary preadipocyte culture cannot be ignored, which include technical difficulties when trying to isolate preadipocytes from other fibroblast-like cells, the relative small proportion of isolated preadipocytes to the total fat tissue required, and the limited life span of primary culture (371).

## 2.5. Culture and Subculture of preadipocytes

Strict aseptic techniques are applied to the following protocols. All the procedures (except the centrifuging step) are performed under a laminar flow cabinet.

1. Prepare supplies as shown in Table 2.5.1.
2. Prepare PGM (the whole preadipocytes growth medium) as shown in Table 2.5.2. Filter the medium and apply it to the following experiments.

3. Fill the flasks with PGM (7 ml/T25 flask). Place the flasks in an incubator (37°C, 5% $CO_2$) for 30 min.

**Table 2.5.1 Supplies needed for subculture and culture of preadipocytes**

| Supply | Catalogue Number | Supply | Catalogue Number |
|---|---|---|---|
| Human white preadipocytes | PromoCell C-12730 | Preadipocyte growth medium | PromoCell C27410 |
| SupplementMix | PromoCell C39425 | 100 x Antibiotic-Antimycotic | ThermoFisher 15240062 |
| T25 flask | Sigma CLS430639U-20EA | 12-wells plate | Sigma CLS3513-50EA |
| Filter | TPP 99250 | Paper towel | - |
| Pipette and Pipette Tip | - | Glovers | - |
| 10% Virkon (in water) | - | 70% Ethanol (in water) | Sigma 51976-500 ML-F |
| Trypsin | ThermoFisher 25200056 | PBS | Gibco 10010023 |
| Hemocytometer | Digital Bio 2-7723-23 | Microscope | - |
| 50 ml centrifuge tube | - | Incubator | - |
| 1.5 ml Eppendorf tube | - | 250 ml beaker | - |
| Distilled water | - | | |

**Table 2.5.2 Preparation of PGM**

| Type | Recipe |
|---|---|
| PGM | 500 ml Preadipocyte Growth Medium,<br>A vial Preadipocyte Growth Medium SupplementMix<br>[Final supplementation concentrations after addition to the growth medium:<br>fetal calf serum (0.05 ml/ml), endothelial cell growth supplement (0.004 ml/ml),<br>epidermal growth factor (recombinant human) (10 ng/ml), hydrocortisone (1 µg/ml), Heparin (90 µg/ml)]<br>5 ml 100 x Antibiotic-Antimycotic (10,000 U/ml penicillin, 10,000 µg/ml streptomycin, and 25µg/ml amphotericin B) |

### 2.5.1. Culture of preadipocytes

Protocol for cryo-preserved cells

1. Thoroughly rinse the cryovial of primary human white preadipocytes [derived from subcutaneous adipose tissue of a female Caucasian subject (BMI: 21; age: 44 years), PromoCell, Germany] with 70% ethanol. Aspirate the excess ethanol from the thread area of

the screw cap. Open the vial and transfer the cells into flasks containing the pre-warmed PGM (0.25 ml/flask).

2. Place the flasks in an incubator (37°C, 5% $CO_2$) for cell attachment. Replace the medium in every 48 h.

Protocol for proliferating cells

1. Warm PGM for 30 min in 37°C water bath.
2. Take the flasks out of the incubator and spray the screw caps thoroughly with 70% ethanol and let them air dry. Aspirate the old PGM from the flasks and replace with the pre-warmed growth medium.
3. Check the cell density under a microscope (Figure 2.3.). The cells are sub-cultured once they have reached 90% confluence (Figure 2.4.).

### 2.5.2. Subculture of preadipocytes

1. Place the trypsin, PBS and growth medium in the 37°C water bath for 30 min. Carefully aspirate the old growth medium from the culture flasks. Add pre-warmed PBS (7 ml/flask) to the non-cell attaching side of the flasks, slowly reverse the flasks to prevent the cells from flushing away, and wash the cells by gently agitating the flasks for 15 sec. Carefully aspirate the PBS from the flasks. Repeat the washing procedure once.
2. Add trypsin (1 X) (1.5 ml/flask) into the flasks and detach the cells at room temperature. Close the flasks and examine the cells under a microscope. When the cells start to detach, gently tap the side of the flasks to loosen the remaining cells.
3. When most of the cells are detached, add PGM (1.5 ml/flask) and gently agitate. Carefully aspirate the cell suspension from the flasks and transfer them into centrifugation tubes (1 flask/tube). Spin down the cells for 3 min at 220 x g.
4. Discard the supernatant. Add 48-60 ml of PGM to each of the tubes to re-suspend the cells.
5. Seed the preadipocytes into 12-wells plates (2 ml/well, seeding density: approximately 5000

cells per $cm^2$). Place the plates in an incubator (37°C, 5% $CO_2$) for cell attachment. Replace the medium in every 48 h.

6. The cells are to be pre-treated once they have reached 90% confluence.

**Figure 2.3 Human white preadipocytes (initial culture)**

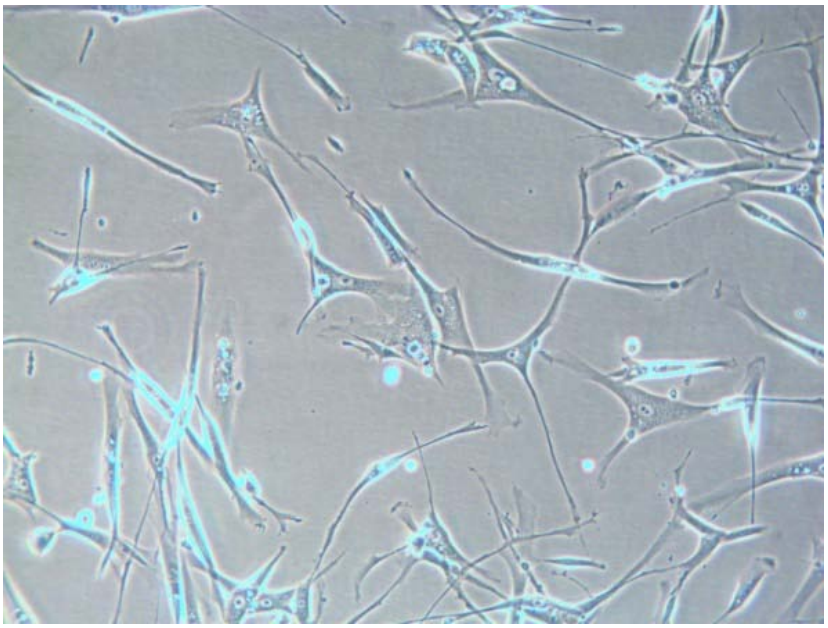

**Figure 2.4 Human white preadipocytes (90% confluent)**

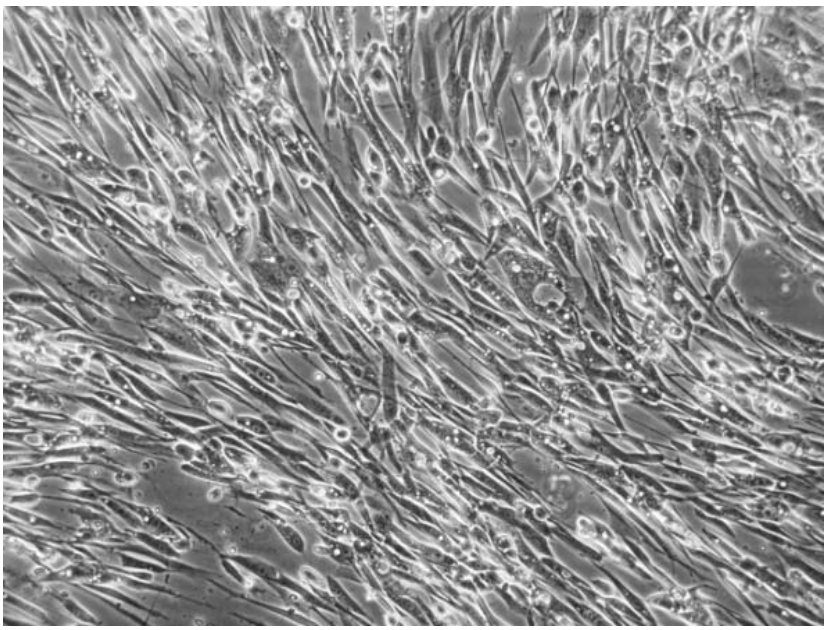

## 2.6. Preadipocyte pre-and treatments

Strict aseptic techniques are applied to the following protocols. All the procedures are performed under a laminar flow cabinet.

1. Prepare reagents and supplies as shown in Table 2.6.1, 2.

**Table 2.6.1 Reagents needed for pre- and treatments of preadipocytes**

| | Catalog Number | Stock Concentration |
|---|---|---|
| IL-1β | Sigma 19401-5UG | 0.1 μg/μl (in water) |
| IL-1β neutralizing antibody | R&D Systems MAB601R-01M | 1 mg/ml (in water) |
| IL-6 neutralizing antibody | R&D Systems AF-206-NA | 1.474 mg/ml |
| $1\alpha,25(OH)_2D_3$ | EnzoB ML-DM2000-0050 | 10 μg/ml (in DMSO) |
| ZK159222 | Bayer | 1 μg/μl (in DMSO) |
| ZK191784 | Bayer | 1 μg/μl (in DMSO) |

**Table 2.6.2 Supplies needed for pre- and treatments of preadipocytes**

| Supply | Catalogue Number | Supply | Catalogue Number |
|---|---|---|---|
| Human white preadipocytes | PromoCell C-12730 | Preadipocyte growth medium | PromoCell C27410 |
| SupplementMix | PromoCell C39425 | 100 x Antibiotic-Antimycotic | ThermoFisher 15240062 |
| Pipette and Pipette Tip | - | Glovers | - |
| 10% Virkon (in water) | - | 70% Ethanol (in water) | Sigma 51976-500 ML-F |
| Untreated and treated MacCM | - | RPMI 1640 medium | Sigma R8758-500 ML |
| Microscope | - | Incubator | - |
| 50 ml centrifuge tube | - | Tube rack | - |
| 1.5 and 2 ml Eppendorf tube | - | 250 ml beaker | - |
| Distilled water | - | Paper towel | - |
| Ice | - | Universal tube | - |
| PBS | Gibco 10010023 | Trizol | ThermoFisher 15596026 |
| Trizma base | Sigma T1503-500G | SDS | Sigma L3771-100G |
| HCl (hydrochloric acid) | Sigma H1758-500 ML | Glycerol | Sigma G5516-100 ML |
| protease inhibitor cocktail | Sigma P8340-1 ML | phosphatase inhibitor cocktail | Sigma P2850-1 ML |
| PH meter | - | | |

2. Culture the preadipocytes alone, or treat them with IL-1β or THP-1-MacCM, or in the presence of cytokine neutralizing antibody for 24 h. Pretreat further groups of the

preadipocytes with VDR agonists [1α,25$(OH)_2D_3$, ZK159222 and ZK191784] for 24 or 48 h, followed by (medium replacement) treatments with IL-1β or THP-1-MacCM in the presence of VDR agonists (as show in Table 2.6.3-6) before culture medium or lysate collection (n = 6 well/ pre- and treatment, all the reagents diluted in PGM).

**Table2.6.3 Pre- and treatment plan of Chapter 3**

| | Pretreatment (24 h) (in PGM) | Treatment (24 h) (in PGM) |
|---|---|---|
| control | - | (25%) RPMI1640 |
| THP-MacCM(25%) | - | (25%) THP-MacCM |
| IL-1βAb(15μg/ml) +MacCM(25%) | - | (25%) THP-MacCM, 15 μg/ml IL-1β antibody |
| IL-6Ab(300ng/ml)+ MacCM(25%) | - | (25%) THP-MacCM, 300 ng/ml IL-6 antibody |
| VD(0.01nM)+MacCM(25%) | 0.01 nM 1α,25$(OH)_2D_3$ | (25%) THP-MacCM, 0.01 nM 1α,25$(OH)_2D_3$ |
| VD(0.01nM)+MacCM(25%) | 0.1 nM 1α,25$(OH)_2D_3$ | (25%) THP-MacCM, 0.1 nM 1α,25$(OH)_2D_3$ |
| VD(0.01nM)+MacCM(25%) | 1 nM 1α,25$(OH)_2D_3$ | (25%) THP-MacCM, 1 nM 1α,25$(OH)_2D_3$ |
| VD(10 nM)+MacCM(25%) | 10 nM 1α,25$(OH)_2D_3$ | (25%) THP-MacCM, 10 nM 1α,25$(OH)_2D_3$ |

**Table 2.6.4 Pre- and treatment plan of Chapter 4**

| | Pretreatment (24 h) (in PGM) | Treatment (24 h) (in PGM) |
|---|---|---|
| control | - | - |
| IL-1β(0.5ng/ml) | - | 0.5 ng/ml IL-1β |
| IL-1β(2ng/ml) | - | 2 ng/ml IL-1β |
| VD(0.01nM)+IL-1β(0.5ng/ml) | 0.01 nM 1α,25$(OH)_2D_3$ | 0.5 ng/ml IL-1β, 0.01 nM 1α,25$(OH)_2D_3$ |
| VD (0.1nM)+IL-1β(0.5ng/ml) | 0.1 nM 1α,25$(OH)_2D_3$ | 0.5 ng/ml IL-1β, 0.1 nM 1α,25$(OH)_2D_3$ |
| VD(1nM)+IL-1β(0.5ng/ml) | 1 nM 1α,25$(OH)_2D_3$ | 0.5 ng/ml IL-1β, 1 nM 1α,25$(OH)_2D_3$ |
| VD(10nM)+IL-1β(0.5ng/ml) | 10 nM 1α,25$(OH)_2D_3$ | 0.5 ng/ml IL-1β, 10 nM 1α,25$(OH)_2D_3$ |
| VD(0.01nM)+IL-1β(2ng/ml) | 0.01 nM 1α,25$(OH)_2D_3$ | 2 ng/ml IL-1β, 0.01 nM 1α,25$(OH)_2D_3$ |
| VD (0.1nM)+IL-1β(2ng/ml) | 0.1 nM 1α,25$(OH)_2D_3$ | 2 ng/ml IL-1β, 0.1 nM 1α,25$(OH)_2D_3$ |
| VD(1nM)+IL-1β(2ng/ml) | 1 nM 1α,25$(OH)_2D_3$ | 2 ng/ml IL-1β, 1 nM 1α,25$(OH)_2D_3$ |
| VD (10nM)+IL-1β(2ng/ml) | 10 nM 1α,25$(OH)_2D_3$ | 2 ng/ml IL-1β, 10 nM 1α,25$(OH)_2D_3$ |

**Table 2.6.5 Pre- and treatment plan of Chapter 5**

| | Pretreatment (48h) (in PGM) | Treatment (24 h) (in PGM) |
|---|---|---|
| control | - | - |
| IL-1β(0.5ng/ml) | - | 0.5 ng/ml IL-1β |
| ZK159222(10nM)+IL-1β(0.5ng/ml) | 10 nM ZK159222 | 0.5 ng/ml IL-1β, 10 nM ZK159222 |
| ZK159222(1μM)+IL-1β(0.5ng/ml) | 1 μM ZK159222 | 0.5 ng/ml IL-1β, 1 μM ZK159222 |
| ZK191784(10nM)+IL-1β(0.5ng/ml) | 10 nM ZK191784 | 0.5 ng/ml IL-1β, 10 nM ZK191784 |
| ZK191784(1μM)+IL-1β(0.5ng/ml) | 1 μM ZK191784 | 0.5 ng/ml IL-1β, 1 μM ZK191784 |
| VD(10nM)+IL-1β(0.5ng/ml) | 10 nM 1α,25$(OH)_2D_3$ | 0.5 ng/ml IL-1β, 10 nM 1α,25$(OH)_2D_3$ |

**Table 2.6.6 Pre- and treatment plan of Chapter 6**

| | Pretreatment (48h) (in PGM) | Treatment (24 h) (in PGM) |
|---|---|---|
| control | - | (25%) RPMI1640 |
| THP-1-MacCM[25%] | - | (25%) THP-1-macrophages (shown in Table 2.3.5) |
| ZK159222(10nM)-MacCM[25%] | 10 nM ZK159222 | (25%) ZK159222 (10 nM)-MacCM (shown in Table 2.3.5) |
| ZK159222(1μM)-MacCM[25%] | 1 μM ZK159222 | (25%) ZK159222 (1 μM )-MacCM (shown in Table 2.3.5) |
| ZK191784(10nM)-MacCM[25%] | 10 nM ZK191784 | (25%) ZK191784 (10 nM)-MacCM (shown in Table 2.3.5) |
| ZK191784(1μM)-MacCM[25%] | 1 μM ZK191784 | (25%) ZK191784 (1 μM )-MacCM (shown in Table 2.3.5) |
| VD(10nM)-MacCM[25%] | 10 nM 1α,25$(OH)_2D_3$ | (25%) 1α,25$(OH)_2D_3$ (10 nM)-MacCM (shown in Table 2.3.5) |

3. Directly collect the culture media (n = 6), store them at -80°C for cytokine array and ELISA.
4. Rinse the treated preadipocytes twice in ice-cold PBS and lyse them with Trizol (n = 6, 250 μl/well), the lysate is then stored at -80°C before analysis.
5. Rinse the treated preadipocytes twice in ice-cold PBS and scrape them into a freshly prepared lysis buffer (n = 6, 100 μl/well) as shown in Table 2.6.7, stored the lysate at -80°C for BCA assay.

**Table 2.6.7 Preparation of the lysis buffer**

| Type | Recipe |
|---|---|
| Lysis Buffer | 50 mM Tris-HCl pH 6.7, 10% Glycerol,<br>4% SDS (sodium dodecyl sulfate)<br>protease inhibitor cocktail (1 ml/10 ml of the lysis buffer),<br>phosphatase inhibitor cocktail (1 ml/100 ml of the lysis buffer) |

## 2.7. Cytokine array

### 2.7.1. Principle

Proteome arrays are often used for detecting protein expression from various samples including serum, plasma, cell, tissue lysates or supernatants (373, 374).

In this technology, firstly, sample (pro-inflammatory factors in our studies) detection requires the binding of 2 distinct antibodies [a capture antibody spotted and fixed on a nitrocellulose membrane and a detection antibody, each binding to a unique epitope of the same sample. Secondly, a (HRP) horseradish peroxidase-linked secondary antibody is added to bind to the detection antibody's Fc region (nonspecific). The binding emits a chemiluminescent signal when reacting with an enhanced chemiluminescent substrate, consequently the signals detected and measured by an X-ray scanner. Reference peptides are printed on the corners of the array to allow for protein relative quantification of the samples (Figure 2.5).

The sandwich-based antibody arrays are rapid, automated, economical, and highly sensitive, consuming small quantities of samples and reagents (375). Their reproducibility also enables quantitative analysis, which confers greater specificity and lower background signal, to be performed (376).

**Figure 2.5 The mechanism of cytokine array (obtained from R&D systems)**

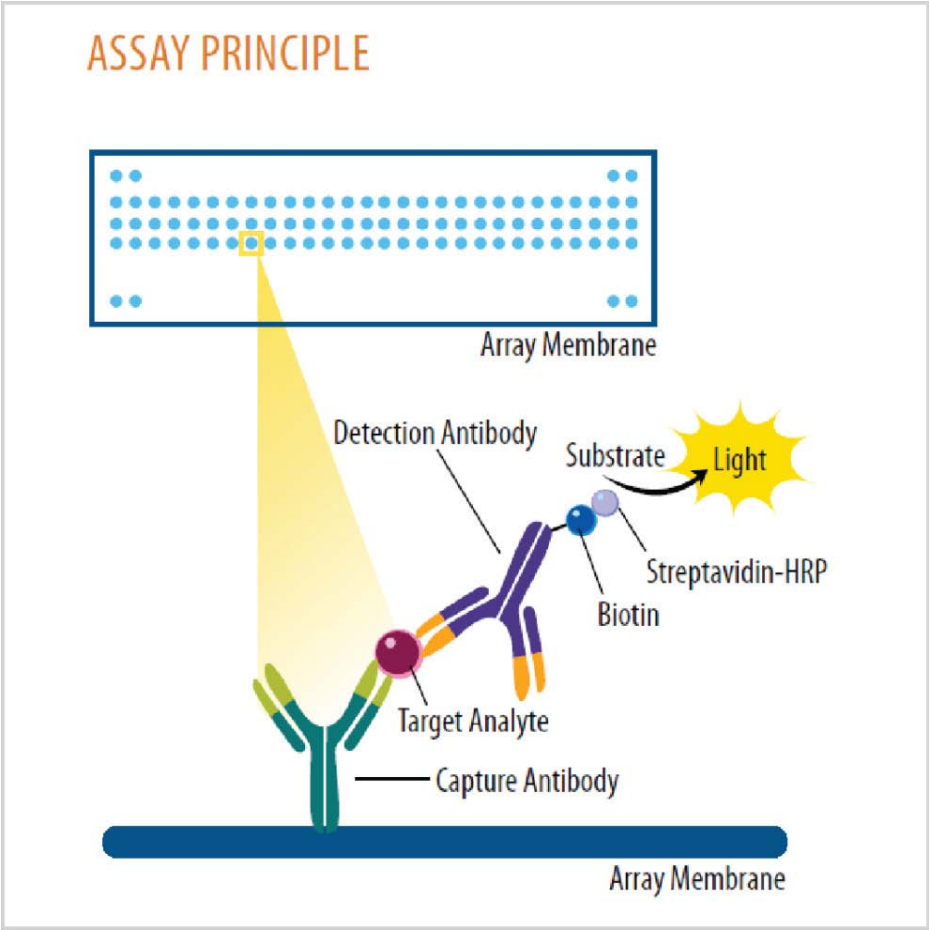


### 2.7.2. General protocol

1. Prepare reagents and supplies as shown in Table 2.7.1, 2.
2. Pipette 2 ml of array buffer 6 (serving as a block buffer) into each well of the 4-well multi-dish.
3. Place array in the dish. The number on the array should be facing upward (upon contact with array buffer 6, the blue dye from the spot will disappear).

**Table 2.7.1 Preparation of the reagents for the cytokine arrays**

| Reagent | Preparation | Catalogue Number |
|---|---|---|
| Human cytokine array | Immediately before use, remove each membrane to be used from between the protective sheets with a flat-tipped tweezers. Handle the membranes with gloved hands and flat-tipped tweezers only. | R&D Systems, ARY005 R&D Systems,ARY022 |
| Detection antibody cocktail | Before use, reconstitute the detection antibody cocktail in 200µL of deionized or distilled water. | |
| 1 x Array buffer 4/6 | *Array buffer 4 may contain a precipitate. Mix well before and during use.* Add 4 ml of array buffer 4 to 8 ml of array buffer 6. Prepare fresh for each use. | |
| 1 x Wash buffer | If crystals have formed in the concentrate, warm the bottles to room temperature and mix gently until the crystals have completely dissolved. Add 40 ml of wash buffer concentrate to 960 ml of distilled water. | |
| Chemi reagent mix | Chemi reagent 1 and 2 should be mixed in equal volumes in 15 minutes of use. Protect from light. 1 ml of the resultant mixtures is required per membrane. | |
| 1 x Streptavidin-HRP | Immediately before use, dilute the Streptavidin-HRP in Array buffer 6. See via label for dilution factor. | |
| *Note: Bring all reagents to room temperature before use.* | | |

**Table 2.7.2 Supplies needed for the cytokine arrays**

| Supply | Catalogue Number | Supply | Catalogue Number |
|---|---|---|---|
| 4-Well multi dish | R&D Systems, ARY005 R&D Systems,ARY022 | Transparent overlay template | R&D Systems, ARY005 R&D Systems,ARY022 |
| Pipette and pipette tip | - | Glovers | - |
| Dnase-free water | ThermoFisher 10977015 | Distilled water | - |
| Rocking platform shaker | - | 500 ml Bottle | - |
| Paper towel | - | Flat-tipped Tweezers | - |
| Plastic sheet protector | - | Plastic container | - |
| ChemiDoc | - | Universal tube | - |
| Marker | - | | |

4. Incubate the array for 1 h on a rocking shaker. Orient the dish so that each array rocks end to end in its well.
5. While the arrays are blocking, prepare samples by mixing 1 ml of Array Buffer 6 and 0.6 ml of the pooled cell culture supernatant together [100 µl of each of the collected media from the treated preadipocytes (n = 6, per treatment)]. Aspirate array buffer 6 from the wells of the dish and add the prepared samples. Place the lid on the dish.
6. Incubate the array overnight at 4 °C on a rocking platform shaker

7. Carefully remove the array and place them into individual containers with 20 ml of 1 X wash buffer. Rinse the dish with distilled water and dry thoroughly.
8. Wash each array 3 times with 1 x wash buffer for 10 min on a rocking platform shaker.
9. For each array, add 30 µl of detection antibody cocktail to 1.5 ml of 1 x Array Buffer 4/6. Pipette 1.5 ml per well of the diluted detection antibody cocktail into the dish.
10. Carefully remove each array from its wash container. Allow excess wash buffer to drain from the array. Return the array to the 4 well-dish containing the diluted detection antibody cocktail, and cover the dish with the lid.
11. Incubate the array for 1 h on a rocking platform shaker.
12. Wash the array as described in step 8 and 9.
13. Pipette 2 ml of 1 X streptavidin-HRP into each well of the 4-well multi-dish.
14. Carefully remove each array from its wash container. Allow excess wash buffer to drain from the array. Return the array to the 4-well multi-dish containing the 1 X streptavidin-HRP. Cover the wells with the lid.
15. Incubate the array for 30 min at room temperature on a rocking platform shaker.
16. Wash the array as described in steps 8 and 9.
17. Carefully remove the array from the dish. Allow excess wash buffer to drain from the array by blotting the lower edge onto paper towels. Return the array to the 4 well multi-dish and pipette 1 ml of the prepared chemi reagent mix evenly onto each array, and cover the lid. Incubate them for 1 min.
18. Carefully remove each array from the dish and allow excess wash buffer to drain from the membrane by blotting the lower edge onto paper towels. Place each array on a plastic sheet protector (the number on the array should be facing upward), then cover it with a transparent overlay template and take care to gently smooth out any air bubbles.
19. Place the array assemblies into the chamber of ChemiDoc for detection.
20. Present results as pixel density relative to the reference controls on the array.

## 2.8. ELISA

### 2.8.1. Principle

Like the proteome array, a ‘sandwich’ ELISA (enzyme-linked immunosorbent assay) is used to detect sample (cell culture media) antigen (pro-inflammatory factors in our studies).

Firstly, a 96-well ELISA microplate is coated with a known quantity of capture antibody that binds to a specific epitope of the antigen, any nonspecific binding sites are blocked with the reagent diluents; secondly, the antigen-containing sample is added to the plate for the capture antibody binding; thirdly, a detection antibody is added to bind to another epitope of the same antigen; finally, a HRP-linked secondary antibodies is added to nonspecifically binds to the detection antibody’s Fc region. The plate is washed to remove any unbound antigen, detection antibody and secondary antibody after each binding step (377).

Subsequently a substrate is added to be converted by HRP into a colormetric signal, the absorbance of which is measured to determine the presence and quantity of antigen (377).

### 2.8.2. General protocol

Before formal assays, several of the samples need to be diluted properly according to the results from the preliminary assays.

1. Prepare reagents and supplies as shown in Table 2.8.1, 2.

**Table 2.8.1 Preparation of the reagents for the ELISAs**

| Reagent | Preparation | Catalogue Number |
|---|---|---|
| Human IL-1β capture antibody | Reconstitute each vial (240 μg) with 0.5 ml of PBS, dilute in PBS to the working concentration (4 μg/ml) before assay. | R&D Systems, DY201-05 |
| Human IL-1β detection antibody | Reconstitute each vial (12 μg) with 1 ml of reagent diluent, dilute in reagent diluent to the working concentration (200 ng/ml) before assay. | |

| | | |
|---|---|---|
| Human IL-1β standard | Reconstitute each vial (55 ng) with 0.5 ml of deionized water. A seven point standard curve using 2-fold serial dilutions in reagent diluent and a high standard of 250 pg/ml is recommended. | |
| Human IL-6 capture antibody | Reconstitute each vial (120 μg) with 0.5 ml of PBS, dilute in PBS to the working concentration (2 μg/ml) before assay. | R&D Systems, DY206-05 |
| Human IL-6 detection antibody | Reconstitute each vial (3 μg) with 1 ml of reagent diluent, dilute in reagent diluent to the working concentration (50 ng/ml) before assay. | |
| Human IL-6 standard | Reconstitute each vial (65 ng) with 0.5 ml of deionized water. A seven point standard curve using 2-fold serial dilutions in reagent diluent and a high standard of 600 pg/ml is recommended. | |
| Human IL-8 capture antibody | Reconstitute each vial (240 μg) with 0.5 ml of PBS, dilute in PBS to the working concentration (4 μg/ml) before assay. | R&D Systems, DY208-05 |
| Human IL-8 detection antibody | Reconstitute each vial (1.2 μg) with 1 ml of reagent diluent, dilute in reagent diluent to the working concentration (20 ng/ml) before assay. | |
| Human IL-8 standard | Reconstitute each vial (40 ng) with 0.5 ml of deionized water. A seven point standard curve using 2-fold serial dilutions in reagent diluent and a high standard of 2000 pg/ml is recommended. | |
| Human CCL-2/MCP-1 capture antibody | Reconstitute each vial (60 μg) with 0.5 ml of PBS, dilute in PBS to the working concentration (1 μg/ml) before assay. | R&D Systems, DY279-05 |
| Human CCL-2/MCP-1 detection antibody | Reconstitute each vial (3 μg) with 1 ml of reagent diluent, dilute in reagent diluent to the working concentration (50 ng/ml) before assay. | |
| Human CCL-2/MCP-1 standard | Reconstitute each vial (70 ng) with 0.5 ml of deionized water. A seven point standard curve using 2-fold serial dilutions in reagent diluent and a high standard of 1000 pg/ml is recommended. | |
| Human CCL-5/RANTES capture antibody | Reconstitute each vial (60 μg) with 0.5 ml of PBS, dilute in PBS to the working concentration (1 μg/ml) before assay. | R&D Systems, DY278-05 |
| Human CCL-5/RANTES detection antibody | Reconstitute each vial (1.2 μg) with 1 ml of reagent diluent, dilute in reagent diluent to the working concentration (20 ng/ml) before assay. | |
| Human CCL-5/RANTES standard | Reconstitute each vial (60 ng) with 0.5 ml of deionized Water. A seven point standard curve using 2-fold serial dilutions in reagent diluent and a high standard of 1000 pg/ml is recommended. | |
| Streptavidin-HRP | Dilute in reagent diluent according to the factor on the label | Within the kits |
| Wash Buffer | Dilute 25 times in distilled water | R&D Systems, WA126 |
| Substrate Solution | Mix substrate A and substrate B at 1:1 (100 μl of the mixture per sample) | R&D Systems, DY999 |

**Table 2.8.2 Supplies needed for the ELISAs**

| Supply | Catalog # | Supply | Catalogue Number |
|---|---|---|---|
| 96 Well microplate | R&D Systems, DY990 | Pipette and pipette tip | - |
| Plate sealer | R&D Systems, DY992 | Glovers | - |
| Dnase-free water | ThermoFisher 10977015 | Distilled water | - |
| PBS | R&D Systems, DY006 | Reagent diluent | R&D systems, DY995 |
| Paper towel | - | 500 ml Bottle | - |
| Trough | - | 15 ml Centrifugation tube | - |
| 25 ml Centrifugation tube | - | Universal tube | - |
| Stop solution | R&D systems, DY995 | Microplate reader | SPECTROstar Nano |

Plate preparation

1. Coat a 96-well microplate with 100 µl per well of the working dilution of Capture Antibody. Seal the plate and incubate overnight at room temperature.
2. Aspirate each well and wash it with Wash Buffer 3 times by filling each-well with wash buffer (200 µl) using a multi-channel pipette (complete removal of liquid at each step is essential for good performance). After the last wash, remove any remaining wash buffer by inverting the plate and blotting it against clean paper towels.
3. Block the plate by adding 200 µl of Reagent Diluent to each well. Incubate it at room temperature for 1 h.
4. Repeat the aspiration/wash as in step 2. The plate is now ready for sample addition.

Assay procedure

1. Add 100 µl of sample or the working dilutions of standards (as shown in Table 2.6.3.) or Blank (Reagent Diluent) per well. Cover the pate with plate sealer and incubate it for 2 h at room temperature.
2. Repeat the aspiration/wash as in step 2 of *plate preparation.*
3. Add 100 µl of the working dilution of Detection Antibody to each well. Cover the plated with a new plate sealer and incubate it for 2 h at room temperature.
4. Repeat the aspiration/wash as in step 2 of *plate preparation*.

5. Add 100 μl of the working dilution of detection streptavidin-HRP to each well. Cover the plate with a new plate sealer and incubate it for 20 min at room temperature. Avoid placing the plate in direct light.
6. Repeat the aspiration/wash as in step 2 of *plate preparation*.
7. Add 100 μl of substrate solution to each well. Cover the plate with a new plate sealer and incubate it for 20 min at room temperature. Avoid placing the plate in direct light.
8. Add 50 μl of stop solution to each well immediately, using a microplate reader to subtract readings at 540 nm from the readings at 450 nm.

Data analysis

1. Average the duplicate readings for each standard control and sample. Subtract the average optical density (O.D) of Blank.
2. Create a standard curve (the standard concentrations are shown in Table 2.8.3) by using computer software to generate a four parameter logistic (4-PL) curve-fit (if samples have been diluted, the concentration read from the standard curve must be multiplied by the dilution factor), as shown in Figure 2.6 - 10.

**Table 2.8.3 The standard concentrations of the ELISAs**

| Type | Concentration range ( pg/ml) | | | | | | |
|---|---|---|---|---|---|---|---|
| IL-1β | 250 | 125 | 62.5 | 31.3 | 15.6 | 7.8 | 3.9 |
| IL-6 | 600 | 300 | 150 | 75 | 37.5 | 18.8 | 9.4 |
| IL-8 | 2000 | 1000 | 500 | 250 | 125 | 62.5 | 31.3 |
| MCP-1 | 1000 | 500 | 250 | 125 | 62.5 | 31.3 | 15.6 |
| RANTES | 1000 | 500 | 250 | 125 | 62.5 | 31.3 | 15.6 |

**Figure 2.6 The standard curve of IL-1β (4-PL curve fit)**

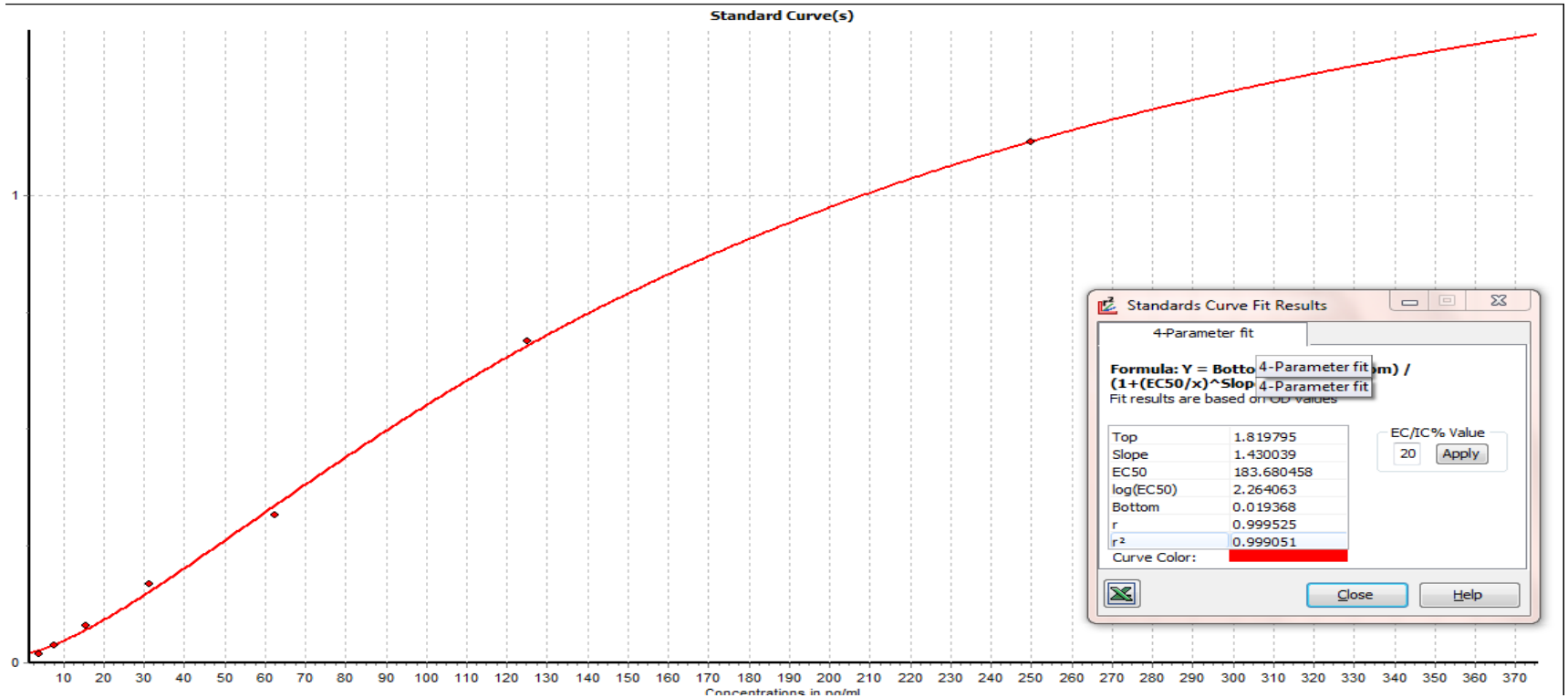

**Figure 2.7 The standard curve of IL-6 (4-PL curve fit)**

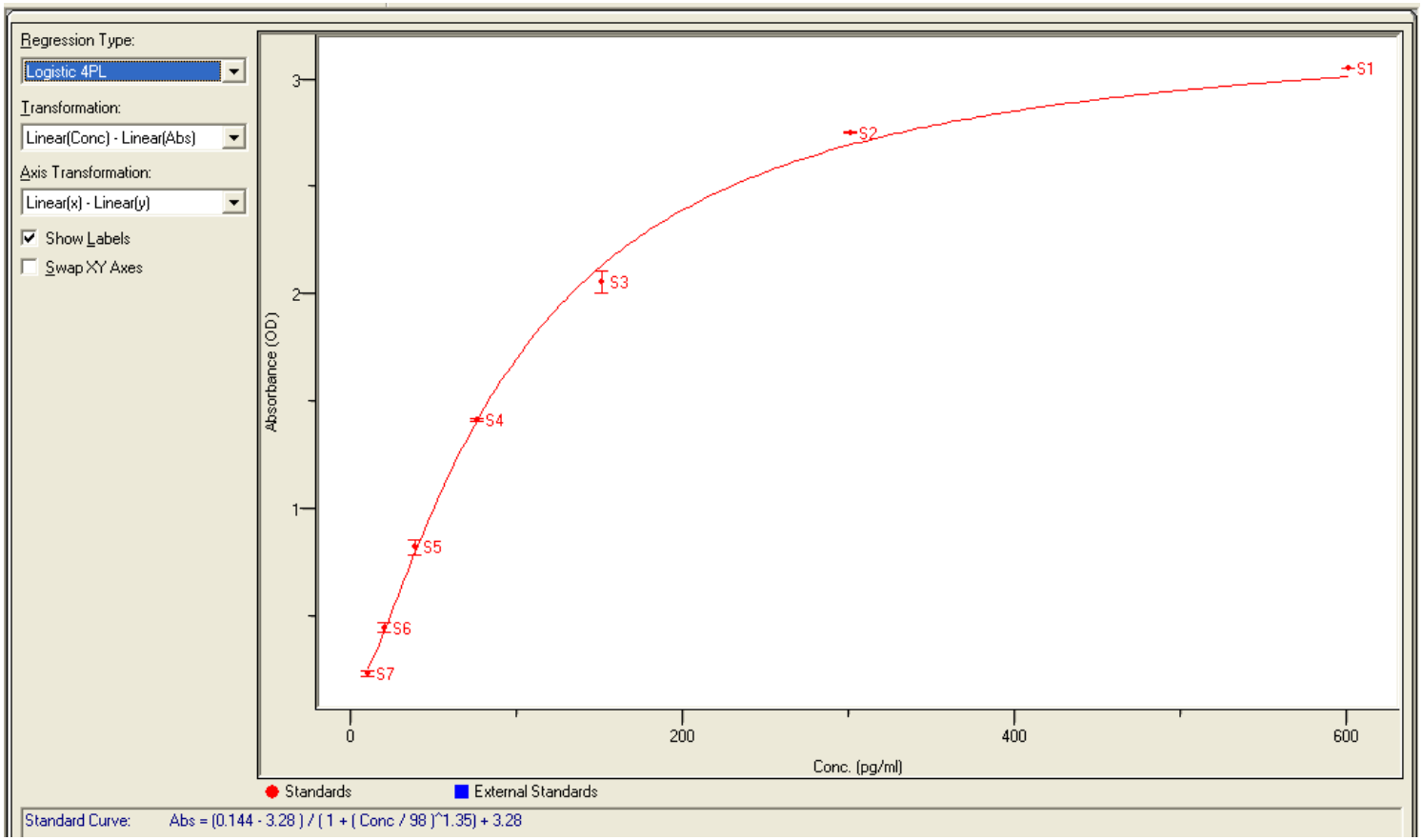

**Figure 2.8 The standard curve of IL-8 (4-PL curve fit)**

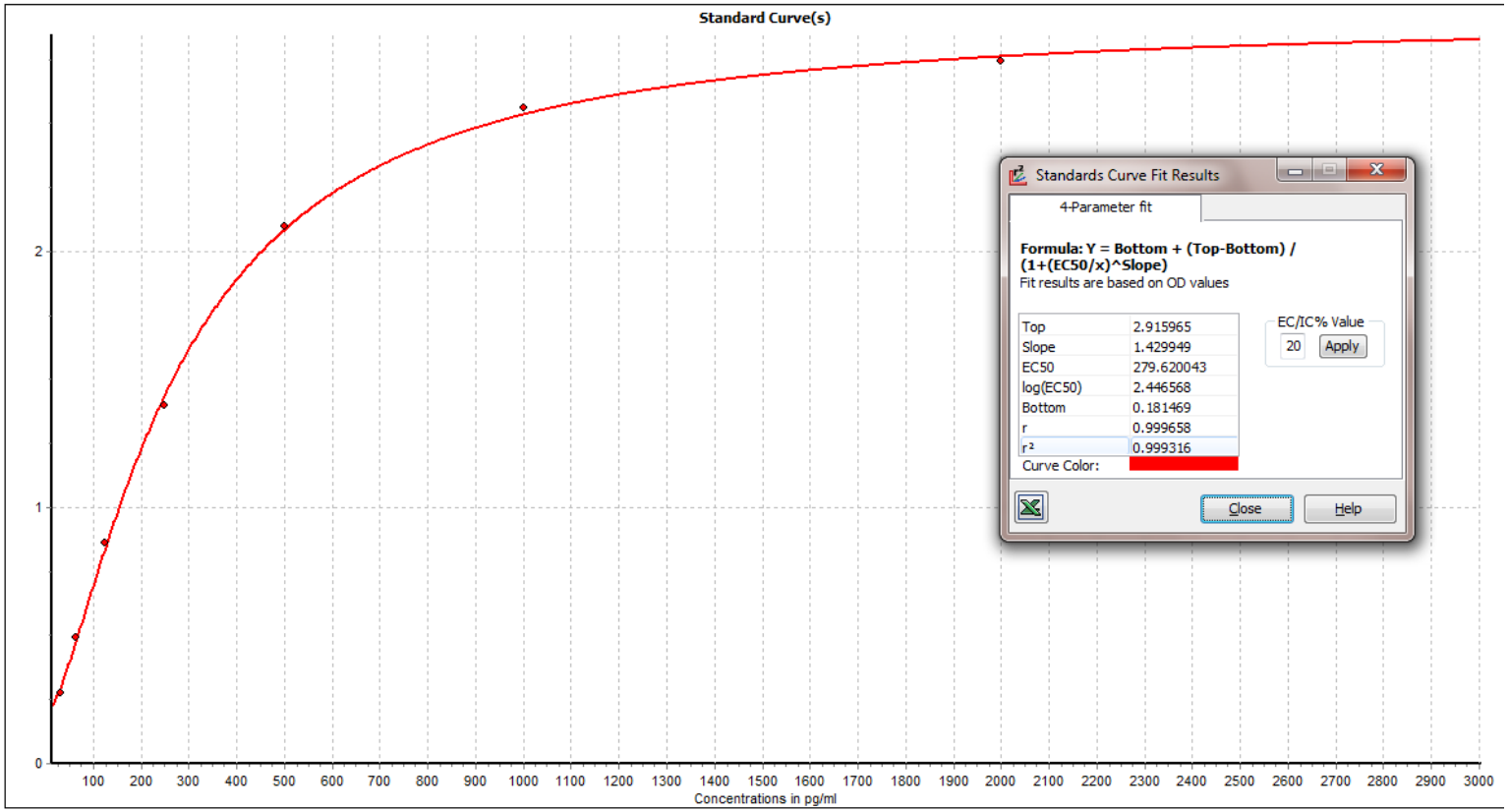

**Figure 2.9 The standard curve of MCP-1 (4-PL curve fit)**

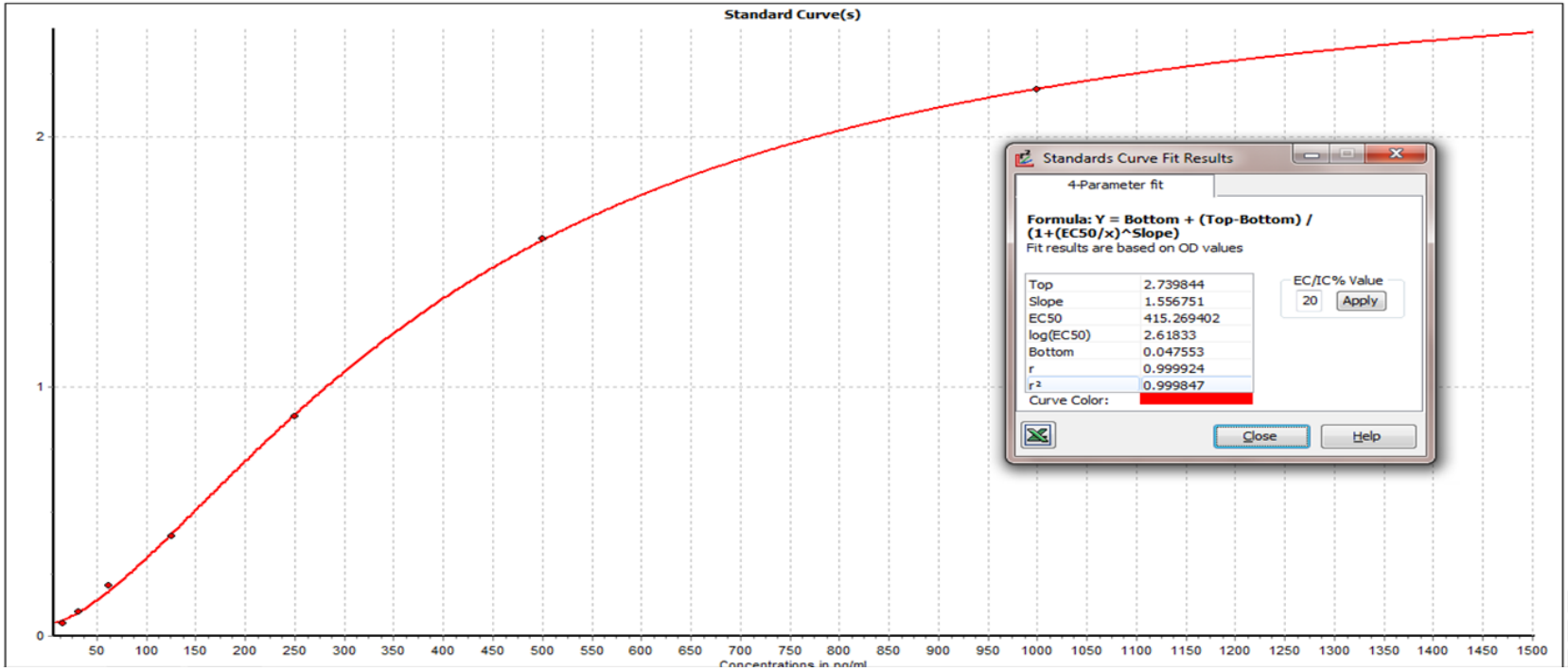

**Figure 2.10 The standard curve of RANTES (4-PL curve fit)**

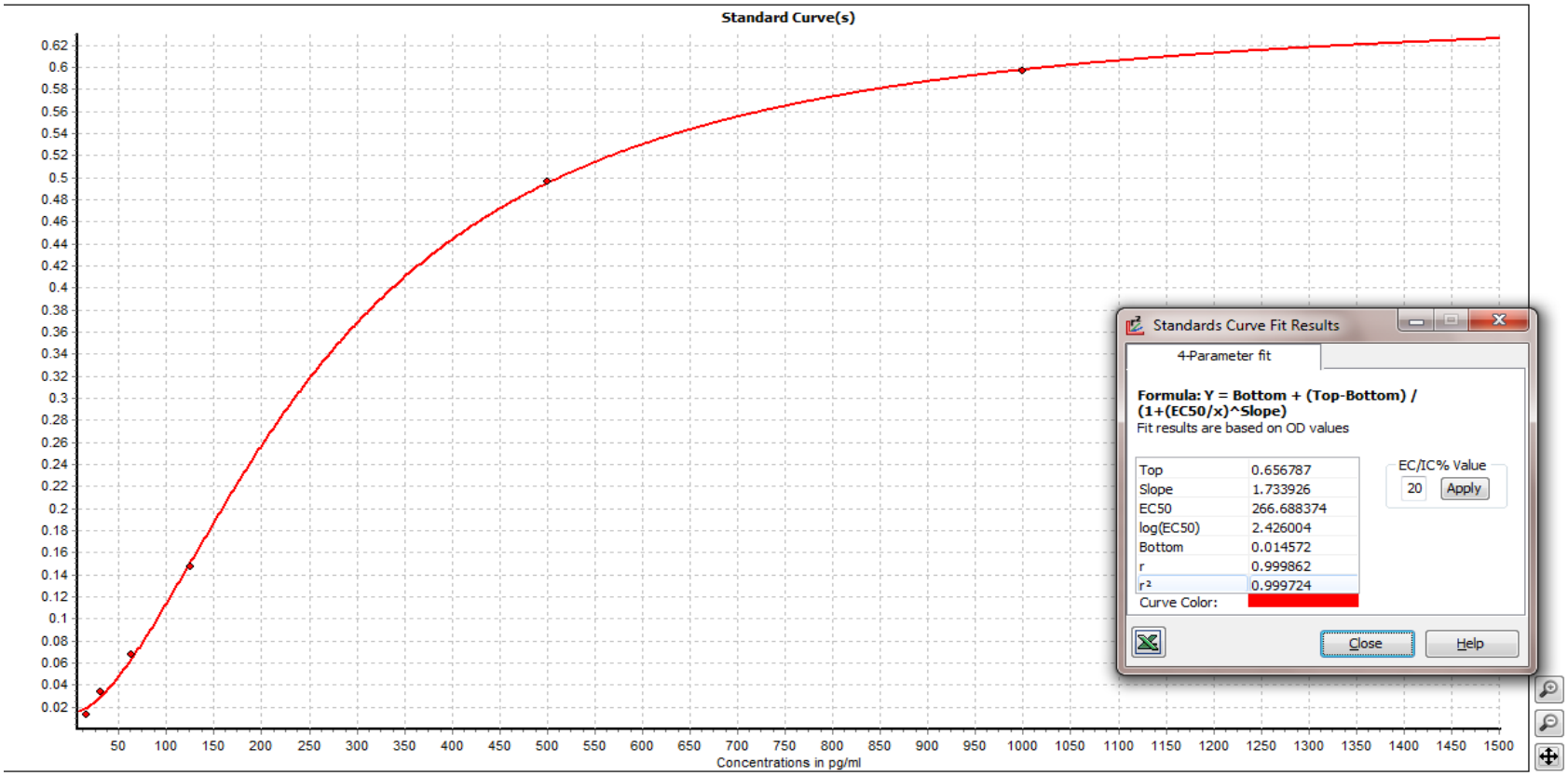

## 2.9. Total RNA isolation and Quantification

### 2.9.1. Principle

Trizol is a monophasic solution of phenol, guanidine isothiocyanate, and other proprietary components which facilitate the isolation of a variety of RNA species of large or small molecular size, and maintains the integrity of RNA due to the highly effective inhibition of RNase activity while disrupting cells and dissolving cell components (378).

Chloroform is added to Trizol-dissolved samples (the treated preadipocytes in our studies), and the homogenate is allowed to separate into a clear upper aqueous layer (containing RNA), an interphase, and a red lower organic layer (containing the DNA and proteins), and then RNA is precipitated from the aqueous layer with isopropanol. The precipitated RNA is washed with ethanol to remove impurities, and then resuspended in DNase-free water for purity determination and quantification.

### 2.9.2. Supply preparation

Prepare supplies as shown in Table 2.9.1.

**Table 2.9.1 Supplies required for total RNA isolation and quantification**

| Supply | Catalogue Number | Supply | Catalogue Number |
|---|---|---|---|
| 1.5 ml EP tube | - | Pipette and pipette tip | - |
| Glovers | - | Fume hood | - |
| goggles | - | Distilled water | - |
| Centrifuge | - | mixer | - |
| ice | - | container | - |
| chloroform | Sigma 288306-100 ML | isopropanol | Sigma 19516-500 ML |
| 75% ethanol (in water) | Sigma 51976-500 ML-F | DNase-free water | ThermoFisher 10977015 |
| NanoDrop | Thermo Scientific | Tube rack | - |

### 2.9.3. Total RNA isolation

The following procedures are operated in a fume cupboard. Always use the appropriate precautions to avoid RNase contamination when preparing and handling RNA.

Phase separation

1. Incubate the frozen (-80°C) Trizol-dissolved cell sample (250 µl) for 5 min at room temperature to permit the complete dissociation of the nucleoprotein complex.
2. Add 100 µl of chloroform into each of the samples.
3. Shake the mixture of chloroform and sample vigorously for 15 min.
4. Centrifuge the mixture at 14,000 rpm for 15 minutes at 4°C to create the three phases, the aqueous layer of which contains RNA.
5. Transfer the aqueous layer to a new 1.5 ml tube by angling the tube at 45º and pipetting the solution out (approximately 50 – 100 µl). Avoid drawing any of the interphase or organic layer into the pipette when removing the aqueous layer.

RNA precipitation

1. Add 25 µl of isopropanol into each of the aqueous samples and vortex the mixture thoroughly.
2. Stand the mixture for 10 min at room temperature.
3. Centrifuge the mixture at 14,000 rpm for 10 min at 4°C to wash off any DNA contamination.
4. Remove the supernatant to a new 1.5 ml tube.
5. Add 225 µl of isopropanol into each of the supernatants and vortex the mixture thoroughly. The RNA is often invisible at this stage and forms a gel-like pellet on the side and bottom of the tube.
6. Stand the mixture for 10 min at room temperature then centrifuge it at 14,000 rmp for 10 min at 4°C.
7. Remove the supernatant from the tube, leaving only the RNA pellet.

RNA wash

1. Add 100 µl of 75% ethanol onto the pellet and centrifuge the mixture at 14,000 rpm for 10 min at 4°C.
2. Remove the supernatant from the tube, and air dry the RNA pellet for 5-10 min. Do not allow the RNA to dry completely, because the pellet can lose solubility.

RNA resuspension

1. Dissolve the RNA pellet in 10 µl RNase-free water by passing the solution up and down several times through a pipette tip.
2. Proceed to downstream applications, or store at -80°C.

### 2.9.4. RNA quantification

Making RNA measurement

1. Bring the samples of isolated RNA to be quantified out of -80°C freezer and chill them in an ice-box.
2. Select the **Nucleic Acid** application from the main menu of the analytic software of the NanoDrop spectrophotometer. If the wavelength verification window appears, ensure the arm is down and click **OK**.
3. Select **RNA-40** from the Type drop-down list and choose **µg/µl** as the concentration unit from the drop-down list adjacent to the color codes concentration box.
4. Select **Add to report** to automatically include all measurements in the current report. The **Add to report** checkbox must be selected prior to a measurement to save the same data to a workbook.
5. Select **Overlay spectra** to display multiple spectra at a time.
6. Pipette 1µl of DNase water as blanking solution onto the bottom pedestal, lower the arm and

click the **Blank** button. The arm must be down for all measurements.

7. Enter a Sample ID in the appropriate filed, load the first sample as described for the blank calibration above and click **Measure**. ~2.0 (the ratio of A260/280) is generally accepted as "pure" for RNA. Abnormal 260/280 ratios usually indicate that the sample is either contaminated by protein or a reagent such as phenol or that there was an issue with the measurement. A lower A260/A280 ratio may be caused by: residual phenol or other reagent associated with the RNA isolation protocol; a very low concentration (<10 ng/μl) of nucleic acid. Whereas a high 260/280 ratio indicates RNA degradation. In addition, the 260/230 values for "pure" nucleic acid are commonly in the range of 2.0-2.2.

After the measurement

1. Simply wipe the upper and lower pedestals using a dry laboratory wipe and the instrument is ready to measure the next sample.
2. Export the report as saving it as **Report, Excel X ML Spreadsheet** (***x ml**) until the last sample has been measured, as shown in Figure 2.11.
3. Print the report out and dilute part of the sample to 0.1 μg/μl according to its yield and purity (the volume of the diluted sample should be higher than 5 μl), then proceed to reverse transcription, or store the un-diluted and diluted samples in the -80°C freezer.

**Figure 2.11 A report exported by NanoDrop in Excel spreadsheet**

| | A | B | C | D | E | F | G | H | I | J | K | L |
|---|---|---|---|---|---|---|---|---|---|---|---|---|
| | # | Sample ID | User name | Date and Time | Nucleic Acid Conc. | Unit | A260 | A280 | 260/280 | 260/230 | Sample Type | Factor |
| 2 | 1 | c1 | nanodrop | 2016/4/28 19:10 | 0.5753 | ng/µl | 14.382 | 7.686 | 1.87 | 0.95 | RNA | 40 |
| 3 | 2 | c2 | nanodrop | 2016/4/28 19:38 | 0.6778 | ng/µl | 16.945 | 9.329 | 1.82 | 1.1 | RNA | 40 |
| 4 | 3 | c3 | nanodrop | 2016/4/28 19:39 | 0.8819 | ng/µl | 22.048 | 12.127 | 1.82 | 0.7 | RNA | 40 |
| 5 | 4 | il1b1 | nanodrop | 2016/4/28 19:40 | 1.0081 | ng/µl | 25.204 | 13.537 | 1.86 | 1.15 | RNA | 40 |
| 6 | 5 | il1b2 | nanodrop | 2016/4/28 19:41 | 2.2997 | ng/µl | 57.492 | 32.137 | 1.79 | 1.33 | RNA | 40 |
| 7 | 6 | il1b3 | nanodrop | 2016/4/28 19:42 | 0.6816 | ng/µl | 17.039 | 9.376 | 1.82 | 0.97 | RNA | 40 |
| 8 | 7 | 8461 | nanodrop | 2016/4/28 19:43 | 0.6264 | ng/µl | 15.66 | 8.426 | 1.86 | 1.02 | RNA | 40 |
| 9 | 8 | 8462 | nanodrop | 2016/4/28 19:44 | 0.5096 | ng/µl | 12.741 | 6.802 | 1.87 | 0.78 | RNA | 40 |
| 10 | 9 | 8463 | nanodrop | 2016/4/28 19:45 | 0.6746 | ng/µl | 16.864 | 9.249 | 1.82 | 1.01 | RNA | 40 |
| 11 | 10 | 8481 | nanodrop | 2016/4/28 19:46 | 0.5962 | ng/µl | 14.905 | 7.963 | 1.87 | 0.84 | RNA | 40 |
| 12 | 11 | 8482 | nanodrop | 2016/4/28 19:47 | 0.6918 | ng/µl | 17.294 | 9.69 | 1.78 | 0.99 | RNA | 40 |
| 13 | 12 | 8483 | nanodrop | 2016/4/28 19:48 | 0.8612 | ng/µl | 21.531 | 11.586 | 1.86 | 1.09 | RNA | 40 |
| 14 | 13 | 2261 | nanodrop | 2016/4/28 19:49 | 1.1985 | ng/µl | 29.963 | 17.669 | 1.7 | 0.43 | RNA | 40 |
| 15 | 14 | 2262 | nanodrop | 2016/4/28 19:50 | 1.6166 | ng/µl | 40.414 | 23.792 | 1.7 | 0.49 | RNA | 40 |
| 16 | 15 | 2263 | nanodrop | 2016/4/28 19:51 | 1.3604 | ng/µl | 34.011 | 20.488 | 1.66 | 0.43 | RNA | 40 |
| 17 | 16 | 2281 | nanodrop | 2016/4/28 19:52 | 0.6491 | ng/µl | 16.228 | 8.846 | 1.83 | 0.95 | RNA | 40 |
| 18 | 17 | 2282 | nanodrop | 2016/4/28 19:53 | 0.5297 | ng/µl | 13.243 | 7.111 | 1.86 | 0.86 | RNA | 40 |
| 19 | 18 | 2283 | nanodrop | 2016/4/28 19:54 | 0.6128 | ng/µl | 15.32 | 8.208 | 1.87 | 0.87 | RNA | 40 |
| 20 | 19 | v81 | nanodrop | 2016/4/28 19:54 | 0.6667 | ng/µl | 16.669 | 9.155 | 1.82 | 0.97 | RNA | 40 |
| 21 | 20 | v82 | nanodrop | 2016/4/28 19:55 | 0.6587 | ng/µl | 16.469 | 8.938 | 1.84 | 0.95 | RNA | 40 |
| 22 | 21 | v83 | nanodrop | 2016/4/28 19:56 | 0.3212 | ng/µl | 8.03 | 4.415 | 1.82 | 0.54 | RNA | 40 |
| 23 | | | | | | | | | | | | |
| 24 | | | | | | | | | | | | |

## 2.10. Reverse transcription and qPCR

### 2.10.1. Principle

The RNA template is first converted into a cDNA (complementary DNA) using a reverse transcriptase. The cDNA is then used as a template for exponential amplification using TaqMan qPCR (quantitative real-time polymerase chain reaction) (379).

The TaqMan probe consist of a fluorophore (FAM, 6-carboxy fluorescein) covalently attached to the 5'-end of the oligonucleotide probe and a quencher at the 3'-end (380). When the fluorophore and the quencher are in proximity, quenching inhibits any fluorescence signals (380). As Taq polymerase extends a specific set of primers and synthesizes nascent strands, the 5' to 3' exonuclease activity of the Taq polymerase degrades the probe that has annealed within the DNA region amplified by the set of primers. The degradation of probe releases the fluorophore from itself and breaks the close proximity to the quencher, thereby relieving the quenching effect and allowing the fluorescence emitted by the fluorophore when excited by the cycler's light source via Förster Resonance Energy Transfer (381).

Hence, the fluorescence detected in the quantitative PCR thermal cycler is directly proportional to the fluorophore released and the amount of cDNA template present in the qPCR.

In addition, a good internal control (with consistent expression levels under experimental conditions) is critical in all quantitative analyses of gene expression, and serial analysis of gene expression on various human samples (brain, breast, colon, pancreas and prostate) has shown that PPIA (peptidylprolyl isomerase A) is a better internal control than β-actin or GAPDH (382) (Figure 2.12).

**Figure 2.12 The consistent expression levels of PPIA**

(A) Chapter 3, (B) Chapter 4, (C) Chapter 5, (D) Chapter 6. Data are means ± SEM for groups of 6. The results were determined using one-way ANOVA with Tukey's post hoc test and confirmed by two independent experiments.

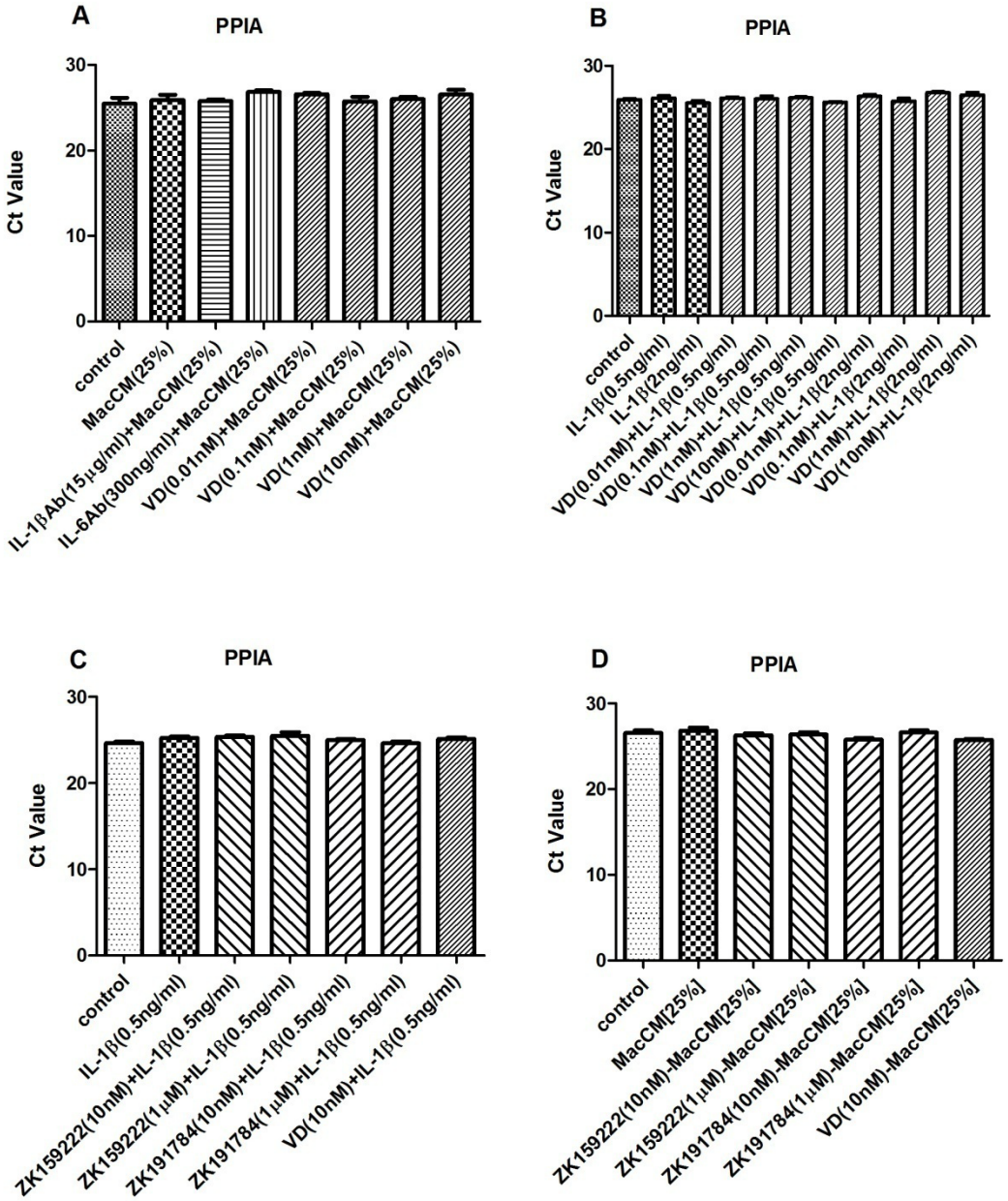

### 2.10.2. Supply preparation

Prepare supplies as shown in Table 2.10.1, 2.

**Table 2.10.1 The sequences of primer sets and probes of the TaqMan assays**

| Gene name | Forward primer | Reverse primer | Probe |
|---|---|---|---|
| **PPIA** | ACGGCGAGCCCTTGG | TTTCTGCTGTCTTTGGGACCT | CGCGTCTCCTTTGAGCTGTTTGCA |
| **IL-1β** | CGGCCACATTTGGTTCTAAGA | AGGGAAGCGGTTGCTCATC | ACCCTCTGTCATTCG |
| **IL-6** | CCTGAACCTTCCAAAGATGG | ACCAGGCAAGTCTCCTCATT | CCAGATTGGAAGCATCCATCTTTTTCA |
| **IL-8** | TGAGAGTGGACCACACTGCG | GCACCCAGTTTTCCTTGGGG | CCAGACAGAGCTCTCTTCCATCAGAAAG |
| **MCP-1** | CGCCTCCAGCATGAAAGTCT | GGAATGAAGGTGGCTGCTATG | TGCCGCCCTTCTGTGCCTGC |
| **RANTES** | TGCATCTGCCTCCCCATATT | AGTGGGCGGGCAATGTAG | CTCGGACACCACACCCTGCTGCT |

**Table 2.10.2 Supplies required for reverse transcription and qPCR**

| Supply | Catalogue Number | Supply | Catalogue Number |
|---|---|---|---|
| 1.5 ml EP tubes | - | Pipette and pipette tip | - |
| Glovers | - | Fume hood | - |
| goggles | - | Distilled water | - |
| Centrifuge | - | Dnase-free water | ThermoFisher 10977015 |
| ice | - | 0.2 ml PCR tube | - |
| 96-wells PCR plate | Star Lab l1402-9700 | Sealing film | Star Lab E2796-3020 |
| Timer | - | Universal tube | - |
| qPCR machine (Mx3000P) | Agilent Technologies | PCR machine | Bio-Rad T100 Thermo Cycler |
| cDNA synthesis kit | Bio-Rad #1708890EDU | qPCR core kit | Eurogentec RT-QP73-05 |
| IL-1β TaqMan assay | Applied Biosystems | IL-6 TaqMan assay | Applied Biosystems |
| IL-8 TaqMan assay | Applied Biosystems | MCP-1 TaqMan assay | Applied Biosystems |
| RANTES TaqMan assay | Applied Biosystems | PPIA TaqMan assay | Applied Biosystems |

### 2.10.3. Reverse transcription

1. Add the following to 0.2 ml tubes to make master mix shown in Table 2.10.3.

**Table 2.10.3 Preparation of the master mix of for the reverse transcription**

| Component | Volume (n = samples) |
|---|---|
| Dnase-free water | 2.5 µl x n |
| 5X Buffer | 2 µl x n |
| iScript enzyme | 0.5 µl x n |
| Total volume | 5 µl x n |

2. Add 0.5 µl of RNA sample (0.1 µg/µl) to the master mix to be reverse-transcribed.
3. Add 0.5µl of Dnase-free water to set up the negative control.
4. Vortex and pulse down the tubes containing the reaction mixture.
5. Heat the tubes at 25°C for 5 min.
6. Heat the tubes at 42°C for 30 min.
7. Heat the tubes at 85°C for 5 min.
8. Freeze the tubes at -20°C for storage, or proceed to qPCR.

### 2.10.4. qPCR

1. Add the following to a 1.5 ml tube to make master mix shown in Table 2.10.4.

**Table 2.10.4 Preparation of the master mix of for the qPCR assays**

| Component | Volume (n = samples) |
|---|---|
| Dnase-free water | 7.8125 µl x n |
| 10X Buffer | 1.25 µl x n |
| $MgCl_2$ | 1.25 µl x n |
| dNTP | 0.5 µl x n |
| 20X TaqMan mix (probes and primers) | 0.625 µl x n |
| GoldStar enzyme | 0.0625 µl x n |
| Total volume | 11.5 µl x n |

2. Add the master mix to a 96-well PCR plate (one reaction per well)
3. Add 1 µl of cDNA sample (in duplicate, including the negative control) to the master mix.
4. Add 1 µl of Dnase-free water to set up the non-template control.

5. Seal the plate and pulse down.
6. Load the plate into a PCR machine and start MxPro program using the thermo profile as 95°C 10min; 95°C 15 sec, 60°C 1 min (40 cycles).
7. After the PCR run, select **Analysis** on the top panel of the plate document page and choose the **Analysis Selection/Setup page**.
8. Select the **Results** page to define the Threshold Value. Use **Log** View (**Y-Axis**) of the **amplification plots**. Place the threshold line above the background signal but in the half of the linear phase of the amplification plot, as shown in Figure 2.13.
9. Select **Text Report** in **Area to analyze** to display the results including the **Column** for **Well**, **Well type**, **Threshold**, **Ct** for each well. **Export** the **Text Report to Excel** and save it as an Excel file.

Data analysis

1. All samples are normalized to the values of PPIA (internal control) (383) and the results are presented as fold changes of Ct value relative to controls using the $2^{-\Delta\Delta ct}$ formula (384).

**Figure 2.13 The log view (y-axis) of IL-1β amplification plot**

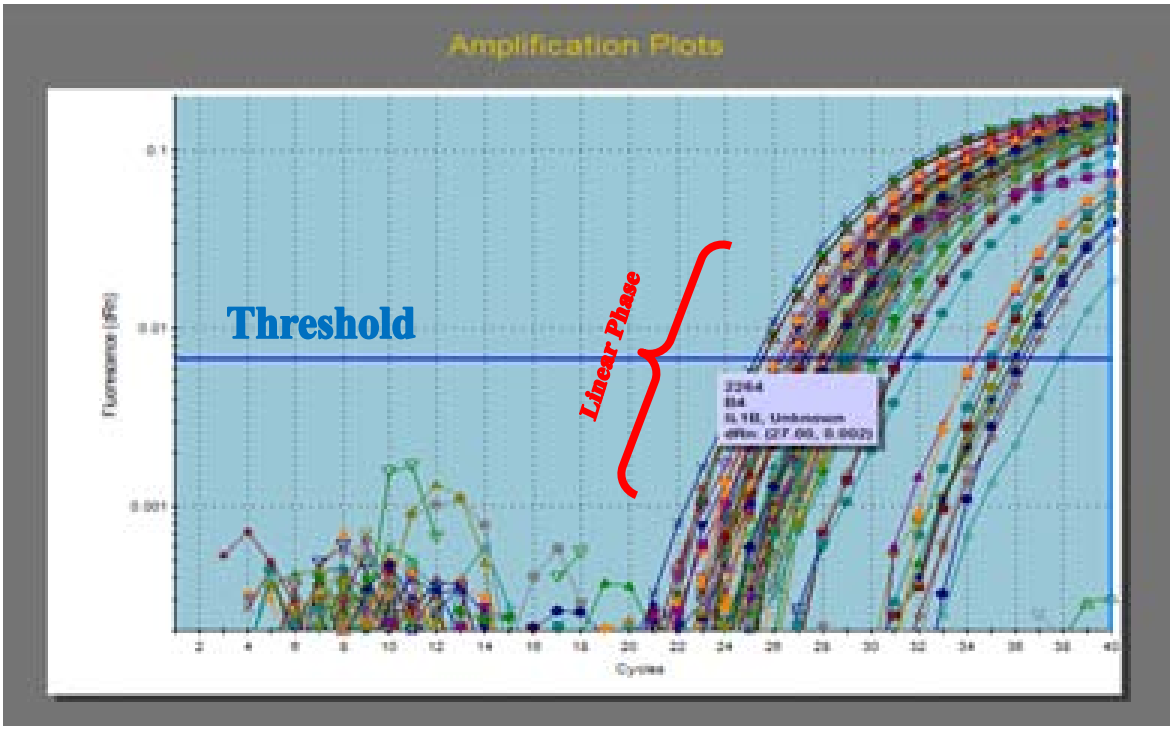

## 2.11. BCA protein assay

### 2.11.1. Principle

The (bicinchoninic acid) BCA protein assay is a biochemical assay for determining the total concentration (0.5 μg/ml to 1.5 mg/ml) of protein in a sample (cell lysates in our studies). Firstly, the peptide bonds in protein reduce $Cu^{2+}$ ions from the copper (II) sulfate to $Cu^{+}$ (a temperature dependent reaction). The amount of $Cu^{2+}$ reduced is proportional to the amount of protein present in the solution. Secondly, two molecules of bicinchoninic acid chelate with each $Cu^{+}$ ion, forming a purple-colored complex that strongly absorbs light at a wavelength of 562 nm. The concentration of protein present in the sample can be quantified by measuring the absorption spectra and comparing with protein solutions of known concentration (385).

### 2.11.2. General protocol

1. Prepare supplies as shown in Table 2.11.1.

**Table 2.11.1 Supplies required for BCA protein assay**

| Supply | Catalogue Number | Supply | Catalogue Number |
|---|---|---|---|
| BCA protein assay kit | ThermoFisher 23227 | Pipettes and pipette tips | - |
| Glovers | - | Fume hood | - |
| Dnase-free water | ThermoFisher 10977015 | 1.5 ml tube | - |
| Centrifuge | - | mixer | - |
| Tube rack | - | container | - |
| Sealing film | Star Lab E2796-3020 | 96-well microplate | ThermoFisher 15045 |
| Microplate reader | - | Ice | |

Preparation of standards

1. Prepare a set of protein standards as shown in Table 2.11.2. Dilute the contents of one BSA (bovine serum albumin) ampoule (concentration: 2,000 μg/ml) into several clean vials (using

Dnase-free water as the diluent).

**Table2.11.2 The preparation of BSA standards**

| Dilution Scheme (Working Range = 20-2,000 µg/ml) | | | |
|---|---|---|---|
| Vial | Volume of diluent original (µl) | Volume and source of BSA (µl) | BSA concentration (µl) |
| A | 0 | 300 of Stock | 2000 |
| B | 125 | 375 of Stock | 1500 |
| C | 325 | 325 of Stock | 1000 |
| D | 175 | 175 of vial B dilution | 750 |
| E | 325 | 325 of vial C dilution | 500 |
| F | 325 | 325 of vial E dilution | 250 |
| G | 325 | 325 of vial F dilution | 125 |
| H | 400 | 100 of vial G dilution | 25 |
| I | 400 | 0 | 0 = Blank |

Preparation of the BCA WR (working reagent)

1. Use the following formula to determine the total volume of WR required
   (# standards + # unknowns) × (2) × (200 µl) = total volume WR required.
2. Prepare WR by mixing 50 parts of BCA Reagent A with 1 part of BCA Reagent B. Note: When Reagent B is first added to Reagent A, turbidity is observed that quickly disappears upon mixing to yield a clear, green WR. Prepare sufficient volume of WR based on the number of samples to be assayed.

Microplate procedure

1. Pipette 10 µl of each standard or unknown sample replicate into a 96-well plate (working range = 125-2000 µg/ml)
2. Add 200 µl of the WR to each well and mix the plate thoroughly on a plate shaker for 30 sec.
3. Cover the plate and incubate it at 37°C for 30 min.
4. Cool the plate to room temperature. Measure the absorbance at 562 nm on a spectrometer.
5. Subtract the average 562 nm absorbance measurement of the Blank standard replicates from

the 562 nm measurements of all other individual standard and unknown sample replicates.

6. Prepare a standard curve by plotting the average Blank-corrected 562 nm measurement for each BSA standard vs. its concentration in µg/ml. Use the standard curve to determine the protein concentration of each unknown sample. Note: linear curve-fitting is used to plot the standard curve, as shown in Figure 2.14.

**Figure 2.14 The standard curve for BCA (linear fit curve)**

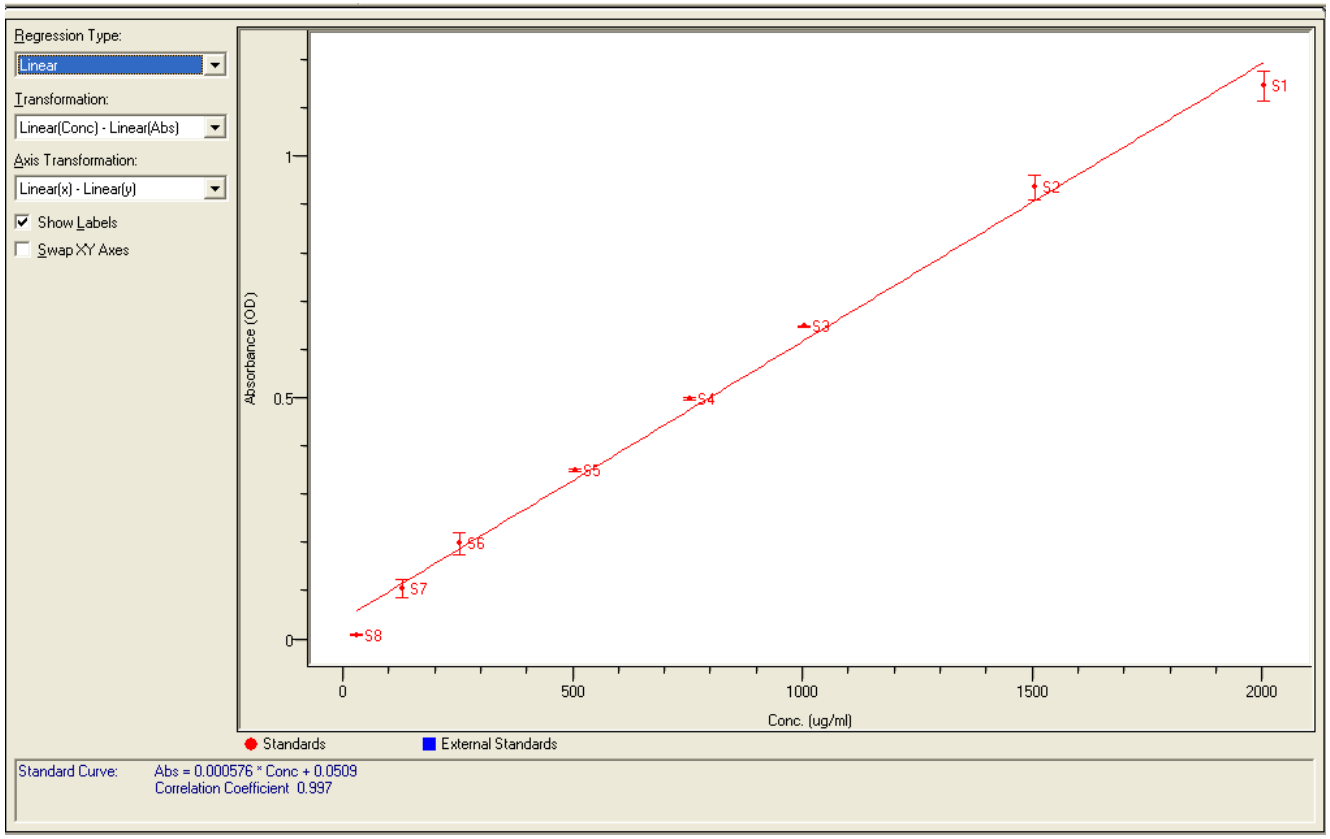

## 2.12. Western blotting

### 2.12.1. Principle

Western blotting is a widely accepted analytical technique used to detect specific proteins in a given sample (denatured cell lysates in our studies). It could detect target protein which is as low as 1 ng due to the high resolution of gel electrophoresis and strong specificity and high sensitivity of immunoassay (386).

Firstly, SDS-PAGE (sodium dodecyl sulfate–polyacrylamide gel electrophoresis) is applied to separate various proteins contained in the given sample by the length of the polypeptide. Secondly, the separated proteins are transferred onto a nitrocellulose membrane, where they are probed with the primary antibodies, and then the HRP-linked secondary antibodies. The binding between the primary and secondary antibodies emits a chemiluminescent signal (protein band) when reacting with an enhanced chemiluminescent substrate, which can be detected and measured by an X-ray scanner. By analyzing location and intensity of the signals, expression details of the target proteins in the given samples could be obtained (386).

### 2.12.2. Supply preparation

Prepare supplies as shown in Table 2.12.1.

**Table 2.12.1 Supplies required for western blotting**

| Supply | Catalogue Number | Supply | Catalogue Number |
|---|---|---|---|
| Pipette and pipette tip | - | Universal tube | - |
| 1.5 ml tube | - | Fume hood | - |
| gloves | - | Dnase-free water | ThermoFisher 10977015 |
| Centrifuge | - | mixer | - |
| Acrylamide kit | Bio-Rad 1610173 | 10% APS (in water) | Bio-Rad 1610700 |
| TEMED | Bio-Rad 1610800 | Short plate | Bio-Rad 1653308 |
| 1.5 mm spacer plate | Bio-Rad 1653312 | Casting stand and clamps | Bio-Rad 1658050 |

| | | | |
|---|---|---|---|
| Combs, 15-wells, 1.5 mm | Bio-Rad 1653366 | Electrophoresis cell | Bio-Rad 1658004 |
| PowerPac | Bio-Rad 1645050 | Gel releaser | Bio-Rad 1653320 |
| Transfer pack | Bio-Rad 1704159 | Roller | Bio-Rad 1651279 |
| Transfer system | Bio-Rad 1704150 | Tweezers | - |
| Plastic containers | - | 500 ml bottles | - |
| Shaker | - | Paper towel | - |
| Protein marker | Bio-Rad 1610374 | Trizma base | Sigma T1503-500G |
| Tricine | Sigma T0377-100G | SDS | Sigma L3771-100G |
| HCl | Sigma H1785-500 ML | Glycerol | Sigma G5516-100 ML |
| Beta-mercaptoethanol | Sigma 465348-5G | Bromophenol Blue | Sigma B0126-25G |
| NaCl (sodium chloride) | SigmaS3014-5KG | Tween-20 | Sigma P9416-50 ML |
| BSA | Sigma 2153-50G | Chemiluminescent substrate | Thermo scientific 2161465 |
| ChemiDoc | - | PH meter | - |
| Plastic wrap | - | 250 ml beaker | - |
| Seal bag | - | Marker | - |
| Heating block | | | |

### 2.12.3. Preparation of gel

1. Prepare resolving gel acrylamide solution by combining equal volumes of resolver A and B solutions in a clean tube (see Table 2.12.2).
2. Hold Mini-PROTEAN plastic cassettes vertically for gel casting. Use a single-row AnyGel™ casting stand to stabilize the cassette during casting. For Bio-Rad handcast glass plates, use a Mini-PROTEAN Tetra cell casting stand to stabilize the plates during casting.
3. Add the required volume of TEMED (tetramethylethylenediamine) and freshly made 10% APS (ammonium persulfate) to the combined resolver solution and mix well. Use 1 ml pipette tip to steadily dispense the solution into the cassette. Do not let bubbles form or solution mix with air. Fill the cassette to 0.5–1 cm below the bottom of the teeth of the comb. Immediately prepare and pour the stacking solution as directed in the next steps.
4. Prepare stacking gel acrylamide solution by combining equal volumes of stacker A and B solutions in a clean tube (see Table 2.12.2).
5. Add required volume of TEMED and freshly made 10% APS to the combined stacker solution and mix well. Pipette solution down the middle of the cassette, filling to the top of

the short plates. Apply slowly and steadily to prevent mixing with the resolving solution. Align and insert the comb in the cassette carefully to prevent air from being trapped under the comb teeth. Allow the gel to polymerize for 30–45 min before electrophoresis.

**Table2.12.2. Preparation of acrylamide gels**

| | 1.5 mm Bio-Rad glass plate (n = gels) | |
|---|---|---|
| | Stacker | Resolver |
| Resolver A | - | 4 ml x n |
| Resolver B | - | 4 ml x n |
| Stacker A | 1.5 ml x n | - |
| Stacker B | 1.5 ml x n | - |
| Total Volume | **3** ml x n | **8** ml x n |
| TEMED | 3 µl x n | 4 µl x n |
| 10% APS | 15 µl x n | 40 µl x n |

### 2.12.4. Electrophoresis

1. Prepare the buffers shown in table 2.12.3.

**Table 2.12.3 Preparation of the buffers for electrophoresis**

| Type | Recipe |
|---|---|
| 1 x Cathode buffer | 100 mM Tris, 100 mM Tricine, 0.1% SDS |
| 1 x Anode buffer | 100 mM Tris-HCl, pH 8.9 |
| 5 x Sample loading buffer | 5% SDS, 50% Glycerol, 0.1% Bromophenol blue, 5% beta-mercaptoethanol, 250 mM Tris-HCl, pH 6.8 |

2. Once the gel is finished polymerization, pluck the comb out carefully and take the glass plates (containing the gel) out of the stands.
3. Place the glass plate into the electrode assembly to make an electrophoresis module. Top up the module (covering all the wells) with cathode buffer, and then load denatured samples (containing 1 x loading buffer, pre-heated at 100°C for 3 min) with equal amount (15-40 µg/lane) into the wells. Load 10 µl of the ladder in the first and last well of each gel.

4. Carefully place the loaded module into the electrophoresis tank, and then fill the outside tank with anode buffer to the mark on the tank wall. Place the lid on the tank, and make sure to match up the black and red leads.
5. Run the samples at 45 V for 30 min followed by 85 V till the samples have run to the bottom of the gel.
6. Turn off the PowerPac and drain the module. Take the glass plates out of the module, then carefully pry the plates open and retrieve the gel. Immediately proceed to the Assembly procedure.

### 2.12.5. Transfer procedure

1. After gel electrophoresis, open the transfer pack and assemble the components on the cassette in order according to the instruction. Use a roller to remove any air trapped between layers. Two mini format gels should be placed on a Midi stack with the foot of each gel toward the center.
2. Place the lid on the cassette and insert it into either bay of the instrument. Lock the cassette by turning the knob clockwise. The upper bay is designated as bay A and the lower is designated as bay B. If running 2 cassettes simultaneously, refer to Table 2.12.4 for acceptable transfer combinations.

**Table 2.12.4 Acceptable transfer combinations**

| | Acceptable | |
|---|---|---|
| Combination | 1 | 2 |
| Upper Bay A | 1 mini gel | 2 mini gel<br>or 1 midi gel |
| Lower Bay B | 1 mini gel | 2 mini gel<br>or 1 midi gel |

3. Press **Turbo** and select the gel type. Press **List** to select the protocol shown in Table 2.12.5. Press **A: Run** or **B: Run** to start the transfer.

**Table 2.12.5 Protocol for transfer**

| Protocol name | MW, kD | Time, min |
|---|---|---|
| 1.5 MM Gel | Any | 10 |

4. Pull the cassette straight out of slot (caution: maybe warm) when **RUN COMPLETE** is displayed on the screen.
5. Disassemble the blotting sandwich and extract the membrane, which is ready for antibody probing or storage in plastic seal bag at -20°C. Discard the remaining transfer pack materials.

### 2.12.6. Antibody detection

Vinculin is the last antibody to be detected with each membrane.

1. Prepare the buffers shown in Table 2.12.6.

**Table 2.12.6 Preparation of the buffers for antibody detection**

| Type | Recipe |
|---|---|
| 1 x Washing buffer | 150 mM NaCl, 0.1% Tween 20, 20 mM Tris, pH 7.5 |
| 1 x Blocking buffer | 5% BSA (bovine serum albumin) in 1 x Washing Buffer |
| 1 x Stripping buffer | 20 ml 10% SDS, 67.5 ml distilled water,<br>0.8 ml Beta-mercaptoethanol, 12.5 ml 0.5M Tris-HCl, pH 6.8 |

2. Place the membrane (the blotted side facing upwards always) in a clean plastic container with a pair of tweezers. Wash the membrane with 1 x washing buffer once then drain the container.
3. Block the membrane with primary antibody (ratios shown in Table 2.12.7) in blocking buffer (5 ml/membrane) on a shaker overnight at 4°C.
4. Wash the membrane in washing buffer 4 x 10 min on a shaker at room temperature.
5. Incubate the membrane with secondary antibody (ratio shown in Table 2.12.8) in blocking buffer (5 ml/membrane) on a shaker for 1 h at room temperature.
6. Wash the membrane in washing buffer 4 x 10 min on a shaker at room temperature.
7. Develop the membrane in pre-mixed chemiluminescent substrate [(1 ml stable peroxide solution + 1 ml enhancer solution)/membrane] for 5 min.

**Table 2.12.7 Primary antibodies for detection**

| Antibody | Catalog number | Ratio |
|---|---|---|
| Phosphorylated relA | CST3033S | 1:2000 |
| Methylated relA | CST13188S | 1:1000 |
| Phosphorylated ERK | CST4377S | 1:2000 |
| Phosphorylated p38 | CST4511S | 1:2000 |
| Phosphorylated eIF-2α | CST3597S | 1:1000 |
| XBP1 | Abcam ab129002 | 2μg/ml |
| Vinculin | Abcam ab37152 | 1:10000 |

**Table 2.12.8 Secondary antibody for detection**

| Antibody | Catalogue number | Ratio |
|---|---|---|
| Anti-rabbit IgG (HRP-linked) | CST7074S | 1:2000 |

### 2.12.7. Signal detection

1. Wrap the membrane in clean plastic sheets and place it in the chamber of ChemiDoc.
2. Select **colormetric** and switch to **filter 1**, capture the image with the ladder.
3. Select chemi and switch to **no filter**, set the **program** (**20 sec, 2000 sec, 100 image)** then capture the image with the protein bands.
4. Merge the colormetric and chemi image then measure pixel densities of the bands.
5. For probing with another antibody, the membrane was incubated with 10 ml of stripping buffer for 10 min followed by washing with PBS and 1 x washing buffer at room temperature on a shaker. Vinculin was the last antibody being probed with each membrane. All samples are normalized to the values of vinculin [it is one of the major components for cell-cell and cell-cell-matrix junctions, and has been used as a loading control in studies regarding the anti-inflammatory effects of VDR agonists on THP-1-MacCM-stimulated human adipocytes (322, 354)].

## 2.13. Statistical analysis

Data was analyzed using GraphPad Prism 5 (GraphPad Software, USA). Results were presented as means ± SEM. The statistical tests used were one-way-ANOVA coupled with Tukey's post hoc test. A value of $P<0.05$ is considered as statistically significant.

# 3. The effects of 1α,25(OH)$_2$D$_3$ on THP-1-MacCM-stimulated human white preadipocytes

## 3.1. Introduction

WAT consists of mature white adipocytes and a SVF including fibroblasts, endothelial cells, immune cells (i.e. macrophages) and preadipocytes (94). Accumulated energy storage in WAT leads to obesity, which could subsequently induce metaflammation characterized by infiltration of macrophages and secretion of pro-inflammatory factors, and further contribute to a series of metabolical disorders, importantly insulin resistance (76). SAT has a higher expandability compared with VAT, for it has a higher angiogenic growth capacity and therefore can more easily expand its capillary network (81). Enhanced subcutaneous lipids storage is mediated by stimulation of adipogenesis, rather than hypertrophy, which might protect against early manifestation of obesity-associated metabolic diseases. For example, MHO individuals are more insulin sensitive, and have smaller adipocytes in SAT, than those adipocytes of MAO individuals that may be able to expand more easily by proliferation (44). However, the protection is relative and when adipogenesis is impaired, hypertrophic SAT subsequently participates in the pathogenesis of obesity associated metabolic disorders (21, 84). In addition, in severely obese patients undergoing bariatric surgery, metaflammation is present in both visceral and subcutaneous tissues, as assessed by the presence of macrophage crown-like structures (88).

It has long been known that macrophages play a key role in influencing the proliferation, survival and differentiation of preadipocytes (For the specific details, please refer to *Introduction* Page 21-23). Several macrophage-secreted factors have been shown to contribute to the anti-differentiation/adipogenic ability of MacCM, especially IL-1β. For instance, the impaired differentiation was significantly associated with the up-regulated expression of IL-1β in the J774-MacCM-treated preadipocytes (144). The anti-adipogenic effect of human THP-1-MacCM on human adipose progenitor cells was exerted via IKKβ phosphorylation and activation of NF-κB, whereas the IKKβ inhibitor (sc-514) could totally abrogate the anti-adipogenic ability of

THP-1-MacCM to promote the differentiation of human preadipocytes (146).

Vitamin D is a fat soluble secosteroid. It has been long proved that adipose tissue is the principal storage site for it and its metabolites, which are mainly encountered in lipid droplets of adipocytes (325). The major circulating form of vitamin D is $25(OH)D_3$, which is also used by clinicians to determine vitamin D status. Serum is the preferred initial test for assessing vitamin D status. Although most laboratories report the normal range to be 50 to 250 nM, the preferred range is 75 to 150 nM (284). However, this form of vitamin D is biologically inactive and must be converted in the kidneys by 1-OHase to the most biologically active form - $1\alpha,25(OH)_2D_3$ (284). The reference value of $1\alpha,25(OH)_2D_3$ is: in males <16 years: 24-86 pg/ml (0.06-0.21 nM), > or =16 years: 18-64 pg/ml (0.04-0.15 nM); in females <16 years: 24-86 pg/ml (0.06-0.21 nM), > or =16 years: 18-78 pg/ml (0.04-0.19 nM) (387). Noteworthy, macrophages in all tissues are capable of expressing 1-hydroxylase and synthesizing $1\alpha,25(OH)_2D_3$ locally (285). Upon extracellular stimuli, $1\alpha,25(OH)_2D_3$ binds to VDR to modulate genomic response of numerous cells and tissues throughout the body in an endocrine, autocrine or paracrine manner (285).

Several *in vitro* studies have demonstrated that $1\alpha,25(OH)_2D_3$ could exert an anti-inflammatory action on adipocytes. For instance, $1\alpha,25(OH)_2D_3$ ($10^{-7}$ M) significantly reduced the release of IL-6 compared with the LPS-stimulated 3T3-L1 cells (24 h) (352). Similarly, $1\alpha,25(OH)_2D_3$ ($10^{-7,-8}$ M) inhibited THP-1-MacCM induced expression of the inflammatory genes of MCP-1, IL-6 and IL-8 in human white adipocytes (24 h) (354). In addition, it has been demonstrated that the anti-inflammatory effects of $1\alpha,25(OH)_2D_3$ ($10^{-8}$ M) were mediated by inhibition of the NF-κB and MAPK signaling pathways (24 h) (354). However, the anti-inflammatory effects of $1\alpha,25(OH)_2D_3$ on human white subcutaneous preadipocytes remains to be characterized in detail.

## 3.2. Aims

The aim of the work described in this chapter was to investigate the anti-inflammatory effects of

$1\alpha,25(OH)_2D_3$ on macrophage-stimulated inflammatory response in human white preadipocytes and the signaling pathways involved. A series of experiments were set up to examine whether:

1. LPS could stimulate THP-1-macrophages to secrete a variety of cytokines, particularly pro-inflammatory factors;
2. THP-1-MacCM could enhance the gene expression of IL-1β, IL-8, IL-6, MCP-1, and RANTES in human white preadipocytes;
3. THP-1-MacCM could enhance the secretion of the pro-inflammatory factors from human white preadipocytes;
4. IL-1β or IL-6 is critical in maintaining the inflammatory response induced by THP-1-MacCM;
5. $1\alpha,25(OH)_2D_3$ could inhibit the secretion or gene expression of the pro-inflammatory factors in THP-1-MacCM-stimulated preadipocytes;
6. THP-1-MacCM could increase the level of phosphorylated relA of the NF-κB pathway as well as phosphorylated ERK or p38 of the MAPK pathways in preadipocytes;
7. $1\alpha,25(OH)_2D_3$ could also modulate the level of phosphorylated eIF-2α of the UPR pathway to exert the anti-inflammatory effects on THP-1-MacCM-stimulated preadipocytes.

## 3.3. Materials and Methods

Culture of human preadipocytes

Preadipocytes were cultured in T25 flasks, and then sub-cultured into 12-well plates (seeding density: 5000 cells per $cm^2$) in PGM (Table 2.5.2) (PromoCell, Germany), and incubated at 37 °C in 95% air and 5% $CO_2$. The pretreatment was initiated when the sub-cultured preadipocytes reached 90% confluence.

Generation of THP-1-MacCM (macrophage conditioned medium)

THP-1 monocytes were cultured in T75 flasks in MGM (Table 2.2.2) (Sigma-Aldrich, UK), and incubated at 37 °C in 95% air and 5% $CO_2$. When the monocytes density reached $1\times10^6$ cells/ml (optimal), the differentiation to macrophages was inducted by 100 nM PMA (Sigma-Aldrich, UK) in MGM for 48 h. Then the THP-1-macrophages were activated by 1 μg/ml LPS and 1mM ATP (Sigma-Aldrich, UK) in MM (Table 2.2.2) for a further 24 h before medium collection. The THP-1-MacCM was filtered through a 0.22 μm filter and stored at −80 °C for preadipocyte treatment.

Preadipocyte pretreatment and treatment

To investigate effects of $1\alpha,25(OH)_2D_3$ on THP-1-MacCM-stimulated preadipocytes, preadipocytes were either cultured alone (control); with (25%) THP-1-MacCM alone [the established protocol (355)], or in the presence of IL-1β neutralizing antibody (15 μg/ml, R&D Systems) [the established protocol (355)] or IL-6 neutralizing antibody (300 ng/ml, R&D Systems) (established by the preliminary work, and the data shown in Appendix 9.2, 3) for 24 h. Further groups of cells were pretreated with $1\alpha,25(OH)_2D_3$ (0.01-10 nM, ENZO Life Sciences, USA) for 24 h [the established protocol (354, 355)], followed by treatments with (25%) THP-1-MacCM and $1\alpha,25(OH)_2D_3$ (0.01-10 nM) for a further 24 h [the established protocol (354, 355)] at 37 °C in 95% air and 5% $CO_2$. When the experiment was completed, cell media were collected for cytokine array and ELISA; preadipocytes were lysed with Trizol for qPCR or lysed with a lysis buffer for western blotting. All samples were stored at -80 °C.

Cytokine array

Secreted cytokines from the treated-preadipocytes or THP-1-macrophages were screened using Human Cytokine Array Panel A (R&D Systems) following the manufacturer's instructions. Before the assays, 100 μl of each of the collected media from the treated-preadipocytes were pooled (n = 6, per group) as the samples to be measured. In addition, 600 μl of (25%) THP-1-MacCM was directly applied unto the array to be screened for cytokines secreted by THP-1-macrophages. The cytokine signals were captured by Molecular Imager ChemiDoc XRS+ System (Bio-Rad,

Hertfordshire, UK), and the results were presented as pixel density relative to the reference controls on the arrays.

ELISA

The secretion levels of pro-inflammatory factors including IL-1β, IL-6, IL-8, MCP-1 and RANTES were measured using human ELISA kits (R&D Systems, UK) following the manufacturer's instructions and SPECTROstar Nano Microplate Reader (BMG LABTECH, Germany). According to the results obtained from the preliminary assays, the collected media from the treated-preadipocytes needed to be diluted properly before applying to these ELISAs. The ELISA result was corrected for total cell protein content [which was measured by Thermo Scientific Pierce BCA Protein Assay Kit) and presented pg(cytokine)/μg(cell protein)].

Real-time PCR

The treated-preadipocytes were rinsed twice in ice-cold PBS, lysed with Trizol and stored at -80°C (Invitrogen, UK). The total RNA was subsequently precipitated from the lysates with isopropanol (Sigma-Aldrich, UK) and re-dissolved in UltraPureDNase/RNase-Free Distilled Water (Thermo Scientific, UK). The RNA concentration was measured by NanoDrop 2000 and the purity was determined by ratio of absorbance at 260 and 280 nm (Thermo Scientific, UK). The first-strand cDNA was synthesized from 0.5μg of the total RNA with iScript cDNA synthesis kit (Bio-Rad, UK) in a final volume of 10 μl (per reaction). Real-time quantitative PCR was performed with a Stratagene Mx3005P instrument system. The gene expression levels of pro-inflammatory factors including IL-1β, IL-6, IL-8, MCP-1, RANTES and internal reference PPIA were measured using TaqMan gene expression assays (Applied Biosystems, UK) and qPCR core kit (Eurogentec, Seraing, Belgium). Each TaqMan reaction contained 10 ng of sample cDNA in a total volume of 12.5 μl (per reaction). The assays were performed in duplicate and the thermo cycling program was set as follows: 95 °C for 10 min followed by 40 cycles (95 °C for 15 sec, 60°C for 1 min). Blank controls without cDNA were run in parallel. All samples were normalized to the values of PPIA and the results were presented as fold changes of Ct value relative to controls using the

$2^{-\Delta\Delta ct}$ formula (384).

Western blotting

The treated-preadipocytes were rinsed twice in ice-cold PBS and scraped into a freshly prepared lysis buffer [50 mM Tris-HCl pH 6.7, 10% Glycerol, 4% SDS protease inhibitor cocktail, phosphatase inhibitor cocktail (Sigma-Aldrich, UK)]. The concentration of the lysate (protein) were measured by Thermo Scientific Pierce BCA Protein Assay Kit and stored at -80°C. Equal amounts of the protein samples (20-30 μg/lane) were separated by SDS-PAGE (Mini Protean Tetra, TGX FastCast premixed acrylamide solutions, Bio-Rad, UK), and transferred to nitrocellulose membranes (Trans-Blot Turbo Midi Nitrocellulose Transfer Packs, Bio-Rad, UK) by Trans-Blot Turbo Transfer System (Bio-Rad, UK) for 10 min (protocol name: 1.5mm gel). For immunodetection, the membranes were respectively blocked for 1 h at room temperature with the blocking buffer [TBS, 0.1% Tween 20, 5% BSA (Sigma-Aldrich, UK)], firstly incubated overnight in the blocking buffer at 4 °C with primary antibodies including phosphorylated relA of the NF-κB signaling pathway, phosphorylated ERK, phosphorylated p38 of the MAPK signaling pathways (New England BioLab, UK) at 1:2000 dilution; phosphorylated (eukaryotic translation initiation factor) eIF-2α in the PERK induced arm of the UPR (New England BioLab, UK) at 1:1000 dilution, and then with a secondary anti-rabbit antibody (New England BioLab, UK) at 1:2000 dilution. Eventually the membranes were probed with vinculin antibody (Abcam, UK) as a loading control. The signals were stained by chemiluminescence (West Pico kit, Pierce, Loughborough, UK), captured and measured by Molecular Imager ChemiDoc XRS+ System (Bio-Rad). The molecular weight of the detected signaling bands was estimated with PageRuler protein markers (Thermo Scientific, UK).

Statistical analysis

Results are presented as means ± SEM. For statistical analysis, one-way-ANOVA coupled with Tukey's post hoc test for independent samples was used. A value of $P<0.05$ was regarded as statistically significant. The analysis and presentation were performed using Prism 5 (GraphPad,

USA).

## 3.4. Results

### 3.4.1. LPS-stimulated THP-1-macrophages secrete a variety of cytokines

In the initial experiments, cytokines released from LPS-stimulated THP-1 macrophages were screened by cytokine array (Figure 3.1, Appendix 9.1). Several pro-inflammatory factors were secreted including GRO-α, RANTES (chemoattractants), IL-8 and slCAM-1 (mainly expressed by neutrophils).

### 3.4.2. THP-1-MacCM enhances cytokine secretion from human preadipocytes, but IL-1β antibody partially blocks the pro-inflammatory effects

A variety of pro-inflammatory factors were secreted including IL-6, IL-8, MCP-1 and RANTES from (25%) THP-1-MacCM-stimulated preadipocytes, but the levels of these cytokines were discernibly reduced by IL-1β antibody (15 μg/ml) (Figure 3.1, Appendix 9.1).

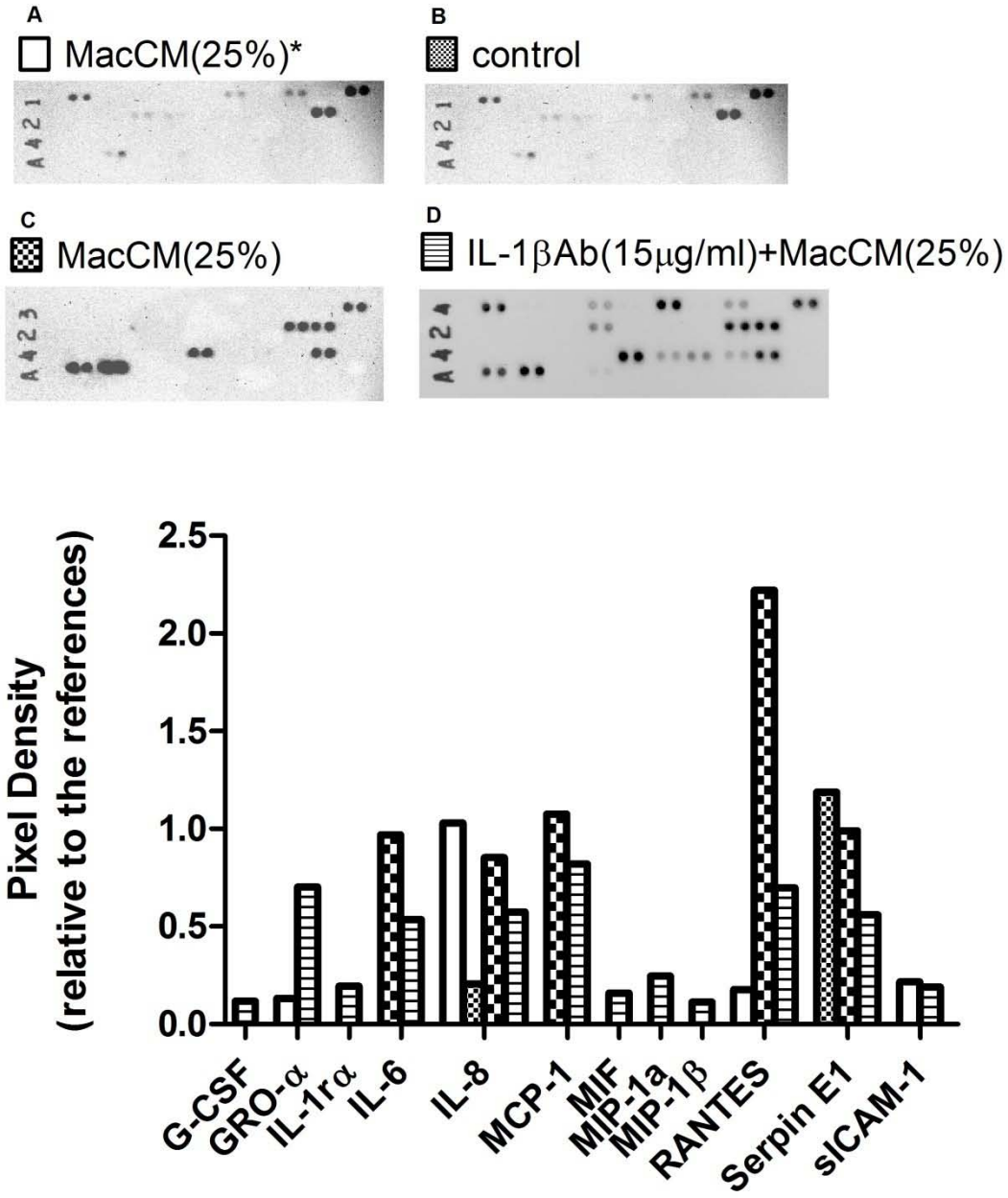


**Figure 3.1 Effects of THP-1-MacCM on cytokine release from human white preadipocytes.** (A) Cytokines [in (25%) THP-1-MacCM] secreted from THP-1-macrophages were screened by cytokine array. Preadipocytes were either cultured alone, with (25%) THP-1-MacCM alone, or in the presence of IL-1β neutralizing antibody (15 μg/ml) for 24 h. Cytokines released from (B) control, (C) (25%) THP-1-MacCM, (D) IL-1β neutralizing antibody (15 μg/ml) were screened by cytokine array. Data are presented as pixel density relative to the reference controls on the arrays.

### 3.4.3. THP-1-MacCM enhances the secretion of the pro-inflammatory factors from human preadipocytes

According to the result on the cytokine array, the pro-inflammatory factors including IL-6, IL-8, MCP-1 and RANTES were selected as indicators of the inflammatory response (metaflammation) of preadipocytes induced by (25%) THP-1-MacCM; IL-1β was also included (though having not included in the cytokine array, it was later confirmed by ELISA that the concentration of IL-1β was approximately 2 ng/ml in THP-1-MacCM).

The ELISA result (Figure 3.2) shows that the secretion levels of these pro-inflammatory factors were dramatically increased by (25%) THP-1-MacCM.

### 3.4.4. IL-1β and IL-6 neutralization inhibit the secretion of the pro-inflammatory factors from THP-1-MacCM-stimulated preadipocytes

The ELISA result (Figure 3.2) shows that IL-1β antibody (15 μg/ml) markedly reduced the secretion levels of IL-1β, IL-6 and IL-8 of (25%) THP-1-MacCM-stimulated preadipocytes, but it did not reduce the secretion levels of MCP-1 and RANTES.

In parallel, the presence of IL-6 antibody (300 ng/ml) exhibited a broader range of blocking effects, since the secretion levels of IL-6, IL-8, MCP-1 and RANTES of (25%) THP-1-MacCM-stimulated preadipocytes were all moderately reduced, but the effects are still partial, as the secretion level of IL-1β was not affected.

### 3.4.5. 1α,25$(OH)_2D_3$ inhibits the secretion of the pro-inflammatory factors from THP-1-MacCM-stimulated preadipocytes

The effects of 1α,25$(OH)_2D_3$ on the cytokine secretion from (25%) THP-1-MacCM-stimulated

preadipocytes are quite complex (Figure 3.2). Firstly, 1α,25$(OH)_2D_3$ (0.01-10 nM) has no effect of the secretion levels of IL-1β and MCP-1. Secondly, the secretion levels of IL-6, IL-8 and RANTES were universally reduced by 1α,25$(OH)_2D_3$ (0.01-10 nM), though some of reductions did not reach the statistical significance. For instance, the level of IL-8 and RANTES by 0.01 nM of 1α,25$(OH)_2D_3$, the level of IL-6 and RANTES by 0.1 nM of 1α,25$(OH)_2D_3$, and IL-8 level by 1 nM of 1α,25$(OH)_2D_3$. Finally, only 10 nM of 1α,25$(OH)_2D_3$ significantly reduced the secretion of MCP-1. In conclusion, 1α,25$(OH)_2D_3$ has an anti-inflammatory effect on THP-1-MacCM-stimulated preadipocytes, in terms of reducing the secretion levels of some pro-inflammatory cytokines. However, there is no straightforward dose-response relationship between the secretion levels of the cytokines and the doses of 1α,25$(OH)_2D_3$ used in these experiments

**Figure 3.2 Effects of 1α,25(OH)$_2$D$_3$ on cytokine release from THP-1-MacCM-stimulated human white preadipocytes.**

Preadipocytes were either cultured alone (control), with (25%) THP-1-MacCM alone, or in the presence of IL-1β neutralizing antibody (15 μg/ml) for 24 h. Further groups of cells were pretreated with 1α,25(OH)$_2$D$_3$ (0.01-10 nM) for 24 h, followed by treatments with (25%) THP-1-MacCM and 1α,25(OH)$_2$D$_3$ (0.01-10 nM) for a further 24 h before medium collection. The release levels of pro-inflammatory factors (A) IL-1β, (B) IL-6, (C) IL-8, (D) MCP-1 and (E) RANTES were measured by ELISA and normalized by protein content in the cellular lysate. Data are means ± SEM for groups of 6. A significant difference to control was indicated by ***(p<0.001); to (25%) THP-1-MacCM by #(p<0.05), ##(p<0.01), ###(p<0.001). The results were determined using one-way ANOVA with Tukey's post hoc test and confirmed by two independent experiments.

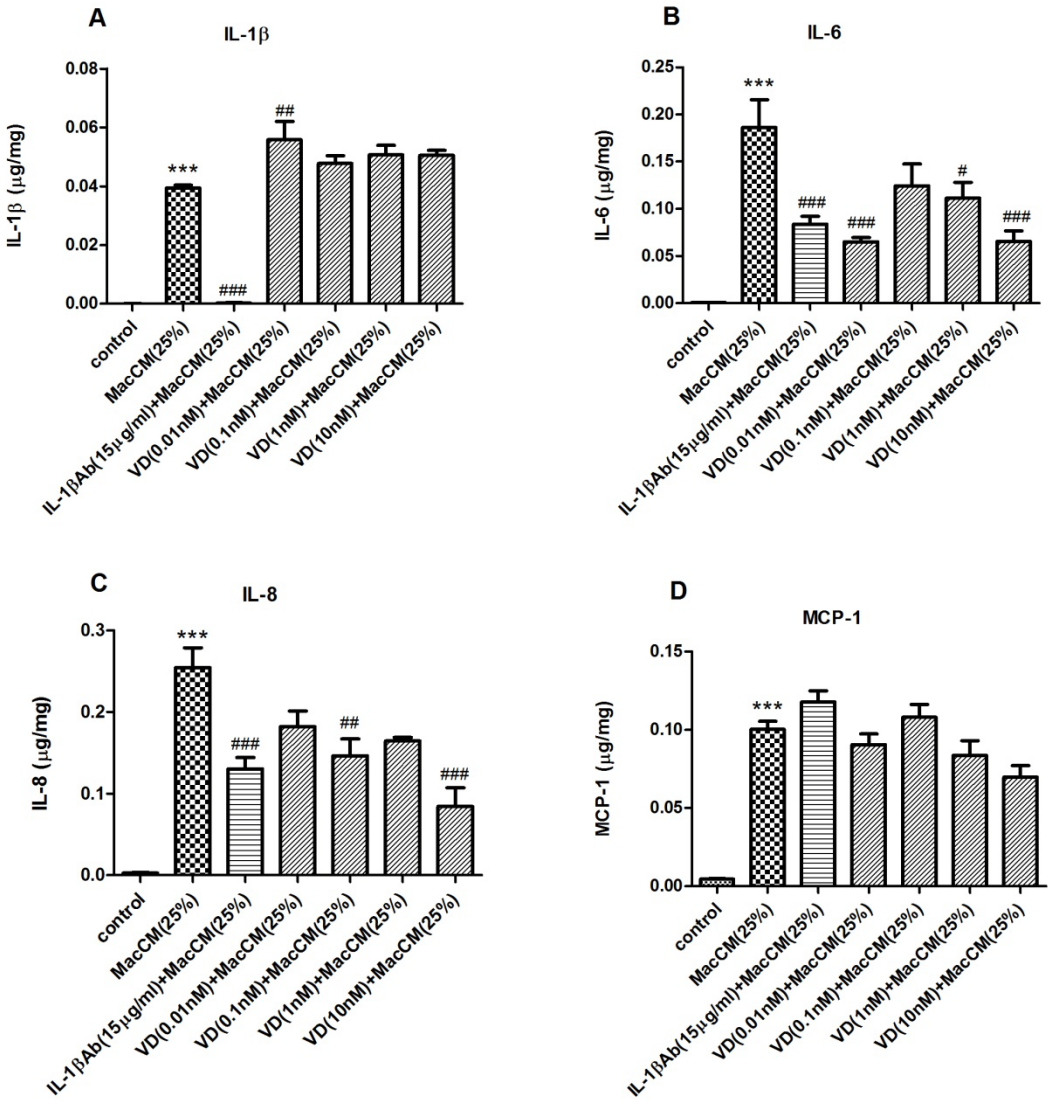

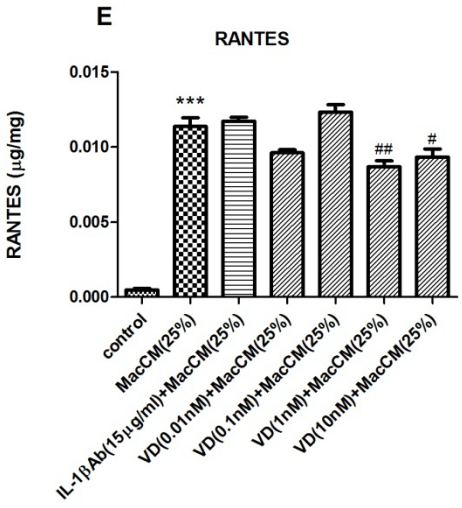
E
RANTES
RANTES (μg/mg)
0.015
0.010
0.005
0.000
***
##
#
control
MacCM(25%)
IL-1βAb(15μg/ml)+MacCM(25%)
VD(0.01nM)+MacCM(25%)
VD(0.1nM)+MacCM(25%)
VD(1nM)+MacCM(25%)
VD(10nM)+MacCM(25%)

### 3.4.6. THP-1-MacCM enhances the gene expression of the pro-inflammatory factors in human preadipocytes

Similar to the secretion levels, the qPCR result (Figure 3.3) shows that the mRNA levels of the pro-inflammatory factors including IL-1β, IL-6, IL-8, MCP-1 and RANTES, were massively increased by (25%) THP-1-MacCM.

### 3.4.7. IL-1β and IL-6 neutralization inhibit the gene expression of the pro-inflammatory factors in THP-1-MacCM-stimulated preadipocytes

(Figure 3.3) IL-1β (15 μg/ml) and IL-6 (300 ng/ml) antibodies also exhibited distinguishable blocking effects on the mRNA levels of IL-1β, IL-6 and IL-8 in (25%) THP-1-MacCM-stimulated preadipocytes. However, the effects are partial, for the levels of MCP-1 are not significant. In addition, though IL-6 antibody markedly decreased the mRNA level of RANTES, whilst IL-1β antibody had no statistically significant effect.

### 3.4.8. 1α,25(OH)$_2$D$_3$ inhibits the gene expression of the pro-inflammatory factors in THP-1-MacCM-stimulated preadipocytes

As with the effects on cytokine secretion, the effects of 1α,25(OH)$_2$D$_3$ on the mRNA levels of (25%) THP-1-MacCM-stimulated preadipocytes are also complicated (Figure 3.3). Firstly, 1α,25(OH)$_2$D$_3$ (0.01-10 nM) treatment was associated with lower mRNA levels of IL-1β and RANTES, and these reducing effects were similar across the range of doses. Secondly, the mRNA levels of IL-6 and IL-8 were only significantly reduced by 1α,25(OH)$_2$D$_3$ (1-10 nM). Finally, 1α,25(OH)$_2$D$_3$ (0.01-10 nM) had no effect on the mRNA levels of RANTES. Taken together, 1α,25(OH)$_2$D$_3$ has an anti-inflammatory effect on THP-1-MacCM-stimulated preadipocytes, with respect to reducing the mRNA levels of IL-1β, IL-6, IL-8 and RANTES. However, there is no consistent dose-response relationship between the mRNA levels of these pro-inflammatory factors

and the doses of $1\alpha,25(OH)_2D_3$ used in these experiments.

**Figure 3.3 Effects of $1\alpha,25(OH)_2D_3$ on cytokine gene expression in THP-1-MacCM-stimulated human white preadipocytes.**

Preadipocytes were either cultured alone (control), with (25%) THP-1-MacCM alone, or in the presence of IL-1β neutralizing antibody (15 μg/ml) or IL-6 neutralizing antibody (300 ng/ml) for 24 h. Further groups of cells were pretreated with $1\alpha,25(OH)_2D_3$ (0.01-10 nM) for 24 h, followed by treatments with (25%) THP-1-MacCM and $1\alpha,25(OH)_2D_3$ (0.01-10 nM) for a further 24 h before Trizol-dissolved lysate collection. The mRNA levels of pro-inflammatory factors (A) IL-1β, (B) IL-6, (C) IL-8, (D) MCP-1 and (E) RANTES were measured by qPCR. Data are means ± SEM for groups of 6. A significant difference to control was indicated by ***($p<0.001$); to (25%) THP-1-MacCM by #($p<0.05$), ##($p<0.01$), ###($p<0.001$). The results were determined using one-way ANOVA with Tukey's post hoc test and confirmed by two independent experiments.

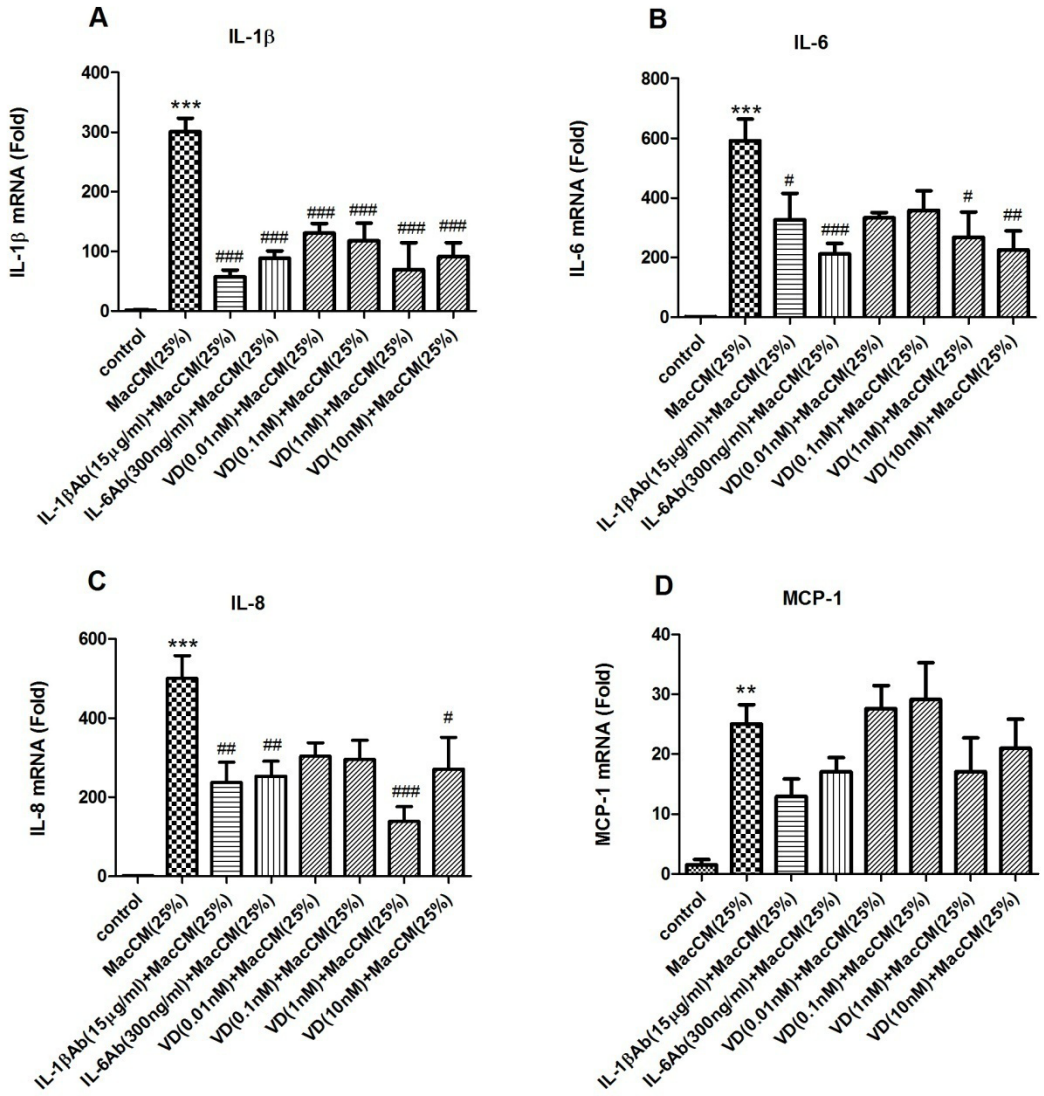

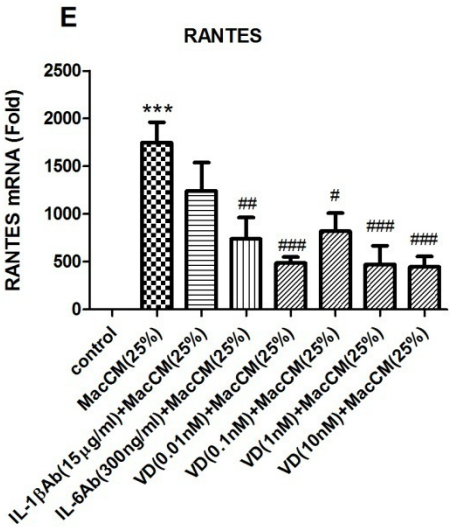
E
RANTES
RANTES mRNA (Fold)
2500
2000
1500
1000
500
0
***
##
###
#
###
###
control
MacCM(25%)
IL-1βAb(15μg/ml)+MacCM(25%)
IL-6Ab(300ng/ml)+MacCM(25%)
VD(0.01nM)+MacCM(25%)
VD(0.1nM)+MacCM(25%)
VD(1nM)+MacCM(25%)
VD(10nM)+MacCM(25%)

### 3.4.9. THP-1-MacCM increases the level of phosphorylated relA in human preadipocytes

To test whether THP-1-MacCM could modulate the NF-κB pathway, the level of phosphorylated relA was measured by western blotting. The result (Figure 3.4) shows that the level of phosphorylated relA was markedly higher in the presence of (25%) THP-1-MacCM, compared to the untreated preadipocytes.

### 3.4.10. IL-1β neutralization reduces the level of phosphorylated relA in THP-1-MacCM-stimulated preadipocytes

By contrast, (Figure 3.4) IL-1β antibody (15 μg/ml) was associated with moderately lower phosphorylated relA in (25%) THP-1-MacCM-stimulated preadipocytes.

### 3.4.11. 1α,25(OH)$_2$D$_3$ (10 nM) reduces the levels of phosphorylated relA in THP-1-MacCM-stimulated preadipocytes

Only 1α,25(OH)$_2$D$_3$ (10 nM) discernibly reduced the level of phosphorylated relA of (25%) THP-1-MacCM-stimulated preadipocytes, while the other doses (0.01-1 nM) had no effect on the levels of phosphorylated relA (Figure 3.4).

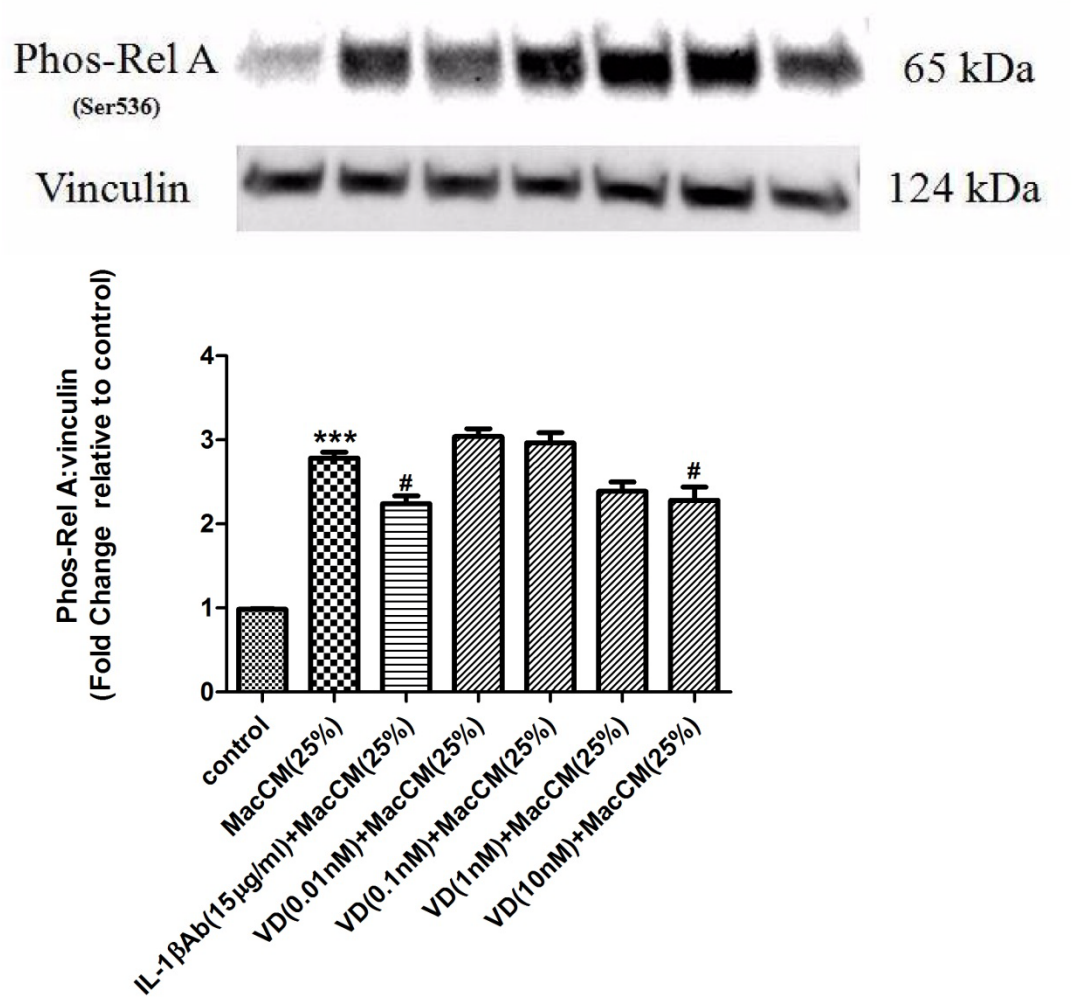


**Figure 3.4 Effects of 1α,25(OH)$_2$D$_3$ on phosphorylated relA in THP-1-MacCM-stimulated human white preadipocytes.**

Preadipocytes were either cultured alone (control), with (25%) THP-1-MacCM alone, or in the presence of IL-1β neutralizing antibody (15 μg/ml) for 24 h. Further groups of cells were pretreated with 1α,25(OH)$_2$D$_3$ (0.01-10 nM) for 24 h, followed by treatments with (25%) THP-1-MacCM and 1α,25(OH)$_2$D$_3$ (0.01-10 nM) for a further 24 h before lysate collection. The levels of phosphorylated relA of the NF-κB signaling pathway were measured by western blotting. Data are means ± SEM for groups of 3. A significant difference to control was indicated by ***($p<0.001$); to (25%) THP-1-MacCM by #($p<0.05$). The results were determined using one-way ANOVA with Tukey's post hoc test and confirmed by two independent experiments.

### 3.4.12. THP-1-MacCM increases the levels of phosphorylated ERK and p38 in human preadipocytes

Like that of phosphorylated relA, (Figure 3.5) the levels of phosphorylated ERK (p44/42) and p38 of the MAPK signaling pathways were significantly increased by (25%) THP-1-MacCM. However, IL-1β antibody (15 μg/ml) did not affect the levels of these signaling molecules in (25%) THP-1-MacCM-stimulated preadipocytes.

### 3.4.13. 1α,25(OH)$_2$D$_3$ (10 nM) reduces the level of phosphorylated ERK in THP-1-MacCM-stimulated preadipocytes

Only 1α,25(OH)$_2$D$_3$ (10 nM) moderately reduced the level of phosphorylated ERK of (25%) THP-1-MacCM-stimulated preadipocytes, while the other doses (0.01-1 nM) had no effect on the levels of phosphorylated ERK or p38; [1α,25(OH)$_2$D$_3$ (10 nM) had no effect on the level of p38, either] (Figure 3.5).

**Figure 3.5 Effects of 1α,25(OH)$_2$D$_3$ on signaling molecules of the MAPK pathways in THP-1-MacCM-stimulated human white preadipocytes.**

Preadipocytes were either cultured alone (control), with (25%) THP-1-MacCM alone, or in the presence of IL-1β neutralizing antibody (15 μg/ml) for 24 h. Further groups of cells were pretreated with 1α,25(OH)$_2$D$_3$ (0.01-10 nM) for 24 h, followed by treatments with (25%) THP-1-MacCM and 1α,25(OH)$_2$D$_3$ (0.01-10 nM) for a further 24 h before lysate collection. The levels of (A) phosphorylated ERK and (B) phosphorylated p38 were measured by western blotting. Data are means ± SEM for groups of 3. A significant difference to control was indicated by ***(p<0.001); to (25%) THP-1-MacCM by ###(p<0.001). The results were determined using one-way ANOVA with Tukey's post hoc test and confirmed by two independent experiments.

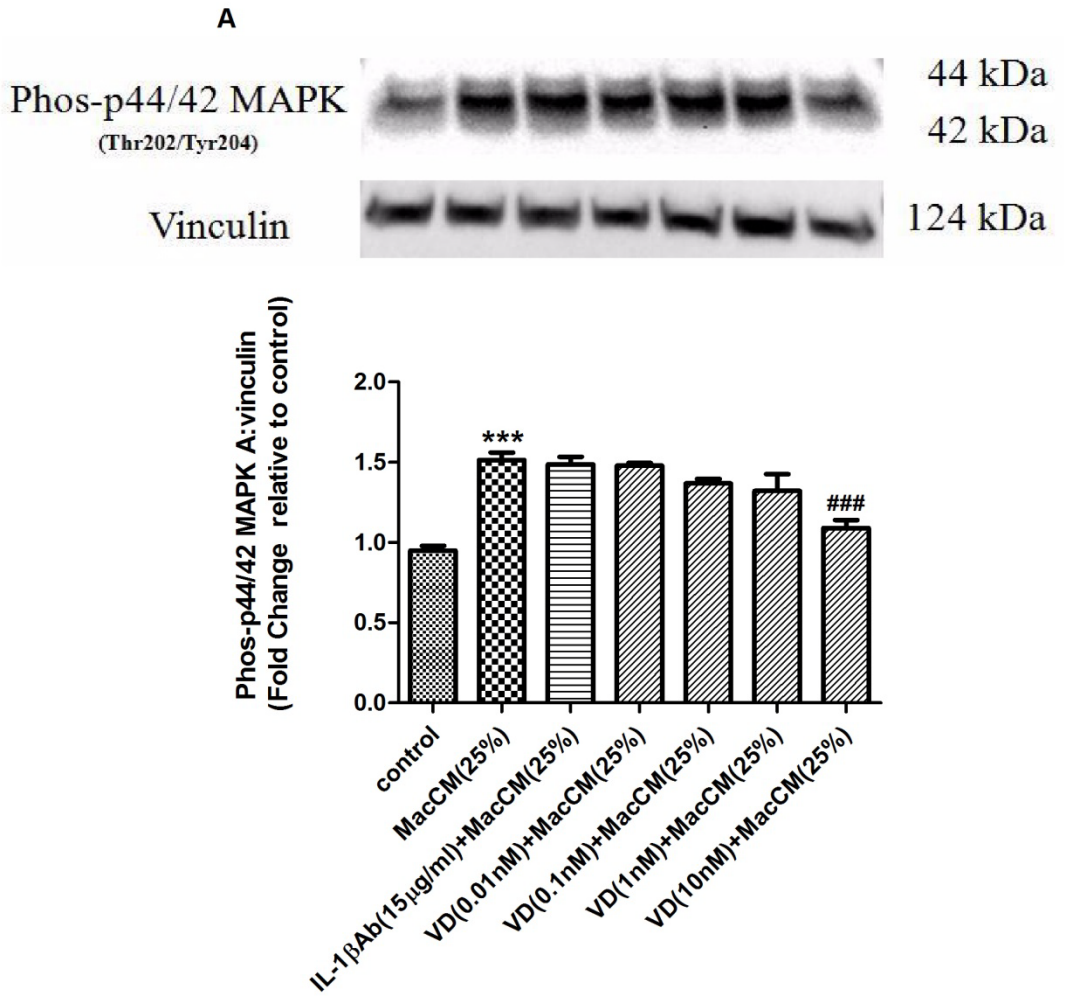

B

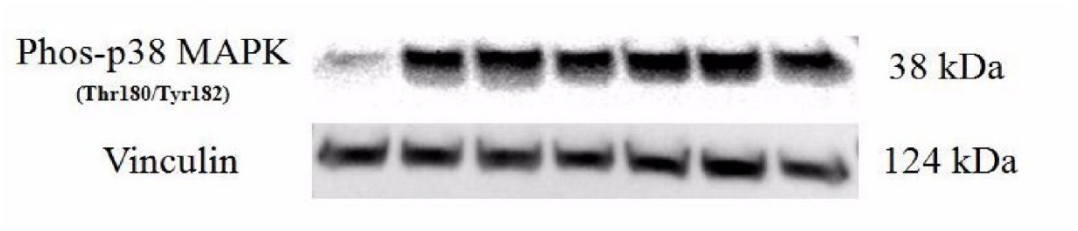
Phos-p38 MAPK
(Thr180/Tyr182)
38 kDa
Vinculin
124 kDa

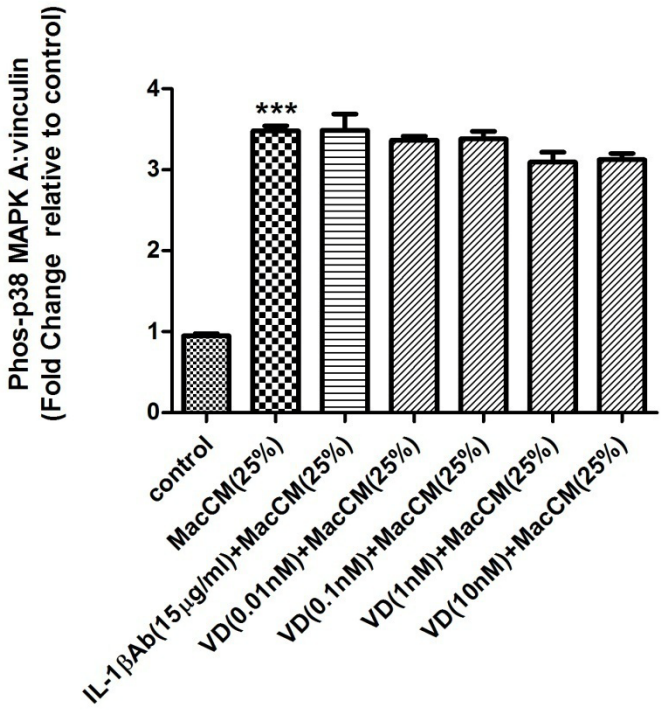
Phos-p38 MAPK A:vinculin
(Fold Change relative to control)
0
1
2
3
4
***
control
MacCM(25%)
IL-1βAb(15μg/ml)+MacCM(25%)
VD(0.01nM)+MacCM(25%)
VD(0.1nM)+MacCM(25%)
VD(1nM)+MacCM(25%)
VD(10nM)+MacCM(25%)

### 3.4.14. THP-1-MacCM increases the level of phosphorylated eIF-2α in human preadipocytes

To test whether THP-1-MacCM could modulate the UPR pathway, the expression levels of phosphorylated eIF-2α were measured by western blotting. The results (Figure 3.6-8) shows that the levels of phosphorylated eIF-2α were markedly increased by (25%) THP-1-MacCM, compared to the untreated preadipocytes.

### 3.4.15. IL-1β neutralization reduces the level of phosphorylated eIF-2α in THP-1-MacCM-stimulated preadipocytes

(Figure 3.6-8) IL-1β antibody (15 μg/ml) moderately reduced the levels of phosphorylated eIF-2α in (25%) THP-1-MacCM-stimulated preadipocytes.

### 3.4.16. 1α,25(OH)$_2$D$_3$ reduces the expression of phosphorylated eIF-2α in THP-1-MacCM-stimulated preadipocytes

(Figure 3.6-8) 1α,25(OH)$_2$D$_3$ (0.01-10 nM) universally reduced the levels of phosphorylated eIF-2α in (25%) THP-1-MacCM-stimulated preadipocytes, and the reducing effects are similar across the range of doses.

**Figure 3.6-8 Effects of $1\alpha,25(OH)_2D_3$ on phosphorylated eIF-2α in THP-1-MacCM-stimulated human white preadipocytes.**

Preadipocytes were either cultured alone (control), with (25%) THP-1-MacCM alone, or in the presence of IL-1β neutralizing antibody (15 μg/ml) for 24 h. Further groups of cells were pretreated with $1\alpha,25(OH)_2D_3$ (0.01-10 nM) for 24 h, followed by treatments with (25%) THP-1-MacCM and $1\alpha,25(OH)_2D_3$ (0.01-10 nM) for a further 24 h before lysate collection. The levels of phosphorylated eIF-2α in the PERK induced arm of the UPR signaling pathways were measured by western blotting. Data are means ± SEM for groups of 3. A significant difference to control was indicated by ***($p<0.001$); to (25%) THP-1-MacCM by #($p<0.05$), ##($p<0.01$), ###($p<0.001$). The results were determined using one-way ANOVA with Tukey's post hoc test.

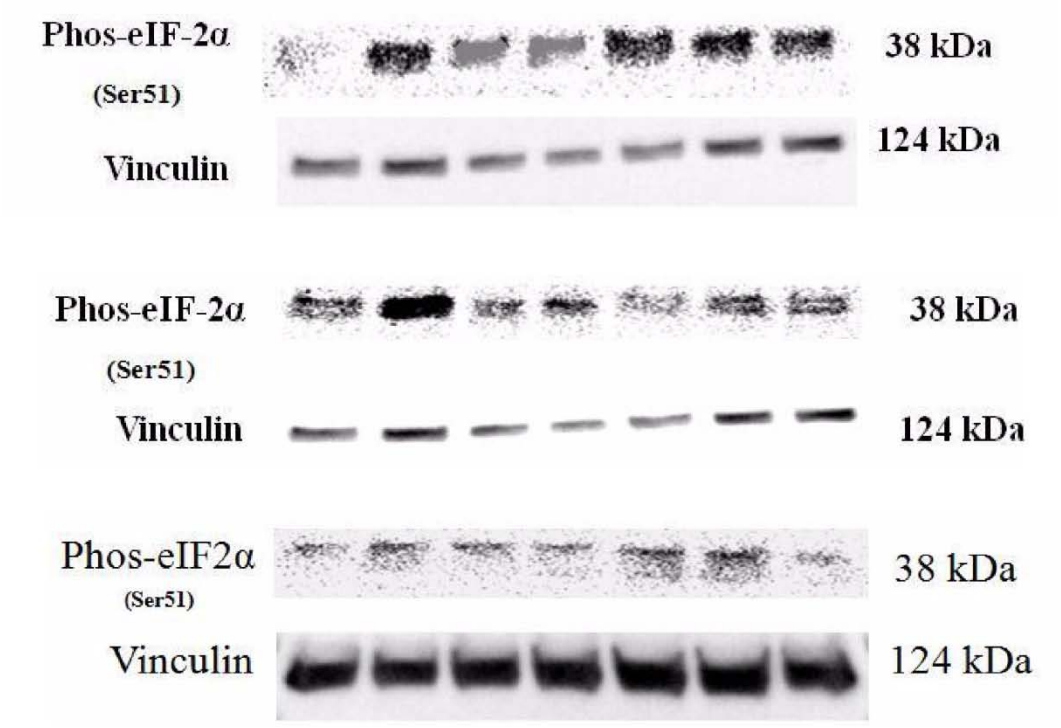
Phos-eIF-2α
(Ser51)
38 kDa
Vinculin
124 kDa
Phos-eIF-2α
(Ser51)
38 kDa
Vinculin
124 kDa
Phos-eIF2α
(Ser51)
38 kDa
Vinculin
124 kDa

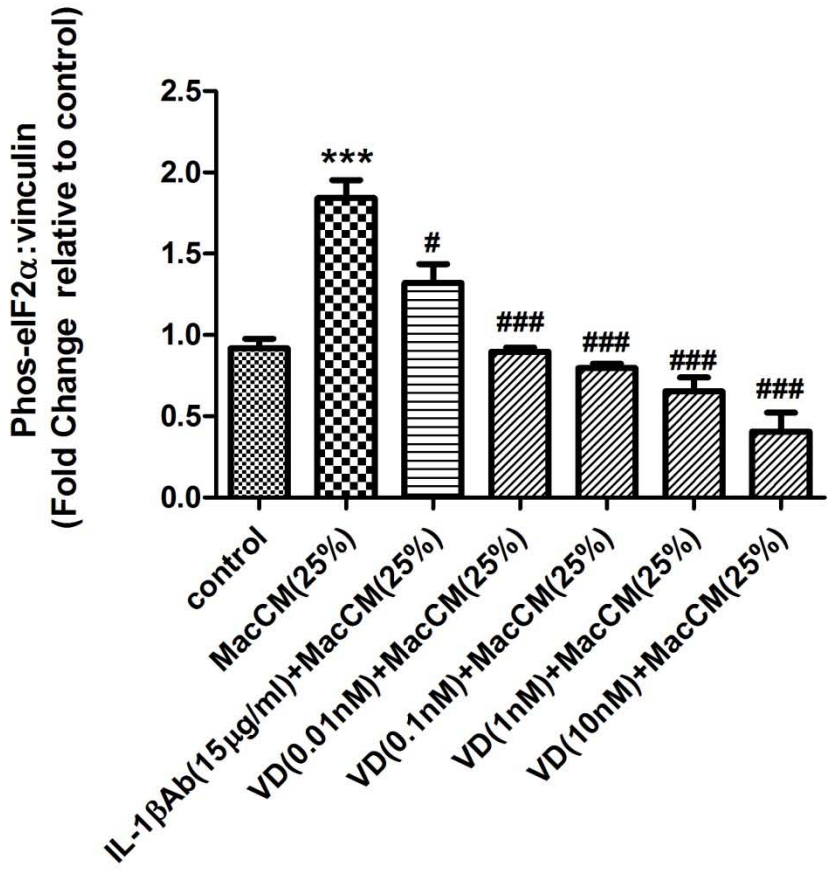
Phos-eIF2α:vinculin
(Fold Change relative to control)
2.5
2.0
1.5
1.0
0.5
0.0
***
#
###
###
###
###
control
MacCM(25%)
IL-1βAb(15μg/ml)+MacCM(25%)
VD(0.01nM)+MacCM(25%)
VD(0.1nM)+MacCM(25%)
VD(1nM)+MacCM(25%)
VD(10nM)+MacCM(25%)

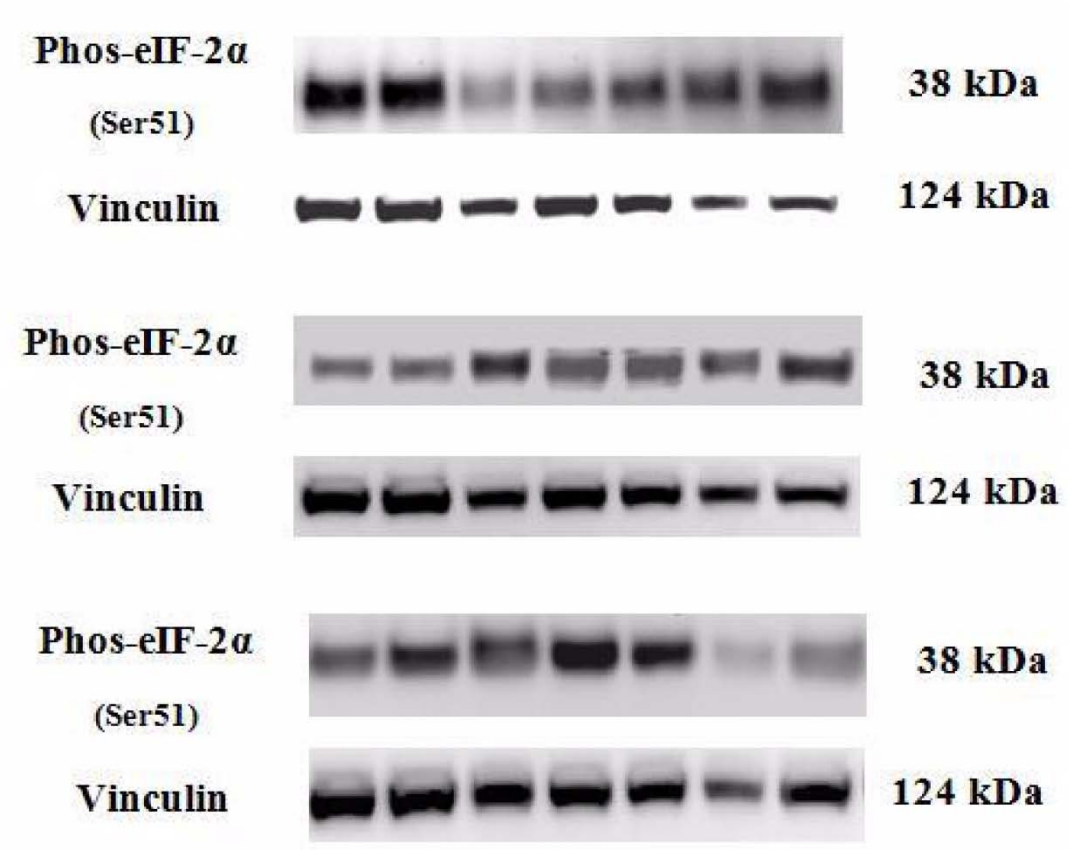
Phos-eIF-2α
(Ser51)
38 kDa
Vinculin
124 kDa
Phos-eIF-2α
(Ser51)
38 kDa
Vinculin
124 kDa
Phos-eIF-2α
(Ser51)
38 kDa
Vinculin
124 kDa

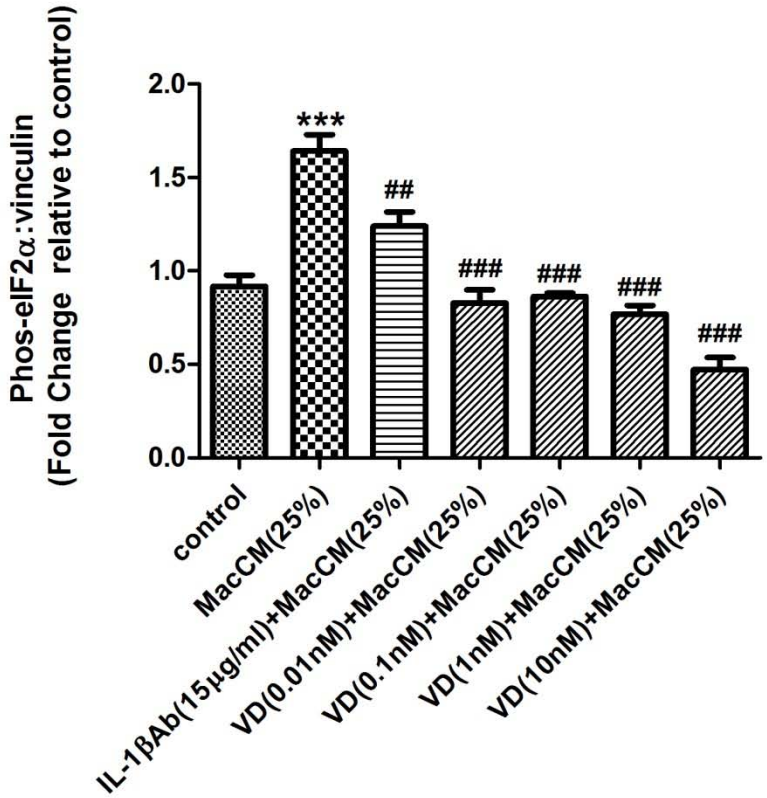
Phos-eIF2α:vinculin
(Fold Change relative to control)
2.0
1.5
1.0
0.5
0.0
***
##
###
###
###
###
control
MacCM(25%)
IL-1βAb(15μg/ml)+MacCM(25%)
VD(0.01nM)+MacCM(25%)
VD(0.1nM)+MacCM(25%)
VD(1nM)+MacCM(25%)
VD(10nM)+MacCM(25%)

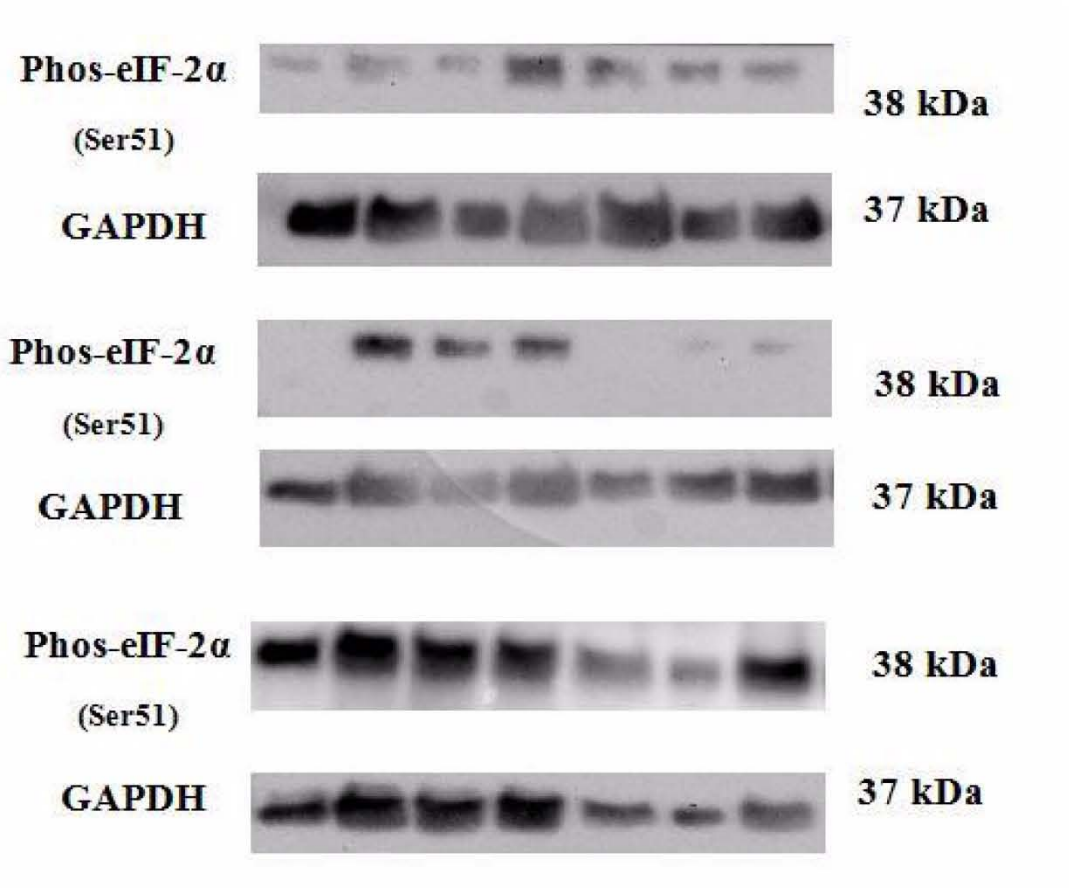
Phos-eIF-2α
(Ser51)
38 kDa
GAPDH
37 kDa
Phos-eIF-2α
(Ser51)
38 kDa
GAPDH
37 kDa
Phos-eIF-2α
(Ser51)
38 kDa
GAPDH
37 kDa

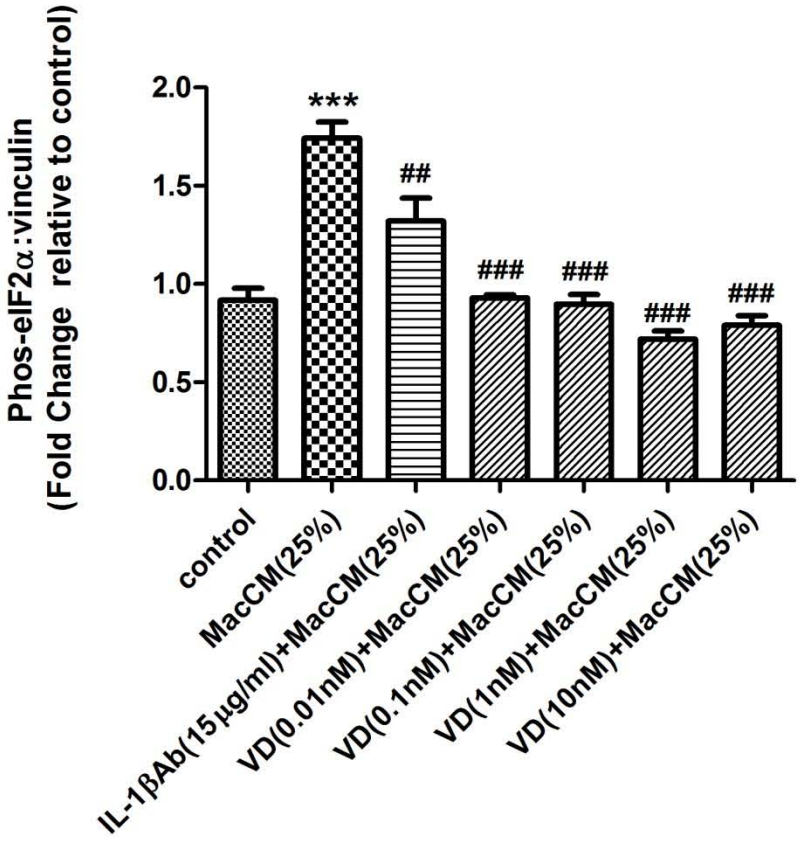
Phos-eIF2α:vinculin
(Fold Change relative to control)
2.0
1.5
1.0
0.5
0.0
***
##
###
###
###
###
control
MacCM(25%)
IL-1βAb(15μg/ml)+MacCM(25%)
VD(0.01nM)+MacCM(25%)
VD(0.1nM)+MacCM(25%)
VD(1nM)+MacCM(25%)
VD(10nM)+MacCM(25%)

## 3.5. Discussion

According to the results of the cytokine array in our study, several pro-inflammatory factors secreted including GRO-α, RANTES, IL-8 and slCAM-1, were secreted from LPS-stimulated THP-1-macrophages. Though having not been screened out by cytokine array, it was later measured by ELISA that the concentration of IL-1β of THP-1-MacCM was 2 ng/ml. It has been reported that microbial products (i.e. LPS and other TLR ligands) or pro-inflammatory cytokines (i.e. IFN-γ and TNF) could stimulate classic M1 macrophages to produce many pro-inflammatory cytokines including TNF-α, IL-1, IL-6, IL-12, Type I IFN, CXCL1-3, CXCL-5 and CXCL-8-10 (235, 237).

In the obese condition, infiltrated macrophages can make up to 40% of all cells of adipose tissue, compared with 10% in the lean controls (21). Interestingly, pre/adipocyte and monocyte/macrophage lineages display many features in common. Moreover, 3T3-L1 preadipocyte cell line rapidly and massively acquired high phagocytic activity, and 60-70% of preadipocytes expressed five macrophage-specific antigens: F4/80, Mac-1, CD80, CD86 and CD45, after having been injected into the peritoneal cavity of nude mice (135). Noteworthy, mouse adipocytes are sensitive to LPS activation and by which could secrete numerous pro-inflammatory factors (such as IL-6) (134). Obesity is also tightly associated with elevated serum levels of FFAs, cholesterol, and especially LPS (242). Hence, the hypothesis that whether metaflammation could be aggravated by the interaction of preadipocytes and macrophages was formed, and was to be tested by *in vitro* model of treating human white preadipocytes with THP-MacCM (collected from LPS-stimulated macrophages) for 24 h. Several cytokines including IL-1β, IL-6, IL-8, MCP-1 and RANTES were selected as indicators of the macrophage-induced inflammatory response of preadipocytes.

It has been demonstrated that adipose tissue can secrete the chemokine IL-8, which predominantly attracts neutrophils (30). Furthermore, the number of infiltrated neutrophils in the VAT of mice transiently increased at 3 and 7 days after initiating HFD feeding (31). Therefore, IL-8 is a potential contributor to metaflammation in obesity. Moreover, MCP-1 secretion by hypertrophic

adipocytes is responsible for macrophage infiltration in WAT of obese rodents and humans (185). CCR-5 also plays a critical role in the regulation of obesity-induced inflammatory response and insulin resistance in WAT, as recent studies have shown that the expression level of CCR-5 was positively correlated with the number of infiltrated macrophage in the WAT of morbidly obese individuals (194). In accordance with the evidence above, the results of qPCR and ELISA show that the gene expression and secretion levels of these pro-inflammatory factors were significantly enhanced by THP-1-MacCM compared to the untreated control.

It has been reported that the expression level of activated IL-1β was significantly enhanced in the VAT and SAT of the overweight subjects (161). Similarly, the gene expression and secretion of IL-1β by preadipocytes was significantly enhanced by THP-1-MacCM in the present study. However, whether IL-1β is pivotal in mediating the macrophage-induced inflammatory response in preadipocytes remains to be clarified. By treating preadipocytes with IL-1β antibody (15 μg/ml) and (25%) THP-1-MacCM, the results show that the gene expression and secretion levels of IL-1β, IL-6 and IL-8 were all significantly reduced by IL-1β neutralization. The levels of MCP-1 and RANTES were also numerically lower but not significantly different compared with the untreated control.

An interesting observation of the current study is that IL-6 could play a role in mediating macrophage-induced inflammatory response in preadipocytes. Like IL-1β, IL-6 is likely to be essential in mediating pro-inflammatory signaling in adipose tissue. Firstly, the plasma level of IL-6 is almost exclusively determined by whole-body adiposity. Secondly, IL-6 is closely associated with obesity induced abnormal metabolism, particularly metaflammation (175). Thirdly, in human hepatocytes, IL-6 has been found to stimulate the synthesis of CRP (one of the strongest indicators of metabolic risk), which was measured by immunoprecipitation (176). The present study has demonstrated that the gene expression and secretion levels of IL-6 and IL-8 were inhibited by IL-6 neutralizing antibody (300 ng/ml). Interestingly, the gene expression level of IL-1β was also significantly inhibited by IL-6 neutralization, though the secretion was not.

In obesity, TNF-α together with FFA, can stimulate the conversion of fatty-acyl-CoA to DAG and

ceramides, thereby activating serine/threonine kinases including MAPK family members (i.e. JNK and ERK), IKK, mTOR, and PKCs in adipose tissue, liver and skeletal muscle, to trigger inflammation and insulin resistance (6, 66). The levels of phosphorylated relA, phosphorylated ERK and p38 were all significantly enhanced by THP-1-MacCM compared to the untreated control, which suggests that the pro-inflammatory factors secreted by macrophages induce metaflammation in preadipocytes by activating the NF-κB and MAPK signaling pathways. Noteworthy, preadipocytes were treated with (25%) MacCM for 24 h and this duration is too long for measurement of IκBa protein due to its complex kinetics. In addition, the interpretation of IκBa levels in this experiment is redundant, as phosphorylated relA alone can be taken as the indicator of NF-κB activation in this experiment. However, the effects of (25%) MacCM or in the presence $1\alpha,25(OH)_2D_3$ (0.01-10 nM) on the levels of IκBa in human preadipocytes, could be studied by undertaking a time-course analysis of western blotting. For example, the levels of IκBa were measured in 2, 5 and 10 min after the stimulation.

It has been shown that $1\alpha,25(OH)_2D_3$ ($10^{-7,-8}$ M) has anti-inflammatory effects on LPS-stimulated 3T3-L1 adipocytes or THP-1-MacCM-stimulated human adipocytes (352, 354). Likewise, the data from our study suggest that $1\alpha,25(OH)_2D_3$ has an inhibitory effect on THP-macrophage-induced production of the major pro-inflammatory factors from human preadipocytes. This is demonstrated by the significant reduction in THP-1-MacCM-triggered gene expression of IL-1β, IL-6, IL-8 and RANTES in preadipocytes treated with $1\alpha,25(OH)_2D_3$ (1, 10 nM). In parallel, the secretion levels of IL-6, IL-8, MCP-1 and RANTES were also significantly inhibited by $1\alpha,25(OH)_2D_3$ (10 nM). Importantly, $1\alpha,25(OH)_2D_3$ (10 nM) had the most potent anti-inflammatory effect compared the other doses (0.01-1 nM). However, there was no obvious dose-response relationship between $1\alpha,25(OH)_2D_3$ and the gene expression or secretion of the pro-inflammatory factors. This is probably because the anti-inflammatory effects of $1\alpha,25(OH)_2D_3$ could be exerted on THP-1-MacCM (IL-1β in Chapter 4 and 5)-stimulated preadipocytes in single or multiple manners (e.g. directly inhibiting the gene expression of the pro-inflammatory factors, genomically or non-genomically blocking inflammatory signaling, increasing eIF-2α of the UPR pathway to abate the translation of the pro-inflammatory factors), the same reason is applied in the late chapters.

The current study has also shown that the NF-κB, MAPK and UPR signaling pathways are involved in the anti-inflammatory action of $1\alpha,25(OH)_2D_3$ in preadipocytes. It has been reported that the VDR transcriptional complex can modulate the expression of vitamin D-responsive genes. These genes include the cytokines such as IL-2, IL-12, TNF-α, IFN-γ, GM-CSF, which are critical in modulating inflammatory response in tissue (307-310). Though, we didn't test whether the regulatory sequence of those pro-inflammatory factor encoding genes were among VDREs, there's a possibility that $1\alpha,25(OH)_2D_3$-VDR transcriptional complex could bind to the regulatory regions (i.e. inhibitor) of IL-1β, IL-6, IL-8 and RANTES, since the results showed that $1\alpha,25(OH)_2D_3$ significantly reduced the gene expression levels of these cytokines. Further assays of chromatin immunoprecipitation could be conducted to investigate that whether the VDR (transcription complex) binds to the regulatory regions of these pro-inflammatory factors. Moreover, VDR-$1\alpha,25(OH)_2D_3$ complex could directly inhibit the expression of some genes by antagonizing the action of certain transcription factors (e.g.NF-AT and NF-κB) (297, 298). The results also show that $1\alpha,25(OH)_2D_3$ (10 nM) significantly reduced the expression levels of phosphorylated relA compared to THP-1-MacCM treated preadipocytes. In addition, it has been shown that relA binds to the promoters of IL-6 and IL-1β, thereby up-regulating the gene transcription (388, 389) Further assays of protein complex immunoprecipitation and chromatin immunoprecipitation could be applied to demonstrate that whether the VDR (transcription complex) binds to phosphorylated relA and the promoter regions of these pro-inflammatory factors. Taken together, $1\alpha,25(OH)_2D_3$ inhibits the gene expression of the pro-inflammatory factors probably by: directly attenuating the transcription by VDRE binding; or blocking the transcription factor relA (NF-κB p65) and attenuating its post translational modification (phosphorylation in this case), thus to indirectly inhibit the gene expression.

Besides the genomic effect of $1\alpha,25(OH)_2D_3$, it has been recognized that by binding VDR on the plasma membrane, $1\alpha,25(OH)_2D_3$ can exert non-genomic actions and the signaling molecules involved include protein kinases, especially MAPKs (311). Moreover, it has been demonstrated that $1\alpha,25(OH)_2D_3$ ($10^{-8}$ M) reduced the levels of phosphorylated ERK and p38 of the MAPK signaling pathways in THP-1-MacCM-stimulated human white subcutaneous adipocytes (24 h) (354). Therefore, the levels of these two signaling molecules were measured by western blotting in

the current study. Like phosphorylated relA, the expression level of phosphorylated ERK were significantly inhibited by 1α,25$(OH)_2D_3$ (10 nM). Phosphorylated p38 was also numerically reduced, but this was not statistically significant. In conclusion, 1α,25$(OH)_2D_3$ could also inhibit the gene expression of the MacCM-induced pro-inflammatory factors, by attenuating the phosphorylated ERK of the MAPK pathway.

Last but not the least, regarding ER stress is a potential contributor to metaflammation in obesity, so the signaling of the UPR pathways was also measured by western blotting. ER stress can be relieved by UPR. The accumulation of incorrectly folded proteins in cytosol triggers the UPR by activating three arms: PERK induced phosphorylated eIF-2α; IRE-1 induced transcription factor XBP-1; and ATF-6 (48). When the arm of PERK is stimulated, the phosphorylated eIF-2α will ubiquinate the incorrectly folded protein thus to attenuate the translation and relieve ER stress (48). Paradoxically, the results showed that the levels of phosphorylated eIF-2α was significantly increased by THP-1-MacCM compared to the control, whilst 1α,25$(OH)_2D_3$ (0.01-10 nM) significantly reduced the levels compared to THP-1-MacCM treated preadipocytes. It has been demonstrated that by activating PERK or IRE-1, UPR can induce a crosstalk with the NF-κB pathway (52). Subsequently the phosphorylation of IKK releases NF-κB, which in nucleus acts as a key transcription factor mediating the inflammatory (54). Though THP-1-MacCM significantly increased the levels of phosphorylated eIF-2α which can attenuate the secretion of the pro-inflammatory factors, it could also interact with the NF-κB signaling pathway to increase the expression of phosphorylated relA, which results in the net effect of enhancing the inflammatory response induced by LPS-stimulated macrophages, whereas by decreasing phosphorylated eIF-2α, 1α,25$(OH)_2D_3$ (0.01-10 nM) might lower the levels of phosphorylated relA to exert the anti-inflammatory effects on human white preadipocytes.

*Limitations*

1. Only preadipocytes studied, as these have similarity to macrophages. The effects might be different in mature adipocytes that make up the majority of human adipose tissue.
2. Although a wide range of 1α,25$(OH)_2D_3$ doses were studied, there is no clear dose-response for many of the observed effects, and the physiological concentrations that are relevant are

unknown at present.

3. Further experiments would be needed to precisely identify the sites and pathways through which 1α,25$(OH)_2D_3$ exerts the observed effects; some of these questions are explored in subsequent chapters.
4. The levels of total unphosphorylated protein(s) including relA, ERK (p42/44), p38 and eIF-2α have not been determined, which is a limitation of the current experiment design. Elevated or decreased phosphorylation levels may be accompanied by increased or decreased protein levels.

In summary, this study demonstrates that THP-1-MacCM significantly enhanced the gene expression and secretion of the pro-inflammatory factors from human preadipocytes. This is probably through increasing the levels of phosphorylated relA of the NF-κB signaling pathway, phosphorylated ERK (p42/44) and p38 of the MAPK pathways, and phosphorylated eIF-2α of the UPR pathway. Among the pro-inflammatory factors, IL-1β and IL-6 are critical in maintaining the inflammatory response. Moreover, 1α,25$(OH)_2D_3$ could inhibit the inflammatory response probably by:

1. Directly attenuating the pro-inflammatory gene expression;
2. Blocking phosphorylated relA to attenuate the pro-inflammatory gene expression;
3. Blocking phosphorylated ERK to attenuate the pro-inflammatory gene expression;
4. Reducing the level of phosphorylated eIF-2α to attenuate phosphorylated relA.

# 4. The effects of 1α,25$(OH)_2D_3$ on IL-1β-stimulated human white preadipocytes

## 4.1. Introduction

Several studies suggest that an array of moderately expressed TNF-α, IL-1β, IL-6, MCP-1 and other chemoattractants are responsible for the infiltration of immune cells into metabolic tissues during obesity, which is critical in the induction and maintenance of metaflammation in human adipose tissue (24, 25). Although the underlying mechanisms remain to be established, several signaling pathways have been implicated. For instance, during metaflammation in human adipocytes, TNF-α or IL-1β activates the JNK, IKKβ and their down-stream cascades including the transcription factors AP-1 as well as NF-κB in the classical receptor-mediated way, thereby up-regulating the gene expression and secretion of the pro-inflammatory factors (24), whereas the expression of the nuclear-receptor PPARγ is down-regulated (26), which may partly explain that the circulating level of adiponectin was negatively correlated with fat mass.

IL-1β is a pleiotropic pro-inflammatory factor that appears to have an important role in initiating and sustaining metabolic abnormalities in obesity, especially metaflammation and insulin resistance (for the specific details, please refer to *Introduction* Page 25-26). Similarly, previous studies from our groups and others have demonstrated that IL-1β stimulated an inflammatory response and dampened insulin sensitivity in human preadipocytes (390). The data from the study described in Chapter 3 also suggest that IL-1β is a major mediator of the macrophage-induced inflammatory response in human preadipocytes (the concentration of IL-1β of THP-1-MacCM was 2 ng/ml measured by ELISA). Furthermore, the interaction of MCP-1 with its receptor CCR-2 and CCR-5 with its ligands (CCL-3, CCL-4 and CCL-5), have also been demonstrated to be crucial for the recruitment of macrophages and the pathogenesis of insulin resistance in obesity (185-187, 193) (for the specific details, please refer to *Introduction* Page 27-29).

It has been shown that 1α,25$(OH)_2D_3$ has a wide range of effects on adipogenesis, adipocyte

apoptosis and metaflammation in adipose tissue (for the specific details, please refer to *Introduction* Page 54-56). Notably, a recent study suggests that pretreatment (24 h) and treatment (24 h) with 1α,25$(OH)_2D_3$ (10 and 100 nM) significantly decreased the expression and secretion of MCP-1 in THP-1-MacCM, TNF-α or IL-1β-stimulated human white preadipocytes (355).

## 4.2. Aims

This study aimed to investigate whether 1α,25$(OH)_2D_3$ has an inhibitory effect on IL-1β-stimulated inflammatory response in human preadipocytes. The experiments were designed to examine whether:

1. IL-1β could enhance the gene expression of IL-1β, IL-8, IL-6, MCP-1 and RANTES in human white preadipocytes;
2. IL-1β enhances the secretion of the pro-inflammatory factors from human white preadipocytes;
3. 1α,25$(OH)_2D_3$ inhibits the secretion or gene expression of the pro-inflammatory cytokines in IL-1β-stimulated preadipocytes;
4. IL-1β increases the level of phosphorylated relA of the NF-κB pathway in preadipocytes;
5. 1α,25$(OH)_2D_3$ could modulate the level of phosphorylated relA of the NF-κB pathway as well as phosphorylated eIF-2α or XBP-1 of the UPR pathways to exert the anti-inflammatory effects on IL-1β-stimulated preadipocytes.

## 4.3. Materials and Methods

Preadipocyte pretreatment and treatment

Culture of human preadipocytes was performed as described in Chapter 3. To investigate the effect

of 1α,25$(OH)_2D_3$ on IL-1β-stimulated preadipocytes, preadipocytes were either cultured alone (control), or with IL-1β (0.5 and 2 ng/ml, Sigma-Aldrich, UK) alone for 24 h. Further groups of cells were pretreated with 1α,25$(OH)_2D_3$ (0.01-10 nM, ENZO Life Sciences, USA) for 24 h [using an established protocol (355)], followed by treatments with IL-1β (0.5 and 2 ng/ml) and 1α,25$(OH)_2D_3$ (0.01-10 nM) for a further 24 h [using an established protocol (355)] at 37°C in 95% air and 5% $CO_2$. When the experiment was completed, cell media were collected for ELISA; preadipocytes were lysed with Trizol for qPCR or lysed with a lysis buffer for western blotting. All samples were stored at -80 °C.

Measurements

ELISA was performed for determining the secretion levels of pro-inflammatory factors including IL-6, IL-8, MCP-1 and RANTES and corrected by total protein content in cellular lysate. Real-time PCR was used to measure the gene expression levels of pro-inflammatory factors including IL-1β, IL-6, IL-8, MCP-1 and internal reference PPIA. For measuring protein levels of phosphorylated relA of the NF-κB signaling pathway, phosphorylated eIF-2α (in the PERK induced arm of the UPR), XBP-1 (at the concentration of 2 μg/ml in the IRE-1 inducted arm of the UPR), western blotting was performed. The laboratory procedures and statistical analyses are described in detail in Chapter 3.

## 4.4. Results

### 4.4.1. IL-1β enhances the secretion of the pro-inflammatory factors from human white preadipocytes

Since the secretion levels of IL-1β, IL-6, IL-8, MCP-1 and RANTES were significantly increased in (25%) THP-1-MacCM-stimulated preadipocytes in Chapter 3, these pro-inflammatory factors

were selected as the indicators of inflammatory response of preadipocytes induced by IL-1β. An ELISA to measure concentrations of IL-1β was not performed, because its secretion level can't be measured accurately in this experiment (the autocrine effect of IL-1β secretion from IL-1β-stimulated preadipocytes is not a simple subtraction).

The results (Figure 4.1, 2) show that IL-1β (0.5 and 2 ng/ml) markedly increased the secretion levels of IL-6, IL-8, MCP-1 and RANTES.

### 4.4.2. 1α,25(OH)$_2$D$_3$ reduces the secretion of the pro-inflammatory factors from IL-1β-stimulated preadipocytes

In general, 1α,25(OH)$_2$D$_3$ (0.01-10 nM) reduced cytokine secretion from (both 0.5 and 2 ng/ml) IL-1β-stimulated preadipocytes, although the effects appeared less consistent in (0.5 ng/ml) IL-1β-stimulated preadipocytes (figures 4.1, 2).

From (0.5 ng/ml) IL-1β-stimulated preadipocytes (Figure 4.1), only the levels of IL-6 were moderately decreased by the full range of doses; the others were partially significantly decreased by 1α,25(OH)$_2$D$_3$. For instance, the levels of IL-8 by 0.1 and 10 nM of 1α,25(OH)$_2$D$_3$, MCP-1 by 1 and 10 nM of 1α,25(OH)$_2$D$_3$ and RANTES by 0.01 and 10 nM of 1α,25(OH)$_2$D$_3$. However, there is no straightforward dose-response relationship between the secretion levels of the cytokines and the doses of 1α,25(OH)$_2$D$_3$ used in these experiments.

In parallel (Figure 4.2), though the levels of IL-8 were only significantly decreased by 0.01 and 0.1 nM of 1α,25(OH)$_2$D$_3$, the levels of IL-6, RANTES (dramatically); and MCP-1 (moderately) were all reduced by all doses (tested) of 1α,25(OH)$_2$D$_3$ (0.01-10 nM) from (2 ng/ml) IL-1β-stimulated preadipocytes. Moreover, the anti-inflammatory effects of 1α,25(OH)$_2$D$_3$ (0.01-10 nM) on cytokine secretion are quite similar across the dose range (0.01-10 nM).

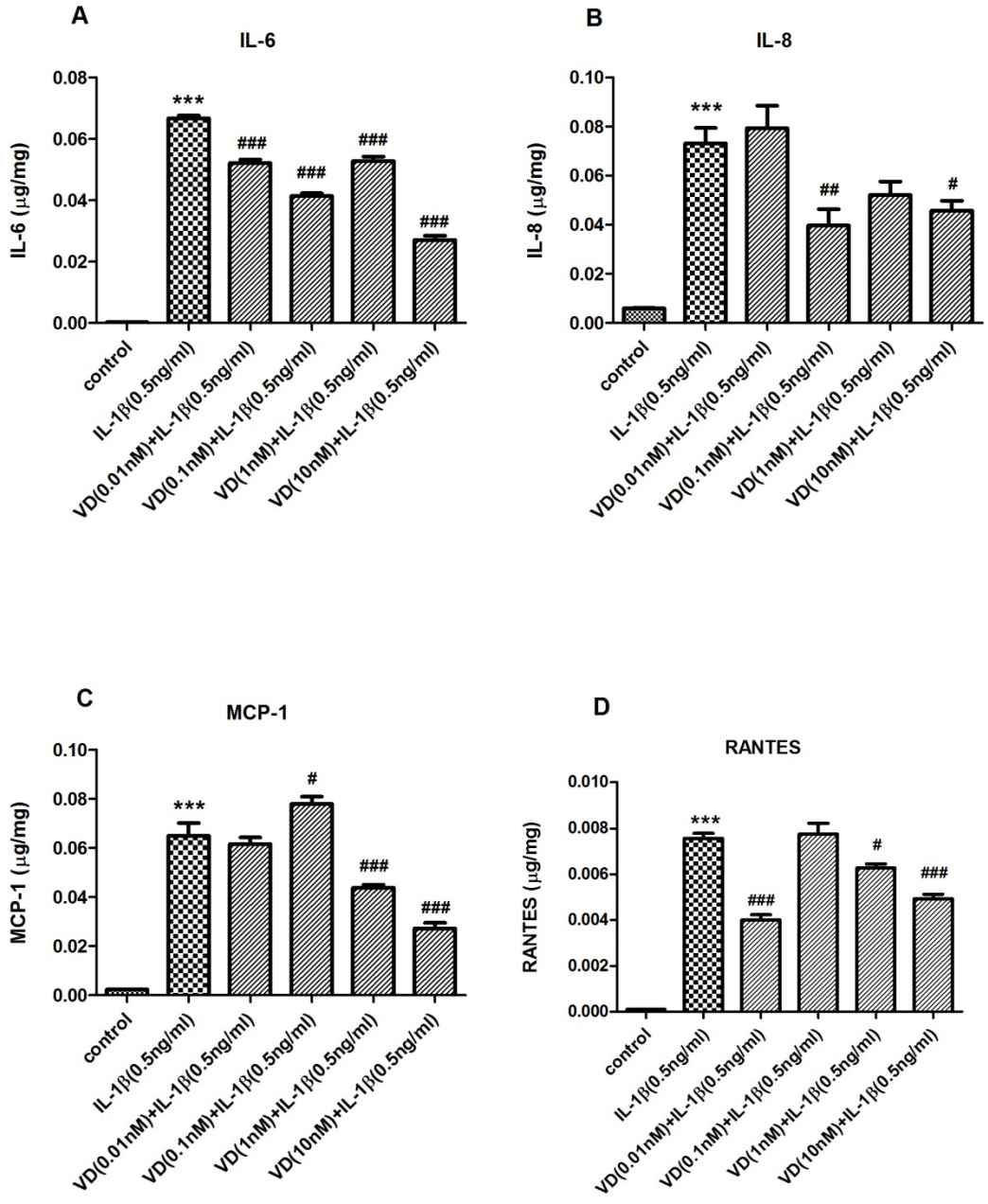


**Figure 4.1 Effects of 1α,25(OH)$_2$D$_3$ on cytokine release from (0.5 ng/ml) IL-1β-stimulated human white preadipocytes.**

Preadipocytes were either cultured alone (control), or with IL-1β (0.5 ng/ml) alone for 24 h. Further groups of cells were pretreated with 1α,25(OH)$_2$D$_3$ (0.01-10 nM) for 24 h, followed by treatments with IL-1β (0.5 ng/ml) and 1α,25(OH)$_2$D$_3$ (0.01-10 nM) for a further 24 h before medium collection. The release levels of pro-inflammatory factors (A) IL-6, (B) IL-8, (C) MCP-1 and (D) RANTES were measured by ELISA and normalized by protein content in the cellular lysate. Data are means ± SEM for groups of 6. A significant difference to control was indicated by ***($p<0.001$); to (0.5 ng/ml) IL-1β by #($p<0.05$), ##($p<0.01$), ###($p<0.001$). The results were determined using one-way ANOVA with Tukey's post hoc test and confirmed by two independent experiments.

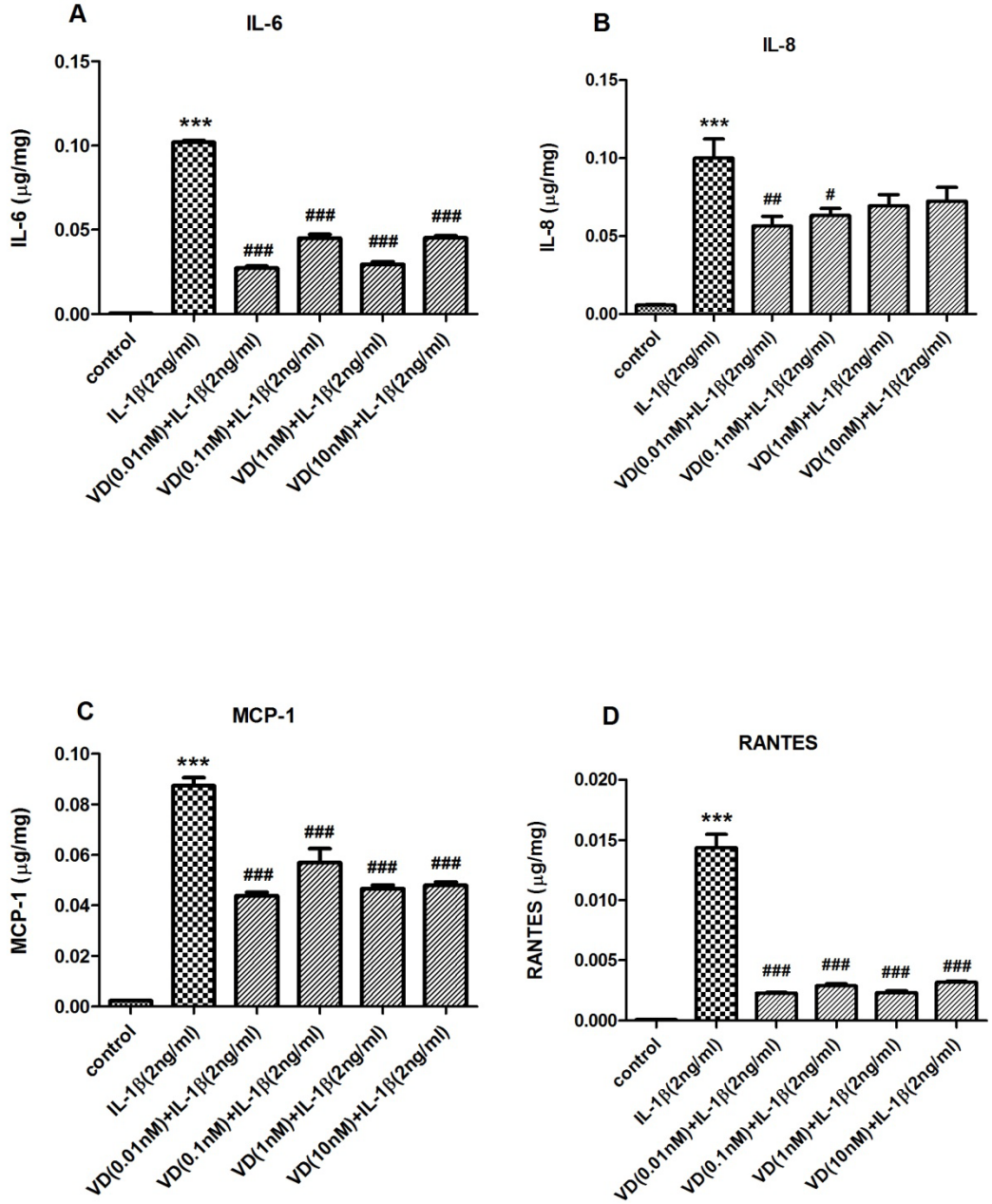


**Figure 4.2 Effects of 1α,25(OH)$_2$D$_3$ on cytokine release from (2 ng/ml) IL-1β-stimulated human white preadipocytes.**

Preadipocytes were either cultured alone (control), or with IL-1β (2 ng/ml) alone for 24 h. Further groups of cells were pretreated with 1α,25(OH)$_2$D$_3$ (0.01-10 nM) for 24 h, followed by treatments with IL-1β (2 ng/ml) and 1α,25(OH)$_2$D$_3$ (0.01-10 nM) for a further 24 h before medium collection. The release levels of pro-inflammatory factors (A) IL-6, (B) IL-8, (C) MCP-1 and (D) RANTES were measured by ELISA and normalized by protein content in the cellular lysate. Data are means ± SEM for groups of 6. A significant difference to control was indicated by ***($p<0.001$); to (2 ng/ml) IL-1β by #($p<0.05$), ##($p<0.01$), ###($p<0.001$). The results were determined using one-way ANOVA with Tukey's post hoc test and confirmed by two independent experiments.

### 4.4.2. IL-1β enhances the gene expression of the pro-inflammatory factors in human white preadipocytes

Similar to the secretion levels, the qPCR results (Figure 4.3, 4) show that the mRNA levels of the pro-inflammatory factors including IL-1β, IL-6, IL-8, MCP-1 and RANTES, were massively increased in (both 0.5 and 2 ng/ml) IL-1β-stimulated preadipocytes.

### 4.4.3. 1α,25(OH)$_2$D$_3$ reduces the gene expression of pro-inflammatory cytokines in IL-1β-stimulated preadipocytes

Except for the mRNA levels of RANTES, which was significantly decreased by all doses, 1α,25(OH)$_2$D$_3$ (0.01-10 nM) had no consistent effects on the mRNA levels of IL-1β, IL-6, IL-8 or MCP-1 in (0.5 ng/ml) IL-1β-stimulated preadipocytes, and in some cases, there appeared to be a modest increase in mRNA levels at low doses of 1α,25(OH)$_2$D$_3$ (IL-8 and MCP-1) (Figure 4.3).

(Figure 4.4) In contrast, 1α,25(OH)$_2$D$_3$ (0.01-10 nM) exhibited extensive anti-inflammatory effects on pro-inflammatory gene transcription in (2 ng/ml) IL-1β-stimulated preadipocytes, apart from 1α,25(OH)$_2$D$_3$ (10 nM) not affecting the mRNA level of IL-6, the rest were all significantly decreased. In addition, the reducing effects of 1α,25(OH)$_2$D$_3$ on the mRNA levels of IL-1β and MCP-1 were marked and similar across the dose range 1α,25(OH)$_2$D$_3$ (0.01-10 nM). However, there is no consistent dose-response relationship between the mRNA levels of the pro-inflammatory cytokines and the doses of 1α,25(OH)$_2$D$_3$ used in these experiments.

**Figure 4.3 Effects of 1α,25(OH)$_2$D$_3$ on cytokine gene expression in (0.5 ng/ml) IL-1β-stimulated human white preadipocytes.**

Preadipocytes were either cultured alone (control), or with IL-1β (0.5 ng/ml) alone for 24 h. Further groups of cells were pretreated with 1α,25(OH)$_2$D$_3$ (0.01-10 nM) for 24 h, followed by treatments with IL-1β (0.5 ng/ml) and 1α,25(OH)$_2$D$_3$ (0.01-10 nM) for a further 24 h before Trizol-dissolved lysate collection. The mRNA levels of pro-inflammatory factors (A) IL-1β, (B) IL-6, (C) IL-8, (D) MCP-1 and (E) RANTES were measured by qPCR. Data are means ± SEM for groups of 6. A significant difference to control was indicated by **(p<0.01), ***(p<0.001); to (0.5 ng/ml) IL-1β by #(p<0.05), ##(p<0.01), ###(p<0.001). The results were determined using one-way ANOVA with Tukey's post hoc test and confirmed by two independent experiments.

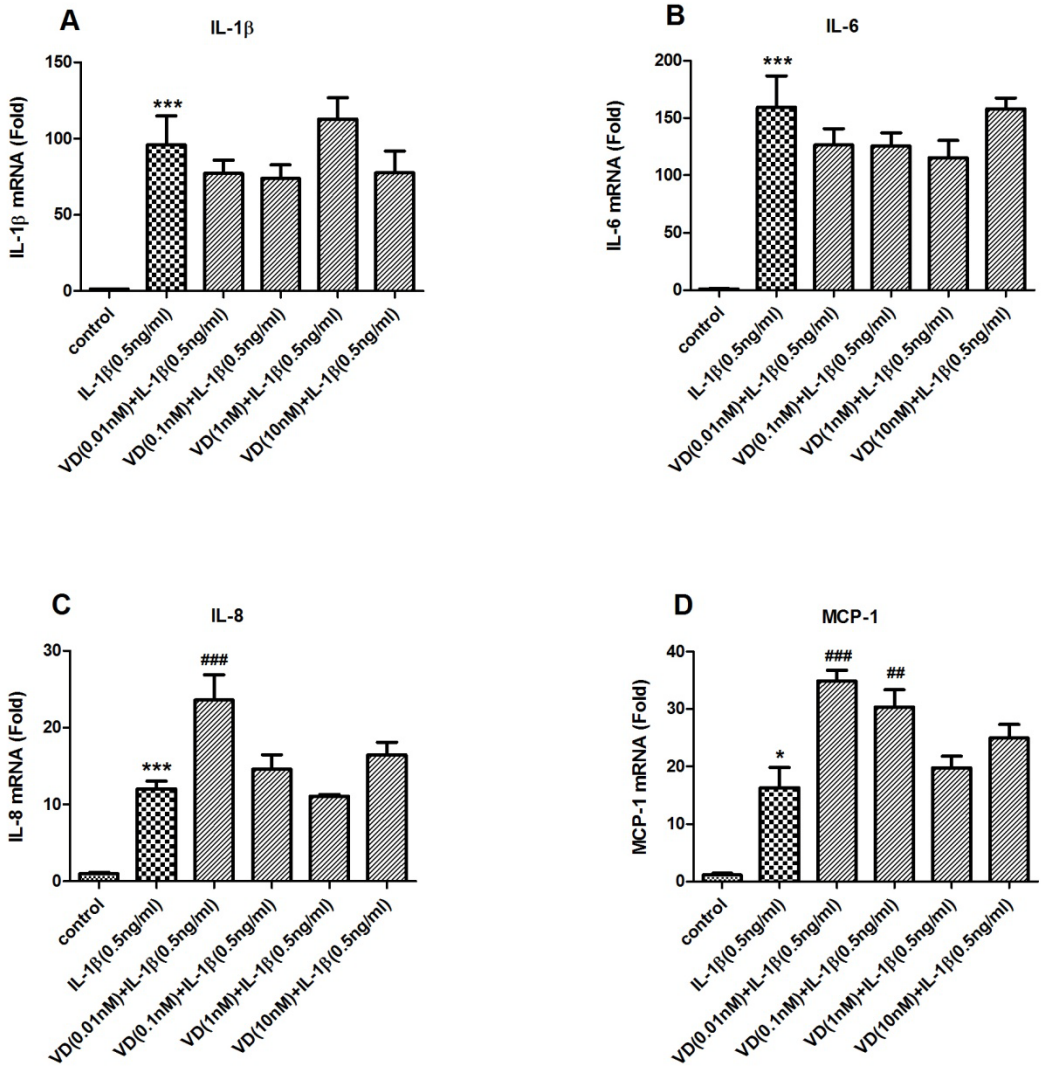

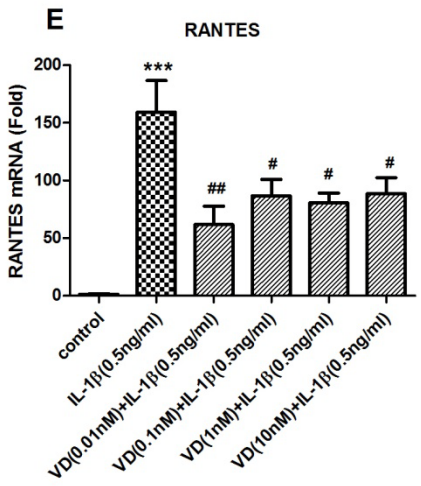
E
RANTES
RANTES mRNA (Fold)
200
150
100
50
0
***
##
#
#
#
control
IL-1β(0.5ng/ml)
VD(0.01nM)+IL-1β(0.5ng/ml)
VD(0.1nM)+IL-1β(0.5ng/ml)
VD(1nM)+IL-1β(0.5ng/ml)
VD(10nM)+IL-1β(0.5ng/ml)

**Figure 4.4 Effects of $1\alpha,25(OH)_2D_3$ on gene expression of cytokine in (2 ng/ml) IL-1β-stimulated human white preadipocytes.**

Preadipocytes were either cultured alone (control), or with IL-1β (2 ng/ml) alone for 24 h. Further groups of cells were pretreated with $1\alpha,25(OH)_2D_3$ (0.01-10 nM) for 24 h, followed by treatments with IL-1β (2 ng/ml) and $1\alpha,25(OH)_2D_3$ (0.01-10 nM) for a further 24 h before Trizol-dissolved lysate collection. The mRNA levels of pro-inflammatory factors (A) IL-1β, (B) IL-6 (B), (C) IL-8, (D) MCP-1 and (E) RANTES were measured by qPCR. Data are means ± SEM for groups of 6. A significant difference to control was indicated by ***($p<0.001$); to (2 ng/ml) IL-1β by #($p<0.05$), ##($p<0.01$), ###($p<0.001$). The results were determined using one-way ANOVA with Tukey's post hoc test and confirmed by two independent experiments.

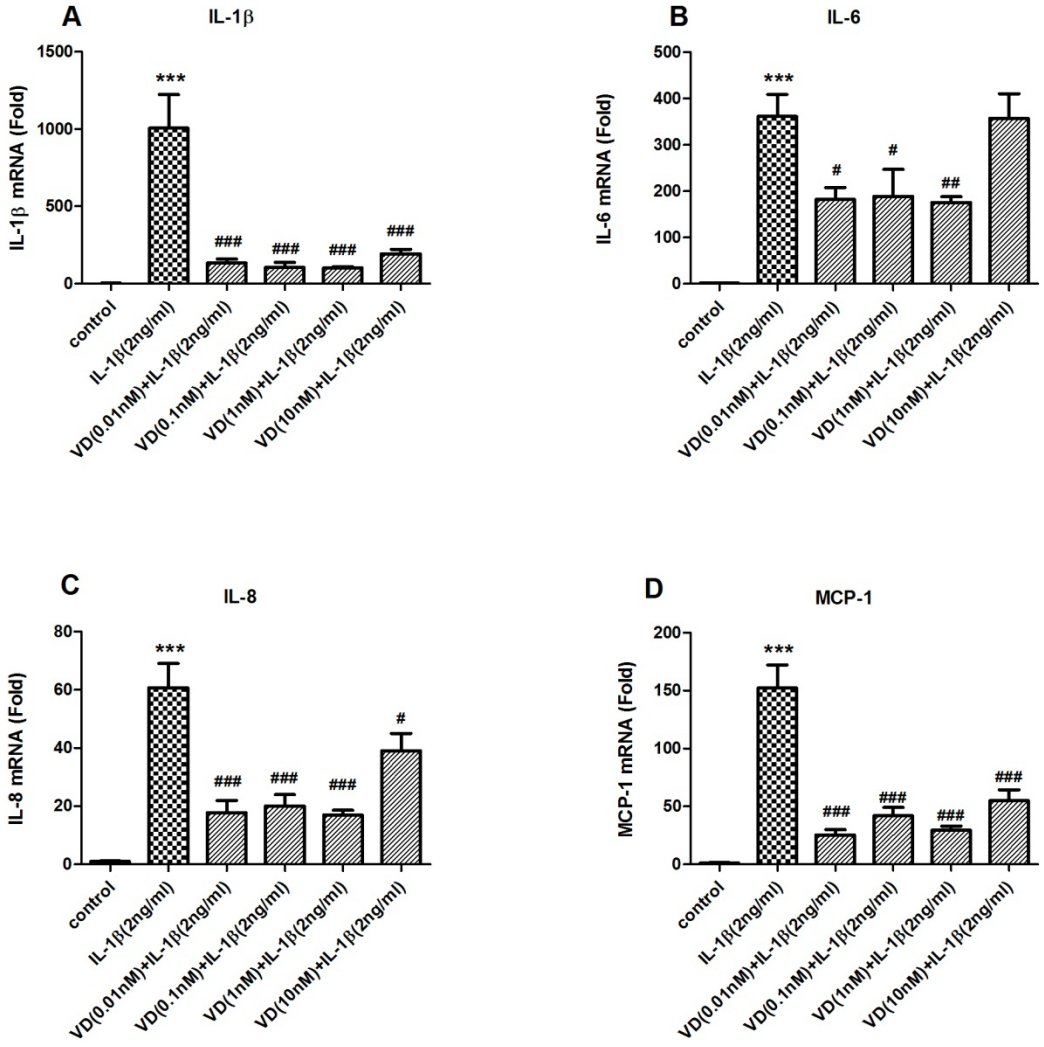

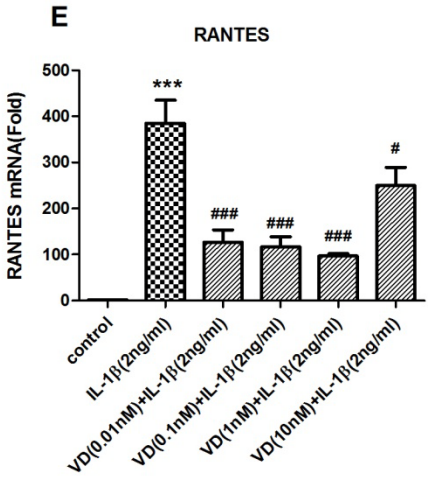
E
RANTES
RANTES mRNA(Fold)
500
400
300
200
100
0
***
###
###
###
#
control
IL-1β(2ng/ml)
VD(0.01nM)+IL-1β(2ng/ml)
VD(0.1nM)+IL-1β(2ng/ml)
VD(1nM)+IL-1β(2ng/ml)
VD(10nM)+IL-1β(2ng/ml)

### 4.4.4. IL-1β increases phosphorylated relA of the NF-κB pathways in human preadipocytes

To test whether IL-1β could modulate the NF-κB pathway, the expression levels of phosphorylated relA were measured by western blotting. The result (Figure 4.5) shows that the levels of phosphorylated relA were markedly higher in the presence of IL-1β (0.5 and 2 ng/ml), compared to the untreated preadipocytes.

However, 1α,25$(OH)_2D_3$ (0.01-10 nM) had no effect on the levels of phosphorylated relA in (0.5 and 2 ng/ml) IL-1β-stimulated preadipocytes.

**Figure 4.5 Effects of 1α,25(OH)$_2$D$_3$ on phosphorylated relA in (0.5 and 2 ng/ml) IL-1β-stimulated human white preadipocytes.**

Preadipocytes were either cultured alone (control), or with IL-1β (0.5 and 2 ng/ml) alone for 24 h. Further groups of cells were pretreated with 1α,25(OH)$_2$D$_3$ (0.01-10 nM) for 24 h, followed by treatments with IL-1β (0.5 and 2 ng/ml) and 1α,25(OH)$_2$D$_3$ (0.01-10 nM) for a further 24 h before lysate collection. The levels of phosphorylated relA (A) (IL-1β 0.5 ng/ml) and (B) (IL-1β 2 ng/ml) were measured by western blotting. Data are means ± SEM for groups of 3. A significant difference to control was indicated by ***($p<0.001$). The results were determined using one-way ANOVA with Tukey's post hoc test and confirmed by two independent experiments.

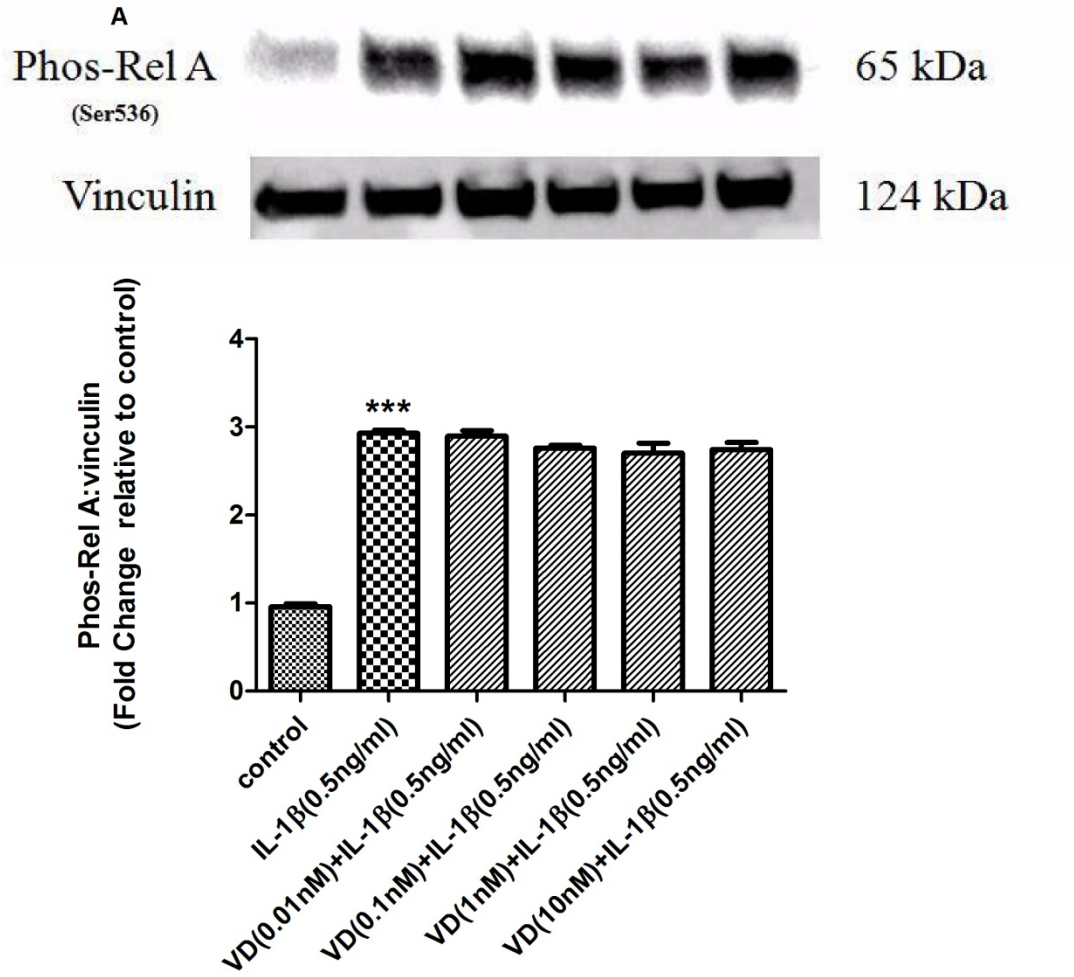

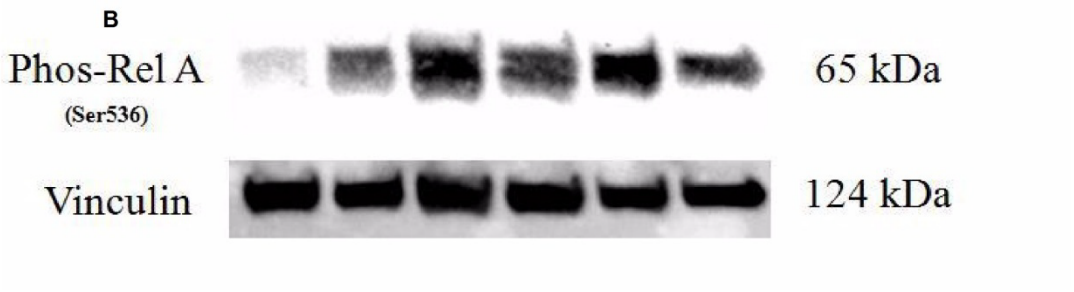
B
Phos-Rel A
(Ser536)
65 kDa
Vinculin
124 kDa

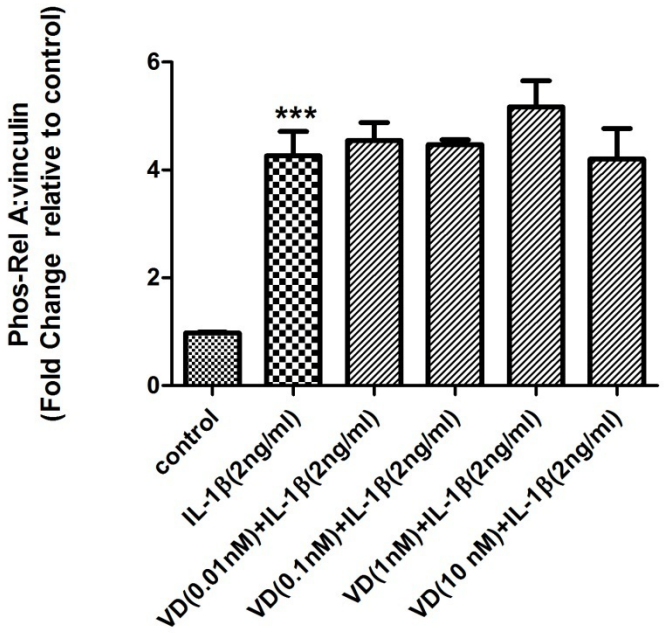
Phos-Rel A:vinculin
(Fold Change relative to control)
6
4
2
0
***
control
IL-1β(2ng/ml)
VD(0.01nM)+IL-1β(2ng/ml)
VD(0.1nM)+IL-1β(2ng/ml)
VD(1nM)+IL-1β(2ng/ml)
VD(10 nM)+IL-1β(2ng/ml)

### 4.4.5. 1α,25(OH)$_2$D$_3$ increases the levels of phosphorylated eIF-2α and XBP-1 of the UPR signaling pathways in IL-1β-stimulated preadipocytes

To test whether IL-1β or 1α,25(OH)$_2$D$_3$ could modulate signaling of the UPR pathways, the expression of phosphorylated eIF-2α and transcription factor XBP-1 were examined (Figure 4.6).

Firstly, IL-1β (0.5 ng/ml) had no effect on the level of phosphorylated eIF-2α, compared to the untreated preadipocytes (Figure 4.6 A).

Secondly, compared to (0.5 ng/ml) IL-1β-stimulated preadipocytes, 1α,25(OH)$_2$D$_3$ (0.01-10 nM) moderately increased the levels of phosphorylated eIF-2α, though the difference by 1 nM of 1α,25(OH)$_2$D$_3$ did not reach the statistical significance (Figure 4.6 A).

Thirdly, the levels of XBP-1 were undetectable in the untreated and (0.5 ng/ml) IL-1β-stimulated preadipocytes, while the levels were markedly increased by 1α,25(OH)$_2$D$_3$ (0.01-10 nM) in (0.5 ng/ml) IL-1β-stimulated preadipocytes (Figure 4.6 B).

Finally, there is no consistent dose-response relationship between the levels of these signaling molecules and the doses of 1α,25(OH)$_2$D$_3$ used in these experiments.

**Figure 4.6 Effects of 1α,25(OH)$_2$D$_3$ on signaling molecules of the UPR signaling pathways in (0.5 ng/ml) IL-1β-stimulated human white preadipocytes.**

Preadipocytes were either cultured alone (control), or with IL-1β (0.5 ng/ml) alone for 24 h. Further groups of cells were pretreated with 1α,25(OH)$_2$D$_3$ (0.01-10 nM) for 24 h, followed by treatments with IL-1β (0.5 ng/ml) and 1α,25(OH)$_2$D$_3$ (0.01-10 nM) for a further 24 h before lysate collection. The levels of (A) phosphorylated eIF-2α and (B) XBP-1 were measured by western blotting. Data are means ± SEM for groups of 3. A significant difference to (0.5 ng/ml) IL-1β was indicated by ###($p<0.001$). The results were determined using one-way ANOVA with Tukey's post hoc test and confirmed by two independent experiments.

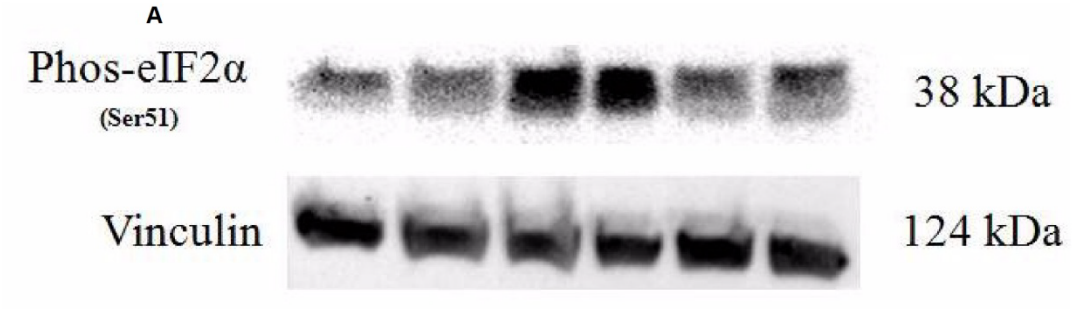


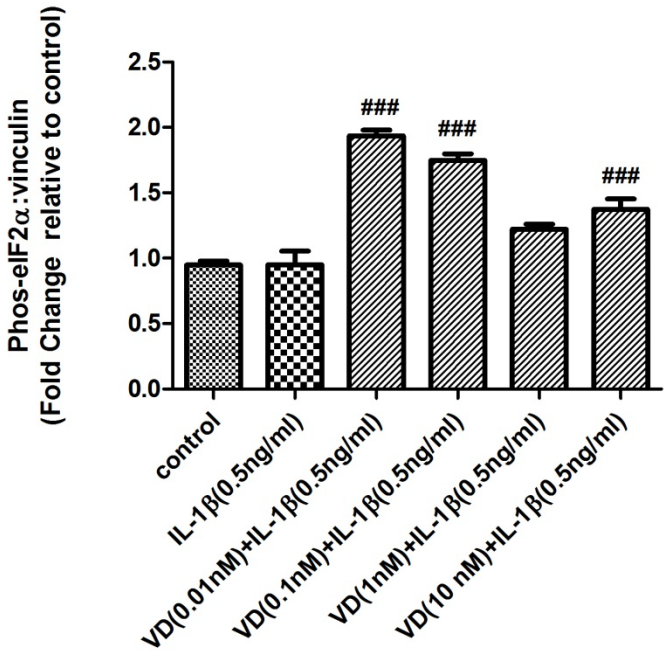

B

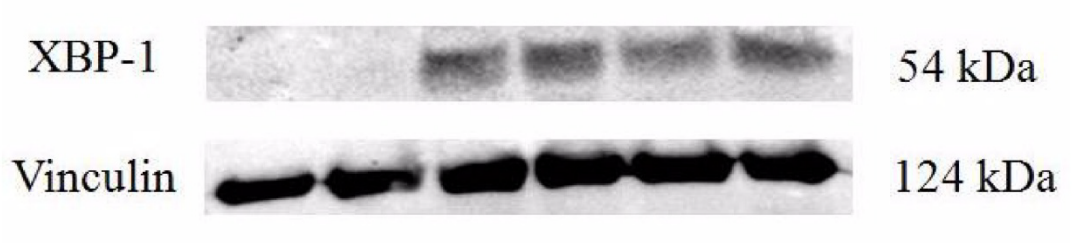
XBP-1
54 kDa
Vinculin
124 kDa

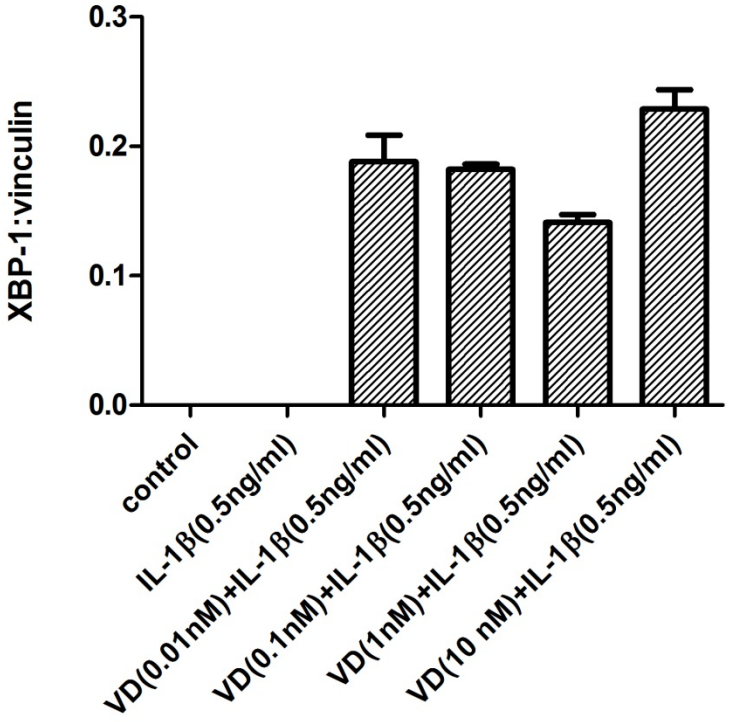
XBP-1:vinculin
0.3
0.2
0.1
0.0
control
IL-1β(0.5ng/ml)
VD(0.01nM)+IL-1β(0.5ng/ml)
VD(0.1nM)+IL-1β(0.5ng/ml)
VD(1nM)+IL-1β(0.5ng/ml)
VD(10 nM)+IL-1β(0.5ng/ml)

### 4.4.6. 1α,25(OH)$_2$D$_3$ increases the levels of phosphorylated eIF-2α of the UPR signaling pathway in IL-1β-stimulated preadipocytes

IL-1β (2 ng/ml) had no effect on the level of phosphorylated eIF-2α, compared to the untreated preadipocytes. While 1α,25(OH)$_2$D$_3$ (0.1-10 nM) was associated with significantly higher levels of phosphorylated eIF-2α in (2 ng/ml) IL-1β-stimulated preadipocytes (Figure 4.7 A).

### 4.4.7. 1α,25(OH)$_2$D$_3$ increases the levels of XBP-1 of the UPR signaling pathway in IL-1β-stimulated preadipocytes

Unlike that of IL-1β (0.5 ng/ml), the increasing effect of XBP-1 level on preadipocytes by IL-1β (2 ng/ml) was distinguishable (Figure 4.7 B).

In parallel, compared to (2 ng/ml) IL-1β-stimulated preadipocytes, 1α,25(OH)$_2$D$_3$ (0.01, 1 and 10 nM) significantly increased the levels of XBP-1, but there is no straightforward dose-response relationship between the levels of XBP-1 and these doses (Figure 4.7 B).

**Figure 4.7 Effects of 1α,25(OH)$_2$D$_3$ on signaling of the UPR signaling pathways in (2 ng/ml) IL-1β-stimulated human white preadipocytes.**

Preadipocytes were either cultured alone (control), or with IL-1β (2 ng/ml) alone for 24 h. Further groups of cells were pretreated with 1α,25(OH)$_2$D$_3$ (0.01-10 nM) for 24 h, followed by treatments with IL-1β (2 ng/ml) and 1α,25(OH)$_2$D$_3$ (0.01-10 nM) for a further 24 h before lysate collection. The levels of (A) phosphorylated eIF-2α and (B) XBP-1 were measured by western blotting. Data are means ± SEM for groups of 3. A significant difference to control was indicated by ***(p<0.001); to (2 ng/ml) IL-1β was indicated by ##(p<0.01), ###(p<0.001). The results were determined using one-way ANOVA with Tukey's post hoc test and confirmed by two independent experiments.

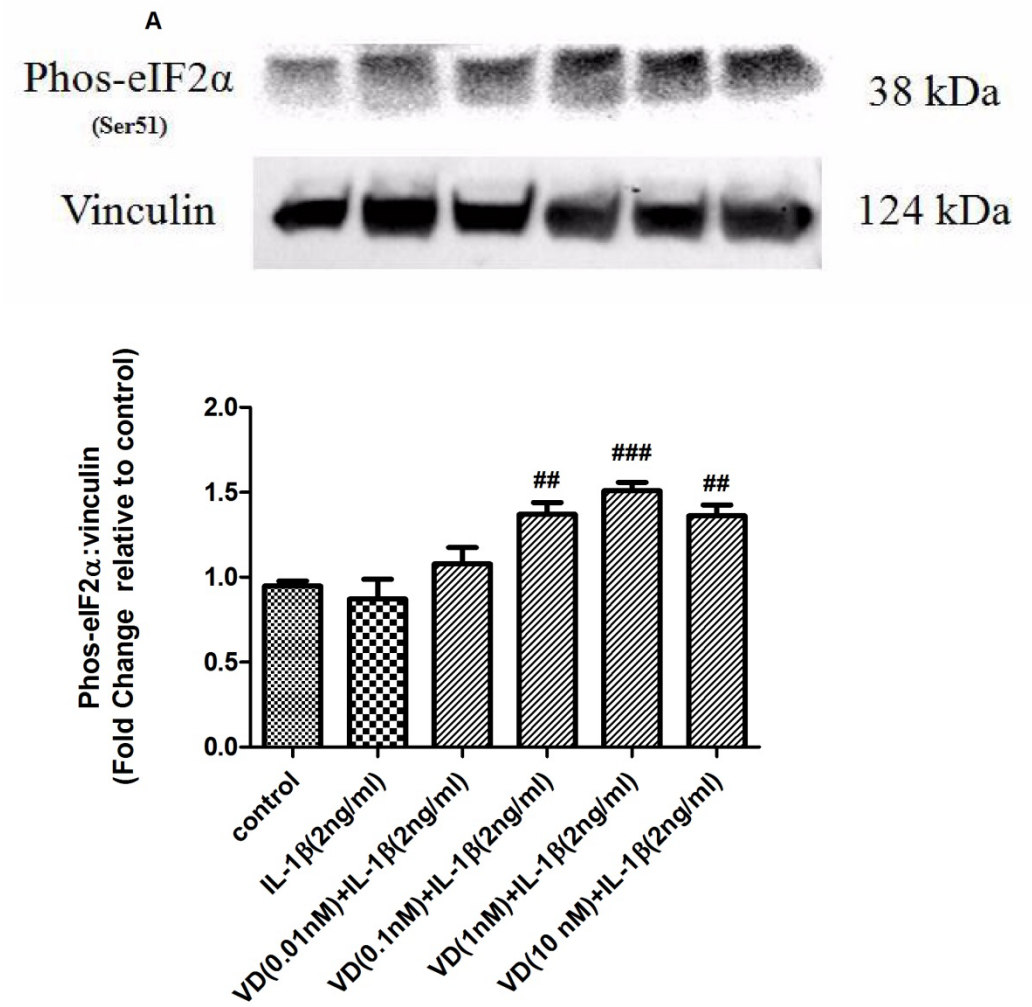

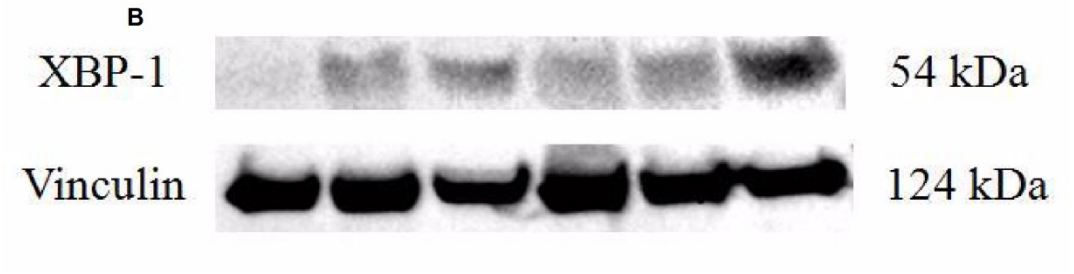
B
XBP-1
54 kDa
Vinculin
124 kDa

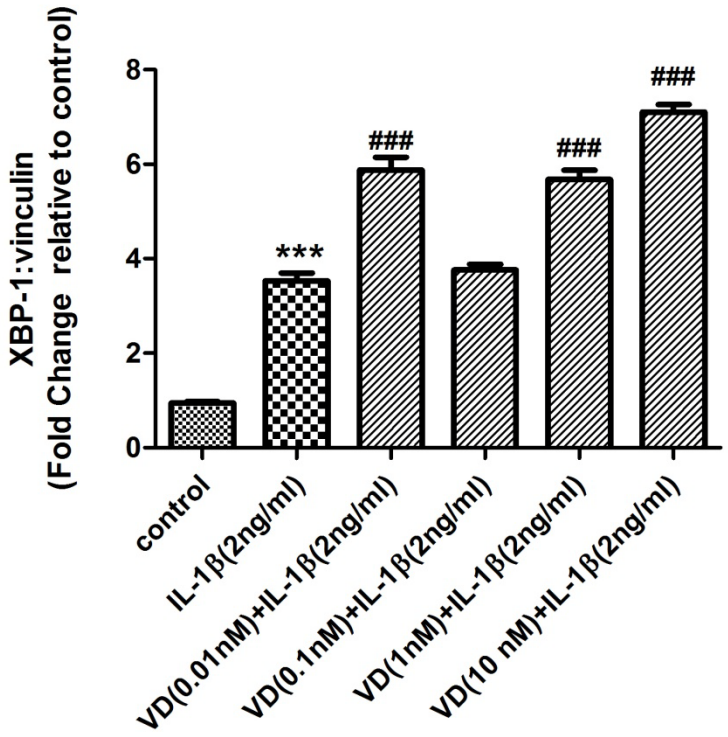
XBP-1:vinculin
(Fold Change relative to control)
8
6
4
2
0
***
###
###
###
control
IL-1β(2ng/ml)
VD(0.01nM)+IL-1β(2ng/ml)
VD(0.1nM)+IL-1β(2ng/ml)
VD(1nM)+IL-1β(2ng/ml)
VD(10 nM)+IL-1β(2ng/ml)

## 4.5. Discussion

The study described in Chapter 3 has demonstrated that the gene expression and secretion levels of the pro-inflammatory factors of THP-1-stimulated preadipocytes were significantly reduced by IL-1β neutralizing antibody. The experiments described in this chapter first aimed to test whether IL-1β (0.5 and 2 ng/ml) alone could induce the inflammatory response from preadipocytes to the same extent as that of LPS-induced macrophages. The dosages of IL-1β were selected according to the results of ELISA (data not shown): the baseline secretion level of IL-1β from LPS-stimulated THP-1-MacCM was approximately 2 ng/ml; preadipocytes were treated with (25%) THP-1-MacCM (the concentration of IL-1β was 0.5 ng/ml) in the study described in Chapter 3. Like (25%) THP-1-MacCM, (0.5 and 2 ng/ml) IL-1β significantly enhanced the gene expression and secretion levels of IL-1β, IL-6, IL-8, MCP-1 and RANTES.

IL-6 stimulates lipolysis, increases FFA levels and whole body fat oxidation (178), whilst it inhibits the secretion of other adipokines, especially adiponectin, an important marker of adipocyte differentiation in human adipocytes (179). Moreover, IL-6 induces metaflammation by up-regulating SOCS3, which in turn impairs the phosphorylation of IRS1 in HepG2 cells (391). Like leptin, the levels of circulating IL-6 are positively correlated with percentage of body fat in human (172). Mice with genetic deletion of IL-6 developed adult-onset obesity, which suggests that IL-6 is involved in the chronic physiological regulation of energy balance; decreased IL-6 signaling is highly associated with weight gain (173). Paradoxically, IL-6 has also an anti-inflammatory effect, since it has been demonstrated that elevated plasma IL-6 by skeletal muscle during exercise inhibited endotoxin-induced plasma TNF-α in humans (392). In addition, IL-6 activates AMPK in rat skeletal muscle by increasing the concentration of cAMP and the AMP to ATP ratio, which suggest that substantial increases in IL-6 concentrations by muscles during exercise, may play a role in glycogen breakdown and lipolysis within skeletal muscle (183). Therefore, in the present study, we selected IL-1β over IL-6 to trigger the inflammatory response in preadipocytes, mainly for the supposed beneficial effects of IL-6.

To test whether IL-1β exerts the pro-inflammatory effects on preadipocytes by increasing the

signaling of the NF-κB pathway, the level of phosphorylated NF-κB was measured by western blotting. We didn't select the signaling with the MAPK pathways because according to the results of Chapter 3, the levels of phosphorylated ERK and p38 were not significantly inhibited by IL-1β neutralization. The NF-κB signaling pathway is activated by a cascade of kinases. When upstream signals converge at the IKK complex and activate IKKβ via phosphorylation, the activated IKKβ phosphorylates and degrades I-κB to release NF-κB p65/p50 heterodimer into the nucleus and binds unto the promoters of inflammatory genes (including TNF-α, IL-1β,COX2, IL-6, IL-12, MCP-1, CCR-2 and CCR-5), which in turn augment metaflammation by recruiting more immune cells into adipose tissue (244). In the present study, like that in THP-1-MacCM-stimulated preadipocytes, the expression levels of phosphorylated NF-κB were significantly enhanced by IL-1β (both 0.5 and 2 ng/ml) compared with the untreated control. Taken together, IL-1β increases the levels of phosphorylated NF-κB, which may lead to enhance the gene expression and secretion of the pro-inflammatory factors in human preadipocytes.

The study described in Chapter 3 also demonstrated that 1α,25$(OH)_2D_3$ (10 nM) significantly inhibited the gene expression and secretion levels of IL-1β, IL-6, IL-8 and RANTES. To investigate whether 1α,25$(OH)_2D_3$ (0.1-10 nM) could inhibit the gene expression and secretion levels of the pro-inflammatory factors, preadipocytes were pre-treated with 1α,25$(OH)_2D_3$ (0.1-10 nM) for 24h, followed by the treatment with IL-1β (0.5, 2 ng/ml) in the presence of 1α,25$(OH)_2D_3$ (0.1-10 nM) for a further 24h. The results show that 1α,25$(OH)_2D_3$ (0.1-10 nM) significantly inhibited the secretion but not the gene expression levels of IL-1β, IL-6, IL-8, MCP-1 and RANTES, compared with IL-1β (0.5 ng/ml) only treated preadipocytes. Surprisingly, the gene expression and secretion levels of these pro-inflammatory factors were significantly inhibited by 1α,25$(OH)_2D_3$ (0.1-10 nM), compared with IL-1β (2 ng/ml) treated preadipocytes. The mechanism underlying 1α,25$(OH)_2D_3$ down-regulating the gene expression of pro-inflammatory factors in an IL-1β dose dependent manner needs to be investigated in the future; although not formally compared, the higher concentration of IL-1β results in a greater inflammatory response (e.g. approx.158-fold increase in IL-6 at 0.5 ng/ml, compared to a 361-fold increase at 2ng/ml), and it may be that the inhibitory effects of 1α,25$(OH)_2D_3$ are only apparent when there is a strong inflammatory response. Like the anti-inflammatory effects on THP-MacCM-stimulated

preadipocytes, there was no apparent dose-response relationship between 1α,25$(OH)_2D_3$ and the gene expression or secretion of the pro-inflammatory factors.

In obesity, as an outcome of excessive intake of energy, enhanced protein synthesis and insufficient chaperone proteins triggers ER stress, but which can be relieved by UPR (48). The activation of UPR is conducted by three arms consisting of PERK, IRE-1 and ATF-6. The consequence of the activation includes inhibition of protein synthesis, enhanced expression of chaperones and clearance of incorrectly folded proteins, and stimulated ER biogenesis (51). In the current study, to test whether 1α,25$(OH)_2D_3$ could modulate the signaling of the UPR pathways, the levels of transcription factors XBP-1 induced by IRE-1, and phosphorylated eIF-2α inducted by PERK, were measured by western blotting. The results show that the level of XBP-1 couldn't be detected in (0.5 ng/ml) IL-1β-stimulated preadipocytes, while 1α,25$(OH)_2D_3$ (0.1-10 nM) increased the levels. Likewise, 1α,25$(OH)_2D_3$ (0.1-10 nM) significantly enhanced the levels of XBP-1 compared to that of (2 ng/ml) IL-1β-stimulated preadipocytes. It has been reported that processing of pro-IL-1β is fully dependent on caspase-8, but neither the UPR proteins (XBP-1 and CHOP) nor the TLR4 adaptor molecule MyD88 are necessary for caspase-8 activation (393). Therefore, the current results suggest that the levels of XBP-1 increased by 1α,25$(OH)_2D_3$ neither contributes nor inhibits the inflammatory response induced by IL-1β.

The study described in Chapter 3 shows that 1α,25$(OH)_2D_3$ may exert the anti-inflammatory effects by reducing the levels of phosphorylated eIF-2α. Paradoxically, the levels of phosphorylated eIF-2α were significantly increased by 1α,25$(OH)_2D_3$, compared with (0.5 and 2 ng/ml) IL-1β-stimulated preadipocytes. This is accentuated by the ELISA and qPCR results, which show that although the gene expression of the pro-inflammatory factors were not significantly reduced by 1α,25$(OH)_2D_3$, the secretion was compared to (0.5 ng/ml) IL-1β-stimulated preadipocytes; and suggest that the increased phosphorylated eIF-2α could ubiquinate the increased levels of mRNA translated products by IL-1β (48), thus significantly inhibiting the secretion of the pro-inflammatory factors. In this sense, 1α,25$(OH)_2D_3$ could also exert anti-inflammatory effects by increasing the levels of phosphorylated eIF-2α of the UPR pathway. In addition, the results might also explain why although 1α,25$(OH)_2D_3$ (10 nM) significantly

reduced the levels of phosphorylated relA in THP-1-MacCM-stimulated preadipocytes in Chapter 3 (the reduced levels of phosphorylated eIF-2α inhibiting the NF-κB pathway), but not by $1\alpha,25(OH)_2D_3$ in (0.5 and 2 ng/ml) IL-1β-stimulated preadipocytes (the increased levels of phosphorylated eIF-2α enhancing the NF-κB pathway).

As demonstrated by the current study, the gene expression levels of the pro-inflammatory factors were significantly inhibited by $1\alpha,25(OH)_2D_3$ (i.e. 10 nM) in (2 ng/ml) IL-1β-stimulated preadipocytes. It has been shown that the VDR transcriptional complex can modulate the expression of vitamin D-responsive genes including cytokines such as IL-2, IL-12, TNF-α, IFN-γ, GM-CSF, which are critical in modulating inflammatory response in tissue (307-310). Therefore, the results suggest that the $1\alpha,25(OH)_2D_3$-VDR transcriptional complex could bind to the promoters of IL-1β, IL-6, IL-8, MCP-1 and RANTES, thereby reducing the gene expression. Further chromatin immunoprecipitation assays are required to clarify this notion.

*Limitations*

1. The levels of total unphosphorylated protein(s) including relA and eIF-2α have not been determined, which is a limitation of the current experiment design. Elevated or decreased phosphorylation levels may be accompanied by increased or decreased protein levels.

In summary, this study demonstrates that IL-1β significantly increased the gene expression and secretion of the pro-inflammatory cytokines, including IL-1β, IL-6, IL-8, MCP-1 and RANTES, from human preadipocytes. This is probably through increasing the level of phosphorylated relA of the NF-κB pathway. $1\alpha,25(OH)_2D_3$ could inhibit the inflammatory response probably by:

1. Directly attenuating the pro-inflammatory gene expression;
2. Increasing the level of phosphorylated eIF-2α of the UPR pathway to attenuate the pro-inflammatory translation.

# 5. The effects of VDR agonists on IL-1β-stimulated human white preadipocytes

## 5.1. Introduction

VDR are generally expressed in a variety of cell lines and primary cells. A large number of studies suggest that it's involved in a variety of processes including cell proliferation, differentiation, and immune-regulation (292). By binding to VDR complex, $1\alpha,25(OH)_2D_3$ modulates the genomic response of numerous cells as well as tissues throughout the body in an endocrine, autocrine or paracrine manner (285). As mentioned before, a large body of evidence suggests that $1\alpha,25(OH)_2D_3$ exerts an anti-inflammatory action on preadipocytes and adipocytes (352-356) (for the specific details, please refer to *Introduction* Page 56).

Though $1\alpha,25(OH)_2D_3$ has anti-inflammatory efficacy in different animal models, which were summarized as systemic lupus erythematosus in lpr/lpr mice; type I diabetes in non-obese diabetic mice; collagen-induced arthritis, experimental allergic encephalomyelitis and inflammatory bowel disease mouse and rat (292), the immuno-modulatory properties are mostly achieved only if very high doses are applied, which can unfortunately lead to the side effect of hypercalcemia. Hence, based on knowledge about the specific interactions between $1\alpha,25(OH)_2D_3$ and the ligand binding pocket in the LBD of the VDR (283), many VDR agonists with the improved biological profile for a potential therapeutic application, have been synthesized (316), and among which are ZK159222 and ZK191784 (318-320, 323, 324) (for the specific details, please refer to *Introduction* Page 50-52).

Noteworthy, a recent study from our group indicates that pretreatment (48 h) and treatment (24 h) with ZK159222 and ZK191784 (100 nM and 1 μM) may have anti-inflammatory actions in THP-1-MacCM-stimulated human white adipocytes (322).

## 5.2. Aims

This study was aimed to investigate whether ZK159222 and ZK191784 have an inhibitory effect on the IL-1β-stimulated inflammatory response in human preadipocytes. Human preadipocytes treated with IL-1β served as an *in vitro* model and $1\alpha,25(OH)_2D_3$ as a positive control to study effects of ZK159222 and ZK191784. The experiments were set up to examine whether:

1. ZK159222 or ZK191784 could inhibit the secretion of the pro-inflammatory factors from IL-1β-stimulated preadipocytes;
2. ZK159222 or ZK191784 could inhibit the gene expression of the pro-inflammatory factors in IL-1β-stimulated preadipocytes;
3. ZK159222 or K191784 could modulate the level of phosphorylated relA or methylated relA of the NF-κB pathway as well as phosphorylated eIF-2α of the UPR pathway.

## 5.3. Materials and Methods

Preadipocyte pretreatment and treatment

Culture of human preadipocytes was performed as described in Chapter 3. To investigate the effect of VDR agonists on IL-1β-stimulated preadipocytes, preadipocytes were either cultured alone (control), or with IL-1β (0.5 ng/ml, Sigma-Aldrich, UK) alone for 24 h. Further groups of cells were pretreated with $1\alpha,25(OH)_2D_3$ (10 nM, ENZO Life Sciences, USA), ZK 159222 (10 nM and 1 μM, Bayer, Germany) or ZK191784 (10 nM and 1 μM, Bayer, Germany) for 48 h [using an established protocol (322)], followed by treatments with IL-1β (0.5 ng/ml) and $1\alpha,25(OH)_2D_3$ (10 nM), ZK 159222 (10 nM and 1 μM) or ZK191784 (10 nM and 1 μM) for a further 24 h [the established protocol (322)] at 37°C in 95% air and 5% $CO_2$. When the experiment was completed, cell media were collected for cytokine array and ELISA; preadipocytes were lysed with Trizol for qPCR or lysed with a lysis buffer for western blotting. All samples were stored at -80 °C.

Cytokine array

Secreted cytokines from the treated preadipocytes were screened using Proteome Profiler Human XL Cytokine Array (R&D Systems) following the manufacturer's instructions. Before the assays, 100 µl of each of the collected media from the treated preadipocytes were pooled (n = 6, per group) as the samples to be measured. The cytokine signals were captured by Molecular Imager ChemiDoc XRS+ System (Bio-Rad, Hertfordshire, UK), and the results were presented as pixel density relative to the reference controls on the arrays.

Other measurements

ELISA was performed for determining the secretion levels of pro-inflammatory factors including IL-6, IL-8, MCP-1 and RANTES and corrected by total protein content in cellular lysate. Real-time PCR was used to measure the gene expression levels of pro-inflammatory factors including IL-1β, IL-6, IL-8, MCP-1 and internal reference PPIA. For measuring protein levels of phosphorylated relA and methylated relA (at 1:1000 dilution) of the NF-κB signaling pathway (the rationale for testing these indictors has been specified in *Discussion* Page 181-182, 183), phosphorylated eIF-2α (in the PERK inducted arm of the UPR), western blotting was performed. The laboratory procedures and statistical analyses are described in detail in Chapter 3.

## 5.4. Results

### 5.4.1. IL-1β enhances the secretion of cytokines from human preadipocytes

In the initial experiments, cytokines released from (0.5 ng/ml) IL-1β-stimulated preadipocytes were screened by cytokine array (Figure 5.1, Appendix 9.4). A variety of cytokines were secreted including pro-inflammatory factors: IL-1β, IL-6, MIF, MIP-1α (specifically expressed by macrophages), GRO-α, MCP-1, MCP-3, RANTES (chemoattractants), IL-8, slCAM-1 (mainly

expressed by neutrophils) and growth factors including angiogenin, EGF, G-CSF, HGF, GDF1, etc.

### 5.4.2. ZK159222 and ZK191784 inhibit the secretion of pro-inflammatory factors from IL-1β-stimulated human preadipocytes

Cytokine release from ZK15922 (1 μM) and ZK191784 (1 μM)-stimulated preadipocytes was also screened by cytokine array. The results (Figure 5.1, Appendix 9.4) show that the secretion of the pro-inflammatory factors including IL-6, IL-8, MCP-1, MCP-3 and RANTES from (0.5 ng/ml) IL-1β-stimulated preadipocytes, were discernibly reduced by the two VDR agonists.

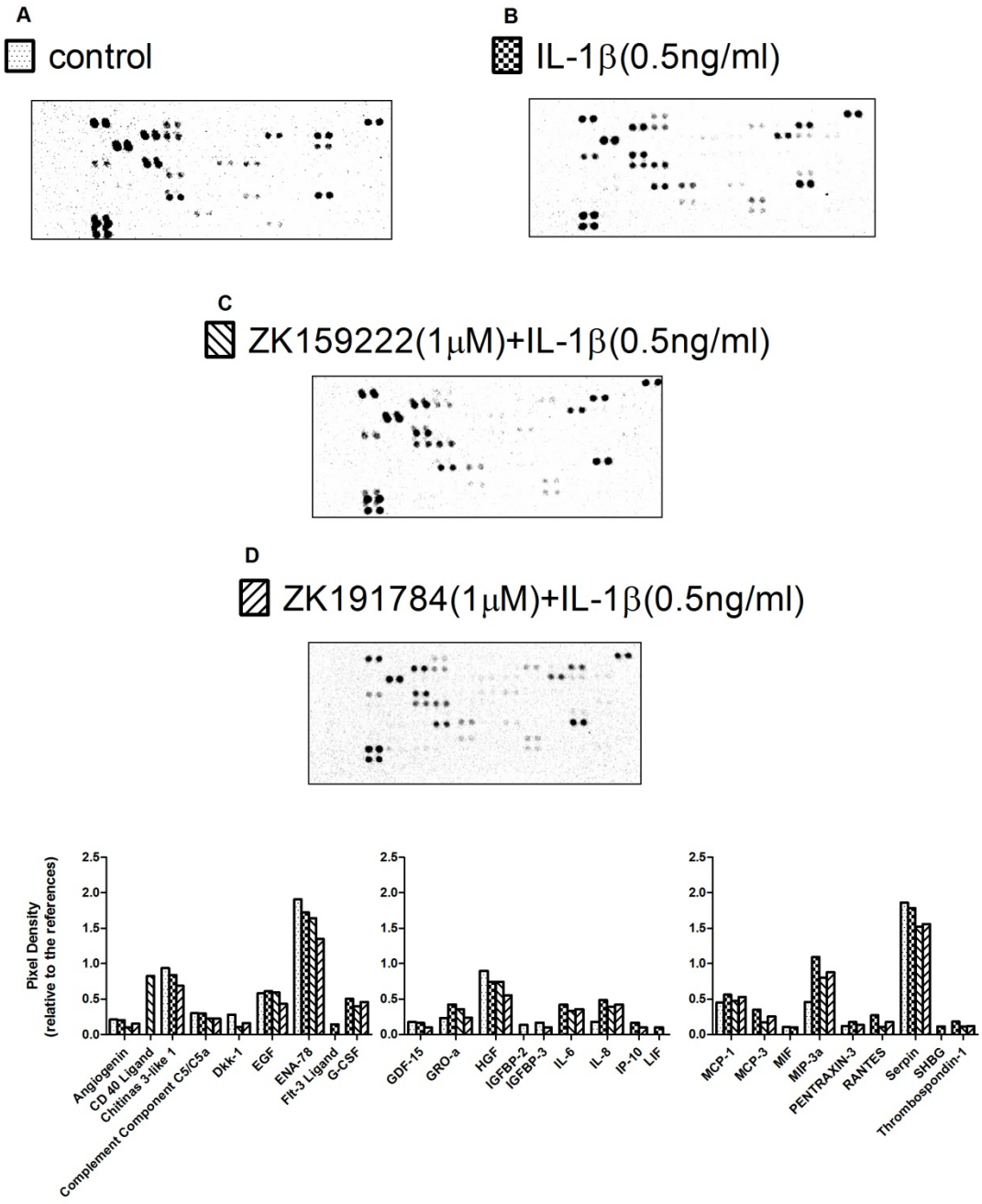


**Figure 5.1 Effects of ZK159222 and ZK191784 on cytokine release from IL-1β-stimulated human white preadipocytes.**

Preadipocytes were pretreated with ZK159222 (1 μM) or ZK191784 (1 μM) for 48 h, followed by treatments with IL-1β (0.5 ng/ml) in the presence of ZK159222 (1 μM) or ZK191784 (1 μM) for a further 24 h before medium collection. The cytokine release levels from (A) control, (B) IL-1β (0.5 ng/ml), (C) ZK159222 (1 μM) and (D) ZK191784 (1 μM) were screened by cytokine array. The results are presented as pixel density relative to the reference controls on the arrays.

### 5.4.3. IL-1β increases the secretion of pro-inflammatory factors from human preadipocytes

According to the result on the cytokine array, the pro-inflammatory factors including IL-6, IL-8, MCP-1 and RANTES were selected as indicators of the inflammatory response, and the result (Figure 5.2) shows that the secretion levels of these pro-inflammatory factors were dramatically increased by IL-1β (0.5 ng/ml) from human preadipocytes.

### 5.4.4. 1α,25(OH)$_2$D$_3$ reduces the secretion of pro-inflammatory factors from IL-1β-stimulated human preadipocytes

(Figure 5.2) 1α,25(OH)$_2$D$_3$ (10 nM) significantly reduced the secretion levels of IL-6, IL-8, MCP-1 and RANTES from (0.5 ng/ml) IL-1β-stimulated preadipocytes.

### 5.4.5. ZK159222 reduces the secretion of pro-inflammatory factors from IL-1β-stimulated human preadipocytes

(Figure 5.2) Firstly, ZK159222 (10 nM and 1 μM) markedly reduced the levels of IL-8 and RANTES from (0.5 ng/ml) IL-1β-stimulated preadipocytes. Secondly, the levels of IL-6 were moderately reduced by ZK159222 (10 nM and 1 μM). Noteworthy, the reducing effects on these pro-inflammatory factors are consistent between the doses. Finally, though the levels of MCP-1 were also moderately reduced by ZK159222 (10 nM and 1 μM), only the difference by ZK159222 (10 nM) was statistically significant, compared to (0.5 ng/ml) IL-1β-stimulated preadipocytes.

### 5.4.6. ZK191784 reduces the secretion of pro-inflammatory factors from IL-1β-stimulated human preadipocytes

(Figure 5.2) The levels of IL-6, IL-8, MCP-1 and RANTES were moderately reduced by ZK191784 (10 nM and 1 μM) compared to (0.5 ng/ml) IL-1β-stimulated preadipocytes, and the reducing effects on these pro-inflammatory factors are consistent between the doses.

.

**Figure 5.2 Effects of VDR agonists on cytokine release from (0.5 ng/ml) IL-1β-stimulated human white preadipocytes.**

Preadipocytes were either cultured alone (control), or with IL-1β (0.5 ng/ml) alone for 24 h. Further groups of cells were pretreated with 1α,25$(OH)_2D_3$ (10 nM) or ZK159222 (10 nM and 1 μM) or ZK191784 (10 nM and 1 μM) for 48 h, followed by treatments with IL-1β (0.5 ng/ml) and 1α,25$(OH)_2D_3$ (10 nM) or ZK159222 (10 nM and 1 μM) or ZK191784 (10 nM and 1 μM) for a further 24 h before medium collection. The release levels of pro-inflammatory factors (A) IL-6, (B) IL-8, (C) MCP-1 and (D) RANTES were measured by ELISA and normalized by protein content in the cellular lysate. Data are means ± SEM for groups of 6. A significant difference to control was indicated by ***($p<0.001$); to (0.5 ng/ml) IL-1β by #($p<0.05$), ##($p<0.01$),###($p<0.001$). The results were determined using one-way ANOVA with Tukey's post hoc test and confirmed by two independent experiments.

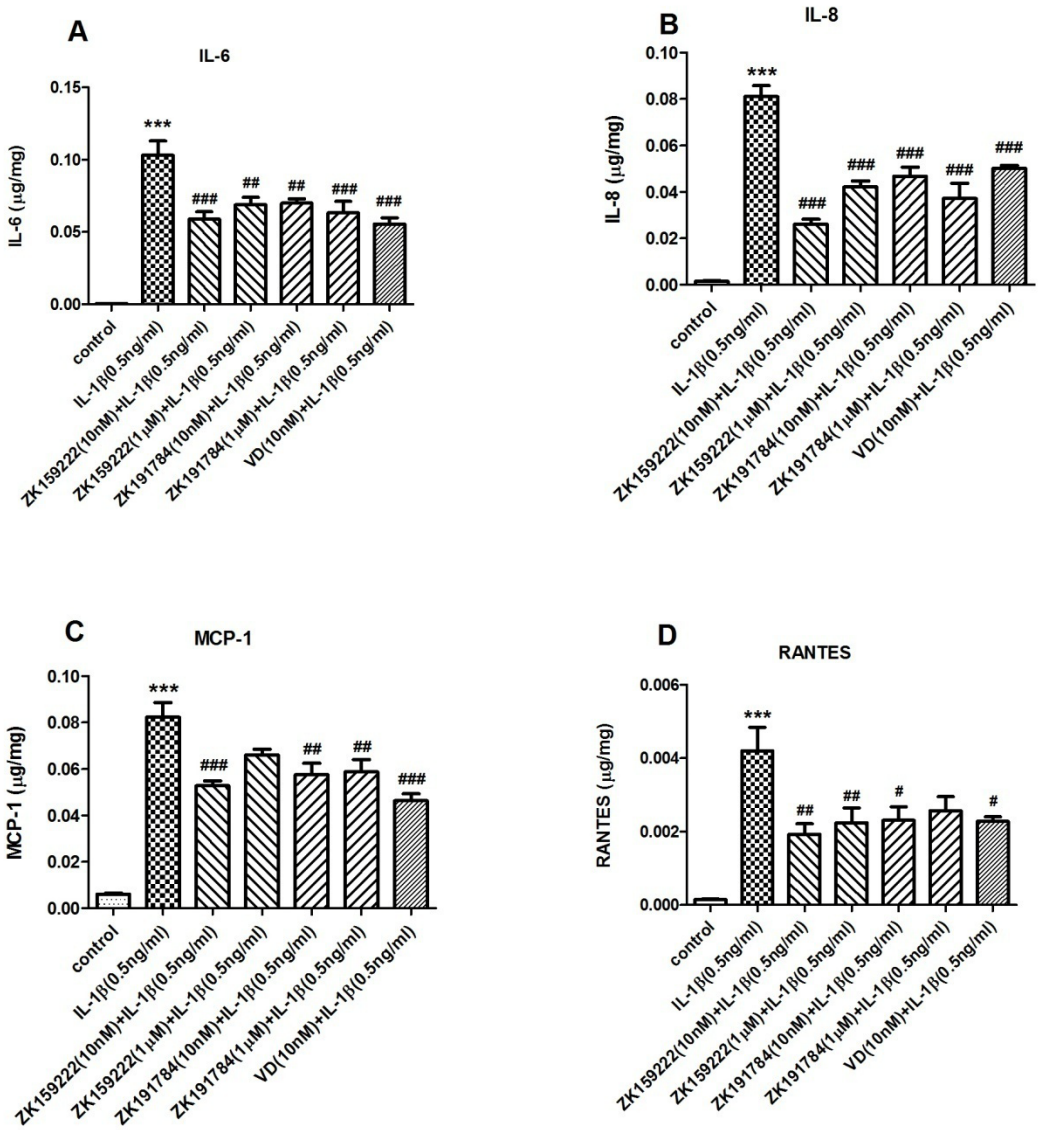

### 5.4.7. IL-1β enhances the gene expression of the pro-inflammatory factors in human preadipocytes

Similar to the secretion levels, the qPCR result (Figure 5.3) shows that the mRNA levels of the pro-inflammatory factors including IL-1β, IL-6, IL-8, MCP-1 and RANTES, were dramatically increased by (0.5 ng/ml) IL-1β in human preadipocytes.

### 5.4.8. 1α,25(OH)$_2$D$_3$ inhibits the gene expression the pro-inflammatory factors in IL-1β-stimulated human preadipocytes

(Figure 5.3) 1α,25(OH)$_2$D$_3$ (10 nM) exhibited distinguishable reducing effects on the mRNA levels of IL-1β, IL-6, IL-8, MCP-1 and RANTES in (0.5 ng/ml) IL-1β-stimulated preadipocytes.

### 5.4.9. ZK159222 inhibits the gene expression the pro-inflammatory factors in IL-1β-stimulated human preadipocytes

(Figure 5.3) Firstly, ZK159222 (10 nM and 1 μM) significantly reduced the mRNA levels of IL-8 in (0.5 ng/ml) IL-1β-stimulated preadipocytes. Secondly, the mRNA levels of IL-6 and MCP-1 were moderately reduced by ZK159222 (10 nM and 1 μM) and the reducing effects on these pro-inflammatory factors are consistent between the doses. Finally, the mRNA level of IL-1β was drastically reduced by ZK159222 (10 nM), but ZK159222 (1 μM) had no effect on the mRNA level of IL-1β in (0.5 ng/ml) IL-1β-stimulated preadipocytes.

### 5.4.10. ZK191784 inhibits the gene expression of the pro-inflammatory factors in IL-1β-stimulated human preadipocytes

(Figure 5.3) ZK191784 (10 nM and 1 μM) markedly reduced the mRNA levels of all the

pro-inflammatory factors in (0.5 ng/ml) IL-1β-stimulated preadipocytes. Moreover, the reducing effects on these pro-inflammatory factors are consistent between the doses.

**Figure 5.3 Effects of VDR agonists on cytokine gene expression in (0.5 ng/ml) IL-1β-stimulated human white preadipocytes.**

Preadipocytes were pretreated with 1α,25$(OH)_2D_3$ (10 nM) or ZK159222 (10 nM, 1 μM) or ZK191784 (10 nM, 1 μM) for 48 h, followed by treatments with IL-1β (0.5 ng/ml) in the presence of 1α,25$(OH)_2D_3$ (10 nM) or ZK159222 (10 nM, 1 μM) or ZK191784 (10 nM, 1 μM) for a further 24 h before Trizol-dissolved lysate collection. The mRNA levels of pro-inflammatory factors (A) IL-1β, (B) IL-6, (C) IL-8, (D) MCP-1 and (E) RANTES were measured by qPCR. Data are means ± SEM for groups of 6. A significant difference to control was indicated by ***($p<0.001$); to (0.5 ng/ml) IL-1β by #($p<0.05$), ##($p<0.01$), ###($p<0.001$). The results were determined using one-way ANOVA with Tukey's post hoc test and confirmed by two independent experiments.

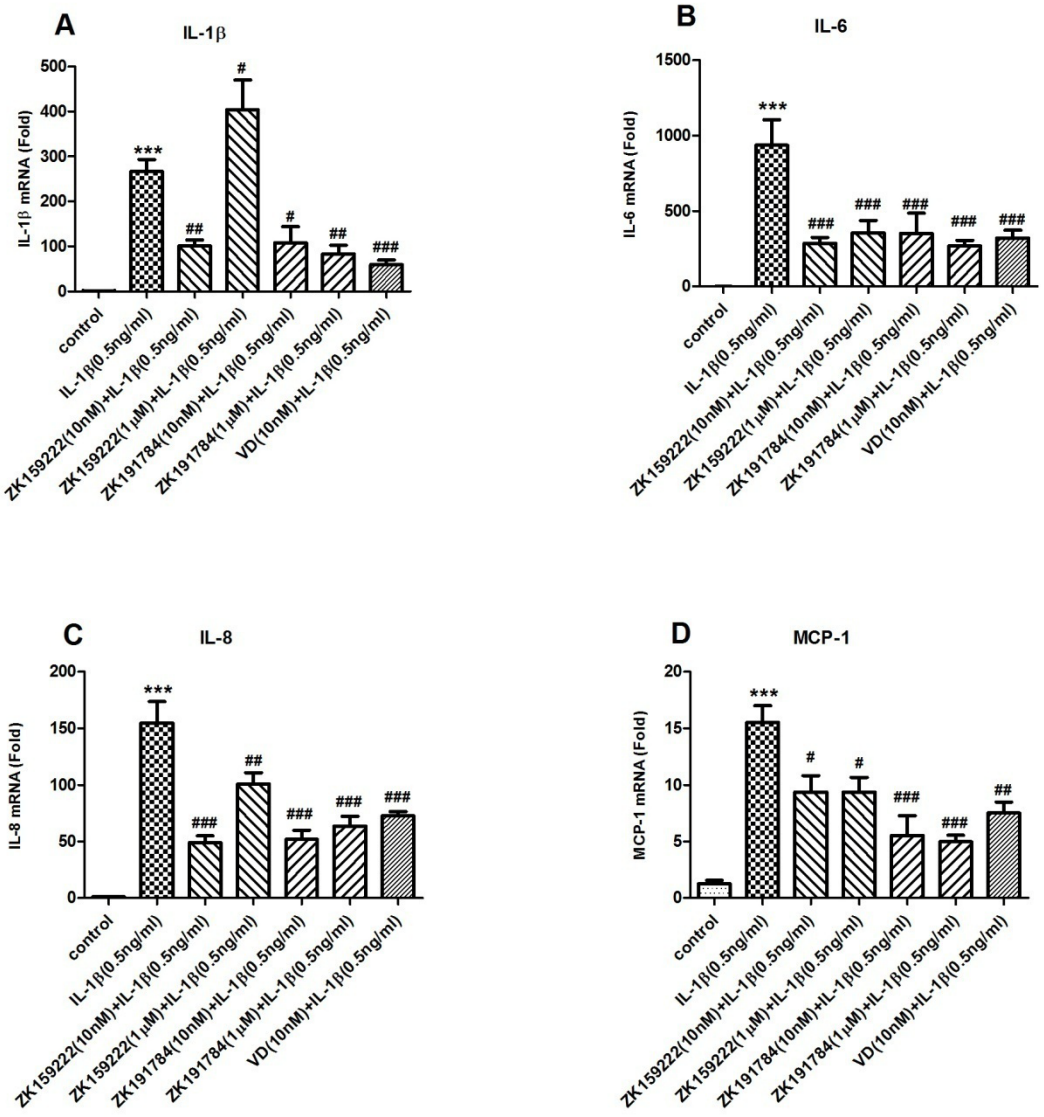

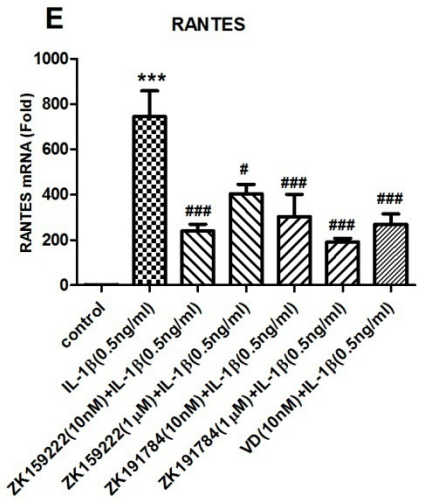
E
RANTES
RANTES mRNA (Fold)
1000
800
600
400
200
0
***
###
#
###
###
###
control
IL-1β(0.5ng/ml)
ZK159222(10nM)+IL-1β(0.5ng/ml)
ZK159222(1μM)+IL-1β(0.5ng/ml)
ZK191784(10nM)+IL-1β(0.5ng/ml)
ZK191784(1μM)+IL-1β(0.5ng/ml)
VD(10nM)+IL-1β(0.5ng/ml)

### 5.4.11. IL-1β stimulates the NF-κB signaling in human preadipocytes

To test whether IL-1β could regulate the post-translational transcription factor relA, the levels of phosphorylated relA and methylated relA of the NF-κB pathway were measured by western blotting. The results (Figure 5.4) show that the level of phosphorylated relA was moderately higher in the presence of (0.5 ng/ml) IL-1β, compared to the untreated preadipocytes. By contrast, the level methylated relA was markedly lower in (0.5 ng/ml) IL-1β-stimulated preadipocytes.

### 5.4.12. ZK159222 and ZK191784 modulate the NF-κB signaling in IL-1β-stimulated preadipocytes

The results (Figure 5.4) show that ZK159222 (1 μM) and ZK191784 (1 μM) mildly reduced the levels of phosphorylated relA, but levels were not affected by 1α,25$(OH)_2D_3$ (10 nM), ZK159222 (10 nM) or ZK191784 (10 nM) in (0.5 ng/ml) IL-1β-stimulated preadipocytes.

In parallel, ZK159222 (10 nM and 1 μM) and ZK191784 (10 nM) were associated with moderately higher levels of methylated relA in (0.5 ng/ml) IL-1β-stimulated preadipocytes. However, ZK191784 (1 μM) and 1α,25$(OH)_2D_3$ (10 nM) had no effect on the levels of methylated relA in (0.5 ng/ml) IL-1β-stimulated preadipocytes.

**Figure 5.4 Effects of VDR agonists on signaling molecules of the NF-κB signaling pathway in (0.5 ng/ml) IL-1β-stimulated human white preadipocytes.**

Preadipocytes were either cultured alone (control), or with IL-1β (0.5 ng/ml) alone for 24 h. Further groups of cells were pretreated with 1α,25$(OH)_2D_3$ (10 nM) or ZK159222 (10 nM and 1 μM) or ZK191784 (10 nM and 1 μM) for 48 h, followed by treatments with IL-1β (0.5 ng/ml) and 1α,25$(OH)_2D_3$ (10 nM) or ZK159222 (10 nM and 1 μM) or ZK191784 (10 nM and 1 μM) for a further 24 h before lysate collection. The levels of (A) phosphorylated relA and (B) methylated relA were measured by western blotting. Data are means ± SEM for groups of 3. A significant difference to control was indicated by ***($p<0.001$); to (0.5 ng/ml) IL-1β by #($p<0.05$), ##($p<0.01$), ###($p<0.001$). The results were determined using one-way ANOVA with Tukey's post hoc test and confirmed by two independent experiments.

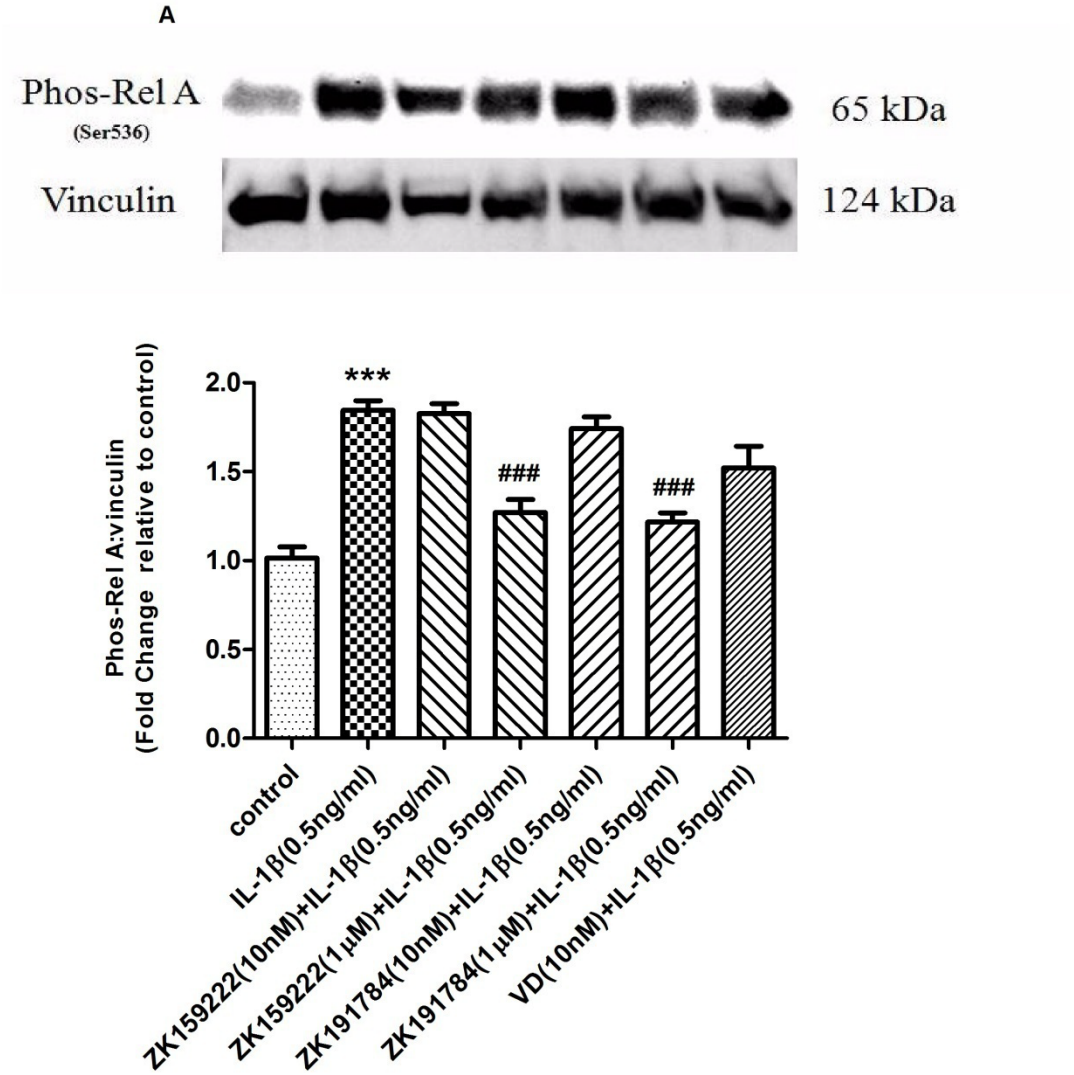

B

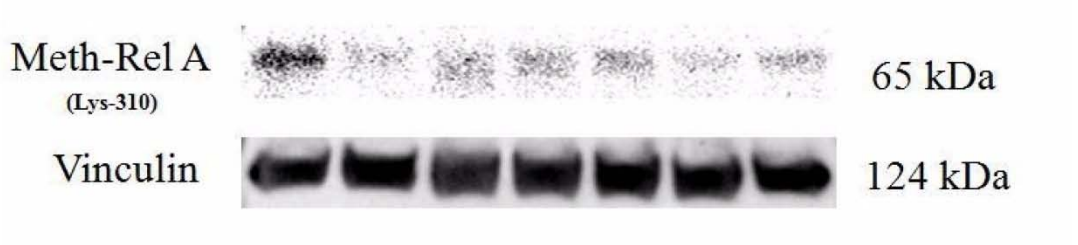
Meth-Rel A
(Lys-310)
65 kDa
Vinculin
124 kDa

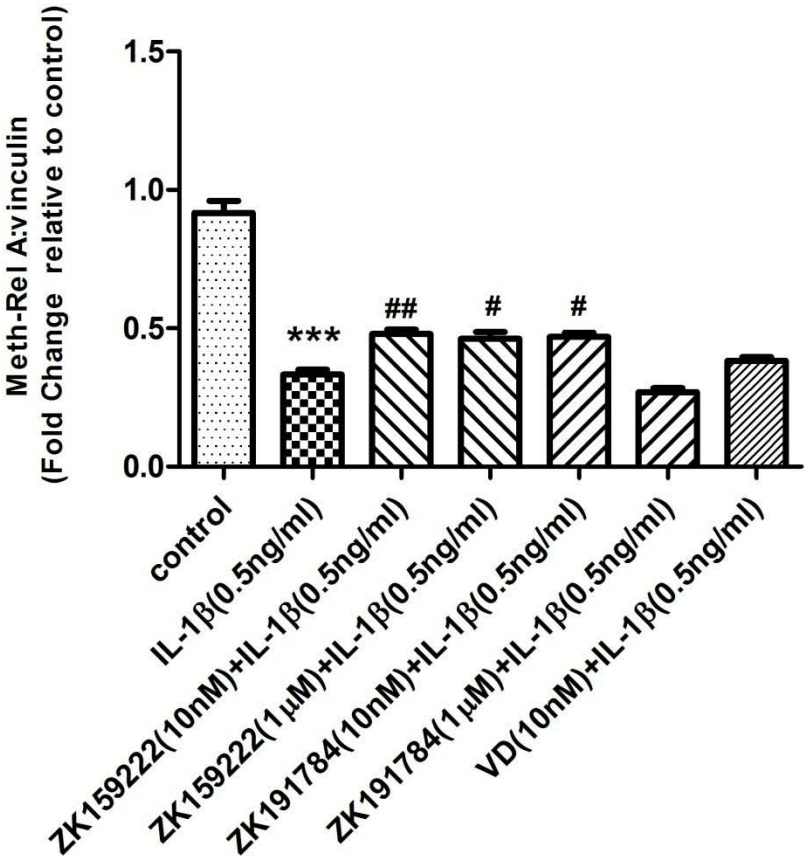
Meth-Rel A:vinculin
(Fold Change relative to control)
1.5
1.0
0.5
0.0
***
##
#
#
control
IL-1β(0.5ng/ml)
ZK159222(10nM)+IL-1β(0.5ng/ml)
ZK159222(1μM)+IL-1β(0.5ng/ml)
ZK191784(10nM)+IL-1β(0.5ng/ml)
ZK191784(1μM)+IL-1β(0.5ng/ml)
VD(10nM)+IL-1β(0.5ng/ml)

### 5.4.13. ZK159222 and ZK191784 increase the levels of phosphorylated eIF-2α in IL-1β-stimulated preadipocytes

To test whether IL-1β (0.5 ng/ml), 1α,25$(OH)_2D_3$ (10 nM), ZK159222 and ZK191784 (10 nM and 1 μM) could modulate signaling of the UPR pathways, the levels of phosphorylated eIF-2α were examined. The result (Figure 5.5) shows that the level of phosphorylated eIF-2α was not affected in (0.5 ng/ml) IL-1β-stimulated preadipocytes.

Only ZK159222 (10 nM) and ZK191784 (1 μM) significantly increased the levels of phosphorylated eIF-2α compared to (0.5 ng/ml), while ZK159222 (1 μM), ZK191784 (10 nM) and 1α,25$(OH)_2D_3$ (10 nM) had no effect on the levels of phosphorylated eIF-2α in (0.5 ng/ml) IL-1β-stimulated preadipocytes.

**Figure 5.5 Effects of VDR agonists on phosphorylated eIF-2α of the UPR signaling pathway in IL-1β-stimulated human white preadipocytes.**

Preadipocytes were either cultured alone (control), or with IL-1β (0.5 ng/ml) alone for 24 h. Further groups of cells were pretreated with 1α,25$(OH)_2D_3$ (10 nM) or ZK159222 (10 nM and 1 μM) or ZK191784 (10 nM and 1 μM) for 48 h, followed by treatments with IL-1β (0.5 ng/ml) and 1α,25$(OH)_2D_3$ (10 nM) or ZK159222 (10 nM and 1 μM) or ZK191784 (10 nM and 1 μM) for a further 24 h before lysate collection. The levels of phosphorylated eIF-2α were measured by western blotting. Data are means ± SEM for groups of 3. A significant difference to (0.5 ng/ml) IL-1β was indicated by ###($p<0.001$). The results were determined using one-way ANOVA with Tukey's post hoc test and confirmed by two independent experiments.

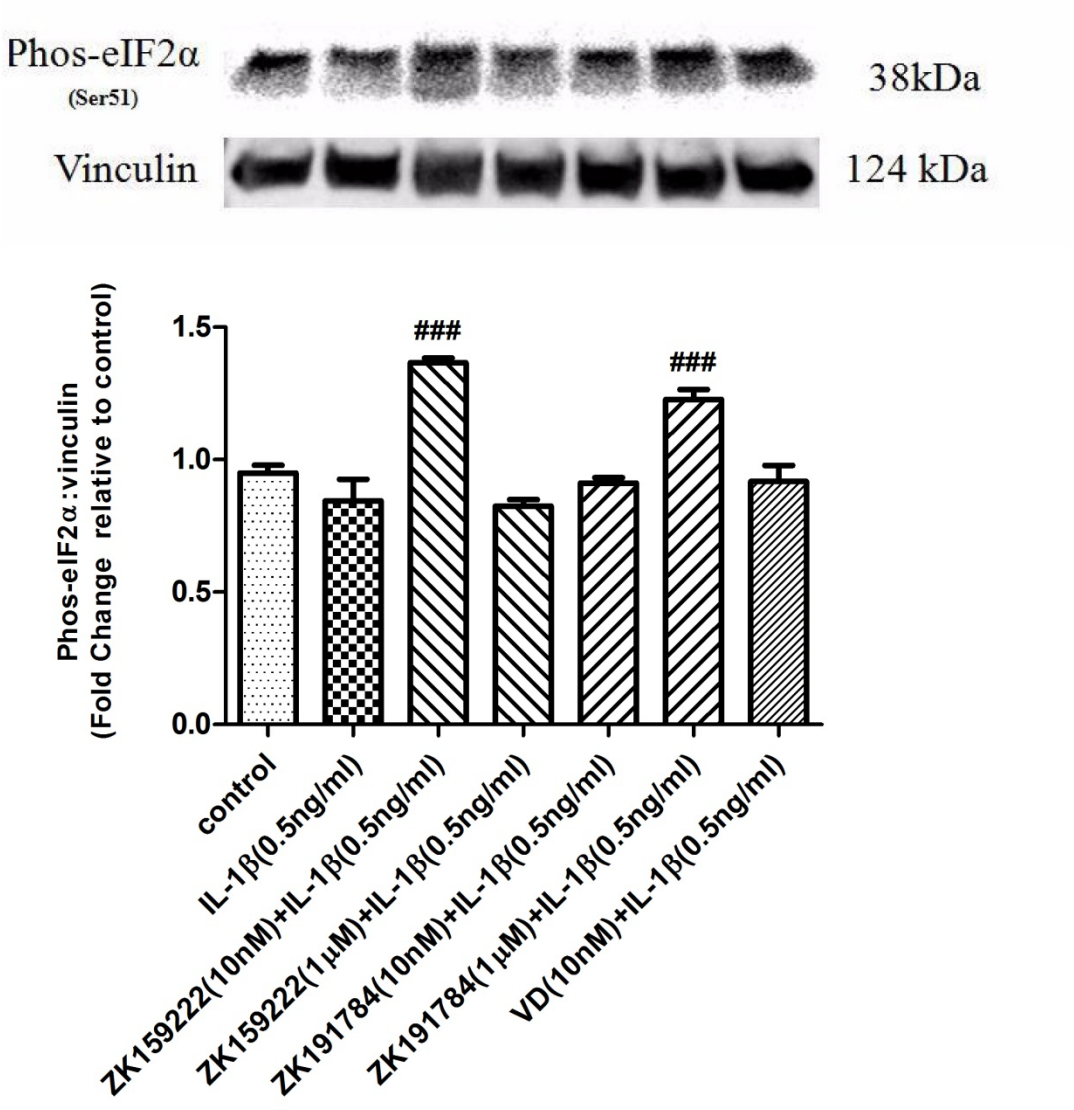

## 5.5. Discussion

The studies described in Chapter 3 and 4 suggested that IL-1β is critical in maintaining the inflammatory response induced by THP-1-MacCM in preadipocytes, since the gene expression and secretion levels of IL-1β, IL-6, IL-8, MCP-1 and RANTES were significantly inhibited by IL-1β neutralization. Moreover, as shown in Chapter 4, the gene expression and secretion levels of these pro-inflammatory factors were significantly enhanced by IL-1β (0.5 and 2 ng/ml). Similarly, the current results of the cytokine array show that IL-1β-stimulated preadipocytes secreted a variety of pro-inflammatory factors including IL-1β, IL-6, IL-8, slCAM-1 (mainly expressed by neutrophils), MIF, MIP-1α (specifically expressed by macrophages), GRO-α, MCP-1, MCP-3 and RANTES, as well as growth factors including angiogenin, EGF, G-CSF, HGF, GDF1, etc. Furthermore, the results of ELISA show that the secretion of the major pro-inflammatory factors was significantly enhanced. Likewise, the gene expression levels of IL-1β, IL-6, IL-8, MCP-1 and RANTES were also significantly enhanced by IL-1β.

To investigate whether IL-1β could modulate the post-translational modified transcription factor relA, thereby enhancing the gene expression of these pro-inflammatory factors, the levels of phosphorylated relA as well as the methylated relA were measured by western blotting. It has been summarized that during metaflammation, TNF-α or IL-1β stimulates JNK, IKKβ, and their down-stream cascades including the transcription factors AP-1 and NF-κB, which process results in elevated pro-inflammatory gene transcription and secretion (24). Similarly, the results of the current study show that IL-1β significantly increased the levels of phosphorylated relA, but reduced the levels of methylated relA. Notably, a very recent study has demonstrated that the SET domain-containing methyltransferase SETD6-mediated methylation attenuates NF-κB gene expression by establishing a G9a-like protein -mediated repressed chromatin state within NF-κB target genes. And in a screen of over 40 human SET domains containing lysine methyltransferases, SETD6 specifically monomethylated relA at Lys310 was only detected in the chromatin-associated fraction of the nucleus, and it occupied the promoters of a subset of NF-κB target genes under basal conditions. However, unlike the methylations of other relA lysines, which are induced by TNF-α-stimulation, TNF-α dramatically reduced the level of methylated relA at

Lys310 in primary immune cells (394), thus methylated relA acts in the opposite way to phosphorylated relA and acts to reduce the inflammatory response. Taken together, IL-1β enhances the gene expression and secretion levels of the pro-inflammatory factors; it also increases phosphorylated relA while reduces methylated relA of the NF-κB signaling pathway.

To investigate whether ZK159222 or ZK191784 could exert anti-inflammatory effects on IL-1β-stimulated preadipocytes, preadipocytes pretreated and treated with 1α,25$(OH)_2D_3$ (10 nM) was used as a positive control in the current study. Consistent with the results shown in Chapter 4, in this study, 1α,25$(OH)_2D_3$ (10 nM) significantly inhibited the secretion levels of IL-6, IL-8, MCP-1 and RANTES compared to (0.5 ng/ml) IL-1β-stimulated preadipocytes. Noteworthy, 1α,25$(OH)_2D_3$ (10 nM) also significantly inhibited the gene expression levels of IL-1β, IL-6, IL-8, MCP-1 and RANTES, which suggests that the prolonged duration of pretreatment [48 h, which was established in the study to explore the anti-inflammatory effects of VDR agonists (ZK159222 and ZK191784) on THP-1-MacCM-stimulated adipocytes (322), compared to 24 h in chapters 3 and 4] could enhance the anti-inflammatory effects on gene inhibition of the pro-inflammatory factors.

A recent study from our group shows that ZK159222 or ZK191784 reduced the production of the pro-inflammatory factors in THP-1-MacCM-stimulated adipocytes (322). Likewise, the results of the current study show that ZK159222 (10 nM and 1 μM) significantly inhibited the gene expression and secretion of the major-pro-inflammatory factors in (0.5 ng/ml) IL-1β-stimulated preadipocytes. It has been reported that ZK191784 exhibited potent immune-suppressive as well as anti-inflammatory activity by inhibiting antigen-induced lymphocyte proliferation and cytokine secretion *in vitro* (323, 324). Similar to the action of ZK159222, this study shows that the gene expression and secretion of the major-pro-inflammatory factors was also significantly inhibited by ZK191784 (10 nM and 1 μM) in (0.5 ng/ml) IL-1β-stimulated preadipocytes. Taken together, the data from the current study suggest that like 1α,25$(OH)_2D_3$, ZK159222 or ZK191784 has anti-inflammatory effects by inhibiting the secretion and gene expression of the pro-inflammatory factors on IL-1β-stimulated preadipocytes.

Moreover, it has been reported that ZK159222 or ZK191784 reduces the levels of phosphorylated relA in THP-1-MacCM-stimulated adipocytes (322). To test whether ZK159222 or ZK191784, like 1α,25$(OH)_2D_3$, could modulate NF-κB signaling in IL-1β-stimulated preadipocytes, the levels of phosphorylated relA and methylated relA were measured in the current study. The results show the levels of phosphorylated relA were significantly inhibited by ZK159222 (1 μM) and ZK191784 (1 μM) in (0.5 ng/ml) IL-1β-stimulated preadipocytes. By contrast, the levels of methylated relA were significantly enhanced by ZK159222 (10 nM and 1 μM) as well as ZK191784 (10 nM). It has been shown that the VDR-1α,25$(OH)_2D_3$ complex directly inhibits the expression (transcription) of some genes by antagonizing the action of certain transcription factors (e.g. NF-AT and NF-κB) (297, 298). Therefore, Like 1α,25$(OH)_2D_3$, ZK15922 and ZK191784 could exert anti-inflammatory effects by inhibiting the expression of phosphorylated relA and/or enhancing methylated relA.

Since the study described in Chapter 4 has demonstrated that 1α,25$(OH)_2D_3$ increases the levels of phosphorylated eIF-2α of the UPR pathway, the current study also examined if ZK159222 or ZK191784 could exert the same effect. The results show that ZK159222 (10 nM) and ZK191784 (1 μM) significantly enhanced the levels of phosphorylated eIF-2α in (0.5 ng/ml) IL-1β-stimulated preadipocytes. Hence, ZK15922 and ZK191784 could also exert the anti-inflammatory by enhancing the levels of phosphorylated eIF-2α of the UPR pathway.

Although 1α,25$(OH)_2D_3$ did not modulate any of the above mentioned signaling pathways in the current study, the results of qPCR suggests that 1α,25$(OH)_2D_3$ probably directly inhibited the gene expression (transcription) of these pro-inflammatory factors by: forming transcriptional complex-corepressor complex, recruiting histone deacetylase activities then deacetylating the lysine residues present in the N-terminal located in histone tails, thus to compact the chromatin and silence those pro-inflammatory genes (303). The same mechanism also applies to ZK159222 and ZK1991784 according the qPCR results.

*Limitations*

1. Not only preadipocytes responding to IL-1β appears to be dose-dependent, but also the

effects of 1α,25$(OH)_2D_3$ seem to be time-dependent [might be caused by the stability of VDR agonists (though unknown)]. A full exploration of this would require repeating the experiment with

1) Average of time exposure (i.e. pretreatment) with 1α,25$(OH)_2D_3$ (e. g. from 6 to 72 h);
2) At a range of doses of IL-1β (e. g. from 0.2 to 5 ng/ml).

2. Likewise, the effects of VDR agonists seem to be dependent on the strength of the inflammatory response, and a minimally effective dose of 1α,25$(OH)_2D_3$ has not been established in dose experiment. Further experiment exploring lower doses of 1α,25$(OH)_2D_3$ might be informative.
3. The levels of total unphosphorylated protein(s) including relA and eIF-2α have not been determined, which is a limitation of the current experiment design. Elevated or decreased phosphorylation levels may be accompanied by increased or decreased protein levels.

In summary, this study demonstrates that IL-1β could potently enhance the gene expression and secretion of the pro-inflammatory factors) in human preadipocytes, by increasing the phosphorylated relA, and reducing the methylated relA of the NF-κB pathway. ZK159222 and ZK191784 might inhibit the inflammatory response by:

1. Directly attenuating the pro-inflammatory gene expression;
2. Reducing level of phosphorylated relA while increasing methylated relA of the NF-κB signaling pathway, to inhibit the pro-inflammatory gene expression;
3. Increasing the level of phosphorylated eIF-2α of the UPR pathway to reduce the pro-inflammatory translation.

# 6. The effects of the combination of VDR agonists and VDR agonist-MacCM on human white preadipocytes

## 6.1. Introduction

The expression of TLR was significantly higher in both immune cells and adipose tissue from overweight and obese human subjects, compared with lean control (395). Moreover, the TLR signaling switches macrophages to M1 phenotype by activating the NF-κB signaling pathway (244), which increases gene transcription and secretion of a variety of pro-inflammatory factors (for the specific details, please refer to *Introduction* Page 36-38), as shown in human and murine adipose tissue (243, 396), but 1α,25$(OH)_2D_3$ (1 μM) could exert an anti-inflammatory effect by inhibiting the gene expression of TLR-2 and TLR-4 in LPS or TNF-α-stimulated human monocyte and macrophages from fresh buffy coats of healthy volunteers (24 h) (397).

The anti-inflammatory effects of 1α,25$(OH)_2D_3$ have been thoroughly explored in human and murine monocytes/macrophages. For example, 1α,25$(OH)_2D_3$ (40 nM) could suppress the listericidal activity, inhibit phagocyte oxidase-mediated oxidative burst and transcription of important IFN-induced genes [including Ccl5, Cxcl10, Cxcl9, Irf2, (Fc gamma receptor) Fcgr1, Fcgr3, and Tlr2] in IFN-stimulated murine BMDMs (48 h). Subsequently, the inhibition of the pro-inflammatory genes was shown to be dependent on a functional VDR and 1α,25$(OH)_2D_3$ acting specifically on IFN-stimulated macrophages. In conclusion, the overall results suggest that the production of 1α,25$(OH)_2D_3$ by IFN-stimulated macrophages might be an important negative feedback mechanism to control innate and inflammatory responses of activated macrophages (398). Furthermore, a recent study has demonstrated that 1α,25$(OH)_2D_3$ and 25$(OH)D_3$ dose dependently (not specified in the paper) inhibited LPS-induced p38 phosphorylation at physiologic concentrations, and the secretion of IL-6 and TNF-α from human monocytes. In parallel, the mRNA level of MAPK phosphatase-1 was significantly up-regulated in human monocytes and murine BMDMs, by increased binding of the VDR and increased histone H4 acetylation at the identified VDRE of the murine and human MKP-1 promoters (399).

It is noteworthy that $1\alpha,25(OH)_2D_3$ also reduced the inflammatory response by polarizing pro-inflammatory M1 macrophages towards anti-inflammatory M2 via the VDR-PPARγ pathway *in vitro*. Zhang et al. reported that under high glucose conditions, RAW264.7 macrophages tend to switch to M1 phenotype characterized by expressing higher iNOS (inducible nitric oxide synthase) as well as pro-inflammatory cytokines including TNF-α and IL-12, whereas $1\alpha,25(OH)_2D_3$ ($10^{-8}$ M) significantly inhibited M1 activation whilst enhanced M2 polarization, demonstrated by up-regulated gene expression of MR (mannose receptor) and (Abelson-related gene) Arg-1; secretion of anti-inflammatory cytokine IL-10, and down-regulated gene expression of M1 marker (iNOS) (24 h) .In addition, the polarizing effect of $1\alpha,25(OH)_2D_3$ could be inhibited by VDR siRNA in RAW264.7 macrophages (24 h) (400).

## 6.2. Aims

This study aimed to investigate whether the combination of pretreatment with VDR agonists and treatment with VDR agonist-MacCM could ameliorate THP-1-MacCM-stimulated pro-inflammatory effects in human preadipocytes. The experiments were set up to examine whether:

1. THP-1-MacCM could enhance the gene expression of IL-1β, IL-8, IL-6, MCP-1 and RANTES in human white preadipocytes;
2. THP-1-MacCM could enhance the secretion of the pro-inflammatory factors from human white preadipocytes;
3. The combination of pretreatment with VDR agonists and treatment with VDR agonist-MacCM could ameliorate the secretion or gene expression of the pro-inflammatory factors in preadipocytes;
4. THP-1-MacCM could increase the levels of phosphorylated relA of the NF-κB pathway as well as phosphorylated ERK or p38 of the MAPK pathways in preadipocytes
5. The combination of pretreatment with VDR agonists and treatment with VDR

agonist-MacCM could reduce the levels of the signaling molecules of the NF-κB and MAPK pathways in preadipocytes.

## 6.3. Materials and Methods

Generation of THP-1-MacCM and VDR agonist-MacCM

Culture of THP-1 monocytes and generation of THP-1-MacCM were performed as described in Chapter 2. The VDR agonist-MacCM were thus generated: ZK159222 (10 nM)-MacCM (generated from THP-1-macrophages treated with 10 nM ZK159222); ZK159222 (1 μM)-MacCM (generated from THP-1-macrophages treated with 1 μM ZK159222); ZK191784 (10 nM)-MacCM (generated from THP-1-macrophages treated with 10 nM ZK191784); ZK191784 (1 μM)-MacCM (generated from THP-1-macrophages treated with 1 μM ZK191784); 1α,25$(OH)_2D_3$ (10 nM)-MacCM (generated from THP-1-macrophages treated with 10 nM of 1α,25$(OH)_2D_3$). All the treatments lasted for 24 h before the VDR agonist-MacCM were collected, filtered through a 0.22 μm filter and then stored at −80°C for preadipocyte treatment.

Preadipocyte pretreatment and treatment

Culture of human preadipocytes was performed as described in Chapter 3. To investigate the effects of the combination of combination of pretreatment with VDR agonists and treatment with VDR agonist-MacCM, preadipocytes were either cultured alone (control), or with (25%) THP-1-MacCM alone for 24 h. Further groups of cells were pretreated with 1α,25$(OH)_2D_3$ (10 nM, ENZO Life Sciences, USA), ZK 159222 (10 nM and 1 μM, Bayer, Germany) or ZK191784 (10 nM and 1 μM, Bayer, Germany) for 48 h [using an established protocol (322)], followed by treatments with (25%) THP-1-MacCM and (25%) VDR agonist-MacCM for a further 24 h [the established protocol (322)] at 37°C in 95% air and 5% $CO_2$ before medium and lysate collection. The cell media for ELISA; the treated preadipocytes lysed with Trizol for qPCR; lysed with lysis

buffer for western blotting, were stored at −80°C.

Measurements

ELISA was performed for determining the secretion levels of pro-inflammatory factors including IL-1β, IL-6, IL-8, MCP-1 and RANTES and corrected by total protein content in cellular lysate. Real-time PCR was used to measure the gene expression levels of pro-inflammatory factors including IL-1β, IL-6, IL-8, MCP-1 and internal reference PPIA. For measuring protein levels of phosphorylated relA of the NF-κB signaling pathway, phosphorylated ERK and p38 of the MAPK signaling pathway, western blotting was performed. The laboratory procedures and statistical analyses are described in detail in Chapter 3.

## 6.4. Results

### 6.4.1. THP-1-MacCM enhances the secretion of the pro-inflammatory factors from human preadipocytes

The ELISA result (Figure 6.1) shows that the secretion levels of IL-1β, IL-6, IL-8, MCP-1 and RANTES were dramatically increased by THP-1-MacCM.

### 6.4.2. The combination of pretreatment with 1α,25(OH)$_2$D$_3$ and treatment with 1α,25(OH)$_2$D$_3$-MacCM ameliorates the secretion of the pro-inflammatory factors from human preadipocytes

(Figure 6.1) The secretion levels of IL-1β, IL-6, IL-8, MCP-1 and RANTES were significantly reduced by the combination of pretreatment with 1α,25(OH)$_2$D$_3$ (10 nM) and treatment with 1α,25(OH)$_2$D$_3$(10nM)-MacCM, compared to the untreated preadipocytes.

### 6.4.3. The combination of pretreatment with ZK159222 and treatment with ZK159222-MacCM ameliorates the secretion of the pro-inflammatory factors from human preadipocytes

(Figure 6.1) Firstly, pretreatments with ZK159222 (10 nM and 1 μM) and treatments with ZK159222 (10 nM and 1 μM)-MacCM dramatically reduced the levels of IL-1β, IL-6 and IL-8. Secondly, the levels of RANTES were moderately reduced by the pre- and treatments compared to the untreated preadipocytes. Noteworthy, the reducing effects on these pro-inflammatory factors are consistent between the groups. Finally, though the levels of MCP-1 were also moderately reduced by the pre- and treatments, only the difference by pretreatment with ZK159222 (10 nM) and treatment with ZK159222(10 nM )-MacCM was statistically significant.

### 6.4.4. The combination of pretreatment with ZK191784 and treatment with ZK191784-MacCM ameliorates the secretion of the pro-inflammatory factors from preadipocytes

(Figure 6.1) Pretreatments with ZK191784 (10 nM and 1 μM) and treatments with ZK191784(10 nM and 1 μM)-MacCM significantly reduced the levels of IL-1β, IL-6, IL-8, MCP-1 and RANTES, and except IL-6, the reducing effects on these pro-inflammatory factors are consistent between the groups.

**Figure 6.1 Effects of the combination of pretreatment with VDR agonists and treatment with VDR agonist-MacCM on cytokine release from human white preadipocytes (after adjustment of ELISA results for total protein).**

Preadipocytes were either cultured alone (control), or with (25%) THP-1-MacCM alone for 24 h. Further groups of cells were pretreated with 1α,25$(OH)_2D_3$ (10 nM) or ZK159222 (10 nM and 1 μM) or ZK191784 (10 nM and 1 μM) for 48 h, followed by treatments with 1α,25$(OH)_2D_3$ (10 nM) or ZK159222 (10 nM and 1 μM) or ZK191784 (10 nM and 1 μM)-MacCM for a further 24 h before medium collection. The release levels of pro-inflammatory factors (A) IL-1β, (B) IL-6, (C) IL-8, (D) MCP-1 and (E) RANTES were measured by ELISA and normalized by protein content in the cellular lysate. Data are means ± SEM for groups of 6. A significant difference to control was indicated by ***(p<0.001); to (25%) THP-1-MacCM by #(p<0.05), ##(p<0.01), ###(p<0.001). The results were determined using one-way ANOVA with Tukey's post hoc test and confirmed by two independent experiments.

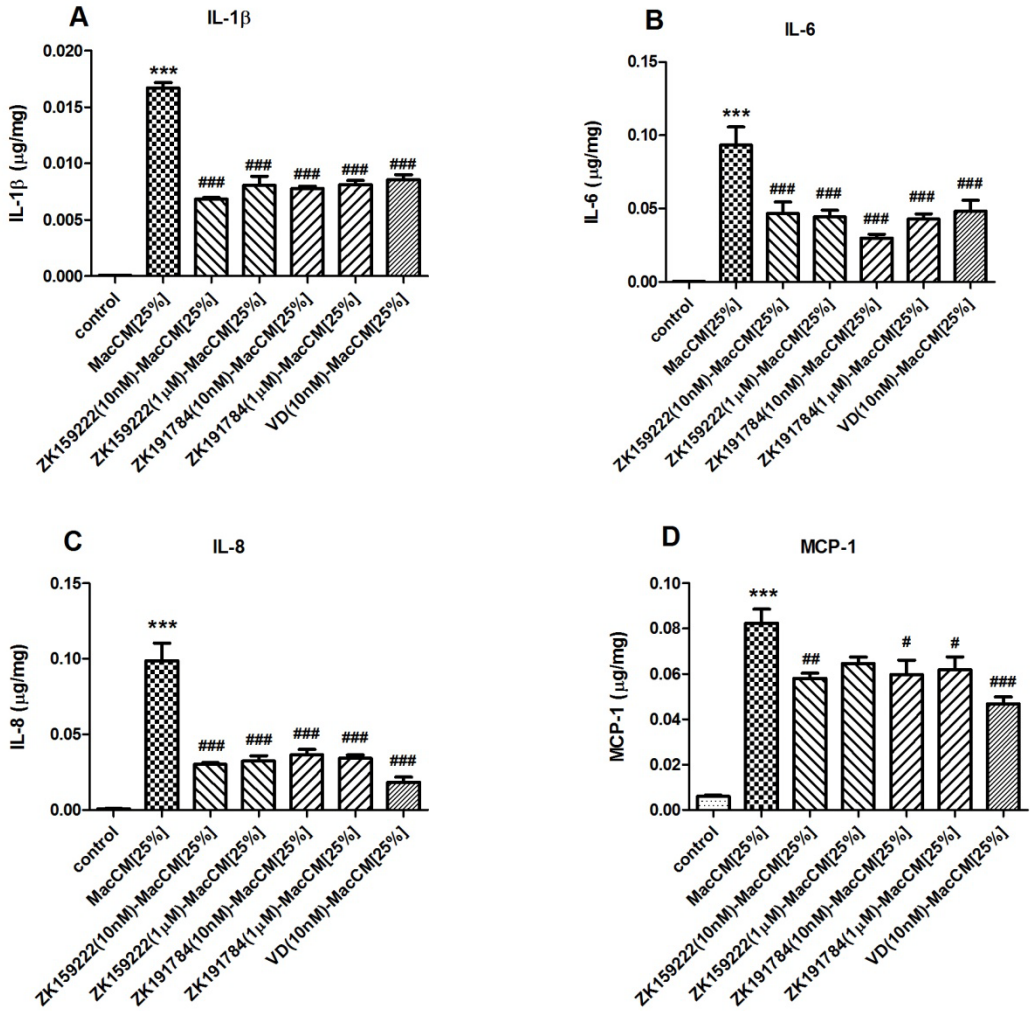

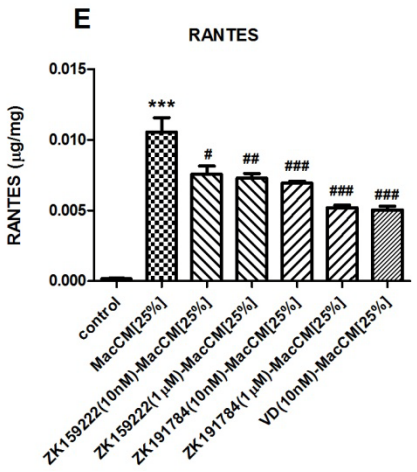
E
RANTES
RANTES (μg/mg)
0.015
0.010
0.005
0.000
***
#
##
###
###
###
control
MacCM[25%]
ZK159222(10nM)-MacCM[25%]
ZK159222(1μM)-MacCM[25%]
ZK191784(10nM)-MacCM[25%]
ZK191784(1μM)-MacCM[25%]
VD(10nM)-MacCM[25%]

### 6.4.5. THP-1-MacCM enhances the gene expression of the pro-inflammatory factors in human preadipocytes

Similar to the secretion levels, the qPCR result (Figure 6.2) shows that the mRNA levels of IL-1β, IL-6, IL-8, MCP-1 and RANTES, were dramatically increased by THP-1-MacCM in human preadipocytes.

### 6.4.6. Pretreatment with 1α,25(OH)$_2$D$_3$ and treatment with 1α,25(OH)$_2$D$_3$-MacCM reduces the gene expression of pro-inflammatory factors in human preadipocytes

(Figure 6.2) The combination of pretreatment with 1α,25(OH)$_2$D$_3$ (10 nM) and treatment with 1α,25(OH)$_2$D$_3$(10 nM)-MacCM exhibited distinguishable reducing effects on the mRNA levels of IL-1β, IL-6, IL-8, MCP-1 and RANTES, compared to those in THP-1-MacCM-stimulated preadipocytes.

### 6.4.7. Pretreatment with ZK159222 followed by treatment with ZK159222-MacCM reduces the gene expression of pro-inflammatory factors in human preadipocytes

Firstly, the mRNA levels of IL-1β were drastically reduced to a similar extent by pretreatments with both doses of ZK159222 (10 nM and 1 μM) and treatments with ZK159222(10 nM and 1 μM)-MacCM, compared to THP-1-MacCM-stimulated preadipocytes (Figure 6.2). Secondly, the combination of pre- and treatment moderately reduced the mRNA levels of IL-6, IL-8 and RANTES, again with no obvious dose-response pattern [though the difference of IL-8 by pretreatment with ZK159222 (10 nM) and treatment with ZK159222(10 nM)-MacCM, is not statistically significant]. Finally, the combination of pre- and treatment had no significant effect on the mRNA levels of MCP-1.

### 6.4.8. The combination of pretreatment with ZK191784 and treatment with ZK191784-MacCM ameliorates the gene expression of pro-inflammatory factors in human preadipocytes, compared to MacCM alone

(Figure 6.2) The mRNA levels of IL-1β, IL-6, IL-8, MCP-1 and RANTES were markedly reduced by pretreatments with ZK191784 (10 nM and 1 μM) and treatments with ZK191784(10 nM and 1 μM)-MacCM, compared to THP-1-MacCM-stimulated preadipocytes [except that of MCP-1 by pretreatment with ZK191784 (1 μM) and treatment with ZK191784(1 μM)-MacCM], with no apparent dose-response relationship.

**Figure 6.2 Effects of the combination of pretreatment with VDR agonists and treatment with VDR agonist-MacCM on cytokine gene expression in human white preadipocytes.**

Preadipocytes were either cultured alone (control), or with (25%) THP-1-MacCM alone for 24 h. Further groups of cells were pretreated with 1α,25$(OH)_2D_3$ (10 nM) or ZK159222 (10 nM and 1 μM) or ZK191784 (10 nM and 1 μM) for 48 h, followed by treatments with 1α,25$(OH)_2D_3$ (10 nM) or ZK159222 (10 nM and 1 μM) or ZK191784 (10 nM and 1 μM)-MacCM for a further 24 h before Trizol-dissolved lysate collection. The mRNA levels of pro-inflammatory factors (A) IL-1β, (B) IL-6, (C) IL-8, (D) MCP-1 and (E) RANTES were measured by qPCR. Data are means ± SEM for groups of 6. A significant difference to control was indicated by ***($p<0.001$); to (25%) THP-1-MacCM by #($p<0.05$), ##($p<0.01$), ###($p<0.001$). The results were determined using one-way ANOVA with Tukey's post hoc test and confirmed by two independent experiments.

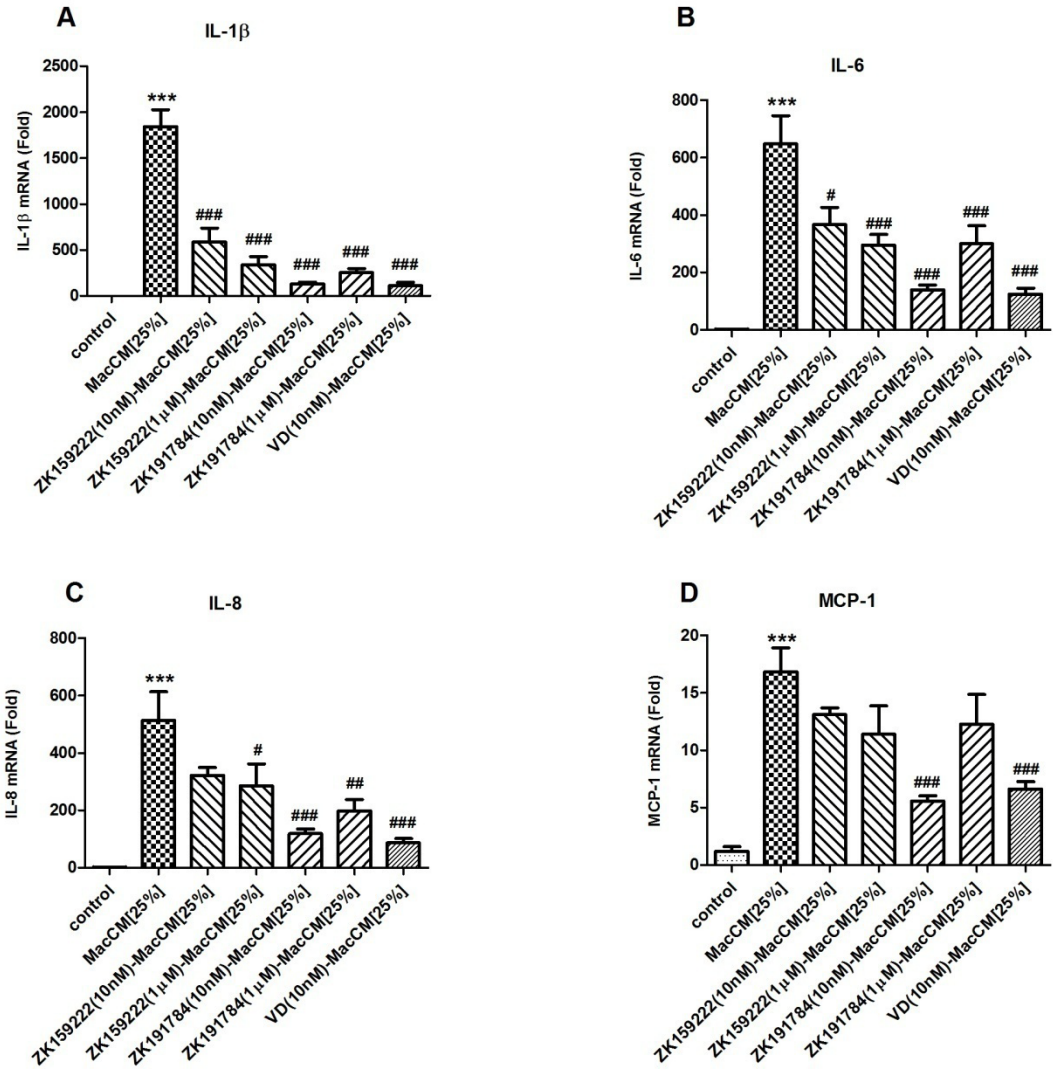

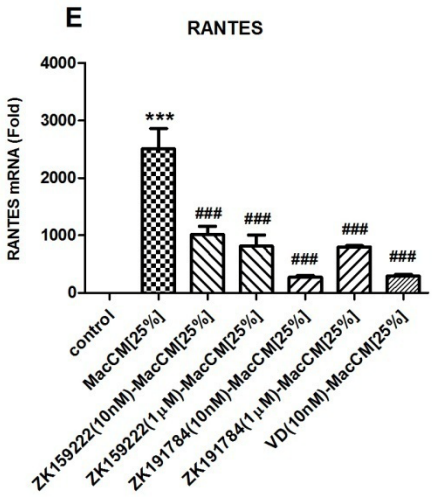
E
RANTES
RANTES mRNA (Fold)
4000
3000
2000
1000
0
***
###
###
###
###
###
control
MacCM[25%]
ZK159222(10nM)-MacCM[25%]
ZK159222(1μM)-MacCM[25%]
ZK191784(10nM)-MacCM[25%]
ZK191784(1μM)-MacCM[25%]
VD(10nM)-MacCM[25%]

### 6.4.9. THP-1-MacCM increases the level of phosphorylated relA in human preadipocytes

To test whether THP-1-MacCM could modulate the NF-κB pathway, the level of phosphorylated relA was measured by western blotting. The result (Figure 6.3) shows that the level of phosphorylated relA was dramatically higher in the presence of THP-1-MacCM, compared to the untreated preadipocytes.

### 6.4.10. The combination of pretreatment with VDR agonists and treatment with VDR agonist-MacCM reduces the levels of phosphorylated relA in human preadipocytes, compared to MacCM alone

The result (Figure 6.3) shows that the levels of phosphorylated relA were moderately and significantly decreased only by pretreatments with 1α,25$(OH)_2D_3$ (10 nM), ZK159222 (1 μM) and ZK191784 (1 μM) and treatments with 1α,25$(OH)_2D_3$(10 nM), ZK159222(1 μM) and ZK191784 (1 μM)-MacCM, compared with THP-1-MacCM treated preadipocytes.

**Figure 6.3 Effects of the combination of pretreatment with VDR agonists and treatment with VDR agonist-MacCM on phosphorylated relA of the NF-κB signaling pathway in human white preadipocytes.**

Preadipocytes were either cultured alone (control), or with (25%) THP-1-MacCM alone for 24 h. Further groups of cells were pretreated with 1α,25$(OH)_2D_3$ (10 nM) or ZK159222 (10 nM and 1 μM) or ZK191784 (10 nM and 1 μM) for 48 h, followed by treatments with 1α,25$(OH)_2D_3$ (10 nM) or ZK159222 (10 nM and 1 μM) or ZK191784 (10 nM and 1 μM)-MacCM for a further 24 h before lysate collection. The levels of phosphorylated relA were measured by western blotting. Data are means ± SEM for groups of 3. A significant difference to control was indicated by ***($p<0.001$); to (25%) THP-1-MacCM by ##($p<0.01$), ###($p<0.001$). The results were determined using one-way ANOVA with Tukey's post hoc test and confirmed by two independent experiments.

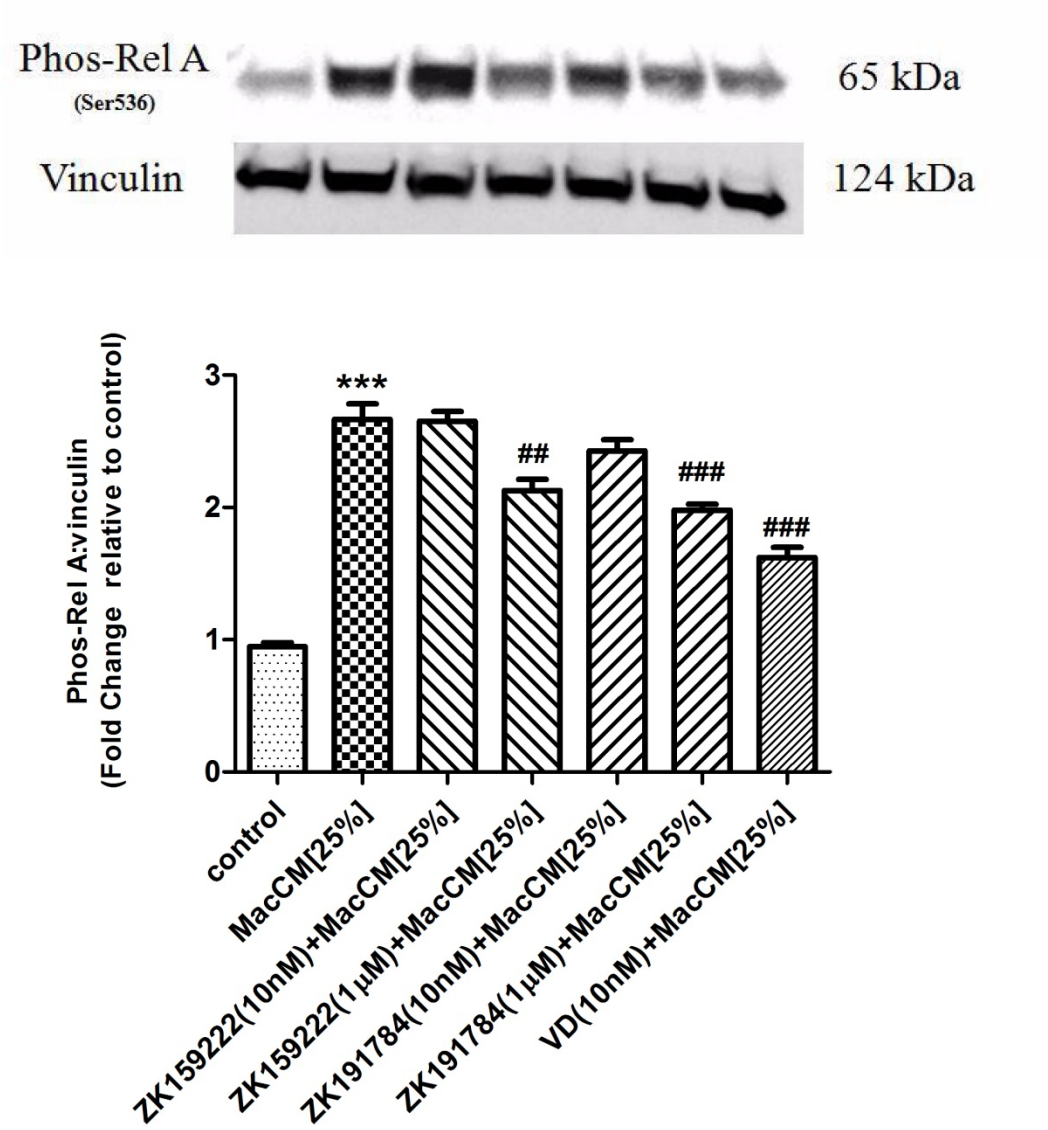

### 6.4.11. THP-1-MacCM increases the levels of phosphorylated ERK and p38 in human preadipocytes

Like that of phosphorylated relA, (Figure 6.4) the levels of phosphorylated ERK (p44/42) and p38 of the MAPK signaling pathways were significantly increased by THP-1-MacCM.

### 6.4.12. The combination of pretreatment with 1α,25(OH)$_2$D$_3$ and treatment with 1α,25(OH)$_2$D$_3$-MacCM reduces the levels of phosphorylated ERK and p38 in human preadipocytes, compared to MacCM alone

(Figure 6.4 A) The level of phosphorylated ERK was moderately reduced by pretreatment with 1α,25(OH)$_2$D$_3$ (10 nM) and treatment with 1α,25(OH)$_2$D$_3$(10 nM)-MacCM in human preadipocytes. (Figure 6.4 B) Moreover, the pre- and treatment dramatically reduced the level of phosphorylated p38, compared to THP-1-MacCM-stimulated preadipocytes.

### 6.4.13. The combination of pretreatment with ZK159222 and treatment with ZK159222-MacCM reduces the levels of phosphorylated ERK and p38 in human preadipocytes

(Figure 6.4 A) Only pretreatment with ZK159222 (1 μM) and treatment with ZK159222 (1 μM)-MacCM significantly reduced the level of phosphorylated ERK in human preadipocytes. (Figure 6.4 B) In parallel, the levels of phosphorylated p38 were moderately reduced by pretreatments with ZK159222 (10 nM and 1 μM) and treatments with ZK159222(10 nM and 1 μM)-MacCM, compared to THP-1-MacCM-stimulated preadipocytes.

### 6.4.14. The combination of pretreatment with ZK191784 and treatment with ZK191784-MacCM ameliorates the levels of phosphorylated p38 in human preadipocytes

(Figure 6.4 B) The levels of phosphorylated p38 were distinguishably and consistently reduced by pretreatments with ZK191784 (10 nM and 1 μM) and treatments with ZK191784(10 nM and 1 μM)-MacCM, compared to THP-1-MacCM-stimulated preadipocytes. (Figure 6.4 A) However, the pre- and treatment had no ameliorating effect on the levels of phosphorylated ERK in human preadipocytes.

**Figure 6.4 Effects of the combination of pretreatment with VDR agonists and treatment with VDR agonist-MacCM on signaling molecules of the MAPK signaling pathways in human white preadipocytes.**

Preadipocytes were either cultured alone (control), or with (25%) THP-1-MacCM alone for 24 h. Further groups of cells were pretreated with 1α,25$(OH)_2D_3$ (10 nM) or ZK159222 (10 nM and 1 μM) or ZK191784 (10 nM and 1 μM) for 48 h, followed by treatments with 1α,25$(OH)_2D_3$ (10 nM) or ZK159222 (10 nM and 1 μM) or ZK191784 (10 nM and 1 μM)-MacCM for a further 24 h before lysate collection. The levels of (A) phosphorylated ERK and (B) phosphorylated p38 were measured by western blotting. Data are means ± SEM for groups of 3. A significant difference to control was indicated by **(p<0.01), ***(p<0.001); to (25%) THP-1-MacCM by #(p<0.05), ##(p<0.01), ###(p<0.001). The results were determined using one-way ANOVA with Tukey's post hoc test and confirmed by two independent experiments.

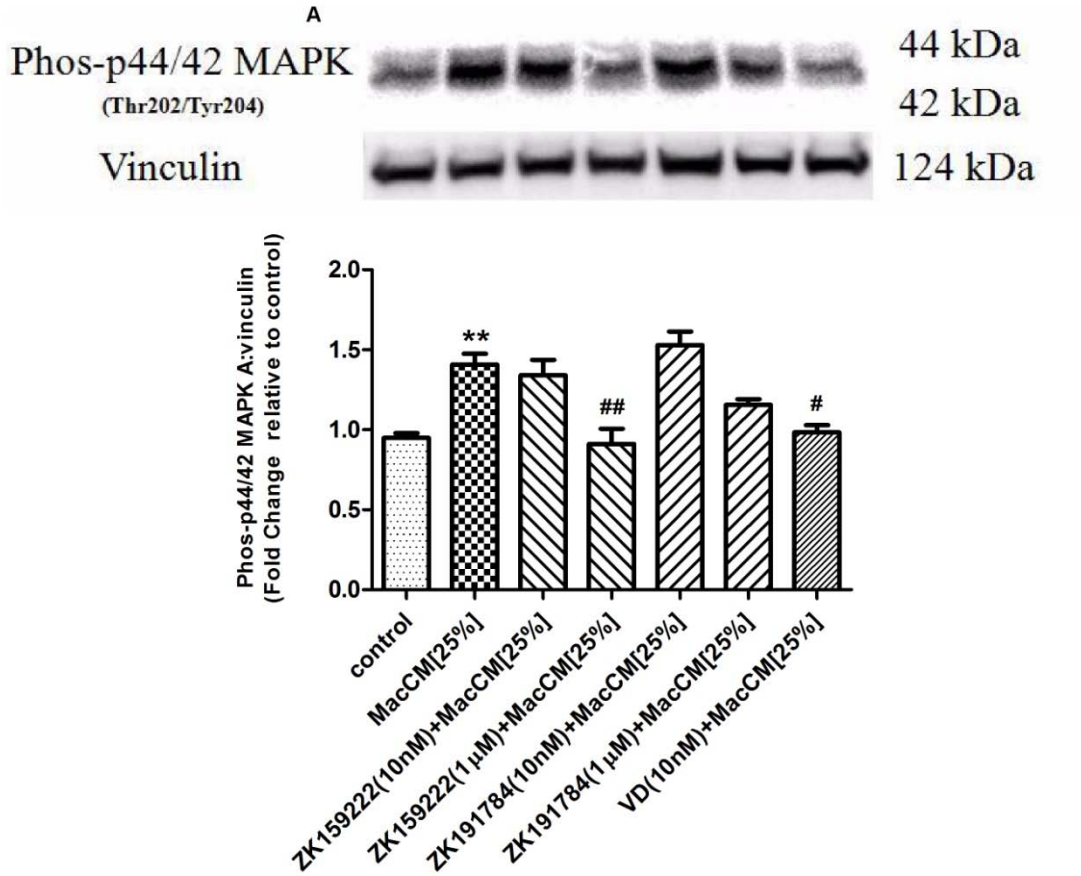

B

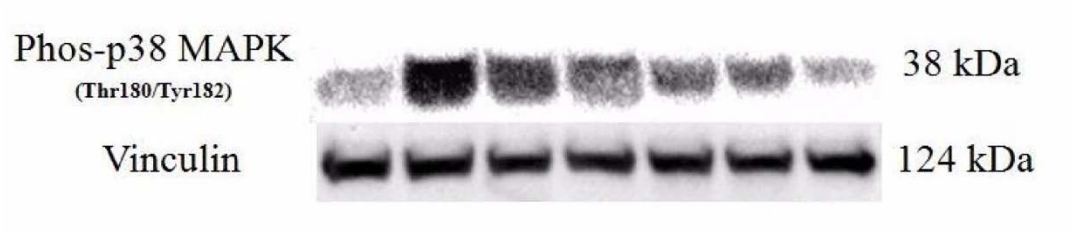
Phos-p38 MAPK
(Thr180/Tyr182)
38 kDa
Vinculin
124 kDa

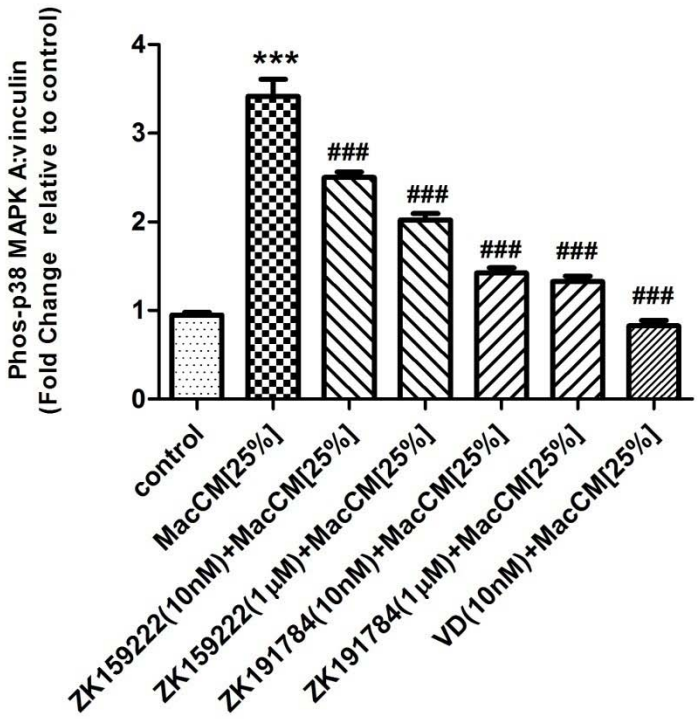
Phos-p38 MAPK A:vinculin
(Fold Change relative to control)
4
3
2
1
0
***
###
###
###
###
###
control
MacCM[25%]
ZK159222(10nM)+MacCM[25%]
ZK159222(1μM)+MacCM[25%]
ZK191784(10nM)+MacCM[25%]
ZK191784(1μM)+MacCM[25%]
VD(10nM)+MacCM[25%]

## 6.5. Discussion

The current study shows that the gene expression and secretion of IL-1β, IL-6, IL-8, MCP-1 and RANTES were markedly reduced by pretreatment with 1α,25$(OH)_2D_3$ (10 nM) and treatment with 1α,25$(OH)_2D_3$(10 nM)-MacCM, compared to THP-1-MacCM-stimulated preadipocytes. Likewise, the pretreatment with the synthesized VDR agonists [ZK159222 (10 nM and 1μM) and ZK191784 (10 nM and 1μM)] and treatment with the synthesized VDR agonist-MacCM significantly ameliorated the gene expression and secretion of these pro-inflammatory factors. In conclusion, the pretreatment with VDR agonists and treatment with VDR agonist-MacCM could attenuate THP-1-MacCM-stimulated inflammatory response in preadipocytes.

Moreover, pretreatments with VDR agonists [1α,25$(OH)_2D_3$ (10 nM), ZK159222 (1 μM) and ZK191784 (1 μM)] and treatments with VDR agonists-MacCM significantly reduced the levels of phosphorylated relA compared with THP-1-MacCM treated preadipocytes. In parallel, the pretreatment with VDR agonists [1α,25$(OH)_2D_3$ (10 nM), ZK159222 (10 nM and 1 μM) and ZK191784 (10 nM and 1 μM)] and treatment with VDR agonists-MacCM dramatically reduced the levels of phosphorylated p38, while the pretreatment with VDR agonists [1α,25$(OH)_2D_3$ (10 nM) and ZK159222 (1 μM)] and treatment with VDR agonists-MacCM significantly reduced the levels of phosphorylated ERK. Taken together, pretreatment with VDR agonists and treatment with VDR agonists-MacCM could lower the levels of phosphorylated relA of the NF-κB pathway, phosphorylated ERK and p38 of the MAPK pathways.

*Limitations*

1. It can't be specified at this stage that whether the ameliorating effects exerted on preadipocytes were by pretreatment with VDR agonists or treatment with VDR-agonist-MacCM. Separate experiments including treating (24 h) human preadipocytes with VDR-agonist-MacCM alone (the pilot study has been done, and the data shown in Appendix 9.5, 6); and pretreating (48 h) and treating (24 h) human preadipocytes with VDR agonists, are to be carried out in the future.
2. To thoroughly examine the potential anti-inflammatory effects of VDR agonist-MacCM

(since the anti-inflammatory effects of VDR agonists on IL-1β-stimulated preadipocytes have been demonstrated in Chapter 5):

a) The secretion and gene expression levels of pro-inflammatory factors (IL-1β, IL-6, IL-8, MCP-1 and RANTES in VDR agonist-MacCM-treated THP-1-macrophages (24 h) should be measured. Moreover, to explore the underlying anti-inflammatory mechanism, the levels of pro-inflammatory signaling molecules (phosphorylated relA of the NF-κB pathway, phosphorylated ERK and p38 of the MAPK pathways) should also be determined.

b) It was mentioned before that $1\alpha,25(OH)_2D_3$ could polarize pro-inflammatory M1 macrophages towards anti-inflammatory M2 (400). To test whether VDR agonists have the polarizing effect on LPS-stimulated THP-1-macrophages, the secretion and gene expression levels of anti-inflammatory factors (i.e. IL-10) in VDR agonist-treated THP-1-macrophages should be measured (24 h). Furthermore, to detect whether M2 markers [Arg-1, CD163, (major histocompatibility complex) MHC II and IL-1R II] on the surface of VDR agonist-treated THP-1-macrophages (24 h), flow cytometry is required for the purpose.

3. The levels of total unphosphorylated protein(s) including relA, ERK (p42/44) and p38 have not been determined, which is a limitation of the current experiment design. Elevated or decreased phosphorylation levels may be accompanied by increased or decreased protein levels.

In summary, this study demonstrates that THP-1-MacCM-stimulated preadipocytes could significantly enhance the gene expression and secretion of the pro-inflammatory factors, by increasing the signaling levels of the NF-κB (phosphorylated relA) and MAPK (phosphorylated ERK and p38) pathways. The combination of pretreatment with VDR agonists and treatment with the VDR agonist-MacCM might decrease the pro-inflammatory secretion and gene expression (compared to THP-1-MacCM-stimulated preadipocytes) by:

1. Directly attenuating the gene expression;
2. Reducing the levels of phosphorylated relA of the NF-κB signaling pathway;
3. Reducing the levels of phosphorylated p38 and ERK of the MAPK signaling pathways.

# 7. Discussion

## 7.1. The inflammatory synergy of preadipocytes

It has been demonstrated that MacCM could increase the pro-inflammatory gene expression and release in mature human adipocytes (322, 354). Likewise, our study shows that MacCM significantly enhanced the gene expression and secretion levels of IL-1β, IL-6, IL-8, MCP-1 and RANTES in human preadipocytes, which suggests that preadipocytes could synergize metaflammation induced by infiltrated macrophages in obesity. In parallel, the gene expression and secretion of the major pro-inflammatory factors were significantly inhibited by IL-1β and IL-6 neutralization. Moreover, IL-1β (0.5 and 2 ng/ml) alone significantly induced the inflammatory response in preadipocytes to a similar extent as that by MacCM. These results are in accordance with good evidence that IL-1β as well as IL-6 could mediate inflammatory response in human adipose tissue (21, 161, 171), and also imply that IL-6 and especially IL-1β secreted from M1 macrophages or preadipocytes are critical in maintaining and aggravating metaflammation in obesity.

The NF-κB and MAPK signaling have been established as pro-inflammatory pathways activated in metaflammation by a number of studies using murine and human MacCM/IL-1β/LPS-stimulated pre/adipocytes and LPS-activated macrophages (134, 141, 144-146, 243, 244, 322, 354, 355). Similarly, the current results show that the levels of phosphorylated relA of the NF-κB pathway, and phosphorylated ERK and p38 of the MAPK pathways, were significantly increased in THP-1-MacCM-stimulated preadipocytes. Though exerting no effect on the signaling molecules of the MAPK pathways (as demonstrated by IL-1β neutralization on Page 130-131), IL-1β (0.5 ng/ml) not only significantly increased the level of phosphorylated relA of the NF-κB pathway [also by IL-1β (2 ng/ml)], but also reduced the levels of methylated relA at Lys 310, which acts in the opposite way (to phosphorylated relA) to enhance the gene transcription of the pro-inflammatory factors (394), and could be added as a new ‘member’ in future research regarding signaling molecules involved in metaflammation.

## 7.2. The anti-inflammatory effects of VDR agonists

The anti-inflammatory effects of 1α,25$(OH)_2D_3$ and its synthesized analogues including ZK159222 and ZK191784 have been shown on mature human adipocytes and murine pre- and adipocytes (322, 352-356). Likewise, pre- (24 h) and treatments (24 h) with 1α,25$(OH)_2D_3$ (0.1-10 nM) significantly inhibited the mRNA levels of IL-1β, IL-6, IL-8 and RANTES in THP-1-MacCM-stimulated preadipocytes (24 h). In parallel with the gene expression, the secretion levels of IL-6, IL-8, MCP-1 and RANTES were also significantly inhibited by the pre- and treatment. However, there was no obvious dose-response relationship between the mRNA or secretion levels of the pro-inflammatory factors and the doses of 1α,25$(OH)_2D_3$.

It is noteworthy that our study also suggests that not only the inflammatory responses induced by IL-1β are dose-dependent, but also the anti-inflammatory effects of 1α,25$(OH)_2D_3$ is time-dependent. For though 1α,25$(OH)_2D_3$ (0.1-10 nM) significantly inhibited the secretion but not the gene expression levels of IL-1β, IL-6, IL-8, MCP-1 and RANTES in (0.5 ng/ml) IL-1β-stimulated preadipocytes, the gene expression and secretion levels of these pro-inflammatory factors were significantly inhibited by 1α,25$(OH)_2D_3$ (0.1-10 nM) in IL-1β (2 ng/ml) treated preadipocytes. Moreover, the gene expression levels of IL-1β, IL-6, IL-8, MCP-1 and RANTES were significantly reduced in (0.5 ng/ml) IL-1β-stimulated preadipocytes that received pre- (48 h) and treatment (24 h) with 1α,25$(OH)_2D_3$ (10 nM), but not in those received pre- (24 h) and treatment (24 h). Again there was no dose-response relationship between the mRNA or secretion level of the pro-inflammatory factors and the dose of 1α,25$(OH)_2D_3$. Hence, to fully explore the nature of inflammatory responses induced by IL-1β and anti-inflammatory efficacies of 1α,25$(OH)_2D_3$, further study with a broadened range of IL-1β and 1α,25$(OH)_2D_3$ doses and pre- and treatment duration is to be carried out.

In addition, similar to the anti-inflammatory effects exerted by pre- (24 and 48 h) and treatments (24 h) with 1α,25$(OH)_2D_3$ (0.1-10 nM), pre- (48 h) and treatments (24 h) with ZK191784 (10 nM and 1 μM) and ZK159222 (10 nM and 1 μM) also significantly reduced the secretion and gene transcription levels of the pro-inflammatory factors in (0.5 ng/ml) IL-1β-stimulated preadipocytes.

Finally, compared to THP-1-MacCM-stimulated preadipocytes, the anti-inflammatory effects of pretreatment with VDR agonists [1α,25$(OH)_2D_3$ (10 nM), ZK15922 (10 nM and 1 μM) and ZK191784 (10 nM and 1 μM)] (48 h) and treatment with VDR agonist-MacCM (24 h) on the pro-inflammatory secretion and gene expression, were also achieved by our study. Whether the effects exerted were by pretreatment with VDR agonists or treatment with VDR-agonist-MacCM is still to be unraveled [the preliminary data (shown in Appendix 9.5, 6) indicate that VDR agonist-MacCM could reduce the pro-inflammatory secretion and gene expression, compared to those by THP-1-MacCM-stimulated preadipocytes], although the anti-inflammatory effects and characterized working mechanism of 1α,25$(OH)_2D_3$ have been demonstrated on murine and human monocytes/macrophages (398-400).

## 7.3. The mechanisms

Similar to the effects of VDR agonists on signaling molecules of NF-κB and MAPK pathways in human adipocytes (322, 354), the western blotting results show that 1α,25$(OH)_2D_3$ (10 nM) significantly inhibited the levels of phosphorylated relA and ERK, compared to THP-1-MacCM-stimulated preadipocytes (24 h). Moreover, ZK15922 and ZK191784 not only reduced the levels of phosphorylated relA, but also increased methylated relA in (0.5 ng/ml) IL-1β-stimulated preadipocytes.

Since ER stress and the coping response-UPR is a potential trigger of metaflammation in obesity (401), the levels of signaling molecules of the UPR pathways were determined in our study. The results show that the levels of phosphorylated eIF-2α were markedly reduced by 1α,25$(OH)_2D_3$ (0.01-10 nM), which indicates that by decreasing phosphorylated eIF-2α, 1α,25$(OH)_2D_3$ could inhibit the UPR-induced NF-κB signaling pathway (52, 53) to exert anti-inflammatory effects on human white preadipocytes. However, in contrast to the effects of 1α,25$(OH)_2D_3$ (0.01-10 nM) in THP-1-MacCM-stimulated preadipocytes, the levels of phosphorylated eIF-2α were significantly increased by 1α,25$(OH)_2D_3$ in (0.5 and 2 ng/ml) IL-1β-stimulated preadipocytes, which could also

be taken as an anti-inflammatory mechanism of 1α,25$(OH)_2D_3$ since phosphorylated eIF-2α could abate the general translation (402). Hence, although the mRNA levels of the pro-inflammatory factors were not significantly inhibited by 1α,25$(OH)_2D_3$ (0.01-10 nM) in (0.5 ng/ml) IL-1β-stimulated preadipocytes (24 h), the secretion could still be reduced (as the ELISA results show) by increasing the level of phosphorylated eIF-2α. Similarly, the reducing effects on the pro-inflammatory production could be exerted by ZK159222 (10 nM) and ZK191784 (1 μM) on (0.5 ng/ml) IL-1β-stimulated preadipocytes in the same way (24 h) (as the western blotting results show). In addition, it could be proposed that VDR agonists activate the UPR pathways in IL-1β-stimulated human preadipocytes and that 1α,25$(OH)_2D_3$ (or ZK159222 and ZK191784) could trigger $Ca^{2+}$ depletion by releasing it from ER stores through IP3R and RyR/$Ca^{2+}$ release channels (349), while the loss of ER $Ca^{2+}$ stores by itself is sufficient to trigger ER stress and apoptosis (403). The evidence of intracellular $Ca^{2+}$ also playing a central role in regulating and sensing key cellular processes, especially the UPR (404, 405) , further supports that VDR agonists might regulate the transportation of ER associated $Ca^{2+}$ to induce the ER stress and the UPR .

In summary,

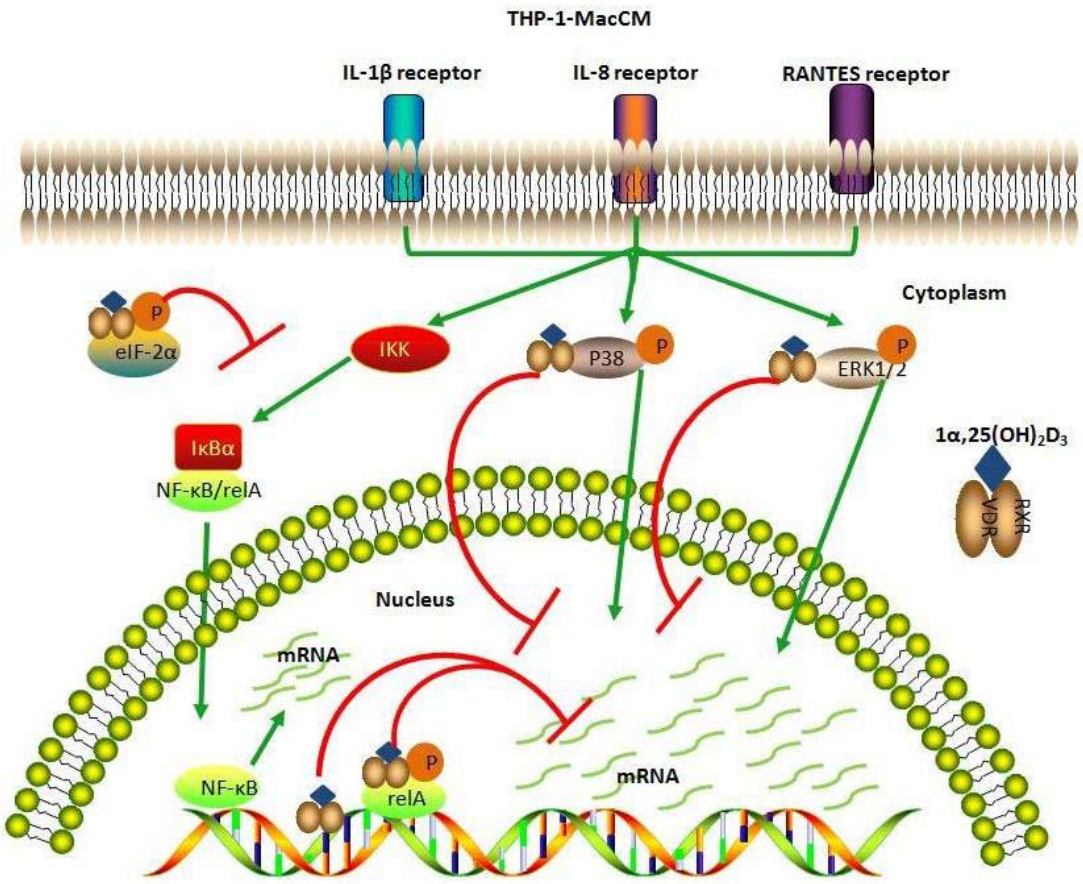


1. Pre- (24 h) and treatment (24 h) with 1α,25$(OH)_2D_3$ (0.1-10 nM) might inhibit (25%) THP-1-MacCM-stimulated inflammatory response in human preadipocytes by:
   a) Directly attenuating the pro-inflammatory gene expression;
   b) Blocking phosphorylated relA of the NF-κB signaling pathway to attenuate the pro-inflammatory gene expression;
   c) Blocking phosphorylated ERK in a non-genomic way to attenuate the pro-inflammatory gene expression;
   d) Reducing phosphorylated eIF-2α to inhibit the NF-κB signaling pathway;

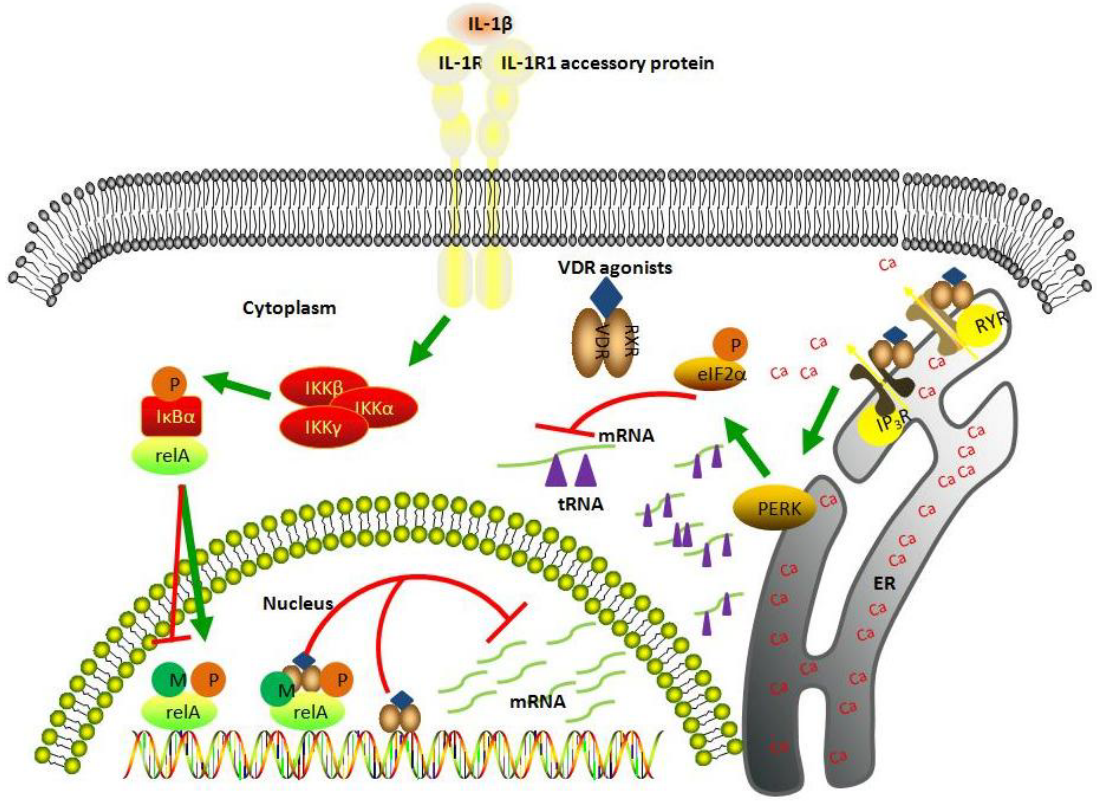


2. Pre- (24 and 48 h) and treatment (24 h) with VDR agonists [1α,25$(OH)_2D_3$ (0.01-10 nM), ZK15922 (10 nM and 1 μM) and ZK191784 (10 nM and 1 μM)] might inhibit (0.5 and 2 ng/ml) IL-1β-stimulated inflammatory response in human preadipocytes by:
   a) Directly attenuating the pro-inflammatory gene expression;
   b) Blocking phosphorylated relA of the NF-κB signaling pathway to attenuate the pro-inflammatory gene expression;
   c) Increasing methylated relA at Lys 310 of the NF-κB signaling pathway to attenuate the pro-inflammatory gene expression
   d) Increasing phosphorylated eIF-2α to abate the pro-inflammatory translation.

## 7.4. The limitations

1. Separate experiments with different time frames should be carried out to address the anti-inflammatory effects of VDR agonists on the pro-inflammatory gene expression and secretion (for 12, 24, 48 and 72 h) and pro- and anti-signaling molecules including un- and modified (phosphorylated and methylated) relA, and phosphorylated ERK, p38 and eIF-2α (for 5, 10, 15, 30 and 60 min);
2. The disparities noted in some experiments regarding gene expression (measured by qPCR) and secretion (measured by ELISA) might be considered a limitation of the study, however there are some possible explanations for this that should be considered. As noted in Chapter 4 and 5, the anti-inflammatory mechanisms involving $1\alpha,25(OH)_2D_3$ in IL-1β-stimulated preadipocytes could be at gene expression level (forming VDR-transcription complex, blocking phosphorylated relA and increasing methylated relA to inhibit the pro-inflammatory gene expression) and secretion level (increasing phosphorylated eIF-2α to directly inhibit the pro-inflammatory translation, and then to reduce the pro-inflammatory release), so the disparity between the secretion and expression data [especially inhibited secretion but unchanged gene expression in (0.01-10 nM) $1\alpha,25(OH)_2D_3$-treated IL-1β-stimulated preadipocytes (24 h)], and even no obvious dose (used in our study)-response relationship between $1\alpha,25(OH)_2D_3$ and the pro-inflammatory mRNA or release levels, might be due to the promiscuity of $1\alpha,25(OH)_2D_3$ in its anti-inflammatory effects on human preadipocytes;
3. Since the cell lysates extracted in the experiments were of the whole cell, only the level of phosphorylated/methylated relA could be measured to determine the activation of the NF-κB signaling pathway, for these post-translationally modified signaling molecules can represent relA the transcription factor in the cell nucleus. To further unravel the mystery of VDR agonists interacting with IL-1β/THP-1-MacCM-induced NF-κB signaling pathway, the nuclear lysates should be extracted and the levels of un- and modified (including phosphorylated and methylated) relA should be measured, to compare with vinculin of the whole cell (the loading control). Likewise, cytoplasmic lysates should also be extracted for the compare among the levels of ERK/p38, phosphorylated ERK/p38 and vinculin of the whole cell;

4. It could be questioned whether total protein or vinculin are the most appropriate methods to help assess whether a specific protein changes in response to treatment. Firstly, the total protein level can be compared across treatment conditions and to untreated cells, which acts as control. Total protein levels should be monitored in reference to a protein that does not change, usually a cytoskeletal protein, for example vinculin, as used in this thesis as a loading control for western blotting. Secondly, western blotting (like qPCR) is a technique to estimate what has happened in a single cell by ruling out influence of cell quantity, so a loading control is necessary to correct for possible differences in the amount of material loaded onto the gel.

## 7.5. Future directions

Animal experiments to be established

1. To generate adipose tissue inflammation *in vivo*:
    a) LPS injection to mouse;
    b) IL-1β injection/infusion to mouse;
    c) Obese mouse models: by HFD or genetic modification (i.e. *ob/ob*)
2. To block the inflammatory response:
    a) IL-1β antibody injection to the mouse;
    b) IL-1β knockout to the mouse;
    c) VDR agonist ($1\alpha,25(OH)_2D_3$, ZK159222 and ZK191784) treatment (by feeding or injection) to the mouse;
3. To measure the outcomes:
    a) Assess the inflammatory status by histology (examine macrophage infiltration) or qPCR (measure the mRNA levels of IL-1β, IL-6, IL-8, MCP-1 and RANTES) in the mouse adipose tissue;
    b) Determine the insulin sensitivity of the mouse by hyperinsulinemic-euglycemic clamp.

## 7.6. Final remarks

The studies aimed to investigate the anti-inflammatory properties of VDR agonists. The results show that pre- (24 and 48 h) and treatment (24 h) with VDR agonists [1α,25$(OH)_2D_3$ (0.01-10 nM), ZK159222 (10 nM and 1 μM) and ZK191784 (10 nM and 1 μM)] significantly inhibited the gene expression and secretion of IL-1β, IL-6, IL-8, MCP-1 and RANTES in (0.5 and 2 ng/ml) IL-1β/(25%) MacCM-stimulated human preadipocytes (24 h). Moreover, pretreatment with VDR agonists [1α,25$(OH)_2D_3$ (0.01-10 nM), ZK159222 (10 nM and 1 μM) and ZK191784 (10 nM and 1 μM)] (48 h) and treatment (24 h) with VDR agonist-MacCM significantly ameliorates the gene expression and secretion of the major inflammatory factors, compared to those of THP-1-MacCM-stimulated preadipocytes. Besides directly attenuating the gene expression of the pro-inflammatory factors, the anti-inflammatory actions of VDR agonists were probably mediated by modulating the NF-κB, MAPK and UPR pathways. The anti-inflammatory mechanism needs to be clarified in the future. In addition, the effects of VDR agonists on insulin resistance also remain to be addressed.

# 8. References


1. Hotamisligil GS, Shargill NS, Spiegelman BM. Adipose expression of tumor necrosis factor-alpha: direct role in obesity-linked insulin resistance. Science. 1993;259(5091):87-91.
2. Hotamisligil GS, Arner P, Caro JF, Atkinson RL, Spiegelman BM. Increased adipose tissue expression of tumor necrosis factor-alpha in human obesity and insulin resistance. The Journal of clinical investigation. 1995;95(5):2409-15. doi: 10.1172/JCI117936.
3. Hotamisligil GS, Spiegelman BM. Tumor necrosis factor alpha: a key component of the obesity-diabetes link. Diabetes. 1994;43(11):1271-8.
4. Hofmann C, Lorenz K, Braithwaite SS, Colca JR, Palazuk BJ, Hotamisligil GS, et al. Altered gene expression for tumor necrosis factor-alpha and its receptors during drug and dietary modulation of insulin resistance. Endocrinology. 1994;134(1):264-70. doi: 10.1210/endo.134.1.8275942.
5. Medzhitov R. Origin and physiological roles of inflammation. Nature. 2008;454(7203):428-35. doi: 10.1038/nature07201.
6. Hotamisligil GS. Inflammation and metabolic disorders. Nature. 2006;444(7121):860-7. doi: 10.1038/nature05485.
7. Gregor MF, Hotamisligil GS. Inflammatory mechanisms in obesity. Annual review of immunology. 2011;29:415-45. doi: 10.1146/annurev-immunol-031210-101322.
8. Ehses JA, Perren A, Eppler E, Ribaux P, Pospisilik JA, Maor-Cahn R, et al. Increased number of islet-associated macrophages in type 2 diabetes. Diabetes. 2007;56(9):2356-70. doi: 10.2337/db06-1650.
9. Cai D, Yuan M, Frantz DF, Melendez PA, Hansen L, Lee J, et al. Local and systemic insulin resistance resulting from hepatic activation of IKK-beta and NF-kappaB. Nature medicine. 2005;11(2):183-90. doi: 10.1038/nm1166.
10. Saghizadeh M, Ong JM, Garvey WT, Henry RR, Kern PA. The expression of TNF alpha by human muscle. Relationship to insulin resistance. The Journal of clinical investigation. 1996;97(4):1111-6. doi: 10.1172/JCI118504.
11. De Souza CT, Araujo EP, Bordin S, Ashimine R, Zollner RL, Boschero AC, et al. Consumption of a fat-rich diet activates a proinflammatory response and induces insulin resistance in the hypothalamus. Endocrinology. 2005;146(10):4192-9. doi: 10.1210/en.2004-1520.
12. Cevenini E, Monti D, Franceschi C. Inflamm-ageing. Current opinion in clinical nutrition and metabolic care. 2013;16(1):14-20. doi: 10.1097/MCO.0b013e32835ada13.
13. Choe SS, Huh JY, Hwang IJ, Kim JI, Kim JB. Adipose Tissue Remodeling: Its Role in Energy Metabolism and Metabolic Disorders. Frontiers in endocrinology. 2016;7:30. doi: 10.3389/fendo.2016.00030.
14. Giordano A, Murano I, Mondini E, Perugini J, Smorlesi A, Severi I, et al. Obese adipocytes show ultrastructural features of stressed cells and die of pyroptosis. Journal of lipid research. 2013;54(9):2423-36. doi: 10.1194/jlr.M038638.
15. Strissel KJ, Stancheva Z, Miyoshi H, Perfield JW, 2nd, DeFuria J, Jick Z, et al. Adipocyte death, adipose tissue remodeling, and obesity complications. Diabetes. 2007;56(12):2910-8. doi: 10.2337/db07-0767.
16. Trayhurn P. Hypoxia and adipose tissue function and dysfunction in obesity. Physiological reviews. 2013;93(1):1-21. doi: 10.1152/physrev.00017.2012.

17. Ye J, Gao Z, Yin J, He Q. Hypoxia is a potential risk factor for chronic inflammation and adiponectin reduction in adipose tissue of ob/ob and dietary obese mice. American journal of physiology Endocrinology and metabolism. 2007;293(4):E1118-28. doi: 10.1152/ajpendo.00435.2007.
18. Hosogai N, Fukuhara A, Oshima K, Miyata Y, Tanaka S, Segawa K, et al. Adipose tissue hypoxia in obesity and its impact on adipocytokine dysregulation. Diabetes. 2007;56(4):901-11. doi: 10.2337/db06-0911.
19. Lee YS, Kim JW, Osborne O, Oh DY, Sasik R, Schenk S, et al. Increased adipocyte O2 consumption triggers HIF-1alpha, causing inflammation and insulin resistance in obesity. Cell. 2014;157(6):1339-52. doi: 10.1016/j.cell.2014.05.012.
20. Xu H, Barnes GT, Yang Q, Tan G, Yang D, Chou CJ, et al. Chronic inflammation in fat plays a crucial role in the development of obesity-related insulin resistance. The Journal of clinical investigation. 2003;112(12):1821-30. doi: 10.1172/JCI19451.
21. Weisberg SP, McCann D, Desai M, Rosenbaum M, Leibel RL, Ferrante AW, Jr. Obesity is associated with macrophage accumulation in adipose tissue. The Journal of clinical investigation. 2003;112(12):1796-808. doi: 10.1172/JCI19246.
22. Ito A, Suganami T, Yamauchi A, Degawa-Yamauchi M, Tanaka M, Kouyama R, et al. Role of CC chemokine receptor 2 in bone marrow cells in the recruitment of macrophages into obese adipose tissue. The Journal of biological chemistry. 2008;283(51):35715-23. doi: 10.1074/jbc.M804220200.
23. Johnson AR, Milner JJ, Makowski L. The inflammation highway: metabolism accelerates inflammatory traffic in obesity. Immunological reviews. 2012;249(1):218-38. doi: 10.1111/j.1600-065X.2012.01151.x.
24. Shoelson SE, Lee J, Goldfine AB. Inflammation and insulin resistance. The Journal of clinical investigation. 2006;116(7):1793-801. doi: 10.1172/JCI29069.
25. Berg AH, Scherer PE. Adipose tissue, inflammation, and cardiovascular disease. Circulation research. 2005;96(9):939-49. doi: 10.1161/01.RES.0000163635.62927.34.
26. Guilherme A, Virbasius JV, Puri V, Czech MP. Adipocyte dysfunctions linking obesity to insulin resistance and type 2 diabetes. Nature reviews Molecular cell biology. 2008;9(5):367-77. doi: 10.1038/nrm2391.
27. Sulston RJ, Learman BS, Zhang B, Scheller EL, Parlee SD, Simon BR, et al. Increased Circulating Adiponectin in Response to Thiazolidinediones: Investigating the Role of Bone Marrow Adipose Tissue. Frontiers in endocrinology. 2016;7:128. doi: 10.3389/fendo.2016.00128.
28. Polyzos SA, Mantzoros CS. Adiponectin as a target for the treatment of nonalcoholic steatohepatitis with thiazolidinediones: A systematic review. Metabolism: clinical and experimental. 2016;65(9):1297-306. doi: 10.1016/j.metabol.2016.05.013.
29. Hotamisligil GS. Inflammation, metaflammation and immunometabolic disorders. Nature. 2017;542(7640):177-85. doi: 10.1038/nature21363.
30. Kobayashi Y. Neutrophil infiltration and chemokines. Critical reviews in immunology. 2006;26(4):307-16.
31. Elgazar-Carmon V, Rudich A, Hadad N, Levy R. Neutrophils transiently infiltrate intra-abdominal fat early in the course of high-fat feeding. Journal of lipid research. 2008;49(9):1894-903. doi: 10.1194/jlr.M800132-JLR200.
32. Wagner JG, Roth RA. Neutrophil migration mechanisms, with an emphasis on the pulmonary vasculature. Pharmacological reviews. 2000;52(3):349-74.
33. WHO. 2014. WHO Fact Files: Ten facts about obesity. Geneva: WHO.

http://www.who.int/features/factfiles/obesity/en/index/html.
34. Chaput JP, Doucet E, Tremblay A. Obesity: a disease or a biological adaptation? An update. Obesity reviews : an official journal of the International Association for the Study of Obesity. 2012;13(8):681-91. doi: 10.1111/j.1467-789X.2012.00992.x.
35. Eckel RH. Obesity: Mechanism and Clinical Management: Lippincott, Williams and Wilkins: Philadelphia, PA; 2003.
36. Crepaldi G, Manzato E. Cardiovascular Risk Factors in the Elderly in Italy. The American journal of geriatric cardiology. 1993;2(5):20-3.
37. Janiszewski PM, Ross R. Effects of weight loss among metabolically healthy obese men and women. Diabetes care. 2010;33(9):1957-9. doi: 10.2337/dc10-0547.
38. Andres R. Effect of obesity on total mortality. Int J Obes. 1980;4(4):381-6.
39. Wildman RP, Muntner P, Reynolds K, McGinn AP, Rajpathak S, Wylie-Rosett J, et al. The obese without cardiometabolic risk factor clustering and the normal weight with cardiometabolic risk factor clustering: prevalence and correlates of 2 phenotypes among the US population (NHANES 1999-2004). Archives of internal medicine. 2008;168(15):1617-24. doi: 10.1001/archinte.168.15.1617.
40. Primeau V, Coderre L, Karelis AD, Brochu M, Lavoie ME, Messier V, et al. Characterizing the profile of obese patients who are metabolically healthy. International journal of obesity. 2011;35(7):971-81. doi: 10.1038/ijo.2010.216.
41. Marini MA, Succurro E, Frontoni S, Hribal ML, Andreozzi F, Lauro R, et al. Metabolically healthy but obese women have an intermediate cardiovascular risk profile between healthy nonobese women and obese insulin-resistant women. Diabetes care. 2007;30(8):2145-7. doi: 10.2337/dc07-0419.
42. Stefan N, Kantartzis K, Machann J, Schick F, Thamer C, Rittig K, et al. Identification and characterization of metabolically benign obesity in humans. Archives of internal medicine. 2008;168(15):1609-16. doi: 10.1001/archinte.168.15.1609.
43. Meigs JB, Wilson PW, Fox CS, Vasan RS, Nathan DM, Sullivan LM, et al. Body mass index, metabolic syndrome, and risk of type 2 diabetes or cardiovascular disease. The Journal of clinical endocrinology and metabolism. 2006;91(8):2906-12. doi: 10.1210/jc.2006-0594.
44. Kloting N, Fasshauer M, Dietrich A, Kovacs P, Schon MR, Kern M, et al. Insulin-sensitive obesity. American journal of physiology Endocrinology and metabolism. 2010;299(3):E506-15. doi: 10.1152/ajpendo.00586.2009.
45. Shin MJ, Hyun YJ, Kim OY, Kim JY, Jang Y, Lee JH. Weight loss effect on inflammation and LDL oxidation in metabolically healthy but obese (MHO) individuals: low inflammation and LDL oxidation in MHO women. International journal of obesity. 2006;30(10):1529-34. doi: 10.1038/sj.ijo.0803304.
46. Cinti S, Mitchell G, Barbatelli G, Murano I, Ceresi E, Faloia E, et al. Adipocyte death defines macrophage localization and function in adipose tissue of obese mice and humans. Journal of lipid research. 2005;46(11):2347-55. doi: 10.1194/jlr.M500294-JLR200.
47. McLaughlin T, Deng A, Yee G, Lamendola C, Reaven G, Tsao PS, et al. Inflammation in subcutaneous adipose tissue: relationship to adipose cell size. Diabetologia. 2010;53(2):369-77. doi: 10.1007/s00125-009-1496-3.
48. Hetz C. The unfolded protein response: controlling cell fate decisions under ER stress and beyond. Nature reviews Molecular cell biology. 2012;13(2):89-102. doi: 10.1038/nrm3270.
49. Chung J, Nguyen AK, Henstridge DC, Holmes AG, Chan MH, Mesa JL, et al. HSP72 protects against obesity-induced insulin resistance. Proceedings of the National Academy of Sciences of the

United States of America. 2008;105(5):1739-44. doi: 10.1073/pnas.0705799105.
50. Ozcan U, Yilmaz E, Ozcan L, Furuhashi M, Vaillancourt E, Smith RO, et al. Chemical chaperones reduce ER stress and restore glucose homeostasis in a mouse model of type 2 diabetes. Science. 2006;313(5790):1137-40. doi: 10.1126/science.1128294.
51. Gregor MF, Hotamisligil GS. Thematic review series: Adipocyte Biology. Adipocyte stress: the endoplasmic reticulum and metabolic disease. Journal of lipid research. 2007;48(9):1905-14. doi: 10.1194/jlr.R700007-JLR200.
52. Hu P, Han Z, Couvillon AD, Kaufman RJ, Exton JH. Autocrine tumor necrosis factor alpha links endoplasmic reticulum stress to the membrane death receptor pathway through IRE1alpha-mediated NF-kappaB activation and down-regulation of TRAF2 expression. Molecular and cellular biology. 2006;26(8):3071-84. doi: 10.1128/MCB.26.8.3071-3084.2006.
53. Deng J, Lu PD, Zhang Y, Scheuner D, Kaufman RJ, Sonenberg N, et al. Translational repression mediates activation of nuclear factor kappa B by phosphorylated translation initiation factor 2. Molecular and cellular biology. 2004;24(23):10161-8. doi: 10.1128/MCB.24.23.10161-10168.2004.
54. Rains JL, Jain SK. Oxidative stress, insulin signaling, and diabetes. Free radical biology & medicine. 2011;50(5):567-75. doi: 10.1016/j.freeradbiomed.2010.12.006.
55. Baud V, Karin M. Signal transduction by tumor necrosis factor and its relatives. Trends in cell biology. 2001;11(9):372-7.
56. Mlinar B, Marc J, Janez A, Pfeifer M. Molecular mechanisms of insulin resistance and associated diseases. Clinica chimica acta; international journal of clinical chemistry. 2007;375(1-2):20-35. doi: 10.1016/j.cca.2006.07.005.
57. de Ferranti S, Mozaffarian D. The perfect storm: obesity, adipocyte dysfunction, and metabolic consequences. Clinical chemistry. 2008;54(6):945-55. doi: 10.1373/clinchem.2007.100156.
58. Inagi R, Ishimoto Y, Nangaku M. Proteostasis in endoplasmic reticulum--new mechanisms in kidney disease. Nature reviews Nephrology. 2014;10(7):369-78. doi: 10.1038/nrneph.2014.67.
59. Santos CX, Tanaka LY, Wosniak J, Laurindo FR. Mechanisms and implications of reactive oxygen species generation during the unfolded protein response: roles of endoplasmic reticulum oxidoreductases, mitochondrial electron transport, and NADPH oxidase. Antioxidants & redox signaling. 2009;11(10):2409-27. doi: 10.1089/ARS.2009.2625.
60. Furukawa S, Fujita T, Shimabukuro M, Iwaki M, Yamada Y, Nakajima Y, et al. Increased oxidative stress in obesity and its impact on metabolic syndrome. The Journal of clinical investigation. 2004;114(12):1752-61. doi: 10.1172/JCI21625.
61. Cassis LA, Police SB, Yiannikouris F, Thatcher SE. Local adipose tissue renin-angiotensin system. Current hypertension reports. 2008;10(2):93-8.
62. Otani H. Oxidative stress as pathogenesis of cardiovascular risk associated with metabolic syndrome. Antioxidants & redox signaling. 2011;15(7):1911-26. doi: 10.1089/ars.2010.3739.
63. Chen B, Wei J, Wang W, Cui G, Zhao Y, Zhu X, et al. Identification of signaling pathways involved in aberrant production of adipokines in adipocytes undergoing oxidative stress. Archives of medical research. 2009;40(4):241-8. doi: 10.1016/j.arcmed.2009.03.007.
64. Imoto K, Kukidome D, Nishikawa T, Matsuhisa T, Sonoda K, Fujisawa K, et al. Impact of mitochondrial reactive oxygen species and apoptosis signal-regulating kinase 1 on insulin signaling. Diabetes. 2006;55(5):1197-204.
65. Lee JY, Ye J, Gao Z, Youn HS, Lee WH, Zhao L, et al. Reciprocal modulation of Toll-like receptor-4 signaling pathways involving MyD88 and phosphatidylinositol 3-kinase/AKT by saturated

and polyunsaturated fatty acids. The Journal of biological chemistry. 2003;278(39):37041-51. doi: 10.1074/jbc.M305213200.
66. Watt MJ, Hevener A, Lancaster GI, Febbraio MA. Ciliary neurotrophic factor prevents acute lipid-induced insulin resistance by attenuating ceramide accumulation and phosphorylation of c-Jun N-terminal kinase in peripheral tissues. Endocrinology. 2006;147(5):2077-85. doi: 10.1210/en.2005-1074.
67. Unger RH, Scherer PE. Gluttony, sloth and the metabolic syndrome: a roadmap to lipotoxicity. Trends in endocrinology and metabolism: TEM. 2010;21(6):345-52. doi: 10.1016/j.tem.2010.01.009.
68. Semenza GL. Oxygen-dependent regulation of mitochondrial respiration by hypoxia-inducible factor 1. The Biochemical journal. 2007;405(1):1-9. doi: 10.1042/BJ20070389.
69. Wood IS, de Heredia FP, Wang B, Trayhurn P. Cellular hypoxia and adipose tissue dysfunction in obesity. The Proceedings of the Nutrition Society. 2009;68(4):370-7. doi: 10.1017/S0029665109990206.
70. Brook CG, Lloyd JK, Wolf OH. Relation between age of onset of obesity and size and number of adipose cells. British medical journal. 1972;2(5804):25-7.
71. Helmlinger G, Yuan F, Dellian M, Jain RK. Interstitial pH and pO2 gradients in solid tumors in vivo: high-resolution measurements reveal a lack of correlation. Nature medicine. 1997;3(2):177-82.
72. Wenger RH. Cellular adaptation to hypoxia: O2-sensing protein hydroxylases, hypoxia-inducible transcription factors, and O2-regulated gene expression. FASEB journal : official publication of the Federation of American Societies for Experimental Biology. 2002;16(10):1151-62. doi: 10.1096/fj.01-0944rev.
73. Wang B, Wood IS, Trayhurn P. Dysregulation of the expression and secretion of inflammation-related adipokines by hypoxia in human adipocytes. Pflugers Archiv : European journal of physiology. 2007;455(3):479-92. doi: 10.1007/s00424-007-0301-8.
74. Lanthier N, Leclercq IA. Adipose tissues as endocrine target organs. Best practice & research Clinical gastroenterology. 2014;28(4):545-58. doi: 10.1016/j.bpg.2014.07.002.
75. Ibrahim MM. Subcutaneous and visceral adipose tissue: structural and functional differences. Obesity reviews : an official journal of the International Association for the Study of Obesity. 2010;11(1):11-8. doi: 10.1111/j.1467-789X.2009.00623.x.
76. Bays HE, Gonzalez-Campoy JM, Bray GA, Kitabchi AE, Bergman DA, Schorr AB, et al. Pathogenic potential of adipose tissue and metabolic consequences of adipocyte hypertrophy and increased visceral adiposity. Expert review of cardiovascular therapy. 2008;6(3):343-68. doi: 10.1586/14779072.6.3.343.
77. Arner P. Not all fat is alike. Lancet. 1998;351(9112):1301-2. doi: 10.1016/S0140-6736(05)79052-8.
78. Wajchenberg BL. Subcutaneous and visceral adipose tissue: their relation to the metabolic syndrome. Endocrine reviews. 2000;21(6):697-738. doi: 10.1210/edrv.21.6.0415.
79. Gealekman O, Guseva N, Hartigan C, Apotheker S, Gorgoglione M, Gurav K, et al. Depot-specific differences and insufficient subcutaneous adipose tissue angiogenesis in human obesity. Circulation. 2011;123(2):186-94. doi: 10.1161/CIRCULATIONAHA.110.970145.
80. Chau YY, Bandiera R, Serrels A, Martinez-Estrada OM, Qing W, Lee M, et al. Visceral and subcutaneous fat have different origins and evidence supports a mesothelial source. Nature cell biology. 2014;16(4):367-75. doi: 10.1038/ncb2922.
81. Van Harmelen V, Rohrig K, Hauner H. Comparison of proliferation and differentiation capacity of

human adipocyte precursor cells from the omental and subcutaneous adipose tissue depot of obese subjects. Metabolism: clinical and experimental. 2004;53(5):632-7.
82. Casteilla L, Penicaud L, Cousin B, Calise D. Choosing an adipose tissue depot for sampling: factors in selection and depot specificity. Methods in molecular biology. 2008;456:23-38. doi: 10.1007/978-1-59745-245-8_2.
83. Frayn KN. Adipose tissue as a buffer for daily lipid flux. Diabetologia. 2002;45(9):1201-10. doi: 10.1007/s00125-002-0873-y.
84. Weyer C, Foley JE, Bogardus C, Tataranni PA, Pratley RE. Enlarged subcutaneous abdominal adipocyte size, but not obesity itself, predicts type II diabetes independent of insulin resistance. Diabetologia. 2000;43(12):1498-506. doi: 10.1007/s001250051560.
85. Harman-Boehm I, Bluher M, Redel H, Sion-Vardy N, Ovadia S, Avinoach E, et al. Macrophage infiltration into omental versus subcutaneous fat across different populations: effect of regional adiposity and the comorbidities of obesity. The Journal of clinical endocrinology and metabolism. 2007;92(6):2240-7. doi: 10.1210/jc.2006-1811.
86. Bradley D, Conte C, Mittendorfer B, Eagon JC, Varela JE, Fabbrini E, et al. Gastric bypass and banding equally improve insulin sensitivity and beta cell function. The Journal of clinical investigation. 2012;122(12):4667-74. doi: 10.1172/JCI64895.
87. Clement K, Viguerie N, Poitou C, Carette C, Pelloux V, Curat CA, et al. Weight loss regulates inflammation-related genes in white adipose tissue of obese subjects. FASEB journal : official publication of the Federation of American Societies for Experimental Biology. 2004;18(14):1657-69. doi: 10.1096/fj.04-2204com.
88. Bigornia SJ, Farb MG, Mott MM, Hess DT, Carmine B, Fiscale A, et al. Relation of depot-specific adipose inflammation to insulin resistance in human obesity. Nutrition & diabetes. 2012;2:e30. doi: 10.1038/nutd.2012.3.
89. Bluher M. Adipose tissue dysfunction contributes to obesity related metabolic diseases. Best practice & research Clinical endocrinology & metabolism. 2013;27(2):163-77. doi: 10.1016/j.beem.2013.02.005.
90. Deveaud C, Beauvoit B, Salin B, Schaeffer J, Rigoulet M. Regional differences in oxidative capacity of rat white adipose tissue are linked to the mitochondrial content of mature adipocytes. Molecular and cellular biochemistry. 2004;267(1-2):157-66.
91. Hocking SL, Wu LE, Guilhaus M, Chisholm DJ, James DE. Intrinsic depot-specific differences in the secretome of adipose tissue, preadipocytes, and adipose tissue-derived microvascular endothelial cells. Diabetes. 2010;59(12):3008-16. doi: 10.2337/db10-0483.
92. Kraunsoe R, Boushel R, Hansen CN, Schjerling P, Qvortrup K, Stockel M, et al. Mitochondrial respiration in subcutaneous and visceral adipose tissue from patients with morbid obesity. The Journal of physiology. 2010;588(Pt 12):2023-32. doi: 10.1113/jphysiol.2009.184754.
93. Schleinitz D, Bottcher Y, Bluher M, Kovacs P. The genetics of fat distribution. Diabetologia. 2014;57(7):1276-86. doi: 10.1007/s00125-014-3214-z.
94. Smas CM, Sul HS. Control of adipocyte differentiation. The Biochemical journal. 1995;309 ( Pt 3):697-710.
95. Kloting N, Bluher M. Adipocyte dysfunction, inflammation and metabolic syndrome. Reviews in endocrine & metabolic disorders. 2014;15(4):277-87. doi: 10.1007/s11154-014-9301-0.
96. Skurk T, Alberti-Huber C, Herder C, Hauner H. Relationship between adipocyte size and adipokine expression and secretion. The Journal of clinical endocrinology and metabolism.

2007;92(3):1023-33. doi: 10.1210/jc.2006-1055.
97. Laurencikiene J, Skurk T, Kulyte A, Heden P, Astrom G, Sjolin E, et al. Regulation of lipolysis in small and large fat cells of the same subject. The Journal of clinical endocrinology and metabolism. 2011;96(12):E2045-9. doi: 10.1210/jc.2011-1702.
98. Bluher M. Are there still healthy obese patients? Current opinion in endocrinology, diabetes, and obesity. 2012;19(5):341-6. doi: 10.1097/MED.0b013e328357f0a3.
99. Cotillard A, Poitou C, Torcivia A, Bouillot JL, Dietrich A, Kloting N, et al. Adipocyte size threshold matters: link with risk of type 2 diabetes and improved insulin resistance after gastric bypass. The Journal of clinical endocrinology and metabolism. 2014;99(8):E1466-70. doi: 10.1210/jc.2014-1074.
100. Stern JS, Batchelor BR, Hollander N, Cohn CK, Hirsch J. Adipose-cell size and immunoreactive insulin levels in obese and normal-weight adults. Lancet. 1972;2(7784):948-51.
101. Laforest S, Labrecque J, Michaud A, Cianflone K, Tchernof A. Adipocyte size as a determinant of metabolic disease and adipose tissue dysfunction. Critical reviews in clinical laboratory sciences. 2015;52(6):301-13. doi: 10.3109/10408363.2015.1041582.
102. Rudich A, Kanety H, Bashan N. Adipose stress-sensing kinases: linking obesity to malfunction. Trends in endocrinology and metabolism: TEM. 2007;18(8):291-9. doi: 10.1016/j.tem.2007.08.006.
103. Bashan N, Dorfman K, Tarnovscki T, Harman-Boehm I, Liberty IF, Bluher M, et al. Mitogen-activated protein kinases, inhibitory-kappaB kinase, and insulin signaling in human omental versus subcutaneous adipose tissue in obesity. Endocrinology. 2007;148(6):2955-62. doi: 10.1210/en.2006-1369.
104. Haase J, Weyer U, Immig K, Kloting N, Bluher M, Eilers J, et al. Local proliferation of macrophages in adipose tissue during obesity-induced inflammation. Diabetologia. 2014;57(3):562-71. doi: 10.1007/s00125-013-3139-y.
105. Bluher M, Kloting N, Wueest S, Schoenle EJ, Schon MR, Dietrich A, et al. Fas and FasL expression in human adipose tissue is related to obesity, insulin resistance, and type 2 diabetes. The Journal of clinical endocrinology and metabolism. 2014;99(1):E36-44. doi: 10.1210/jc.2013-2488.
106. Keuper M, Bluher M, Schon MR, Moller P, Dzyakanchuk A, Amrein K, et al. An inflammatory micro-environment promotes human adipocyte apoptosis. Molecular and cellular endocrinology. 2011;339(1-2):105-13. doi: 10.1016/j.mce.2011.04.004.
107. Alkhouri N, Gornicka A, Berk MP, Thapaliya S, Dixon LJ, Kashyap S, et al. Adipocyte apoptosis, a link between obesity, insulin resistance, and hepatic steatosis. The Journal of biological chemistry. 2010;285(5):3428-38. doi: 10.1074/jbc.M109.074252.
108. Waring P, Mullbacher A. Cell death induced by the Fas/Fas ligand pathway and its role in pathology. Immunology and cell biology. 1999;77(4):312-7. doi: 10.1046/j.1440-1711.1999.00837.x.
109. Rapold RA, Wueest S, Knoepfel A, Schoenle EJ, Konrad D. Fas activates lipolysis in a Ca2+-CaMKII-dependent manner in 3T3-L1 adipocytes. Journal of lipid research. 2013;54(1):63-70. doi: 10.1194/jlr.M028035.
110. Wueest S, Rapold RA, Schoenle EJ, Konrad D. Fas activation in adipocytes impairs insulin-stimulated glucose uptake by reducing Akt. FEBS letters. 2010;584(19):4187-92. doi: 10.1016/j.febslet.2010.08.052.
111. Wueest S, Rapold RA, Schumann DM, Rytka JM, Schildknecht A, Nov O, et al. Deletion of Fas in adipocytes relieves adipose tissue inflammation and hepatic manifestations of obesity in mice. The Journal of clinical investigation. 2010;120(1):191-202. doi: 10.1172/JCI38388.

112. Klionsky DJ. Autophagy revisited: a conversation with Christian de Duve. Autophagy. 2008;4(6):740-3.
113. Maixner N, Kovsan J, Harman-Boehm I, Bluher M, Bashan N, Rudich A. Autophagy in adipose tissue. Obesity facts. 2012;5(5):710-21. doi: 10.1159/000343983.
114. Kovsan J, Bluher M, Tarnovscki T, Kloting N, Kirshtein B, Madar L, et al. Altered autophagy in human adipose tissues in obesity. The Journal of clinical endocrinology and metabolism. 2011;96(2):E268-77. doi: 10.1210/jc.2010-1681.
115. Kosacka J, Koch K, Gericke M, Nowicki M, Heiker JT, Kloting I, et al. The polygenetically inherited metabolic syndrome of male WOKW rats is associated with enhanced autophagy in adipose tissue. Diabetology & metabolic syndrome. 2013;5:23. doi: 10.1186/1758-5996-5-23.
116. Zhang Y, Goldman S, Baerga R, Zhao Y, Komatsu M, Jin S. Adipose-specific deletion of autophagy-related gene 7 (atg7) in mice reveals a role in adipogenesis. Proceedings of the National Academy of Sciences of the United States of America. 2009;106(47):19860-5. doi: 10.1073/pnas.0906048106.
117. Sengenes C, Lolmede K, Zakaroff-Girard A, Busse R, Bouloumie A. Preadipocytes in the human subcutaneous adipose tissue display distinct features from the adult mesenchymal and hematopoietic stem cells. Journal of cellular physiology. 2005;205(1):114-22. doi: 10.1002/jcp.20381.
118. Church CD, Berry R, Rodeheffer MS. Isolation and study of adipocyte precursors. Methods in enzymology. 2014;537:31-46. doi: 10.1016/B978-0-12-411619-1.00003-3.
119. Rodeheffer MS, Birsoy K, Friedman JM. Identification of white adipocyte progenitor cells in vivo. Cell. 2008;135(2):240-9. doi: 10.1016/j.cell.2008.09.036.
120. Rosen ED, Hsu CH, Wang X, Sakai S, Freeman MW, Gonzalez FJ, et al. C/EBPalpha induces adipogenesis through PPARgamma: a unified pathway. Genes & development. 2002;16(1):22-6. doi: 10.1101/gad.948702.
121. Wu Z, Rosen ED, Brun R, Hauser S, Adelmant G, Troy AE, et al. Cross-regulation of C/EBP alpha and PPAR gamma controls the transcriptional pathway of adipogenesis and insulin sensitivity. Molecular cell. 1999;3(2):151-8.
122. Ross SE, Hemati N, Longo KA, Bennett CN, Lucas PC, Erickson RL, et al. Inhibition of adipogenesis by Wnt signaling. Science. 2000;289(5481):950-3.
123. Huang H, Song TJ, Li X, Hu L, He Q, Liu M, et al. BMP signaling pathway is required for commitment of C3H10T1/2 pluripotent stem cells to the adipocyte lineage. Proceedings of the National Academy of Sciences of the United States of America. 2009;106(31):12670-5. doi: 10.1073/pnas.0906266106.
124. Smith PJ, Wise LS, Berkowitz R, Wan C, Rubin CS. Insulin-like growth factor-I is an essential regulator of the differentiation of 3T3-L1 adipocytes. The Journal of biological chemistry. 1988;263(19):9402-8.
125. Kim JB, Wright HM, Wright M, Spiegelman BM. ADD1/SREBP1 activates PPARgamma through the production of endogenous ligand. Proceedings of the National Academy of Sciences of the United States of America. 1998;95(8):4333-7.
126. Kim JB, Spiegelman BM. ADD1/SREBP1 promotes adipocyte differentiation and gene expression linked to fatty acid metabolism. Genes & development. 1996;10(9):1096-107.
127. Kusminski CM, Holland WL, Sun K, Park J, Spurgin SB, Lin Y, et al. MitoNEET-driven alterations in adipocyte mitochondrial activity reveal a crucial adaptive process that preserves insulin sensitivity in obesity. Nature medicine. 2012;18(10):1539-49. doi: 10.1038/nm.2899.

128. Yamauchi T, Kamon J, Waki H, Imai Y, Shimozawa N, Hioki K, et al. Globular adiponectin protected ob/ob mice from diabetes and ApoE-deficient mice from atherosclerosis. The Journal of biological chemistry. 2003;278(4):2461-8. doi: 10.1074/jbc.M209033200.
129. Saltiel AR, Olefsky JM. Thiazolidinediones in the treatment of insulin resistance and type II diabetes. Diabetes. 1996;45(12):1661-9.
130. Lehmann JM, Moore LB, Smith-Oliver TA, Wilkison WO, Willson TM, Kliewer SA. An antidiabetic thiazolidinedione is a high affinity ligand for peroxisome proliferator-activated receptor gamma (PPAR gamma). The Journal of biological chemistry. 1995;270(22):12953-6.
131. Huang X, Ordemann J, Muller JM, Dubiel W. The COP9 signalosome, cullin 3 and Keap1 supercomplex regulates CHOP stability and adipogenesis. Biology open. 2012;1(8):705-10. doi: 10.1242/bio.20121875.
132. Cousin B, Andre M, Casteilla L, Penicaud L. Altered macrophage-like functions of preadipocytes in inflammation and genetic obesity. Journal of cellular physiology. 2001;186(3):380-6. doi: 10.1002/1097-4652(2001)9999:9999<000::AID-JCP1038>3.0.CO;2-T.
133. Cousin B, Munoz O, Andre M, Fontanilles AM, Dani C, Cousin JL, et al. A role for preadipocytes as macrophage-like cells. FASEB journal : official publication of the Federation of American Societies for Experimental Biology. 1999;13(2):305-12.
134. Lin Y, Lee H, Berg AH, Lisanti MP, Shapiro L, Scherer PE. The lipopolysaccharide-activated toll-like receptor (TLR)-4 induces synthesis of the closely related receptor TLR-2 in adipocytes. The Journal of biological chemistry. 2000;275(32):24255-63. doi: 10.1074/jbc.M002137200.
135. Charriere G, Cousin B, Arnaud E, Andre M, Bacou F, Penicaud L, et al. Preadipocyte conversion to macrophage. Evidence of plasticity. The Journal of biological chemistry. 2003;278(11):9850-5. doi: 10.1074/jbc.M210811200.
136. Maumus M, Sengenes C, Decaunes P, Zakaroff-Girard A, Bourlier V, Lafontan M, et al. Evidence of in situ proliferation of adult adipose tissue-derived progenitor cells: influence of fat mass microenvironment and growth. The Journal of clinical endocrinology and metabolism. 2008;93(10):4098-106. doi: 10.1210/jc.2008-0044.
137. Zaragosi LE, Wdziekonski B, Villageois P, Keophiphath M, Maumus M, Tchkonia T, et al. Activin a plays a critical role in proliferation and differentiation of human adipose progenitors. Diabetes. 2010;59(10):2513-21. doi: 10.2337/db10-0013.
138. Keophiphath M, Achard V, Henegar C, Rouault C, Clement K, Lacasa D. Macrophage-secreted factors promote a profibrotic phenotype in human preadipocytes. Molecular endocrinology. 2009;23(1):11-24. doi: 10.1210/me.2008-0183.
139. Neese RA, Misell LM, Turner S, Chu A, Kim J, Cesar D, et al. Measurement in vivo of proliferation rates of slow turnover cells by 2H2O labeling of the deoxyribose moiety of DNA. Proceedings of the National Academy of Sciences of the United States of America. 2002;99(24):15345-50. doi: 10.1073/pnas.232551499.
140. Molgat AS, Gagnon A, Sorisky A. Preadipocyte apoptosis is prevented by macrophage-conditioned medium in a PDGF-dependent manner. American journal of physiology Cell physiology. 2009;296(4):C757-65. doi: 10.1152/ajpcell.00617.2008.
141. Molgat AS, Gagnon A, Sorisky A. Macrophage-induced preadipocyte survival depends on signaling through Akt, ERK1/2, and reactive oxygen species. Experimental cell research. 2011;317(4):521-30. doi: 10.1016/j.yexcr.2010.10.024.
142. Molgat AS, Gagnon A, Foster C, Sorisky A. The activation state of macrophages alters their

ability to suppress preadipocyte apoptosis. The Journal of endocrinology. 2012;214(1):21-9. doi: 10.1530/JOE-12-0114.
143. Constant VA, Gagnon A, Landry A, Sorisky A. Macrophage-conditioned medium inhibits the differentiation of 3T3-L1 and human abdominal preadipocytes. Diabetologia. 2006;49(6):1402-11. doi: 10.1007/s00125-006-0253-0.
144. Lu C, Kumar PA, Fan Y, Sperling MA, Menon RK. A novel effect of growth hormone on macrophage modulates macrophage-dependent adipocyte differentiation. Endocrinology. 2010;151(5):2189-99. doi: 10.1210/en.2009-1194.
145. Constant VA, Gagnon A, Yarmo M, Sorisky A. The antiadipogenic effect of macrophage-conditioned medium depends on ERK1/2 activation. Metabolism: clinical and experimental. 2008;57(4):465-72. doi: 10.1016/j.metabol.2007.11.005.
146. Yarmo MN, Gagnon A, Sorisky A. The anti-adipogenic effect of macrophage-conditioned medium requires the IKKbeta/NF-kappaB pathway. Hormone and metabolic research = Hormon- und Stoffwechselforschung = Hormones et metabolisme. 2010;42(12):831-6. doi: 10.1055/s-0030-1263124.
147. de Luca C, Olefsky JM. Stressed out about obesity and insulin resistance. Nature medicine. 2006;12(1):41-2; discussion 2. doi: 10.1038/nm0106-41.
148. Cone RD. Anatomy and regulation of the central melanocortin system. Nature neuroscience. 2005;8(5):571-8. doi: 10.1038/nn1455.
149. de Luca C, Olefsky JM. Inflammation and insulin resistance. FEBS letters. 2008;582(1):97-105. doi: 10.1016/j.febslet.2007.11.057.
150. Taniguchi CM, Emanuelli B, Kahn CR. Critical nodes in signalling pathways: insights into insulin action. Nature reviews Molecular cell biology. 2006;7(2):85-96. doi: 10.1038/nrm1837.
151. Pickersgill L, Litherland GJ, Greenberg AS, Walker M, Yeaman SJ. Key role for ceramides in mediating insulin resistance in human muscle cells. The Journal of biological chemistry. 2007;282(17):12583-9. doi: 10.1074/jbc.M611157200.
152. Lee JS, Pinnamaneni SK, Eo SJ, Cho IH, Pyo JH, Kim CK, et al. Saturated, but not n-6 polyunsaturated, fatty acids induce insulin resistance: role of intramuscular accumulation of lipid metabolites. Journal of applied physiology. 2006;100(5):1467-74. doi: 10.1152/japplphysiol.01438.2005.
153. Yu C, Chen Y, Cline GW, Zhang D, Zong H, Wang Y, et al. Mechanism by which fatty acids inhibit insulin activation of insulin receptor substrate-1 (IRS-1)-associated phosphatidylinositol 3-kinase activity in muscle. The Journal of biological chemistry. 2002;277(52):50230-6. doi: 10.1074/jbc.M200958200.
154. Aguirre V, Werner ED, Giraud J, Lee YH, Shoelson SE, White MF. Phosphorylation of Ser307 in insulin receptor substrate-1 blocks interactions with the insulin receptor and inhibits insulin action. The Journal of biological chemistry. 2002;277(2):1531-7. doi: 10.1074/jbc.M101521200.
155. Rui L, Yuan M, Frantz D, Shoelson S, White MF. SOCS-1 and SOCS-3 block insulin signaling by ubiquitin-mediated degradation of IRS1 and IRS2. The Journal of biological chemistry. 2002;277(44):42394-8. doi: 10.1074/jbc.C200444200.
156. Zavaroni I, Bonora E, Pagliara M, Dall'Aglio E, Luchetti L, Buonanno G, et al. Risk factors for coronary artery disease in healthy persons with hyperinsulinemia and normal glucose tolerance. The New England journal of medicine. 1989;320(11):702-6. doi: 10.1056/NEJM198903163201105.
157. Reaven GM. Banting lecture 1988. Role of insulin resistance in human disease. Diabetes. 1988;37(12):1595-607.

158. Lillioja S, Mott DM, Spraul M, Ferraro R, Foley JE, Ravussin E, et al. Insulin resistance and insulin secretory dysfunction as precursors of non-insulin-dependent diabetes mellitus. Prospective studies of Pima Indians. The New England journal of medicine. 1993;329(27):1988-92. doi: 10.1056/NEJM199312303292703.
159. Akdis M, Burgler S, Crameri R, Eiwegger T, Fujita H, Gomez E, et al. Interleukins, from 1 to 37, and interferon-gamma: receptors, functions, and roles in diseases. The Journal of allergy and clinical immunology. 2011;127(3):701-21 e1-70. doi: 10.1016/j.jaci.2010.11.050.
160. Dinarello CA. Immunological and inflammatory functions of the interleukin-1 family. Annual review of immunology. 2009;27:519-50. doi: 10.1146/annurev.immunol.021908.132612.
161. Koenen TB, Stienstra R, van Tits LJ, Joosten LA, van Velzen JF, Hijmans A, et al. The inflammasome and caspase-1 activation: a new mechanism underlying increased inflammatory activity in human visceral adipose tissue. Endocrinology. 2011;152(10):3769-78. doi: 10.1210/en.2010-1480.
162. Stienstra R, Joosten LA, Koenen T, van Tits B, van Diepen JA, van den Berg SA, et al. The inflammasome-mediated caspase-1 activation controls adipocyte differentiation and insulin sensitivity. Cell metabolism. 2010;12(6):593-605. doi: 10.1016/j.cmet.2010.11.011.
163. Jager J, Gremeaux T, Cormont M, Le Marchand-Brustel Y, Tanti JF. Interleukin-1beta-induced insulin resistance in adipocytes through down-regulation of insulin receptor substrate-1 expression. Endocrinology. 2007;148(1):241-51. doi: 10.1210/en.2006-0692.
164. McGillicuddy FC, Harford KA, Reynolds CM, Oliver E, Claessens M, Mills KH, et al. Lack of interleukin-1 receptor I (IL-1RI) protects mice from high-fat diet-induced adipose tissue inflammation coincident with improved glucose homeostasis. Diabetes. 2011;60(6):1688-98. doi: 10.2337/db10-1278.
165. Larsen CM, Faulenbach M, Vaag A, Volund A, Ehses JA, Seifert B, et al. Interleukin-1-receptor antagonist in type 2 diabetes mellitus. The New England journal of medicine. 2007;356(15):1517-26. doi: 10.1056/NEJMoa065213.
166. Mizushima N, Levine B. Autophagy in mammalian development and differentiation. Nature cell biology. 2010;12(9):823-30. doi: 10.1038/ncb0910-823.
167. Reggiori F, Klionsky DJ. Autophagosomes: biogenesis from scratch? Current opinion in cell biology. 2005;17(4):415-22. doi: 10.1016/j.ceb.2005.06.007.
168. Ost A, Svensson K, Ruishalme I, Brannmark C, Franck N, Krook H, et al. Attenuated mTOR signaling and enhanced autophagy in adipocytes from obese patients with type 2 diabetes. Molecular medicine. 2010;16(7-8):235-46. doi: 10.2119/molmed.2010.00023.
169. Tack CJ, Stienstra R, Joosten LA, Netea MG. Inflammation links excess fat to insulin resistance: the role of the interleukin-1 family. Immunological reviews. 2012;249(1):239-52. doi: 10.1111/j.1600-065X.2012.01145.x.
170. Harris J, Hartman M, Roche C, Zeng SG, O'Shea A, Sharp FA, et al. Autophagy controls IL-1beta secretion by targeting pro-IL-1beta for degradation. The Journal of biological chemistry. 2011;286(11):9587-97. doi: 10.1074/jbc.M110.202911.
171. Eder K, Baffy N, Falus A, Fulop AK. The major inflammatory mediator interleukin-6 and obesity. Inflammation research : official journal of the European Histamine Research Society [et al]. 2009;58(11):727-36. doi: 10.1007/s00011-009-0060-4.
172. Fried SK, Bunkin DA, Greenberg AS. Omental and subcutaneous adipose tissues of obese subjects release interleukin-6: depot difference and regulation by glucocorticoid. The Journal of clinical endocrinology and metabolism. 1998;83(3):847-50. doi: 10.1210/jcem.83.3.4660.

173. Wallenius V, Wallenius K, Ahren B, Rudling M, Carlsten H, Dickson SL, et al. Interleukin-6-deficient mice develop mature-onset obesity. Nature medicine. 2002;8(1):75-9. doi: 10.1038/nm0102-75.
174. Plata-Salaman CR. Immunoregulators in the nervous system. Neuroscience and biobehavioral reviews. 1991;15(2):185-215.
175. Wassmann S, Stumpf M, Strehlow K, Schmid A, Schieffer B, Bohm M, et al. Interleukin-6 induces oxidative stress and endothelial dysfunction by overexpression of the angiotensin II type 1 receptor. Circulation research. 2004;94(4):534-41. doi: 10.1161/01.RES.0000115557.25127.8D.
176. Castell JV, Gomez-Lechon MJ, David M, Hirano T, Kishimoto T, Heinrich PC. Recombinant human interleukin-6 (IL-6/BSF-2/HSF) regulates the synthesis of acute phase proteins in human hepatocytes. FEBS letters. 1988;232(2):347-50.
177. Burke AP, Tracy RP, Kolodgie F, Malcom GT, Zieske A, Kutys R, et al. Elevated C-reactive protein values and atherosclerosis in sudden coronary death: association with different pathologies. Circulation. 2002;105(17):2019-23.
178. van Hall G, Steensberg A, Sacchetti M, Fischer C, Keller C, Schjerling P, et al. Interleukin-6 stimulates lipolysis and fat oxidation in humans. The Journal of clinical endocrinology and metabolism. 2003;88(7):3005-10. doi: 10.1210/jc.2002-021687.
179. Sopasakis VR, Sandqvist M, Gustafson B, Hammarstedt A, Schmelz M, Yang X, et al. High local concentrations and effects on differentiation implicate interleukin-6 as a paracrine regulator. Obesity research. 2004;12(3):454-60. doi: 10.1038/oby.2004.51.
180. Ellingsgaard H, Hauselmann I, Schuler B, Habib AM, Baggio LL, Meier DT, et al. Interleukin-6 enhances insulin secretion by increasing glucagon-like peptide-1 secretion from L cells and alpha cells. Nature medicine. 2011;17(11):1481-9. doi: 10.1038/nm.2513.
181. Kern PA, Ranganathan S, Li C, Wood L, Ranganathan G. Adipose tissue tumor necrosis factor and interleukin-6 expression in human obesity and insulin resistance. American journal of physiology Endocrinology and metabolism. 2001;280(5):E745-51.
182. Pricola KL, Kuhn NZ, Haleem-Smith H, Song Y, Tuan RS. Interleukin-6 maintains bone marrow-derived mesenchymal stem cell stemness by an ERK1/2-dependent mechanism. Journal of cellular biochemistry. 2009;108(3):577-88. doi: 10.1002/jcb.22289.
183. Starkie R, Ostrowski SR, Jauffred S, Febbraio M, Pedersen BK. Exercise and IL-6 infusion inhibit endotoxin-induced TNF-alpha production in humans. FASEB journal : official publication of the Federation of American Societies for Experimental Biology. 2003;17(8):884-6. doi: 10.1096/fj.02-0670fje.
184. Makki K, Froguel P, Wolowczuk I. Adipose tissue in obesity-related inflammation and insulin resistance: cells, cytokines, and chemokines. ISRN inflammation. 2013;2013:139239. doi: 10.1155/2013/139239.
185. Kim CS, Park HS, Kawada T, Kim JH, Lim D, Hubbard NE, et al. Circulating levels of MCP-1 and IL-8 are elevated in human obese subjects and associated with obesity-related parameters. International journal of obesity. 2006;30(9):1347-55. doi: 10.1038/sj.ijo.0803259.
186. Weisberg SP, Hunter D, Huber R, Lemieux J, Slaymaker S, Vaddi K, et al. CCR2 modulates inflammatory and metabolic effects of high-fat feeding. The Journal of clinical investigation. 2006;116(1):115-24. doi: 10.1172/JCI24335.
187. Kamei N, Tobe K, Suzuki R, Ohsugi M, Watanabe T, Kubota N, et al. Overexpression of monocyte chemoattractant protein-1 in adipose tissues causes macrophage recruitment and insulin

resistance. The Journal of biological chemistry. 2006;281(36):26602-14. doi: 10.1074/jbc.M601284200.
188. Tamura Y, Sugimoto M, Murayama T, Ueda Y, Kanamori H, Ono K, et al. Inhibition of CCR2 ameliorates insulin resistance and hepatic steatosis in db/db mice. Arteriosclerosis, thrombosis, and vascular biology. 2008;28(12):2195-201. doi: 10.1161/ATVBAHA.108.168633.
189. Kirk EA, Sagawa ZK, McDonald TO, O'Brien KD, Heinecke JW. Monocyte chemoattractant protein deficiency fails to restrain macrophage infiltration into adipose tissue [corrected]. Diabetes. 2008;57(5):1254-61. doi: 10.2337/db07-1061.
190. Inouye KE, Shi H, Howard JK, Daly CH, Lord GM, Rollins BJ, et al. Absence of CC chemokine ligand 2 does not limit obesity-associated infiltration of macrophages into adipose tissue. Diabetes. 2007;56(9):2242-50. doi: 10.2337/db07-0425.
191. Miyakawa T, Obaru K, Maeda K, Harada S, Mitsuya H. Identification of amino acid residues critical for LD78beta, a variant of human macrophage inflammatory protein-1alpha, binding to CCR5 and inhibition of R5 human immunodeficiency virus type 1 replication. The Journal of biological chemistry. 2002;277(7):4649-55. doi: 10.1074/jbc.M109198200.
192. Struyf S, Menten P, Lenaerts JP, Put W, D'Haese A, De Clercq E, et al. Diverging binding capacities of natural LD78beta isoforms of macrophage inflammatory protein-1alpha to the CC chemokine receptors 1, 3 and 5 affect their anti-HIV-1 activity and chemotactic potencies for neutrophils and eosinophils. European journal of immunology. 2001;31(7):2170-8.
193. Kitade H, Sawamoto K, Nagashimada M, Inoue H, Yamamoto Y, Sai Y, et al. CCR5 plays a critical role in obesity-induced adipose tissue inflammation and insulin resistance by regulating both macrophage recruitment and M1/M2 status. Diabetes. 2012;61(7):1680-90. doi: 10.2337/db11-1506.
194. Huber J, Kiefer FW, Zeyda M, Ludvik B, Silberhumer GR, Prager G, et al. CC chemokine and CC chemokine receptor profiles in visceral and subcutaneous adipose tissue are altered in human obesity. The Journal of clinical endocrinology and metabolism. 2008;93(8):3215-21. doi: 10.1210/jc.2007-2630.
195. Betz MJ, Enerback S. Human Brown Adipose Tissue: What We Have Learned So Far. Diabetes. 2015;64(7):2352-60. doi: 10.2337/db15-0146.
196. Cannon B, Nedergaard J. Brown adipose tissue: function and physiological significance. Physiological reviews. 2004;84(1):277-359. doi: 10.1152/physrev.00015.2003.
197. Harms M, Seale P. Brown and beige fat: development, function and therapeutic potential. Nature medicine. 2013;19(10):1252-63. doi: 10.1038/nm.3361.
198. Rothwell NJ, Stock MJ. A role for brown adipose tissue in diet-induced thermogenesis. Nature. 1979;281(5726):31-5.
199. Ravussin Y, Xiao C, Gavrilova O, Reitman ML. Effect of intermittent cold exposure on brown fat activation, obesity, and energy homeostasis in mice. PloS one. 2014;9(1):e85876. doi: 10.1371/journal.pone.0085876.
200. Hondares E, Iglesias R, Giralt A, Gonzalez FJ, Giralt M, Mampel T, et al. Thermogenic activation induces FGF21 expression and release in brown adipose tissue. The Journal of biological chemistry. 2011;286(15):12983-90. doi: 10.1074/jbc.M110.215889.
201. Sarruf DA, Thaler JP, Morton GJ, German J, Fischer JD, Ogimoto K, et al. Fibroblast growth factor 21 action in the brain increases energy expenditure and insulin sensitivity in obese rats. Diabetes. 2010;59(7):1817-24. doi: 10.2337/db09-1878.
202. Stanford KI, Middelbeek RJ, Townsend KL, An D, Nygaard EB, Hitchcox KM, et al. Brown

adipose tissue regulates glucose homeostasis and insulin sensitivity. The Journal of clinical investigation. 2013;123(1):215-23. doi: 10.1172/JCI62308.
203. Barbatelli G, Murano I, Madsen L, Hao Q, Jimenez M, Kristiansen K, et al. The emergence of cold-induced brown adipocytes in mouse white fat depots is determined predominantly by white to brown adipocyte transdifferentiation. American journal of physiology Endocrinology and metabolism. 2010;298(6):E1244-53. doi: 10.1152/ajpendo.00600.2009.
204. Rosenwald M, Perdikari A, Rulicke T, Wolfrum C. Bi-directional interconversion of brite and white adipocytes. Nature cell biology. 2013;15(6):659-67. doi: 10.1038/ncb2740.
205. Lee YH, Petkova AP, Mottillo EP, Granneman JG. In vivo identification of bipotential adipocyte progenitors recruited by beta3-adrenoceptor activation and high-fat feeding. Cell metabolism. 2012;15(4):480-91. doi: 10.1016/j.cmet.2012.03.009.
206. Grant R, Youm YH, Ravussin A, Dixit VD. Quantification of adipose tissue leukocytosis in obesity. Methods in molecular biology. 2013;1040:195-209. doi: 10.1007/978-1-62703-523-1_15.
207. Permana PA, Menge C, Reaven PD. Macrophage-secreted factors induce adipocyte inflammation and insulin resistance. Biochemical and biophysical research communications. 2006;341(2):507-14. doi: 10.1016/j.bbrc.2006.01.012.
208. Trellakis S, Rydleuskaya A, Fischer C, Canbay A, Tagay S, Scherag A, et al. Low adiponectin, high levels of apoptosis and increased peripheral blood neutrophil activity in healthy obese subjects. Obesity facts. 2012;5(3):305-18. doi: 10.1159/000339452.
209. Jeffery E, Church CD, Holtrup B, Colman L, Rodeheffer MS. Rapid depot-specific activation of adipocyte precursor cells at the onset of obesity. Nature cell biology. 2015;17(4):376-85. doi: 10.1038/ncb3122.
210. Talukdar S, Oh DY, Bandyopadhyay G, Li D, Xu J, McNelis J, et al. Neutrophils mediate insulin resistance in mice fed a high-fat diet through secreted elastase. Nature medicine. 2012;18(9):1407-12. doi: 10.1038/nm.2885.
211. Wu D, Molofsky AB, Liang HE, Ricardo-Gonzalez RR, Jouihan HA, Bando JK, et al. Eosinophils sustain adipose alternatively activated macrophages associated with glucose homeostasis. Science. 2011;332(6026):243-7. doi: 10.1126/science.1201475.
212. Kurashima Y, Kiyono H. New era for mucosal mast cells: their roles in inflammation, allergic immune responses and adjuvant development. Experimental & molecular medicine. 2014;46:e83. doi: 10.1038/emm.2014.7.
213. Hirai S, Ohyane C, Kim YI, Lin S, Goto T, Takahashi N, et al. Involvement of mast cells in adipose tissue fibrosis. American journal of physiology Endocrinology and metabolism. 2014;306(3):E247-55. doi: 10.1152/ajpendo.00056.2013.
214. Altintas MM, Azad A, Nayer B, Contreras G, Zaias J, Faul C, et al. Mast cells, macrophages, and crown-like structures distinguish subcutaneous from visceral fat in mice. Journal of lipid research. 2011;52(3):480-8. doi: 10.1194/jlr.M011338.
215. Liu J, Divoux A, Sun J, Zhang J, Clement K, Glickman JN, et al. Genetic deficiency and pharmacological stabilization of mast cells reduce diet-induced obesity and diabetes in mice. Nature medicine. 2009;15(8):940-5. doi: 10.1038/nm.1994.
216. Divoux A, Moutel S, Poitou C, Lacasa D, Veyrie N, Aissat A, et al. Mast cells in human adipose tissue: link with morbid obesity, inflammatory status, and diabetes. The Journal of clinical endocrinology and metabolism. 2012;97(9):E1677-85. doi: 10.1210/jc.2012-1532.
217. Pessin JE, Kwon H. How does high-fat diet induce adipose tissue fibrosis? Journal of

investigative medicine : the official publication of the American Federation for Clinical Research. 2012;60(8):1147-50. doi: 10.2310/JIM.0b013e318271fdb9.
218. Ghigliotti G, Barisione C, Garibaldi S, Fabbi P, Brunelli C, Spallarossa P, et al. Adipose tissue immune response: novel triggers and consequences for chronic inflammatory conditions. Inflammation. 2014;37(4):1337-53. doi: 10.1007/s10753-014-9914-1.
219. Bertola A, Ciucci T, Rousseau D, Bourlier V, Duffaut C, Bonnafous S, et al. Identification of adipose tissue dendritic cells correlated with obesity-associated insulin-resistance and inducing Th17 responses in mice and patients. Diabetes. 2012;61(9):2238-47. doi: 10.2337/db11-1274.
220. Stefanovic-Racic M, Yang X, Turner MS, Mantell BS, Stolz DB, Sumpter TL, et al. Dendritic cells promote macrophage infiltration and comprise a substantial proportion of obesity-associated increases in CD11c+ cells in adipose tissue and liver. Diabetes. 2012;61(9):2330-9. doi: 10.2337/db11-1523.
221. Chen Y, Tian J, Tian X, Tang X, Rui K, Tong J, et al. Adipose tissue dendritic cells enhances inflammation by prompting the generation of Th17 cells. PloS one. 2014;9(3):e92450. doi: 10.1371/journal.pone.0092450.
222. Wensveen FM, Jelencic V, Valentic S, Sestan M, Wensveen TT, Theurich S, et al. NK cells link obesity-induced adipose stress to inflammation and insulin resistance. Nature immunology. 2015;16(4):376-85. doi: 10.1038/ni.3120.
223. Taniguchi M, Seino K, Nakayama T. The NKT cell system: bridging innate and acquired immunity. Nature immunology. 2003;4(12):1164-5. doi: 10.1038/ni1203-1164.
224.Godfrey DI, MacDonald HR, Kronenberg M, Smyth MJ, Van Kaer L. NKT cells: what's in a name? Nature reviews Immunology. 2004;4(3):231-7. doi: 10.1038/nri1309.
225. Huh JY, Kim JI, Park YJ, Hwang IJ, Lee YS, Sohn JH, et al. A novel function of adipocytes in lipid antigen presentation to iNKT cells. Molecular and cellular biology. 2013;33(2):328-39. doi: 10.1128/MCB.00552-12.
226. Lynch L, O'Shea D, Winter DC, Geoghegan J, Doherty DG, O'Farrelly C. Invariant NKT cells and CD1d(+) cells amass in human omentum and are depleted in patients with cancer and obesity. European journal of immunology. 2009;39(7):1893-901. doi: 10.1002/eji.200939349.
227. Nishimura S, Manabe I, Nagasaki M, Eto K, Yamashita H, Ohsugi M, et al. CD8+ effector T cells contribute to macrophage recruitment and adipose tissue inflammation in obesity. Nature medicine. 2009;15(8):914-20. doi: 10.1038/nm.1964.
228. Feuerer M, Herrero L, Cipolletta D, Naaz A, Wong J, Nayer A, et al. Lean, but not obese, fat is enriched for a unique population of regulatory T cells that affect metabolic parameters. Nature medicine. 2009;15(8):930-9. doi: 10.1038/nm.2002.
229. Poutahidis T, Kleinewietfeld M, Smillie C, Levkovich T, Perrotta A, Bhela S, et al. Microbial reprogramming inhibits Western diet-associated obesity. PloS one. 2013;8(7):e68596. doi: 10.1371/journal.pone.0068596.
230. Rocha VZ, Folco EJ, Sukhova G, Shimizu K, Gotsman I, Vernon AH, et al. Interferon-gamma, a Th1 cytokine, regulates fat inflammation: a role for adaptive immunity in obesity. Circulation research. 2008;103(5):467-76. doi: 10.1161/CIRCRESAHA.108.177105.
231. Khan IM, Dai Perrard XY, Perrard JL, Mansoori A, Smith CW, Wu H, et al. Attenuated adipose tissue and skeletal muscle inflammation in obese mice with combined CD4+ and CD8+ T cell deficiency. Atherosclerosis. 2014;233(2):419-28. doi: 10.1016/j.atherosclerosis.2014.01.011.
232. Zhao R, Tang D, Yi S, Li W, Wu C, Lu Y, et al. Elevated peripheral frequencies of Th22 cells: a

novel potent participant in obesity and type 2 diabetes. PloS one. 2014;9(1):e85770. doi: 10.1371/journal.pone.0085770.
233. Winer S, Chan Y, Paltser G, Truong D, Tsui H, Bahrami J, et al. Normalization of obesity-associated insulin resistance through immunotherapy. Nature medicine. 2009;15(8):921-9. doi: 10.1038/nm.2001.
234. Priceman SJ, Kujawski M, Shen S, Cherryholmes GA, Lee H, Zhang C, et al. Regulation of adipose tissue T cell subsets by Stat3 is crucial for diet-induced obesity and insulin resistance. Proceedings of the National Academy of Sciences of the United States of America. 2013;110(32):13079-84. doi: 10.1073/pnas.1311557110.
235. Verreck FA, de Boer T, Langenberg DM, Hoeve MA, Kramer M, Vaisberg E, et al. Human IL-23-producing type 1 macrophages promote but IL-10-producing type 2 macrophages subvert immunity to (myco)bacteria. Proceedings of the National Academy of Sciences of the United States of America. 2004;101(13):4560-5. doi: 10.1073/pnas.0400983101.
236. Sica A, Mantovani A. Macrophage plasticity and polarization: in vivo veritas. The Journal of clinical investigation. 2012;122(3):787-95. doi: 10.1172/JCI59643.
237. Martinez FO, Helming L, Gordon S. Alternative activation of macrophages: an immunologic functional perspective. Annual review of immunology. 2009;27:451-83. doi: 10.1146/annurev.immunol.021908.132532.
238. Mosser DM. The many faces of macrophage activation. Journal of leukocyte biology. 2003;73(2):209-12.
239. Saccani A, Schioppa T, Porta C, Biswas SK, Nebuloni M, Vago L, et al. p50 nuclear factor-kappaB overexpression in tumor-associated macrophages inhibits M1 inflammatory responses and antitumor resistance. Cancer research. 2006;66(23):11432-40. doi: 10.1158/0008-5472.CAN-06-1867.
240. Guiducci C, Vicari AP, Sangaletti S, Trinchieri G, Colombo MP. Redirecting in vivo elicited tumor infiltrating macrophages and dendritic cells towards tumor rejection. Cancer research. 2005;65(8):3437-46. doi: 10.1158/0008-5472.CAN-04-4262.
241. Escribese MM, Casas M, Corbi AL. Influence of low oxygen tensions on macrophage polarization. Immunobiology. 2012;217(12):1233-40. doi: 10.1016/j.imbio.2012.07.002.
242. Caricilli AM, Picardi PK, de Abreu LL, Ueno M, Prada PO, Ropelle ER, et al. Gut microbiota is a key modulator of insulin resistance in TLR 2 knockout mice. PLoS biology. 2011;9(12):e1001212. doi: 10.1371/journal.pbio.1001212.
243. Wang N, Liang H, Zen K. Molecular mechanisms that influence the macrophage m1-m2 polarization balance. Frontiers in immunology. 2014;5:614. doi: 10.3389/fimmu.2014.00614.
244. Kosteli A, Sugaru E, Haemmerle G, Martin JF, Lei J, Zechner R, et al. Weight loss and lipolysis promote a dynamic immune response in murine adipose tissue. The Journal of clinical investigation. 2010;120(10):3466-79. doi: 10.1172/JCI42845.
245. Tschopp J, Martinon F, Burns K. NALPs: a novel protein family involved in inflammation. Nature reviews Molecular cell biology. 2003;4(2):95-104. doi: 10.1038/nrm1019.
246. Inohara, Chamaillard, McDonald C, Nunez G. NOD-LRR proteins: role in host-microbial interactions and inflammatory disease. Annual review of biochemistry. 2005;74:355-83. doi: 10.1146/annurev.biochem.74.082803.133347.
247. Shaw MH, Reimer T, Kim YG, Nunez G. NOD-like receptors (NLRs): bona fide intracellular microbial sensors. Current opinion in immunology. 2008;20(4):377-82. doi: 10.1016/j.coi.2008.06.001.

248. Hitotsumatsu O, Ahmad RC, Tavares R, Wang M, Philpott D, Turer EE, et al. The ubiquitin-editing enzyme A20 restricts nucleotide-binding oligomerization domain containing 2-triggered signals. Immunity. 2008;28(3):381-90. doi: 10.1016/j.immuni.2008.02.002.
249. Hasegawa M, Fujimoto Y, Lucas PC, Nakano H, Fukase K, Nunez G, et al. A critical role of RICK/RIP2 polyubiquitination in Nod-induced NF-kappaB activation. The EMBO journal. 2008;27(2):373-83. doi: 10.1038/sj.emboj.7601962.
250. Timmer AM, Nizet V. IKKbeta/NF-kappaB and the miscreant macrophage. The Journal of experimental medicine. 2008;205(6):1255-9. doi: 10.1084/jem.20081056.
251. Martinon F, Burns K, Tschopp J. The inflammasome: a molecular platform triggering activation of inflammatory caspases and processing of proIL-beta. Molecular cell. 2002;10(2):417-26.
252. Kofler J, Wiley CA. Microglia: key innate immune cells of the brain. Toxicologic pathology. 2011;39(1):103-14. doi: 10.1177/0192623310387619.
253. Vandanmagsar B, Youm YH, Ravussin A, Galgani JE, Stadler K, Mynatt RL, et al. The NLRP3 inflammasome instigates obesity-induced inflammation and insulin resistance. Nature medicine. 2011;17(2):179-88. doi: 10.1038/nm.2279.
254. Krausgruber T, Blazek K, Smallie T, Alzabin S, Lockstone H, Sahgal N, et al. IRF5 promotes inflammatory macrophage polarization and TH1-TH17 responses. Nature immunology. 2011;12(3):231-8. doi: 10.1038/ni.1990.
255. Fleetwood AJ, Dinh H, Cook AD, Hertzog PJ, Hamilton JA. GM-CSF- and M-CSF-dependent macrophage phenotypes display differential dependence on type I interferon signaling. Journal of leukocyte biology. 2009;86(2):411-21. doi: 10.1189/jlb.1108702.
256. Donlin LT, Jayatilleke A, Giannopoulou EG, Kalliolias GD, Ivashkiv LB. Modulation of TNF-induced macrophage polarization by synovial fibroblasts. Journal of immunology. 2014;193(5):2373-83. doi: 10.4049/jimmunol.1400486.
257. Baltimore D, Boldin MP, O'Connell RM, Rao DS, Taganov KD. MicroRNAs: new regulators of immune cell development and function. Nature immunology. 2008;9(8):839-45. doi: 10.1038/ni.f.209.
258. Graff JW, Dickson AM, Clay G, McCaffrey AP, Wilson ME. Identifying functional microRNAs in macrophages with polarized phenotypes. The Journal of biological chemistry. 2012;287(26):21816-25. doi: 10.1074/jbc.M111.327031.
259. Taganov KD, Boldin MP, Chang KJ, Baltimore D. NF-kappaB-dependent induction of microRNA miR-146, an inhibitor targeted to signaling proteins of innate immune responses. Proceedings of the National Academy of Sciences of the United States of America. 2006;103(33):12481-6. doi: 10.1073/pnas.0605298103.
260. Biswas SK, Lopez-Collazo E. Endotoxin tolerance: new mechanisms, molecules and clinical significance. Trends in immunology. 2009;30(10):475-87. doi: 10.1016/j.it.2009.07.009.
261. Zhuang G, Meng C, Guo X, Cheruku PS, Shi L, Xu H, et al. A novel regulator of macrophage activation: miR-223 in obesity-associated adipose tissue inflammation. Circulation. 2012;125(23):2892-903. doi: 10.1161/CIRCULATIONAHA.111.087817.
262. Lumeng CN, DelProposto JB, Westcott DJ, Saltiel AR. Phenotypic switching of adipose tissue macrophages with obesity is generated by spatiotemporal differences in macrophage subtypes. Diabetes. 2008;57(12):3239-46. doi: 10.2337/db08-0872.
263. Mills CD, Kincaid K, Alt JM, Heilman MJ, Hill AM. M-1/M-2 macrophages and the Th1/Th2 paradigm. Journal of immunology. 2000;164(12):6166-73.
264. Biswas SK, Mantovani A. Macrophage plasticity and interaction with lymphocyte subsets: cancer

as a paradigm. Nature immunology. 2010;11(10):889-96. doi: 10.1038/ni.1937.
265. Liu G, Ma H, Qiu L, Li L, Cao Y, Ma J, et al. Phenotypic and functional switch of macrophages induced by regulatory CD4+CD25+ T cells in mice. Immunology and cell biology. 2011;89(1):130-42. doi: 10.1038/icb.2010.70.
266. Vieira-Potter VJ. Inflammation and macrophage modulation in adipose tissues. Cellular microbiology. 2014;16(10):1484-92. doi: 10.1111/cmi.12336.
267. Spits H, Artis D, Colonna M, Diefenbach A, Di Santo JP, Eberl G, et al. Innate lymphoid cells--a proposal for uniform nomenclature. Nature reviews Immunology. 2013;13(2):145-9. doi: 10.1038/nri3365.
268. Kim BS, Artis D. Group 2 innate lymphoid cells in health and disease. Cold Spring Harbor perspectives in biology. 2015;7(5). doi: 10.1101/cshperspect.a016337.
269. Cayrol C, Girard JP. IL-33: an alarmin cytokine with crucial roles in innate immunity, inflammation and allergy. Current opinion in immunology. 2014;31:31-7. doi: 10.1016/j.coi.2014.09.004.
270. Han JM, Wu D, Denroche HC, Yao Y, Verchere CB, Levings MK. IL-33 Reverses an Obesity-Induced Deficit in Visceral Adipose Tissue ST2+ T Regulatory Cells and Ameliorates Adipose Tissue Inflammation and Insulin Resistance. Journal of immunology. 2015;194(10):4777-83. doi: 10.4049/jimmunol.1500020.
271. Park-Min KH, Antoniv TT, Ivashkiv LB. Regulation of macrophage phenotype by long-term exposure to IL-10. Immunobiology. 2005;210(2-4):77-86. doi: 10.1016/j.imbio.2005.05.002.
272. O'Farrell AM, Liu Y, Moore KW, Mui AL. IL-10 inhibits macrophage activation and proliferation by distinct signaling mechanisms: evidence for Stat3-dependent and -independent pathways. The EMBO journal. 1998;17(4):1006-18. doi: 10.1093/emboj/17.4.1006.
273. Nelms K, Keegan AD, Zamorano J, Ryan JJ, Paul WE. The IL-4 receptor: signaling mechanisms and biologic functions. Annual review of immunology. 1999;17:701-38. doi: 10.1146/annurev.immunol.17.1.701.
274. Shirey KA, Pletneva LM, Puche AC, Keegan AD, Prince GA, Blanco JC, et al. Control of RSV-induced lung injury by alternatively activated macrophages is IL-4R alpha-, TLR4-, and IFN-beta-dependent. Mucosal immunology. 2010;3(3):291-300. doi: 10.1038/mi.2010.6.
275. Martinez FO, Helming L, Milde R, Varin A, Melgert BN, Draijer C, et al. Genetic programs expressed in resting and IL-4 alternatively activated mouse and human macrophages: similarities and differences. Blood. 2013;121(9):e57-69. doi: 10.1182/blood-2012-06-436212.
276. Whyte CS, Bishop ET, Ruckerl D, Gaspar-Pereira S, Barker RN, Allen JE, et al. Suppressor of cytokine signaling (SOCS)1 is a key determinant of differential macrophage activation and function. Journal of leukocyte biology. 2011;90(5):845-54. doi: 10.1189/jlb.1110644.
277. Narayana Y, Balaji KN. NOTCH1 up-regulation and signaling involved in Mycobacterium bovis BCG-induced SOCS3 expression in macrophages. The Journal of biological chemistry. 2008;283(18):12501-11. doi: 10.1074/jbc.M709960200.
278. Babaev VR, Yancey PG, Ryzhov SV, Kon V, Breyer MD, Magnuson MA, et al. Conditional knockout of macrophage PPARgamma increases atherosclerosis in C57BL/6 and low-density lipoprotein receptor-deficient mice. Arteriosclerosis, thrombosis, and vascular biology. 2005;25(8):1647-53. doi: 10.1161/01.ATV.0000173413.31789.1a.
279. Odegaard JI, Ricardo-Gonzalez RR, Goforth MH, Morel CR, Subramanian V, Mukundan L, et al. Macrophage-specific PPARgamma controls alternative activation and improves insulin resistance.

Nature. 2007;447(7148):1116-20. doi: 10.1038/nature05894.
280. Kang K, Reilly SM, Karabacak V, Gangl MR, Fitzgerald K, Hatano B, et al. Adipocyte-derived Th2 cytokines and myeloid PPARdelta regulate macrophage polarization and insulin sensitivity. Cell metabolism. 2008;7(6):485-95. doi: 10.1016/j.cmet.2008.04.002.
281. Pludowski P, Holick MF, Pilz S, Wagner CL, Hollis BW, Grant WB, et al. Vitamin D effects on musculoskeletal health, immunity, autoimmunity, cardiovascular disease, cancer, fertility, pregnancy, dementia and mortality-a review of recent evidence. Autoimmunity reviews. 2013;12(10):976-89. doi: 10.1016/j.autrev.2013.02.004.
282. Arnson Y, Amital H, Shoenfeld Y. Vitamin D and autoimmunity: new aetiological and therapeutic considerations. Annals of the rheumatic diseases. 2007;66(9):1137-42. doi: 10.1136/ard.2007.069831.
283. Vojinovic J. Vitamin D receptor agonists' anti-inflammatory properties. Annals of the New York Academy of Sciences. 2014;1317:47-56. doi: 10.1111/nyas.12429.
284. Holick MF. Vitamin D deficiency. The New England journal of medicine. 2007;357(3):266-81. doi: 10.1056/NEJMra070553.
285. Adams JS, Hewison M. Update in vitamin D. The Journal of clinical endocrinology and metabolism. 2010;95(2):471-8. doi: 10.1210/jc.2009-1773.
286. Jurutka PW, Bartik L, Whitfield GK, Mathern DR, Barthel TK, Gurevich M, et al. Vitamin D receptor: key roles in bone mineral pathophysiology, molecular mechanism of action, and novel nutritional ligands. Journal of bone and mineral research : the official journal of the American Society for Bone and Mineral Research. 2007;22 Suppl 2:V2-10. doi: 10.1359/jbmr.07s216.
287. Hollis BW. Assessment of vitamin D nutritional and hormonal status: what to measure and how to do it. Calcified tissue international. 1996;58(1):4-5.
288. Norman AW, Mizwicki MT, Norman DP. Steroid-hormone rapid actions, membrane receptors and a conformational ensemble model. Nature reviews Drug discovery. 2004;3(1):27-41. doi: 10.1038/nrd1283.
289. Ranganathan P. Genetics of bone loss in rheumatoid arthritis--role of vitamin D receptor polymorphisms. Rheumatology. 2009;48(4):342-6. doi: 10.1093/rheumatology/ken473.
290. Crofts LA, Hancock MS, Morrison NA, Eisman JA. Multiple promoters direct the tissue-specific expression of novel N-terminal variant human vitamin D receptor gene transcripts. Proceedings of the National Academy of Sciences of the United States of America. 1998;95(18):10529-34.
291. Pinette KV, Yee YK, Amegadzie BY, Nagpal S. Vitamin D receptor as a drug discovery target. Mini reviews in medicinal chemistry. 2003;3(3):193-204.
292. Nagpal S, Na S, Rathnachalam R. Noncalcemic actions of vitamin D receptor ligands. Endocrine reviews. 2005;26(5):662-87. doi: 10.1210/er.2004-0002.
293. Barsony J, Pike JW, DeLuca HF, Marx SJ. Immunocytology with microwave-fixed fibroblasts shows 1 alpha,25-dihydroxyvitamin D3-dependent rapid and estrogen-dependent slow reorganization of vitamin D receptors. The Journal of cell biology. 1990;111(6 Pt 1):2385-95.
294. Cheskis B, Freedman LP. Ligand modulates the conversion of DNA-bound vitamin D3 receptor (VDR) homodimers into VDR-retinoid X receptor heterodimers. Molecular and cellular biology. 1994;14(5):3329-38.
295. Prufer K, Racz A, Lin GC, Barsony J. Dimerization with retinoid X receptors promotes nuclear localization and subnuclear targeting of vitamin D receptors. The Journal of biological chemistry. 2000;275(52):41114-23. doi: 10.1074/jbc.M003791200.
296. Eduardo-Canosa S, Fraga R, Sigueiro R, Marco M, Rochel N, Moras D, et al. Design and

synthesis of active vitamin D analogs. The Journal of steroid biochemistry and molecular biology. 2010;121(1-2):7-12. doi: 10.1016/j.jsbmb.2010.03.036.
297. Harant H, Andrew PJ, Reddy GS, Foglar E, Lindley IJ. 1alpha,25-dihydroxyvitamin D3 and a variety of its natural metabolites transcriptionally repress nuclear-factor-kappaB-mediated interleukin-8 gene expression. European journal of biochemistry. 1997;250(1):63-71.
298. Alroy I, Towers TL, Freedman LP. Transcriptional repression of the interleukin-2 gene by vitamin D3: direct inhibition of NFATp/AP-1 complex formation by a nuclear hormone receptor. Molecular and cellular biology. 1995;15(10):5789-99.
299. Sutton AL, MacDonald PN. Vitamin D: more than a "bone-a-fide" hormone. Molecular endocrinology. 2003;17(5):777-91. doi: 10.1210/me.2002-0363.
300. Rachez C, Gamble M, Chang CP, Atkins GB, Lazar MA, Freedman LP. The DRIP complex and SRC-1/p160 coactivators share similar nuclear receptor binding determinants but constitute functionally distinct complexes. Molecular and cellular biology. 2000;20(8):2718-26.
301. Hermanson O, Glass CK, Rosenfeld MG. Nuclear receptor coregulators: multiple modes of modification. Trends in endocrinology and metabolism: TEM. 2002;13(2):55-60.
302. Rachez C, Suldan Z, Ward J, Chang CP, Burakov D, Erdjument-Bromage H, et al. A novel protein complex that interacts with the vitamin D3 receptor in a ligand-dependent manner and enhances VDR transactivation in a cell-free system. Genes & development. 1998;12(12):1787-800.
303. Hu X, Li Y, Lazar MA. Determinants of CoRNR-dependent repression complex assembly on nuclear hormone receptors. Molecular and cellular biology. 2001;21(5):1747-58. doi: 10.1128/MCB.21.5.1747-1758.2001.
304. van de Kerkhof PC. Reduction of epidermal abnormalities and inflammatory changes in psoriatic plaques during treatment with vitamin D3 analogs. The journal of investigative dermatology Symposium proceedings. 1996;1(1):78-81.
305. Kremer R, Karaplis AC, Henderson J, Gulliver W, Banville D, Hendy GN, et al. Regulation of parathyroid hormone-like peptide in cultured normal human keratinocytes. Effect of growth factors and 1,25 dihydroxyvitamin D3 on gene expression and secretion. The Journal of clinical investigation. 1991;87(3):884-93. doi: 10.1172/JCI115094.
306. Hashimoto K, Matsumoto K, Higashiyama M, Nishida Y, Yoshikawa K. Growth-inhibitory effects of 1,25-dihydroxyvitamin D3 on normal and psoriatic keratinocytes. The British journal of dermatology. 1990;123(1):93-8.
307. D'Ambrosio D, Cippitelli M, Cocciolo MG, Mazzeo D, Di Lucia P, Lang R, et al. Inhibition of IL-12 production by 1,25-dihydroxyvitamin D3. Involvement of NF-kappaB downregulation in transcriptional repression of the p40 gene. The Journal of clinical investigation. 1998;101(1):252-62. doi: 10.1172/JCI1050.
308. Muller K, Bendtzen K. 1,25-Dihydroxyvitamin D3 as a natural regulator of human immune functions. The journal of investigative dermatology Symposium proceedings. 1996;1(1):68-71.
309. Tobler A, Gasson J, Reichel H, Norman AW, Koeffler HP. Granulocyte-macrophage colony-stimulating factor. Sensitive and receptor-mediated regulation by 1,25-dihydroxyvitamin D3 in normal human peripheral blood lymphocytes. The Journal of clinical investigation. 1987;79(6):1700-5. doi: 10.1172/JCI113009.
310. Manolagas SC, Provvedini DM, Tsoukas CD. Interactions of 1,25-dihydroxyvitamin D3 and the immune system. Molecular and cellular endocrinology. 1985;43(2-3):113-22.
311. Doroudi M, Schwartz Z, Boyan BD. Membrane-mediated actions of 1,25-dihydroxy vitamin D3:

a review of the roles of phospholipase A2 activating protein and Ca(2+)/calmodulin-dependent protein kinase II. The Journal of steroid biochemistry and molecular biology. 2015;147:81-4. doi: 10.1016/j.jsbmb.2014.11.002.
312. Dwivedi PP, Gao XH, Tan JC, Evdokiou A, Ferrante A, Morris HA, et al. A role for the phosphatidylinositol 3-kinase--protein kinase C zeta--Sp1 pathway in the 1,25-dihydroxyvitamin D3 induction of the 25-hydroxyvitamin D3 24-hydroxylase gene in human kidney cells. Cellular signalling. 2010;22(3):543-52. doi: 10.1016/j.cellsig.2009.11.009.
313. Nutchey BK, Kaplan JS, Dwivedi PP, Omdahl JL, Ferrante A, May BK, et al. Molecular action of 1,25-dihydroxyvitamin D3 and phorbol ester on the activation of the rat cytochrome P450C24 (CYP24) promoter: role of MAP kinase activities and identification of an important transcription factor binding site. The Biochemical journal. 2005;389(Pt 3):753-62. doi: 10.1042/BJ20041947.
314. Dwivedi PP, Hii CS, Ferrante A, Tan J, Der CJ, Omdahl JL, et al. Role of MAP kinases in the 1,25-dihydroxyvitamin D3-induced transactivation of the rat cytochrome P450C24 (CYP24) promoter. Specific functions for ERK1/ERK2 and ERK5. The Journal of biological chemistry. 2002;277(33):29643-53. doi: 10.1074/jbc.M204561200.
315. Saini V, Nadeem M, Kolb C, Weinstock-Guttman B. Vitamin D: role in pathogenesis of multiple sclerosis. Multiple sclerosis: a mechanistic review. 2015;1:pp127-52. doi: 10.1016/B978-0-12-800763-1.00007.5.
316. Adorini L. 1,25-Dihydroxyvitamin D3 analogs as potential therapies in transplantation. Current opinion in investigational drugs. 2002;3(10):1458-63.
317. Herdick M, Steinmeyer A, Carlberg C. Antagonistic action of a 25-carboxylic ester analogue of 1alpha, 25-dihydroxyvitamin D3 is mediated by a lack of ligand-induced vitamin D receptor interaction with coactivators. The Journal of biological chemistry. 2000;275(22):16506-12. doi: 10.1074/jbc.M910000199.
318. Nijenhuis T, van der Eerden BC, Zugel U, Steinmeyer A, Weinans H, Hoenderop JG, et al. The novel vitamin D analog ZK191784 as an intestine-specific vitamin D antagonist. FASEB journal : official publication of the Federation of American Societies for Experimental Biology. 2006;20(12):2171-3. doi: 10.1096/fj.05-5515fje.
319. Herdick M, Steinmeyer A, Carlberg C. Carboxylic ester antagonists of 1alpha,25-dihydroxyvitamin D(3) show cell-specific actions. Chemistry & biology. 2000;7(11):885-94.
320. Wiesinger H, Ulrich M, Fahnrich M, Haberey M. ZK 159222: a novel vitamin D receptor partial agonist. Journal of Dermatological Science. 1998;16(Supplement 1):S60. doi: 10.1016/S0923-1811(98)83356-2.
321. Mangelsdorf DJ, Umesono K, Kliewer SA, Borgmeyer U, Ong ES, Evans RM. A direct repeat in the cellular retinol-binding protein type II gene confers differential regulation by RXR and RAR. Cell. 1991;66(3):555-61.
322. Ding C, Wilding JP, Bing C. Vitamin D3 analogues ZK159222 and Zk191784 have anti-inflammatory properties in human adipocytes. Endocrinol Metab Genet. 2016;1:1-8. doi: doi: 10.15761/EMG.1000101.
323. Zugel U, Steinmeyer A, Giesen C, Asadullah K. A novel immunosuppressive 1alpha,25-dihydroxyvitamin D3 analog with reduced hypercalcemic activity. The Journal of investigative dermatology. 2002;119(6):1434-42. doi: 10.1046/j.1523-1747.2002.19623.x.
324. Norman AW, Bishop JE, Bula CM, Olivera CJ, Mizwicki MT, Zanello LP, et al. Molecular tools for study of genomic and rapid signal transduction responses initiated by 1 alpha,25(OH)(2)-vitamin

D(3). Steroids. 2002;67(6):457-66.
325. Malmberg P, Karlsson T, Svensson H, Lonn M, Carlsson NG, Sandberg AS, et al. A new approach to measuring vitamin D in human adipose tissue using time-of-flight secondary ion mass spectrometry: a pilot study. Journal of photochemistry and photobiology B, Biology. 2014;138:295-301. doi: 10.1016/j.jphotobiol.2014.06.008.
326. Heaney RP, Recker RR, Grote J, Horst RL, Armas LA. Vitamin D(3) is more potent than vitamin D(2) in humans. The Journal of clinical endocrinology and metabolism. 2011;96(3):E447-52. doi: 10.1210/jc.2010-2230.
327. Rosenstreich SJ, Rich C, Volwiler W. Deposition in and release of vitamin D3 from body fat: evidence for a storage site in the rat. The Journal of clinical investigation. 1971;50(3):679-87. doi: 10.1172/JCI106538.
328. Lawson DE, Douglas J, Lean M, Sedrani S. Estimation of vitamin D3 and 25-hydroxyvitamin D3 in muscle and adipose tissue of rats and man. Clinica chimica acta; international journal of clinical chemistry. 1986;157(2):175-81.
329. Blum M, Dolnikowski G, Seyoum E, Harris SS, Booth SL, Peterson J, et al. Vitamin D(3) in fat tissue. Endocrine. 2008;33(1):90-4. doi: 10.1007/s12020-008-9051-4.
330. Brouwer DA, van Beek J, Ferwerda H, Brugman AM, van der Klis FR, van der Heiden HJ, et al. Rat adipose tissue rapidly accumulates and slowly releases an orally-administered high vitamin D dose. The British journal of nutrition. 1998;79(6):527-32.
331. Mawer EB, Backhouse J, Holman CA, Lumb GA, Stanbury SW. The distribution and storage of vitamin D and its metabolites in human tissues. Clinical science. 1972;43(3):413-31.
332. Wamberg L, Christiansen T, Paulsen SK, Fisker S, Rask P, Rejnmark L, et al. Expression of vitamin D-metabolizing enzymes in human adipose tissue -- the effect of obesity and diet-induced weight loss. International journal of obesity. 2013;37(5):651-7. doi: 10.1038/ijo.2012.112.
333. Ellero S, Chakhtoura G, Barreau C, Langouet S, Benelli C, Penicaud L, et al. Xenobiotic-metabolizing cytochromes p450 in human white adipose tissue: expression and induction. Drug metabolism and disposition: the biological fate of chemicals. 2010;38(4):679-86. doi: 10.1124/dmd.109.029249.
334. Nimitphong H, Holick MF, Fried SK, Lee MJ. 25-hydroxyvitamin D(3) and 1,25-dihydroxyvitamin D(3) promote the differentiation of human subcutaneous preadipocytes. PloS one. 2012;7(12):e52171. doi: 10.1371/journal.pone.0052171.
335. Li J, Byrne ME, Chang E, Jiang Y, Donkin SS, Buhman KK, et al. 1alpha,25-Dihydroxyvitamin D hydroxylase in adipocytes. The Journal of steroid biochemistry and molecular biology. 2008;112(1-3):122-6. doi: 10.1016/j.jsbmb.2008.09.006.
336. Jones G, Prosser DE, Kaufmann M. 25-Hydroxyvitamin D-24-hydroxylase (CYP24A1): its important role in the degradation of vitamin D. Archives of biochemistry and biophysics. 2012;523(1):9-18. doi: 10.1016/j.abb.2011.11.003.
337. Mahajan A, Stahl CH. Dihydroxy-cholecalciferol stimulates adipocytic differentiation of porcine mesenchymal stem cells. The Journal of nutritional biochemistry. 2009;20(7):512-20. doi: 10.1016/j.jnutbio.2008.05.010.
338. Narvaez CJ, Simmons KM, Brunton J, Salinero A, Chittur SV, Welsh JE. Induction of STEAP4 correlates with 1,25-dihydroxyvitamin D3 stimulation of adipogenesis in mesenchymal progenitor cells derived from human adipose tissue. Journal of cellular physiology. 2013;228(10):2024-36. doi: 10.1002/jcp.24371.

339. Fu M, Sun T, Bookout AL, Downes M, Yu RT, Evans RM, et al. A Nuclear Receptor Atlas: 3T3-L1 adipogenesis. Molecular endocrinology. 2005;19(10):2437-50. doi: 10.1210/me.2004-0539.
340. Blumberg JM, Tzameli I, Astapova I, Lam FS, Flier JS, Hollenberg AN. Complex role of the vitamin D receptor and its ligand in adipogenesis in 3T3-L1 cells. The Journal of biological chemistry. 2006;281(16):11205-13. doi: 10.1074/jbc.M510343200.
341. Kong J, Li YC. Molecular mechanism of 1,25-dihydroxyvitamin D3 inhibition of adipogenesis in 3T3-L1 cells. American journal of physiology Endocrinology and metabolism. 2006;290(5):E916-24. doi: 10.1152/ajpendo.00410.2005.
342. Lee H, Bae S, Yoon Y. Anti-adipogenic effects of 1,25-dihydroxyvitamin D3 are mediated by the maintenance of the wingless-type MMTV integration site/beta-catenin pathway. International journal of molecular medicine. 2012;30(5):1219-24. doi: 10.3892/ijmm.2012.1101.
343. Cianferotti L, Demay MB. VDR-mediated inhibition of DKK1 and SFRP2 suppresses adipogenic differentiation of murine bone marrow stromal cells. Journal of cellular biochemistry. 2007;101(1):80-8. doi: 10.1002/jcb.21151.
344. Le TT, Cheng JX. Single-cell profiling reveals the origin of phenotypic variability in adipogenesis. PloS one. 2009;4(4):e5189. doi: 10.1371/journal.pone.0005189.
345. Sun X, Morris KL, Zemel MB. Role of calcitriol and cortisol on human adipocyte proliferation and oxidative and inflammatory stress: a microarray study. Journal of nutrigenetics and nutrigenomics. 2008;1(1-2):30-48. doi: 10.1159/000109873.
346. Sun X, Zemel MB. Role of uncoupling protein 2 (UCP2) expression and 1alpha, 25-dihydroxyvitamin D3 in modulating adipocyte apoptosis. FASEB journal : official publication of the Federation of American Societies for Experimental Biology. 2004;18(12):1430-2. doi: 10.1096/fj.04-1971fje.
347. Zemel MB, Sun X. Calcitriol and energy metabolism. Nutrition reviews. 2008;66(10 Suppl 2):S139-46. doi: 10.1111/j.1753-4887.2008.00099.x.
348. Sergeev IN, Song Q. High vitamin D and calcium intakes reduce diet-induced obesity in mice by increasing adipose tissue apoptosis. Molecular nutrition & food research. 2014;58(6):1342-8. doi: 10.1002/mnfr.201300503.
349. Sergeev IN. 1,25-Dihydroxyvitamin D3 induces Ca2+-mediated apoptosis in adipocytes via activation of calpain and caspase-12. Biochemical and biophysical research communications. 2009;384(1):18-21. doi: 10.1016/j.bbrc.2009.04.078.
350. Sergeev IN. Calcium as a mediator of 1,25-dihydroxyvitamin D3-induced apoptosis. The Journal of steroid biochemistry and molecular biology. 2004;89-90(1-5):419-25. doi: 10.1016/j.jsbmb.2004.03.010.
351. Wamberg L, Cullberg KB, Rejnmark L, Richelsen B, Pedersen SB. Investigations of the anti-inflammatory effects of vitamin D in adipose tissue: results from an in vitro study and a randomized controlled trial. Hormone and metabolic research = Hormon- und Stoffwechselforschung = Hormones et metabolisme. 2013;45(6):456-62. doi: 10.1055/s-0032-1331746.
352. Lira FS, Rosa JC, Cunha CA, Ribeiro EB, do Nascimento CO, Oyama LM, et al. Supplementing alpha-tocopherol (vitamin E) and vitamin D3 in high fat diet decrease IL-6 production in murine epididymal adipose tissue and 3T3-L1 adipocytes following LPS stimulation. Lipids in health and disease. 2011;10:37. doi: 10.1186/1476-511X-10-37.
353. Lorente-Cebrian S, Eriksson A, Dunlop T, Mejhert N, Dahlman I, Astrom G, et al. Differential effects of 1alpha,25-dihydroxycholecalciferol on MCP-1 and adiponectin production in human white

adipocytes. European journal of nutrition. 2012;51(3):335-42. doi: 10.1007/s00394-011-0218-z.
354. Ding C, Wilding JP, Bing C. 1,25-dihydroxyvitamin D3 protects against macrophage-induced activation of NFkappaB and MAPK signalling and chemokine release in human adipocytes. PloS one. 2013;8(4):e61707. doi: 10.1371/journal.pone.0061707.
355. Gao D, Trayhurn P, Bing C. 1,25-Dihydroxyvitamin D3 inhibits the cytokine-induced secretion of MCP-1 and reduces monocyte recruitment by human preadipocytes. International journal of obesity. 2013;37(3):357-65. doi: 10.1038/ijo.2012.53.
356. Marcotorchino J, Gouranton E, Romier B, Tourniaire F, Astier J, Malezet C, et al. Vitamin D reduces the inflammatory response and restores glucose uptake in adipocytes. Molecular nutrition & food research. 2012;56(12):1771-82. doi: 10.1002/mnfr.201200383.
357. Jeffery LE, Burke F, Mura M, Zheng Y, Qureshi OS, Hewison M, et al. 1,25-Dihydroxyvitamin D3 and IL-2 combine to inhibit T cell production of inflammatory cytokines and promote development of regulatory T cells expressing CTLA-4 and FoxP3. Journal of immunology. 2009;183(9):5458-67. doi: 10.4049/jimmunol.0803217.
358. Zeng H, Chi H. Metabolic control of regulatory T cell development and function. Trends in immunology. 2015;36(1):3-12. doi: 10.1016/j.it.2014.08.003.
359. Tsuchiya S, Yamabe M, Yamaguchi Y, Kobayashi Y, Konno T, Tada K. Establishment and characterization of a human acute monocytic leukemia cell line (THP-1). International journal of cancer. 1980;26(2):171-6.
360. Daigneault M, Preston JA, Marriott HM, Whyte MK, Dockrell DH. The identification of markers of macrophage differentiation in PMA-stimulated THP-1 cells and monocyte-derived macrophages. PloS one. 2010;5(1):e8668. doi: 10.1371/journal.pone.0008668.
361. Schwende H, Fitzke E, Ambs P, Dieter P. Differences in the state of differentiation of THP-1 cells induced by phorbol ester and 1,25-dihydroxyvitamin D3. Journal of leukocyte biology. 1996;59(4):555-61.
362. Tsuchiya S, Kobayashi Y, Goto Y, Okumura H, Nakae S, Konno T, et al. Induction of maturation in cultured human monocytic leukemia cells by a phorbol diester. Cancer research. 1982;42(4):1530-6.
363. Chanput W, Mes JJ, Wichers HJ. THP-1 cell line: an in vitro cell model for immune modulation approach. International immunopharmacology. 2014;23(1):37-45. doi: 10.1016/j.intimp.2014.08.002.
364. Cousins RJ, Blanchard RK, Popp MP, Liu L, Cao J, Moore JB, et al. A global view of the selectivity of zinc deprivation and excess on genes expressed in human THP-1 mononuclear cells. Proceedings of the National Academy of Sciences of the United States of America. 2003;100(12):6952-7. doi: 10.1073/pnas.0732111100.
365. Hjort MR, Brenyo AJ, Finkelstein JN, Frampton MW, LoMonaco MB, Stewart JC, et al. Alveolar epithelial cell-macrophage interactions affect oxygen-stimulated interleukin-8 release. Inflammation. 2003;27(3):137-45.
366. Ueki K, Tabeta K, Yoshie H, Yamazaki K. Self-heat shock protein 60 induces tumour necrosis factor-alpha in monocyte-derived macrophage: possible role in chronic inflammatory periodontal disease. Clinical and experimental immunology. 2002;127(1):72-7.
367. Smiderle FR, Ruthes AC, van Arkel J, Chanput W, Iacomini M, Wichers HJ, et al. Polysaccharides from Agaricus bisporus and Agaricus brasiliensis show similarities in their structures and their immunomodulatory effects on human monocytic THP-1 cells. BMC complementary and alternative medicine. 2011;11:58. doi: 10.1186/1472-6882-11-58.
368. Sharif O, Bolshakov VN, Raines S, Newham P, Perkins ND. Transcriptional profiling of the LPS

induced NF-kappaB response in macrophages. BMC immunology. 2007;8:1. doi: 10.1186/1471-2172-8-1.
369. Caprio M, Fabbrini E, Isidori AM, Aversa A, Fabbri A. Leptin in reproduction. Trends in endocrinology and metabolism: TEM. 2001;12(2):65-72.
370. Wellen KE, Hotamisligil GS. Inflammation, stress, and diabetes. The Journal of clinical investigation. 2005;115(5):1111-9. doi: 10.1172/JCI25102.
371. Armani A, Mammi C, Marzolla V, Calanchini M, Antelmi A, Rosano GM, et al. Cellular models for understanding adipogenesis, adipose dysfunction, and obesity. Journal of cellular biochemistry. 2010;110(3):564-72. doi: 10.1002/jcb.22598.
372. Sethi JK, Vidal-Puig AJ. Thematic review series: adipocyte biology. Adipose tissue function and plasticity orchestrate nutritional adaptation. Journal of lipid research. 2007;48(6):1253-62. doi: 10.1194/jlr.R700005-JLR200.
373. Lin Y, Huang R, Cao X, Wang SM, Shi Q, Huang RP. Detection of multiple cytokines by protein arrays from cell lysate and tissue lysate. Clinical chemistry and laboratory medicine. 2003;41(2):139-45. doi: 10.1515/CCLM.2003.023.
374. Wilson JJ, Burgess R, Mao YQ, Luo S, Tang H, Jones VS, et al. Antibody arrays in biomarker discovery. Advances in clinical chemistry. 2015;69:255-324. doi: 10.1016/bs.acc.2015.01.002.
375. Mitchell P. A perspective on protein microarrays. Nature biotechnology. 2002;20(3):225-9. doi: 10.1038/nbt0302-225.
376. Zeng Q, Chen W. The functional behavior of a macrophage/fibroblast co-culture model derived from normal and diabetic mice with a marine gelatin-oxidized alginate hydrogel. Biomaterials. 2010;31(22):5772-81. doi: 10.1016/j.biomaterials.2010.04.022.
377. Schmidt SD, Mazzella MJ, Nixon RA, Mathews PM. Abeta measurement by enzyme-linked immunosorbent assay. Methods in molecular biology. 2012;849:507-27. doi: 10.1007/978-1-61779-551-0_34.
378. Chomczynski P, Sacchi N. Single-step method of RNA isolation by acid guanidinium thiocyanate-phenol-chloroform extraction. Analytical biochemistry. 1987;162(1):156-9. doi: 10.1006/abio.1987.9999.
379. Freeman WM, Walker SJ, Vrana KE. Quantitative RT-PCR: pitfalls and potential. BioTechniques. 1999;26(1):112-22, 24-5.
380. Kutyavin IV, Afonina IA, Mills A, Gorn VV, Lukhtanov EA, Belousov ES, et al. 3'-minor groove binder-DNA probes increase sequence specificity at PCR extension temperatures. Nucleic acids research. 2000;28(2):655-61.
381. Bustin SA. Absolute quantification of mRNA using real-time reverse transcription polymerase chain reaction assays. Journal of molecular endocrinology. 2000;25(2):169-93.
382. Feroze-Merzoug F, Berquin IM, Dey J, Chen YQ. Peptidylprolyl isomerase A (PPIA) as a preferred internal control over GAPDH and beta-actin in quantitative RNA analyses. BioTechniques. 2002;32(4):776-8, 80, 82.
383. Radonic A, Thulke S, Mackay IM, Landt O, Siegert W, Nitsche A. Guideline to reference gene selection for quantitative real-time PCR. Biochemical and biophysical research communications. 2004;313(4):856-62.
384. Schmittgen TD, Livak KJ. Analyzing real-time PCR data by the comparative C(T) method. Nature protocols. 2008;3(6):1101-8.
385. Smith PK, Krohn RI, Hermanson GT, Mallia AK, Gartner FH, Provenzano MD, et al.

Measurement of protein using bicinchoninic acid. Analytical biochemistry. 1985;150(1):76-85.
386. Mahmood T, Yang PC. Western blot: technique, theory, and trouble shooting. North American journal of medical sciences. 2012;4(9):429-34. doi: 10.4103/1947-2714.100998.
387. DB E, RK R. Vitamin D and its metabolites. Textbook of Clinical Chemisty Third edition Edited by CA Burtis, ER Ashwood. 1999:pp 1417-23.
388. Hiscott J, Marois J, Garoufalis J, D'Addario M, Roulston A, Kwan I, et al. Characterization of a functional NF-kappa B site in the human interleukin 1 beta promoter: evidence for a positive autoregulatory loop. Molecular and cellular biology. 1993;13(10):6231-40.
389. Libermann TA, Baltimore D. Activation of interleukin-6 gene expression through the NF-kappa B transcription factor. Molecular and cellular biology. 1990;10(5):2327-34.
390. Gao D, Madi M, Ding C, Fok M, Steele T, Ford C, et al. Interleukin-1beta mediates macrophage-induced impairment of insulin signaling in human primary adipocytes. American journal of physiology Endocrinology and metabolism. 2014;307(3):E289-304. doi: 10.1152/ajpendo.00430.2013.
391. Senn JJ, Klover PJ, Nowak IA, Zimmers TA, Koniaris LG, Furlanetto RW, et al. Suppressor of cytokine signaling-3 (SOCS-3), a potential mediator of interleukin-6-dependent insulin resistance in hepatocytes. The Journal of biological chemistry. 2003;278(16):13740-6. doi: 10.1074/jbc.M210689200.
392. Febbraio MA, Steensberg A, Starkie RL, McConell GK, Kingwell BA. Skeletal muscle interleukin-6 and tumor necrosis factor-alpha release in healthy subjects and patients with type 2 diabetes at rest and during exercise. Metabolism: clinical and experimental. 2003;52(7):939-44.
393. Shenderov K, Riteau N, Yip R, Mayer-Barber KD, Oland S, Hieny S, et al. Cutting edge: Endoplasmic reticulum stress licenses macrophages to produce mature IL-1beta in response to TLR4 stimulation through a caspase-8- and TRIF-dependent pathway. Journal of immunology. 2014;192(5):2029-33. doi: 10.4049/jimmunol.1302549.
394. Levy D, Kuo AJ, Chang Y, Schaefer U, Kitson C, Cheung P, et al. Lysine methylation of the NF-kappaB subunit RelA by SETD6 couples activity of the histone methyltransferase GLP at chromatin to tonic repression of NF-kappaB signaling. Nature immunology. 2011;12(1):29-36. doi: 10.1038/ni.1968.
395. Ahmad R, Al-Mass A, Atizado V, Al-Hubail A, Al-Ghimlas F, Al-Arouj M, et al. Elevated expression of the toll like receptors 2 and 4 in obese individuals: its significance for obesity-induced inflammation. Journal of inflammation. 2012;9(1):48. doi: 10.1186/1476-9255-9-48.
396. Vitseva OI, Tanriverdi K, Tchkonia TT, Kirkland JL, McDonnell ME, Apovian CM, et al. Inducible Toll-like receptor and NF-kappaB regulatory pathway expression in human adipose tissue. Obesity. 2008;16(5):932-7. doi: 10.1038/oby.2008.25.
397. Di Rosa M, Malaguarnera G, De Gregorio C, Palumbo M, Nunnari G, Malaguarnera L. Immuno-modulatory effects of vitamin D3 in human monocyte and macrophages. Cellular immunology. 2012;280(1):36-43. doi: 10.1016/j.cellimm.2012.10.009.
398. Helming L, Bose J, Ehrchen J, Schiebe S, Frahm T, Geffers R, et al. 1alpha,25-Dihydroxyvitamin D3 is a potent suppressor of interferon gamma-mediated macrophage activation. Blood. 2005;106(13):4351-8. doi: 10.1182/blood-2005-03-1029.
399. Zhang Y, Leung DY, Richers BN, Liu Y, Remigio LK, Riches DW, et al. Vitamin D inhibits monocyte/macrophage proinflammatory cytokine production by targeting MAPK phosphatase-1. Journal of immunology. 2012;188(5):2127-35. doi: 10.4049/jimmunol.1102412.

400. Zhang X, Zhou M, Guo Y, Song Z, Liu B. 1,25-Dihydroxyvitamin D(3) Promotes High Glucose-Induced M1 Macrophage Switching to M2 via the VDR-PPARgamma Signaling Pathway. BioMed research international. 2015;2015:157834. doi: 10.1155/2015/157834.
401. Boden G. Endoplasmic reticulum stress: another link between obesity and insulin resistance/inflammation? Diabetes. 2009;58(3):518-9. doi: 10.2337/db08-1746.
402. de Haro C, Mendez R, Santoyo J. The eIF-2alpha kinases and the control of protein synthesis. FASEB journal : official publication of the Federation of American Societies for Experimental Biology. 1996;10(12):1378-87.
403. Yoshida I, Monji A, Tashiro K, Nakamura K, Inoue R, Kanba S. Depletion of intracellular Ca2+ store itself may be a major factor in thapsigargin-induced ER stress and apoptosis in PC12 cells. Neurochemistry international. 2006;48(8):696-702. doi: 10.1016/j.neuint.2005.12.012.
404. Decuypere JP, Monaco G, Bultynck G, Missiaen L, De Smedt H, Parys JB. The IP(3) receptor-mitochondria connection in apoptosis and autophagy. Biochimica et biophysica acta. 2011;1813(5):1003-13. doi: 10.1016/j.bbamcr.2010.11.023.
405. Harr MW, Distelhorst CW. Apoptosis and autophagy: decoding calcium signals that mediate life or death. Cold Spring Harbor perspectives in biology. 2010;2(10):a005579. doi: 10.1101/cshperspect.a005579.

# 9. Appendix

## 9.1. The summary of cytokine secretion of Chapter 3

| | THP-1-MacCM (25%)* | Control | THP-1-MacCM (25%) | IL-1β antibody (15 μg/ml) |
|---|---|---|---|---|
| G-CSF | - | - | - | 0.1185404 |
| GRO-α | 0.1319586 | - | - | 0.7023741 |
| IL-1Ra | - | - | - | 0.1953415 |
| IL-6 | - | - | 0.9698434 | 0.5358791 |
| IL-8 | 1.031219 | 0.2082694 | 0.8538878 | 0.5741403 |
| MCP-1 | - | - | 1.075745 | 0.8201016 |
| MIF | - | - | - | 0.1598375 |
| MIP-1β | - | - | - | 0.1129619 |
| MIP-1α | - | - | - | 0.2468504 |
| RANTES | 0.1786312 | - | 2.221326 | 0.6981524 |
| Serpin E1 | - | 1.188645 | 0.990583 | 0.5595829 |
| sICAM-1 | 0.2167966 | - | - | 0.1913958 |

*The results are presented in fold change of pixel density (relative to the references on the proteome array).*

## 9.2. Effects of IL-6 antibody on cytokine release from THP-1-MacCM-stimulated human white preadipocytes

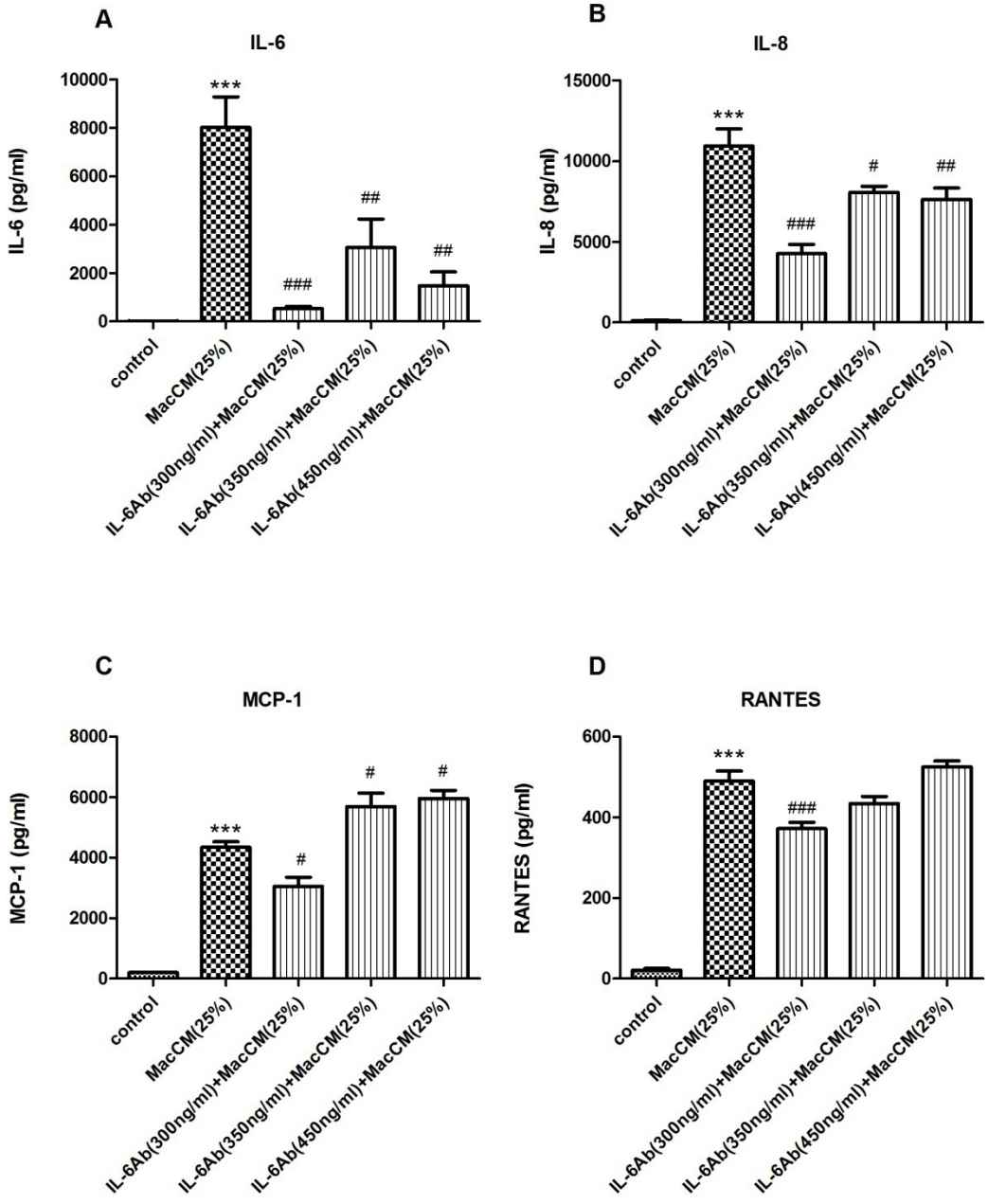


Preadipocytes were either cultured alone (control), with (25%) THP-1-MacCM alone, or in the presence of IL-6 neutralizing antibody (300, 350 and 400 ng/ml) for 24 h before medium collection. The release levels of pro-inflammatory factors (A) IL-6, (B) IL-8, (C) MCP-1 and (D) RANTES were measured by ELISA. Data are means ± SEM for groups of 6. A significant difference to control was indicated by ***($p<0.001$); to (25%) THP-1-MacCM by #($p<0.05$), ##($p<0.01$), ###($p<0.001$). The results were determined using one-way ANOVA with Tukey's post hoc test.

## 9.3. Effects of IL-6 antibody on cytokine gene expression in THP-1-MacCM-stimulated human white preadipocytes

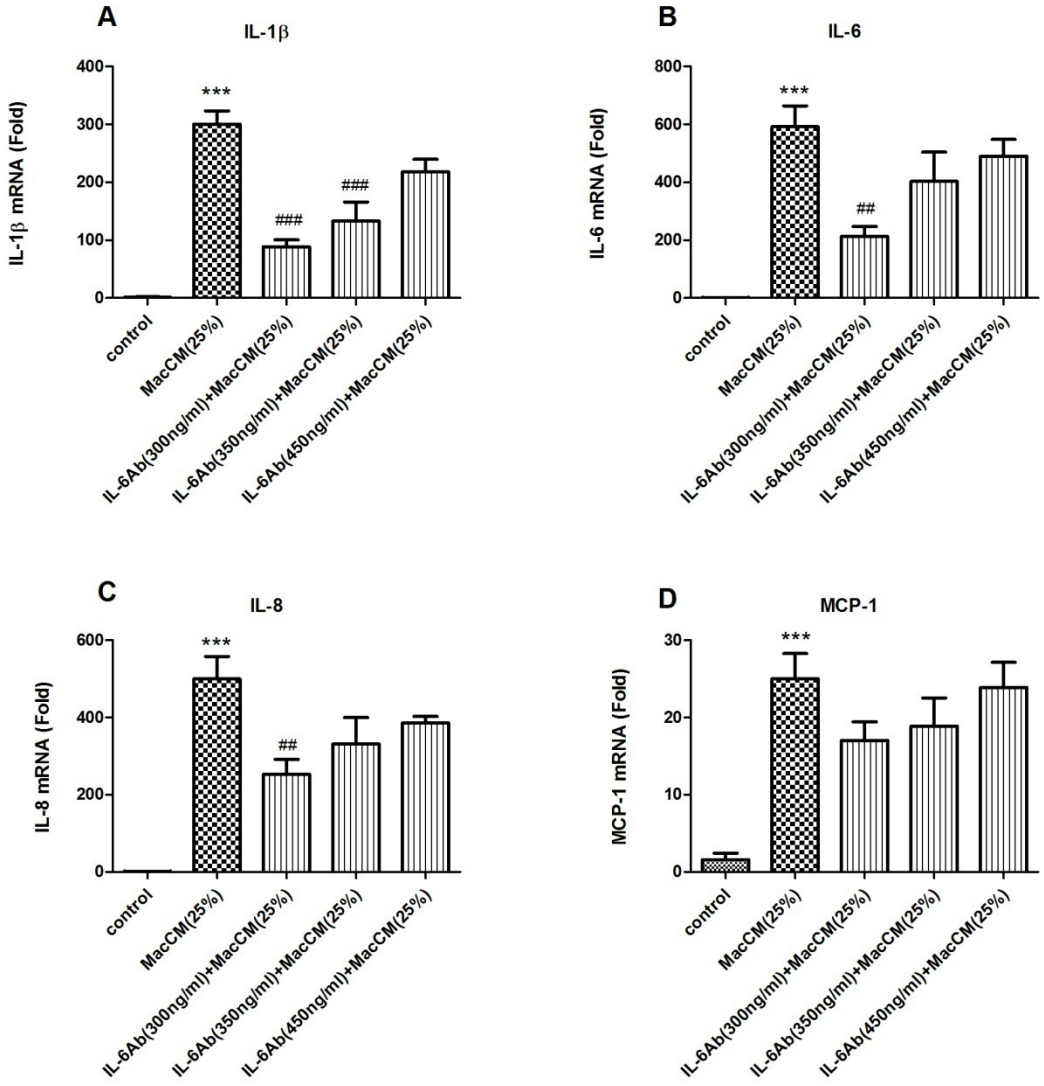

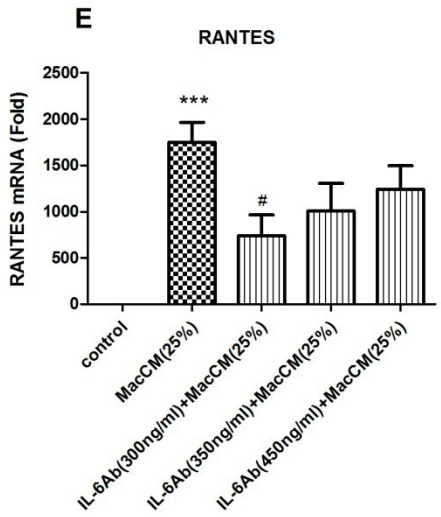


Preadipocytes were either cultured alone (control), with (25%) THP-1-MacCM alone, or in the presence of IL-6 neutralizing antibody (300, 350 and 400 ng/ml) for 24 h before Trizol-dissolved lysate collection. The mRNA levels of pro-inflammatory factors (A) IL-1β, (B) IL-6, (C) IL-8, (D) MCP-1 and (E) RANTES were measured by qPCR. Data are means ± SEM for groups of 6. A significant difference to control was indicated by ***($p<0.001$); to (25%) THP-1-MacCM by #($p<0.05$), ##($p<0.01$), ###($p<0.001$). The results were determined using one-way ANOVA with Tukey's post hoc test.

## 9.4. The summary of cytokine secretion of Chapter 5

| | Control | IL-1β (0.5 ng/ml) | ZK159222 (1 μM) | ZK191784 (1 μM) |
|---|---|---|---|---|
| Angiogenin | 0.2125524 | 0.2038048 | 0.09923838 | 0.1524558 |
| CD 40 Ligand | - | - | 0.8288996 | - |
| Chitinas 3-like 1 | 0.935989 | 0.8394657 | - | 0.6883796 |
| Complement Component C5/C5a | 0.303930 | 0.294674 | 0.2249955 | 0.2249371 |
| Dkk-1 | 0.2813234 | - | 0.1055688 | 0.1644258 |
| EGF | 0.5809314 | 0.6144629 | 0.5926872 | 0.4367681 |
| ENA-78 | 1.905615 | 1.721861 | 1.642727 | 1.349148 |
| FGF-7 | - | - | - | - |
| Flt-3 Ligand | - | 0.1448068 | - | - |
| G-CSF | - | 0.503077 | 0.3989667 | 0.4587737 |
| GDF-15 | 0.1764942 | 0.1647092 | | 0.1012699 |
| GRO-α | 0.233063 | 0.422392 | 0.3582508 | 0.2398946 |
| HGF | 0.8961962 | 0.7456259 | 0.7454289 | 0.5537399 |
| ICAM-1 | - | - | - | - |
| IGFBP-2 | 0.1367003 | - | - | - |
| IGFBP-3 | 0.1681335 | - | - | 0.1029851 |
| IL-6 | - | 0.420650 | 0.3334813 | 0.3584065 |
| IL-8 | 0.1798735 | 0.486144 | 0.3954694 | 0.4225234 |
| IP-10 | - | 0.1664159 | - | 0.100023 |
| LIF | - | 0.1029121 | - | - |
| MCP-1 | 0.4498097 | 0.5610289 | 0.4734685 | 0.5295422 |
| MCP-3 | - | 0.3525286 | 0.1744396 | 0.2575721 |
| MIF | 0.106795 | 0.1033987 | - | - |
| MIP-3α | 0.4598199 | 1.093482 | 0.8006401 | 0.8811694 |
| PENTRAXIN-3 | 0.1215895 | 0.1763251 | - | 0.1394787 |
| RANTES | - | 0.2716343 | 0.1065614 | 0.1761037 |
| Serpin | 1.862303 | 1.783751 | 1.522748 | 1.558629 |
| SHBG | - | 0.1165364 | - | - |
| Thrombospondin-1 | - | 0.1832954 | 0.1113202 | 0.1194948 |

*The results are presented in fold change of pixel density (relative to the references on the proteome array).*

## 9.5. Effects of VDR agonist-MacCM on cytokine release from human white preadipocytes

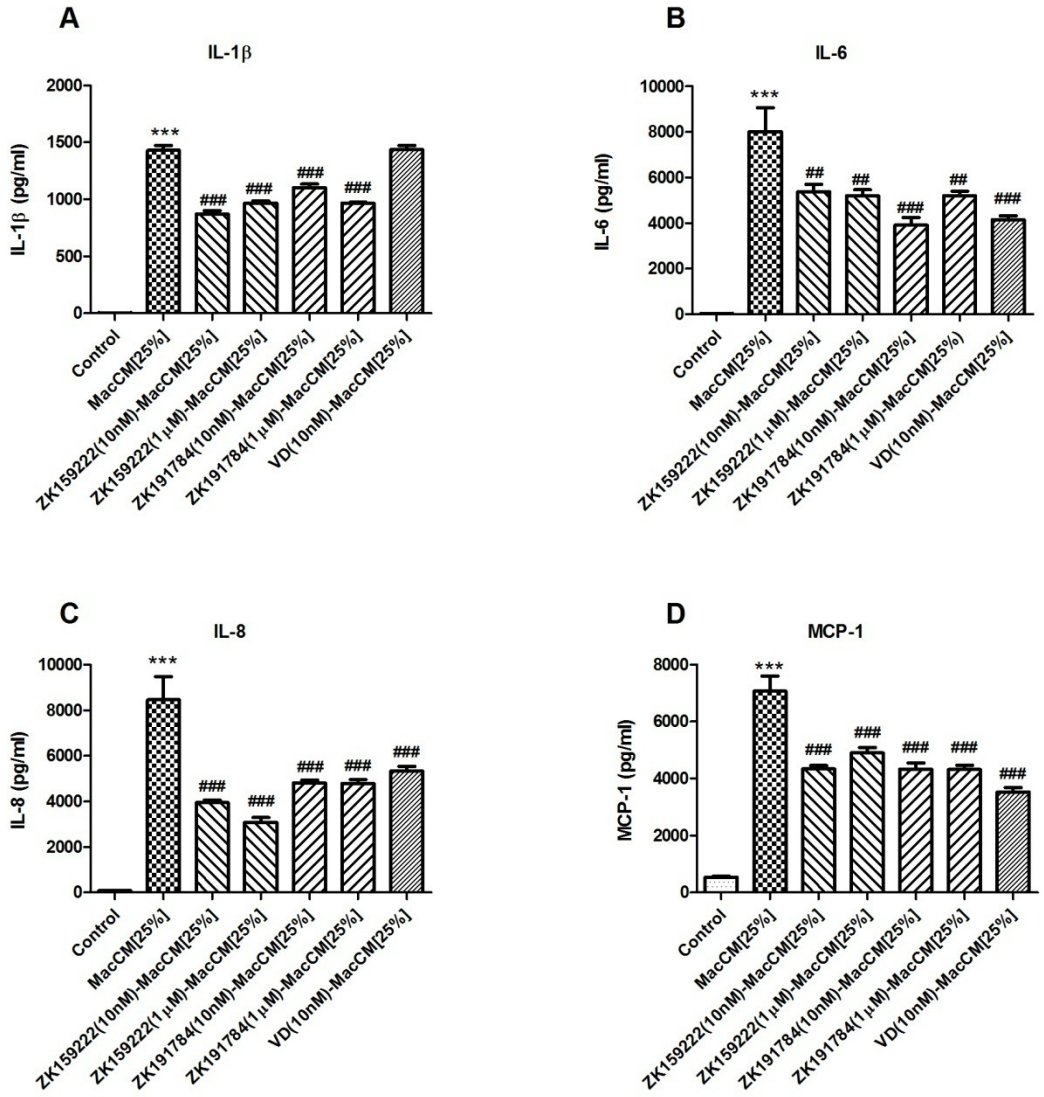

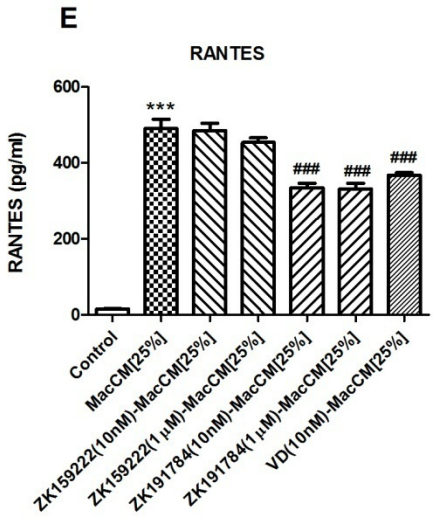


Preadipocytes were either cultured alone (control), or with (25%) THP-1-MacCM alone, or with [1α,25$(OH)_2D_3$ (10 nM), ZK159222 (10 nM and 1 μM) and ZK191784 (10 nM and 1 μM)] VDR agonist-MacCM for 24 h before medium collection. The release levels of pro-inflammatory factors (A) IL-1β, (B) IL-6, (C) IL-8, (D) MCP-1 and (E) RANTES were measured by ELISA. Data are means ± SEM for groups of 6. A significant difference to control was indicated by ***($p<0.001$); to (25%) THP-1-MacCM by ##($p<0.01$), ###($p<0.001$). The results were determined using one-way ANOVA with Tukey's post hoc test.

## 9.6. Effects of VDR agonist-MacCM on cytokine gene expression in human white preadipocytes

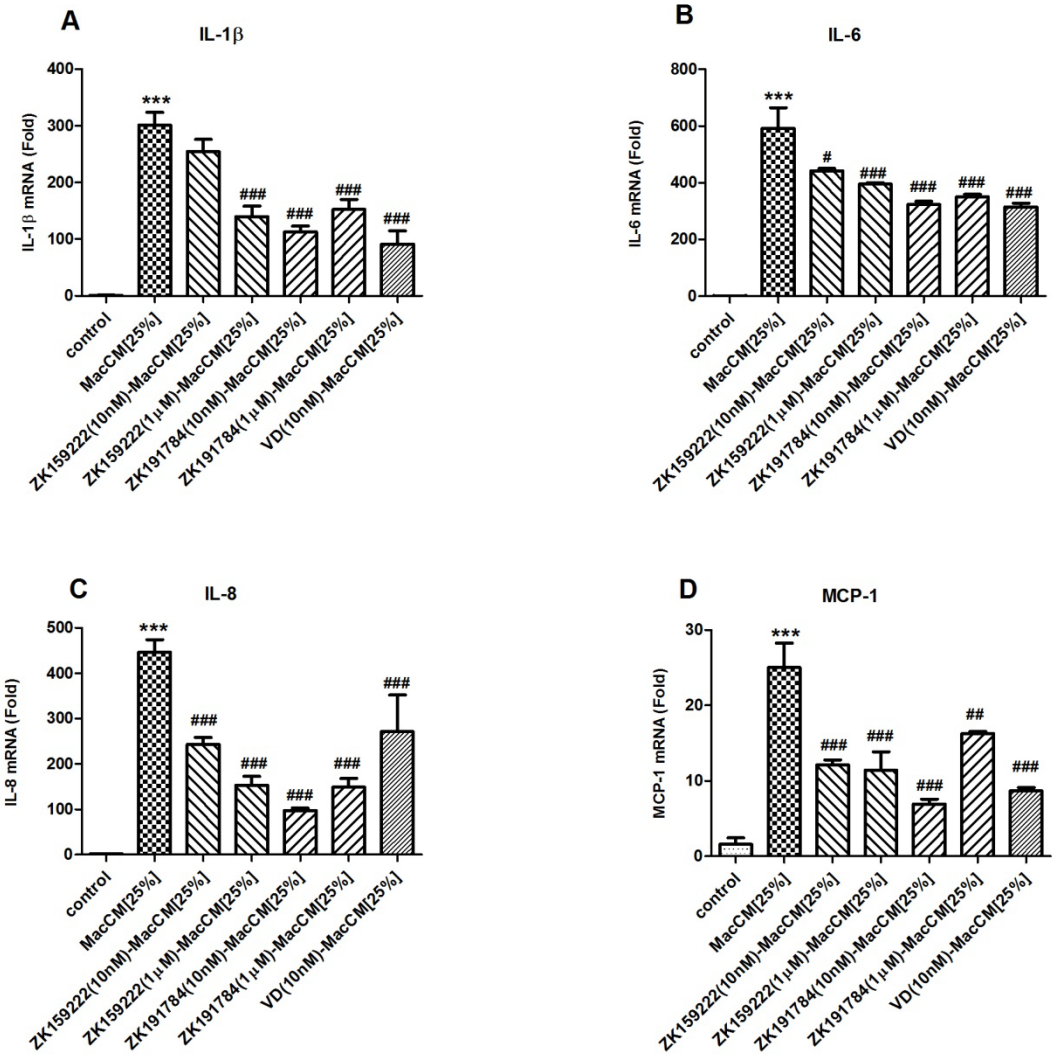

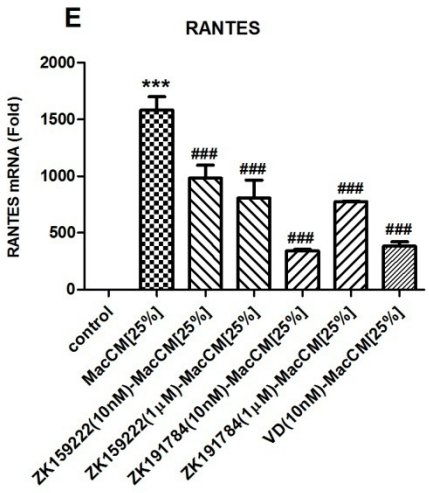


Preadipocytes were either cultured alone (control), or with (25%) THP-1-MacCM alone, or with [1α,25$(OH)_2D_3$ (10 nM), ZK159222 (10 nM and 1 μM) and ZK191784 (10 nM and 1 μM)] VDR agonist-MacCM for 24 h before Trizol-dissolved lysate collection. The mRNA levels of pro-inflammatory factors (A) IL-1β, (B) IL-6, (C) IL-8, (D) MCP-1 and (E) RANTES were measured by ELISA. Data are means ± SEM for groups of 6. A significant difference to control was indicated by ***($p<0.001$); to (25%) THP-1-MacCM by ##($p<0.01$), ###($p<0.001$). The results were determined using one-way ANOVA with Tukey's post hoc test.